HORMETIC DIETARY PHYTOCHEMICALS FROM WESTERN CANADIAN PLANTS: IDENTIFICATION, CHARACTERIZATION AND MECHANISTIC INSIGHTS

A Thesis Submitted to the College of

Graduate Studies and Research

In Partial Fulfillment of the Requirements

For the Degree of Doctor of Philosophy

In the Department of Biology

University of Saskatchewan

Saskatoon

By

David James Konkin

PERMISSION TO USE

In presenting this thesis/dissertation in partial fulfillment of the requirements for a Postgraduate degree from the University of Saskatchewan, I agree that the Libraries of this University may make it freely available for inspection. I further agree that permission for copying of this thesis/dissertation in any manner, in whole or in part, for scholarly purposes may be granted by the professor who supervised my thesis/dissertation work or, in their absence, by the Head of the Department or the Dean of the College in which my thesis work was done. It is understood that any copying or publication or use of this thesis/dissertation or parts thereof for financial gain shall not be allowed without my written permission. It is also understood that due recognition shall be given to me and to the University of Saskatchewan in any scholarly use which may be made of any material in my thesis/dissertation.

DISCLAIMER

Reference in this thesis/dissertation to any specific commercial products, process, or service by trade name, trademark, manufacturer, or otherwise, does not constitute or imply its endorsement, recommendation, or favoring by the University of Saskatchewan. The views and opinions of the author expressed herein do not state or reflect those of the University of Saskatchewan, and shall not be used for advertising or product endorsement purposes.

Requests for permission to copy or to make other uses of materials in this thesis/dissertation in whole or part should be addressed to:

Head of the Department of Biology

University of Saskatchewan

Saskatoon, Saskatchewan S7N 5E2

Canada

ABSTRACT

Activation of mammalian stress responsive pathways by plant secondary metabolites may contribute to the protection against certain chronic diseases afforded by fruit and vegetable consumption. This work focuses on the identification of plant compounds that activate the stress-responsive enzyme quinone reductase (QR) by stabilizing the transcription factor NF-E2 related factor-2 (Nrf2). Screening methanolic extracts of plants from Western Canada for QR induction in a mouse hepatoma cell line (Hepa-1c1c7) led to the identification of twenty-one extracts capable of doubling the activity of QR. Bioassay-guided fractionation of six extracts led to the identification of novel classes of compounds with QR-inducing activity including fatty-acid derived polyacetylenes, phthalides, and cannabinoids. Studies using low molecular weight thiols and the recombinantly expressed protein Keap1, the principal negative regulator of Nrf2, supported a mechanism of QR activation involving covalent modification of Keap1 cysteines for the polyacetylenes and phthalides. Analysis of transcriptional changes in response to treatment with a panel of QR-inducing compounds provided strong support for Nrf2 activation by the polyacetylene (3*S*,8*S*)-falcarindiol and the isothiocyanate (*R*)-sulforaphane and weaker support for the compounds (3*R*,8*S*)-falcarindiol, 6-isovaleryl-umbelliferone (6-IVU) and (*Z*)-ligustilide. Additionally, transcript level analyses supported a role for the aryl-hydrocarbon receptor in QR-activation by (3*R*,8*S*)-falcarindiol, (*Z*)-ligustilide, (*R*)-sulforaphane, 6-IVU and cannabidiol and suggested that treatment with polyacetylenes with a (3*R*)-configuration, (*Z*)-ligustilide and 6-IVU causes substantial changes in the expression of genes associated with lipid homeostasis and energy metabolism. As a whole, this work provides evidence that compounds that activate QR (and Nrf2) are widely distributed in the Canadian flora. However, of these QR activators, few are active at concentrations that are expected to be achieved through dietary consumption. Nevertheless, the most exceptional compounds isolated in this work, the compounds (3*S*,8*S*)-falcarindiol and epoxyfalcarindiol are highly potent and appear to be or are expected to be specific for activating Nrf2 and thus warrant attention with respect to dietary implications and as drug candidate leads.

ACKNOWLEDGEMENTS

I would like to thank my supervisor Jon Page and committee members Peta Bonham-Smith, Jo-Anne Dillon, Bernhard Juurlink, and Ed Krol for their guidance and encouragement.

I thank Nick Page for his help with collecting plant material, Eric Bol for his involvement in extraction of plant material, Yuping Lu for instruction on phytochemical separations, Paula Ashe for help with cell culture, Steve Ambrose, Doug Olsen, Randy Purves and Haixia Zhang for assistance with mass spectrometry, Ken Nelson and Chantelle Benson for guidance on chemistry, Larissa Ramsay for help with bioinformatics, Enwu Liu for assistance with molecular biology and Sandra Polvi for help with plant tissue culture and plant care. I would also like to thank my colleagues Jana Nagel, Andrea Todd, Shawn Clark, Jake Stout, Steve Gagne and Lana Culley for many productive discussions and good company.

I would like to acknowledge the generous financial support from NSERC, the NRC graduate student supplemental scholarship program, the NRC Plants for Health and Wellness program and the U of S Dean's scholarship.

DEDICATIONS

I would like to dedicate this thesis to my grandparents, Valentina and Alexander Konkin and May and James Bedwell who nurtured my interest in biology at an early age and continue to provide me with inspiration. I would also like to thank my parents and family for all their support. I dedicate a special thanks to my wife Rochelle Bondarenko for her encouragement and support.

TABLE OF CONTENTS

LIST OF TABLES

LIST OF FIGURES

LIST OF ABBREVIATIONS

ABTS	2,2'-azino-bis(3-ethylbenzothiazoline-6-sulphonic acid)
AhR	aryl-hydrocarbon receptor
ARE	antioxidant responsive element
ARNT	aryl-hydrocarbon receptor nuclear translocator
ATP	adenosine triphosphate
BTB	broad complex-tramtrac-bric-a-brac
BSA	bovine serum albumin
bZIP	basic leucine zipper
C_{50}	concentration required to increase activity of QR by 50%
CAR	constitutive androstane receptor
CB	cannabinoid
CBD	cannabidiol
CBDA	cannabidiolic acid
CBP	Cre-binding protein
CD	concentration required to double the activity of the enzyme quinone reductase relative to solvent-treated controls
$CDCl_3$	deuterated chloroform
cDNA	complimentary DNA
CI	chemopreventive index (ratio of the cell viability IC_{50} and QR CD values)
CPDB	Consensus Path Database
CT	charcoal-treated
CYP	cytochrome P450
DE3	prophage lambda DE3
DG	double glycine repeat
DLG	aspartatic acid-leucine-glycine
DMSO	dimethylsulfoxide
D-PBS	Dulbecco's phosphate buffered saline
DPPH	diphenylpicrylhydrazyl
DTT	dithiothreitol
EDTA	ethylenediaminetetraacetic acid
ESR-1	estrogen receptor-1
ETGE	glutamic acid-threonine-glycine-glutamic acid
FOXO	forkhead box protein O
FBS	fetal bovine serum
FRAP	ferric reducing antioxidant capacity
GO	gene ontology
GR	glucocorticoid receptor
GSH	glutathione (reduced form)
HIF-α	hypoxia inducible factor-α
HMBC	heteronuclear multiple bond correlation
HMQC	heteronuclear multiple quantum coherence
HO-1	heme oxygenase-1
HPLC	high performance liquid chromatography

HRESIMS	high resolution electrospray ionization mass spectrometry
IC_{50}	inhibitory concentration required to reduce the radical concentration or cellular viability by 50%
IKK	IκB kinase
IPTG	isopropyl β-D-1-thiogalactopyranoside
IVR	intervening region
IκB	inhibitor of NF-κB
Keap1	kelch-like ECH-associated protein 1
LB	lysogeny broth
LPS	lipopolysaccharide
MALDI	matrix-assisted laser desorption ionization
MAPK	mitogen-activated protein kinase
MeCN	acetonitrile
MeOD	deuterated methanol
MS	mass spectrometry
MTT	3-(4,5-dimethylthiazol-2-yl)-2,5-diphenyltetrazolium bromide
NADPH	reduced form of nicotinamide adenine dinucleotide phosphate
NF-E2	nuclear factor-erythroid derived 2
NF-κB	nuclear factor of kappa light chain gene enhancer in β cells
NMR	nuclear magnetic resonance
NOE	nuclear overhauser effect
NRC	National Research Council of Canada
Nrf2	nuclear factor-erythroid derived 2-related factor 2
PCA	principal component analysis
PERK	PKR-like endoplasmic reticulum kinase
PGAM5	phosphoglycerate mutase family member 5
PXR	pregnane X receptor
QR	NAD(P)H-quinone oxidoreductase-1
qRT-PCR	quantitative real-time reverse-transcriptase polymerase chain reaction
RF	radiofrequency
RIN	RNA integrity number
RNA-seq	RNA sequencing
ROS	reactive oxygen species
RPKM	reads mapped per kilobase of gene per million reads mapped
SAGE	serial analysis of gene expression
SDS-PAGE	sodium dodecylsulfate polyacrylamide gel electrophoresis
SPE	solid phase extraction
SREBP	sterol responsive element binding protein
TBA	TATA-binding protein
THC	Δ^9-tetrahydrocannabinol
THCA	Δ^9-tetrahydrocannabinolic acid
TLC	thin layer chromatography
TOF	time of flight
TOF/TOF	tandem time of flight
UV	ultraviolet

UV-VIS	ultraviolet-visible
XRE	xenobiotic response element

CHAPTER 1

GENERAL INTRODUCTION

1.1. Diet and health

The impact of diet on health has been recognized for centuries. Sailors stocking citrus fruits to prevent scurvy is a classic example. Basic nutritional requirements must be met to prevent diseases of deficiency. The development of our understanding of basic nutrition and the prevention of deficiency-associated diseases can be regarded as one of the great medical successes of the 20th century. However, the mechanisms by which diet affects the development of chronic diseases are inadequately understood. A large body of epidemiological research links intake of fruits, vegetables and whole grains above the levels required for basic nutritional needs to decreased incidence of chronic diseases such as cardiovascular diseases and certain cancers including those of the of the respiratory and gastrointestinal tracts (WHO 2003; Dauchet et al. 2006; He et al. 2006; Vainio et al. 2006; He et al. 2007; WCRF-AICR 2007). Typical reductions in risk are in the range of 10-20% for intake of 3-10 servings of fruits and vegetables per day (WHO 2003).

In addition to plant intake, other dietary habits may also be protective against diseases of aging. Low to moderate alcohol consumption is associated with decreased mortality (Grønbæk 2004) and reduced caloric intake promotes longevity in a range of organisms (Fontana et al. 2010). What link if any exists amongst these seemingly disparate dietary interventions? A commonality exists in their ability to cause mild stress and by doing so, activate adaptive stress responses (Mattson 2008).

1.2. Hormesis

Stress in biological systems can be defined as a perturbation of homeostasis. Homeostasis refers to the process of maintaining a constant internal environment. Organisms are constantly dealing with both externally and internally-derived stresses. Examples of stresses at the biochemical level include alterations in pH, osmotic pressure, gas concentrations (oxygen, carbon dioxide) as well as exposure to foreign compounds (xenobiotics).

It has long been acknowledged that a mild dose of stress can be beneficial and show the opposite effect of a large dose. For example, low doses of physical or mental exercise lead to enhanced performance, whereas high doses are debilitating (Radak et al. 2008). The phenomenon that small quantities of an agent cause the opposite effect of large quantities is known as hormesis (Calabrese et al. 2007). Calabrese and colleagues have shown that hormesis is a widely observed biological phenomenon (Calabrese et al. 2003; Calabrese 2008). As shown in Figure 1-1, typical hormetic response curves display a J or inverted U shape depending on the endpoint measured (Hayes 2006). The traditional dose-response relationships, the threshold model and linear non-threshold model, are presented for comparison. These traditional models are often used in toxicological studies for extrapolation from high doses to low doses. However, this practice does not accurately predict the effects of low doses in situations where hormesis occurs. Therefore, despite the additional efforts required, testing at low doses is essential to accurately determine a dose response. It should be noted that hormesis is not always beneficial. For example, low concentrations of some anti-cancer drugs and herbicides have been shown to increase tumour and weed growth, respectively (Wiedman et al. 1972; Calabrese et al. 2003).

The hormetic dose-response can occur as the result of direct stimulation, overcompensation in response to a disruption of homeostasis or as an adaptive response to protect against further insult (Calabrese 2008). By activating stress responses at low doses that do not overwhelm the cell, hormetic agents can increase capacity for dealing with stress including that from other insults. An example of such cross protection occurs in mosquito larvae exposed to high, but sub-lethal temperatures. These mosquitoes not only show increased tolerance to subsequent exposures to higher temperatures, but also show increased resistance to the insecticide propoxur (Patil et al. 1996).

From an evolutionary perspective, hormetic mechanisms confer a survival advantage by increasing the ability to cope and adapt to environmental and internal harms. Of particular importance to heterotrophs is the ability to cope with noxious compounds found in the food they consume.

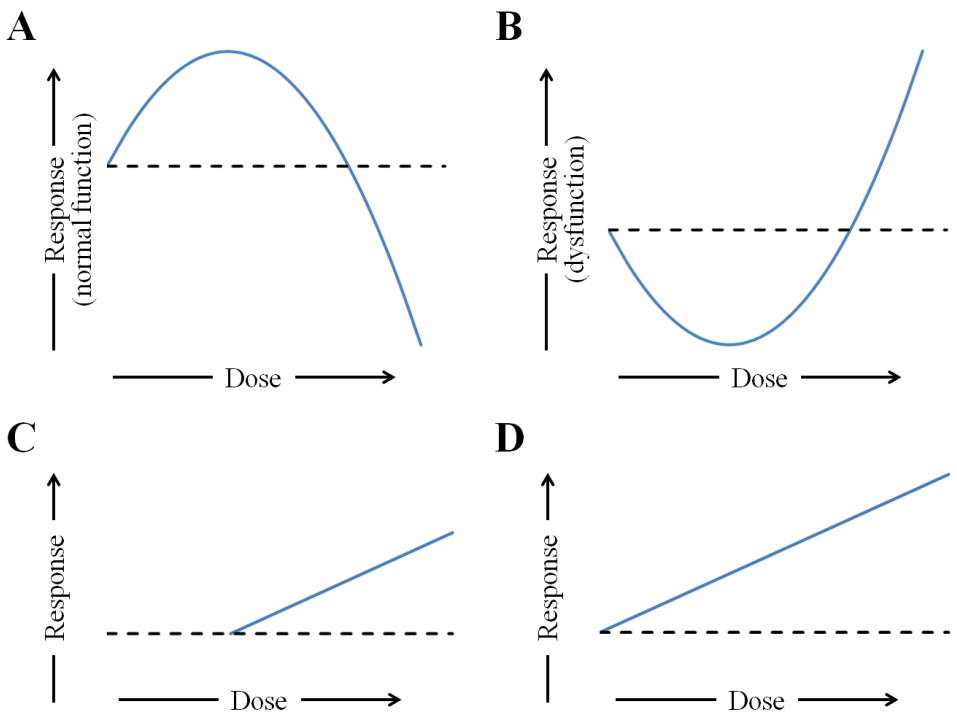

Figure 1-1. Dose response curves. (a) Inverted U-shaped hormetic model portraying low-dose enhancement and high-dose impairment of normal function. (b) J-shaped hormetic model portraying low-dose reduction and high-dose augmentation of adverse dysfunction. (c) The threshold model. (d) The linear non-threshold model. Redrawn from (Hayes 2006).

1.2.1. Dietary hormesis

There is increasing support for the ability of dietary agents and caloric restriction to prevent chronic diseases by activating hormetic pathways (Mattson 2008; Son et al. 2008). In other words, our diet can modulate adaptive stress responses that, in addition to protection potentially harmful dietary compounds, may offer protection against chronic diseases. Examples of the signalling pathways involved include those mediated by the transcription factors nuclear factor-erythroid-derived 2-related factor-2 (Nrf2) and nuclear factor of kappa light chain gene enhancer in β cells (NF-κB), as well as cell-survival signalling kinases and histone deacetylases including sirtuins. These regulatory proteins in turn influence the expression of antioxidant proteins, xenobiotic-metabolizing enzymes, transporters, growth factors, proteasomal proteins, heat shock proteins, and DNA repair enzymes.

Several signalling pathways may work in concert during a hormetic response. For example, the benefits of caloric restriction in mice include extension of life span and increased resistance to chemically induced carcinogenesis (Fontana et al. 2010). While sirtuin-forkhead box protein O (FOXO) pathways are suspected to confer life span extension, the Kelch-like ECH-associated protein 1 (Keap1)-Nrf2-antioxidant responsive element (ARE) pathway (described below) has been shown to be responsible for chemopreventive benefits (Guarente et al. 2005; Pearson et al. 2008). Although the upstream events that lead to the activation of these pathways are not completely understood it is evident that these signalling pathways form an integral part of the overall hormetic effect.

1.2.2. Phytochemicals as activators of hormetic stress responses

Plants produce an estimated 200,000 metabolites, the majority of which are specialized compounds called phytochemicals (Goodacre et al. 2004). These compounds are not required for basic metabolism and serve supplementary ecological roles such as deterring herbivory, communication with other plants or mutualistic microorganisms, inhibiting the growth of neighboring plants, combating infections, and attracting seed dispersers and pollinators (Wink 2010).

The diversity of phytochemicals has been exploited by humans as a primary source of medicines and investigational drugs. Paclitaxel (anti-cancer), morphine (analgesic) and artemisinin (antimalarial) are examples of important phytochemical drugs used in Western medicine. Additionally, plant-based medicines are integral to many widely practiced traditional medicines such as Ayurveda and traditional Chinese medicine. Although not all traditional medicines have undergone scientific scrutiny, in many cases the active phytochemicals have been isolated and are used as drugs today (Fabricant et al. 2001).

Human exposure to phytochemicals is not limited to plant-derived medicines. Food plants, spices, tea and coffee provide dietary exposure to a wide range of phytochemicals on a daily basis. Along with fibre, these compounds are thought to be responsible for benefits such as protection against certain cancers and diseases of aging that are afforded by plant consumption.

As plants have historically comprised an important part of the human diet it is not surprising that stress responses exist for coping with exposure to a range of potentially harmful phytochemicals. What was unexpected however, was the finding that these same stress responses may protect against diseases of aging. The reason for this cross-protection is that stresses associated with exposure to phytochemicals, such as electrophilic metabolites, reactive oxygen species and inflammation, are also associated with the pathogenesis of diseases of aging. Activation of these stress responses is hormetic: at low doses the increased protection afforded by activation of the stress response outweighs the harms of exposure whereas at high doses the protective response is overwhelmed. Therefore it is essential to identify compounds with the greatest selectivity for activating a stress response as these compounds will have a large therapeutic window and greater overall positive effects.

Examples of such hormetic stress-response-activating phytochemicals include sulforaphane, curcumin, xanthohumol and quercetin (Uda et al. 1997; Thimmulappa et al. 2002; Dietz et al. 2005; Scapagnini et al. 2006). Sulforaphane is an isothiocyanate which can be obtained in high amounts from broccoli sprouts. Sulforaphane and related isothiocyanates impart the spicy taste of broccoli sprouts and other cruciferous vegetables. Curcumin I is a bright yellow polyphenol abundant in the roots of turmeric (*Curcuma longa*). Xanthohumol is a prenylated chalcone from hop (*Humulus lupulus*). Quercetin is a flavonoid found in high amounts in onions, and fruits such as strawberries and apples (Hertog et al. 1992). Although these compounds have been shown to modulate numerous cellular pathways, they share the ability to modulate what is emerging as an exceptionally important pathway, the Keap1-Nrf2-ARE axis (Bacon et al. 2003; Surh 2003; Menon et al. 2007; Dinkova-Kostova et al. 2008).

1.3. The Keap1-Nrf2-ARE axis

The transcription factor Nrf2 is a master regulator of cellular antioxidant and protective capacity (Kobayashi et al. 2006). Nrf2 directs the expression of numerous cytoprotective genes (see Table 1-1 for a partial list) through transcriptional enhancers called antioxidant responsive elements (ARE, also known as electrophile responsive elements). Examples of compounds that activate Nrf2-mediated transcription (Nrf2 activators) are presented in Table 1-2.

Table 1-1. Cytoprotective genes regulated by Nrf2 (modified from (Holtzclaw et al. 2004))

Gene name	Cytoprotective role	Reference(s)
QUINONE REDUCTASE (QR)	Diverts quinones from redox cycling and sulfhydryl depletion, maintains vitamin E in reduced form, stabilizes p53	(Ross et al. 2000)
GLUTATHIONE S-TRANSFERASES	Conjugates electrophiles, detoxifies oxidants, reduces peroxides, regenerates reduced ascorbate	(Talalay et al. 1978; Kelly et al. 2000)
HEME OXYGENASE-1 (HO-1)	Rate limiting step in heme degradation leading to production of the protective molecules bilirubin and carbon monoxide	(Gong et al. 2002)
γ-GLUTAMYLCYSTEINE SYNTHETASE	GSH synthesis	(Mulcahy et al. 1995)
GLUTATHIONE REDUCTASE	Regenerates reduced glutathione	(Ansher et al. 1986)
GLUTATHIONE CONJUGATE EXPORTER	Eliminates glutathione conjugates	(Bock et al. 2000)
THIOREDOXIN	Reduces oxidants	(Kim et al. 2001)
THIOREDOXIN REDUCTASE	Regenerates reduced thioredoxin	(Cho et al. 2004)
UDP-GLUCURONOSYLTRANSFERASES	Conjugates UDP to electrophiles	(Talalay et al. 1978; Bock et al. 2000)
AFLATOXIN ALDEHYDE REDUCTASE	Detoxifies aflatoxin B_1	(Kelly et al. 2000)
DIHYDRODIOL DEHYDROGENASE	Epoxide metabolism	(Ciaccio et al. 1994)
CATALASE	Converts hydrogen peroxide to molecular oxygen and water	(Otieno et al. 2000; Cho et al. 2005)
SUPEROXIDE DISMUTASE	Converts superoxide to hydrogen peroxide	(Otieno et al. 2000)
FERRITIN	Sequesters Fe	(Pietsch et al. 2003; Cho et al. 2005)
MULTIDRUG RESISTANCE PROTEINS 1 AND 2	Export of xenobiotics	(Bock et al. 2000; Cho et al. 2005)
LEUKOTRIENE B_4 DEHYDROGENASE	Suppresses inflammation	(Primiano et al. 1998)

Table 1-2. Endogenous Nrf2 activators

Compound	Structure	Class	Reference
15-Deoxy-$\Delta^{12,14}$-prostaglandin J_2	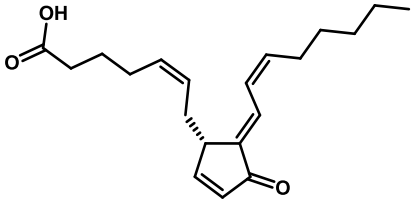	Prostaglandin	(Kim et al. 2008)
Nitric oxide		Gas	(Buckley et al. 2008)
S-Nitrosocysteine	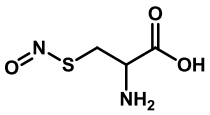	Cysteine-gas adduct	(Buckley et al. 2008)

Table 1-3. Plant-derived Nrf2 activators

Plant compound	Structure	Class	Sources	Reference
Quercetin	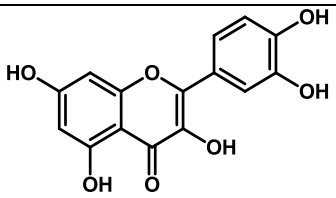	Flavonoid	Fruits, onion	(Lee-Hilz et al. 2006)
Sulforaphane	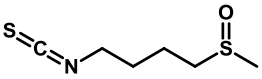	Isothiocyanate	Broccoli	(Thimmulappa et al. 2002)
Xanthohumol	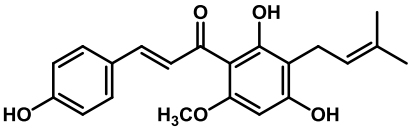	Chalcone	Hop	(Dietz et al. 2005)
Resveratrol	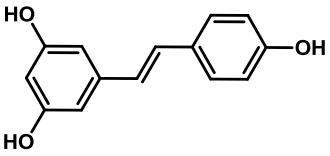	Stilbene	Grape	(Kode et al. 2008)
Ixocarpalactone A	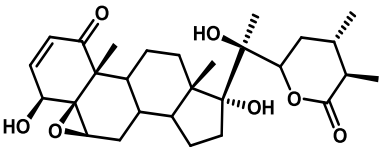	Withanolide	Tomatillo	(Su et al. 2004)
Curcumin I	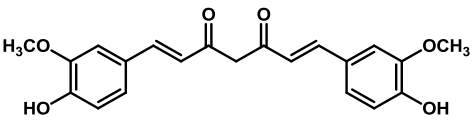	Polyphenol	Turmeric	(Scapagnini et al. 2006)

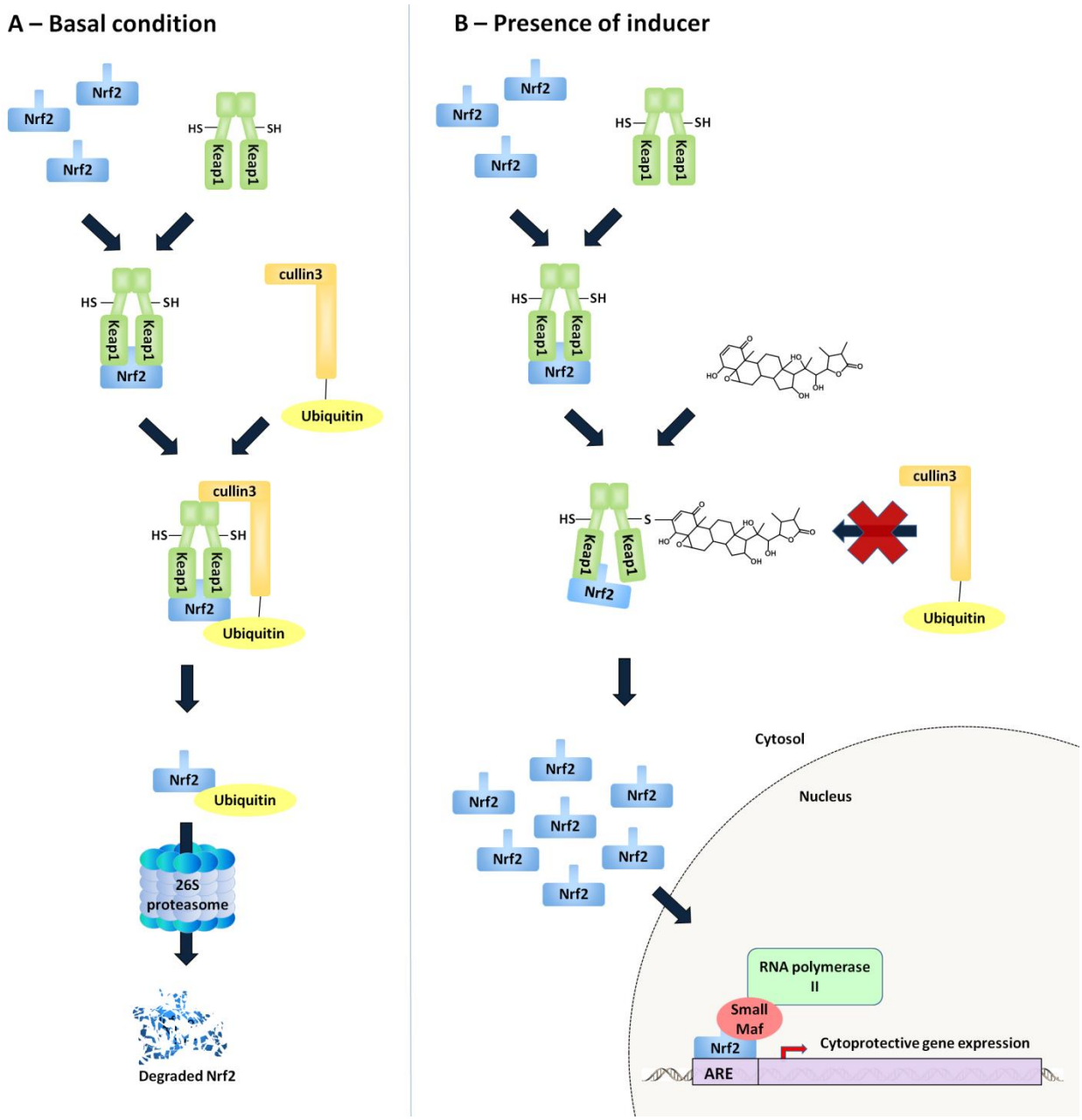

Figure 1-2. Regulation of Nrf2 by Keap1. (A) Under basal conditions Nrf2 associates with Keap1 and is ubiquitylated by the ubiquitin ligase, Cullin3, and consequently degraded. (B) Nrf2-activators, such as the withanolide depicted here, cause a conformational change in Keap1 such that Cullin3 can no longer ubiquitylate Nrf2. Inhibition of Nrf2 degradation leads to the accumulation of Nrf2 and the activation of Nrf2 targeted genes.

Nrf2 is constitutively expressed and under basal conditions is degraded by the ubiquitin proteasomal pathway with a half life of less than 20 min (Kobayashi et al. 2006). A cytosolic

protein, Keap1, mediates the degradation of Nrf2 by acting as an adapter for a Cullin3-based ubiquitin ligase (Figure 1-2) (Kobayashi et al. 2004; Zhang et al. 2004). Ubiquitin ligases are proteins that regulate, often with the co-operation of an adapter protein, the abundance of target proteins by mediating their ubiquitylation. Ubiquitylation then serves as a signal for the proteasomal degradation of the target protein, in this case Nrf2.

Keap1 possesses several reactive cysteine residues. Modification of these cysteine residues by Nrf2 activators such as sulforaphane (Tables 1-2 and 1-3), interferes with the ability of Keap1 to function as a ubiquitin ligase adapter and thus stabilizes Nrf2. Nrf2 then translocates to the nucleus and directs transcription of genes that possess an ARE. Although it is clear that Nrf2 is a vital component of the adaptive stress machinery, some of the details regarding the regulation of this transcription factor and the related implications for human health await investigation. Here I briefly summarize the discovery and current state of knowledge regarding the Keap1-Nrf2-ARE axis.

1.3.1. The discovery of Nrf2 and its targets

The discovery of Nrf2 was a result of the investigation of xenobiotic detoxification. The detoxification of xenobiotics often involves metabolism to make the compound more polar and therefore, more easily excreted. Classically, xenobiotic metabolism is divided into two phases (Williams 1959). First, polar functionalities are introduced by phase I enzymes which include many cytochrome P450 superfamily enzymes. Phase II (conjugating) enzymes then add large polar moieties such as glucuronic acid, sulphate, acetate or glutathione to the products of phase I metabolism thereby deactivating and assisting elimination of the xenobiotic.

Investigation of the promoter regions of several phase II genes led to the identification of a common regulatory sequence. This sequence was named the ARE as it was responsive to several phenolic antioxidants (Rushmore et al. 1990; Favreau et al. 1991). Similarity of the ARE motif to the binding motif of the transcription factor, nuclear factor-erythroid derived 2 (NF-E2), led to the investigation of transcription factors related to NF-E2 and the subsequent identification of Nrf2 as the primary mediator of gene expression through the ARE (Itoh et al. 1997). Nrf2 has been identified in several vertebrates including human, rat, mouse, chicken, zebrafish, and the African clawed frog (Malik et al. 2009).

1.3.2. Insights from Nrf2$^{-/-}$ mice

Nrf2$^{-/-}$ mice are viable and can survive under normal laboratory conditions. However, these mice commonly develop lupus-like autoimmune disorders (Ma et al. 2006) and display increased sensitivity to acute toxicity, carcinogen exposure, as well as inflammation and oxidative stress. Unlike Nrf2$^{+/+}$ mice, Nrf2$^{-/-}$ mice are not protected from these insults by dietary Nrf2 activators (Kobayashi et al. 2006). Nrf2-deficient mice display increased acetaminophen-induced hepatotoxicity (Enomoto et al. 2001), diesel exhaust-induced DNA adduct formation (Aoki et al. 2001), cisplatin-induced nephrotoxicity (Liu et al. 2009), damage from ischemia reperfusion in kidney and brain (Shih et al. 2005; Liu et al. 2009), elastase-induced pulmonary inflammation and emphysema (Ishii et al. 2005), chemically-induced skin papilloma (auf dem Keller et al. 2006) and streptozotocin-induced diabetic nephropathy (Jiang et al. 2010) and are unable to efficiently resolve inflammation (Itoh et al. 2004).

Microarray analyses of Nrf2$^{-/-}$ mice have led to the discovery that in addition to antioxidant proteins and xenobiotic metabolizing enzymes Nrf2 also regulates the transcription of heat shock proteins, proteasomal subunits, transporters, enzymes involved in regeneration of reduced nicotinamide adenine dinucleotide phosphate (NADPH) and primary metabolism, as well as numerous kinases, phosphatases, transcription factors, immunity related proteins, cell adhesion proteins, cell cycle and growth regulating proteins (Li et al. 2002; Thimmulappa et al. 2002; Kwak et al. 2003; Lee et al. 2003; Lee et al. 2003; Kraft et al. 2004; Li et al. 2004; Cho et al. 2005; Hu et al. 2006; Hu et al. 2006; Shen et al. 2006; Yates et al. 2009). Subsequently, direct evidence for Nrf2-regulation of some of these genes has been reported (Pietsch et al. 2003).

Thus, Nrf2 has a multifaceted set of targets that increase the capacity of the cell for dealing with both endogenous and exogenous chemical insults: phase II xenobiotic-metabolizing enzymes deactivate harmful xenobiotics; antioxidant proteins and enzymes neutralize reactive oxygen and nitrogen species and bolster the levels of intracellular small molecule antioxidants such as glutathione; efflux transporters remove products of phase II metabolism; influx transporters provide the necessary compounds to enable the above responses (i.e. entry of the amino acids necessary for glutathione synthesis) and heat shock proteins and the proteasome aid in the refolding or elimination of denatured proteins caused by reactive oxygen species (ROS) or

reactive metabolites. In addition, regulation of the cell signalling machinery including kinases, phosphatases, transcription factors, and proteins regulating cell cycle and growth allow for coordination of cellular events.

As the cellular harms of inflammation and xenobiotic exposure are often the same, (e.g. electrophiles, reactive oxygen species, dysfunctional proteins) it makes sense that there is a convergence of the response to these superficially different stresses through Nrf2 activation. Exploiting this convergence is the basis for using dietary Nrf2 activators for disease prevention as controlled activation of Nrf2 by dietary agents will confer cross-protection against inflammation and redox stress that are thought to underlie the development of chronic diseases.

How are these different stimuli integrated into a single consolidated Nrf2-driven response? Keap1, the sensor protein regulating the cellular abundance of Nrf2, is responsive to both electrophilic endogenous signalling molecules and electrophilic xenobiotics.

1.3.3. Regulation of Nrf2 by Keap1

In 1999, it was noted that disruption of the N-terminal domain of Nrf2 enhanced the activity of Nrf2 and was hypothesized that this domain may interact with a negative regulator (Itoh et al. 1999). This repressor was identified by yeast-2-hybrid screening and named Keap1 (Itoh et al. 1999). Constitutive activation of Nrf2 in Keap1$^{-/-}$ mice verified the repression of Nrf2 by Keap1 (Wakabayashi et al. 2003).

Keap1 possesses numerous cysteine residues (25 in mouse, 27 in human), several of which are highly reactive toward electrophiles due to their proximity to basic residues (Snyder et al. 1981; Itoh et al. 2004). Keap1 represses Nrf2 by acting as an adapter for a Cullin3-based ubiquitin ligase thereby directing Nrf2 degradation (Figure 1-2) (Cullinan et al. 2004; Kobayashi et al. 2004). Small molecule Nrf2 activators are thought to cause a conformational change in the structure of Keap1, which impairs the ability of Keap1 to direct the ubiquitylation of Nrf2 and may result in ubiquitylation of Keap1 itself (Eggler et al. 2005). This model is supported by experiments using a protein synthesis inhibitor showing that only *de novo* synthesized Nrf2 translocates to the nucleus and by experiments showing that proteasome inhibitors lead to the nuclear accumulation of Nrf2 (Stewart et al. 2003; Kobayashi et al. 2006).

1.3.3.1. Keap1 and Nrf2 structure

High resolution structures of Keap1 and Nrf2 are not available, although a low-resolution cryo-EM-based structure was recently published for mouse Keap1 ((Ogura et al. 2010) Figure1-3). Keap1 possesses several distinct domains; a Broad complex-Tramtrac-Bric-a-brac (BTB) domain near the N-terminus is necessary for dimerization and interaction with Cullin3, a double glycine repeat (DG) domain which is necessary for interaction with Nrf2 and an intervening region (IVR) (Figure 1-3).

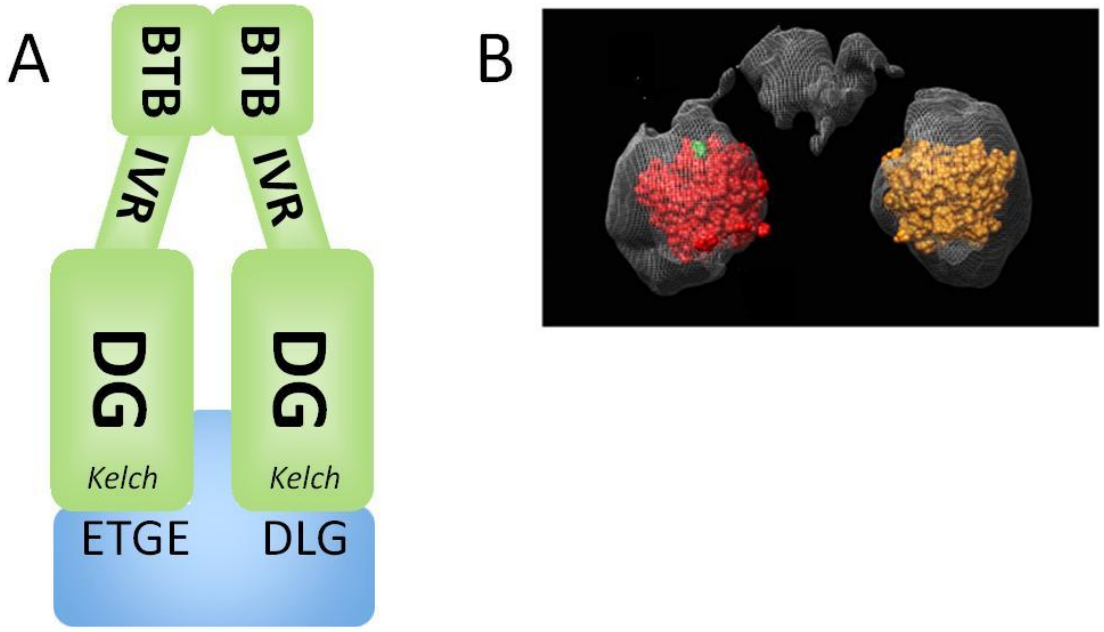

Figure 1-3. Keap1 and Nrf2 structures. A) Cartoon depicting important domains and regions of Keap1 (*green*, shown as a dimer) and Nrf2 (*blue*). BTB = Broad complex-Tramtrac-Bric-a-brac, IVR = intervening region, DG = double glycine repeat, ETGE = glutamic acid-threonine-glycine-glutamic acid, DLG = aspartatic acid-leucine-glycine.B) Keap1 dimer cryo-EM density map superimposed on the x-ray diffraction-based structure of the Keap1-DG domain (*orange* or *red*). Modified from (Ogura et al. 2010).

Nrf2 possesses two motifs, DLG (aspartatic acid-leucine-glycine) and ETGE (glutamic acid-threonine-glycine-glutamic acid), that can bind a Kelch motif of the Keap1 DG domain, albeit with 100-fold difference in affinity (Tong et al. 2006; Tong et al. 2006; Tong et al. 2007). The "hinge and latch model" proposes that the high affinity ETGE-Kelch interaction functions as

a hinge whereas the lower affinity DLG-Kelch interaction (on the other Keap1 monomer) functions as a latch that can be opened by modification of Keap1 such that the lysines on Nrf2 targeted for ubiquitylation are out of reach of the Cullin3 ubiquitin ligase. Consistent with this model, the lysine residues that are ubiquitylated in Nrf2 lie between the DLG and ETGE motifs (Zhang et al. 2004).

1.3.3.2. Modification of Keap1 cysteines results in impaired ubiquitylation of Nrf2

Modification of cysteine residues of Keap1, either by alkylation or oxidation, has long been thought to be the molecular sensor for electrophilic compounds. Due to the presence of electron withdrawing groups, electrophilic compounds have a region that is deficient in electrons and are susceptible to reactions with nucleophiles, which are electron-rich. Under basic conditions, the thiol group of cysteine is deprotonated to form the thiolate ion which is an effective nucleophile. As several of the cysteines of Keap1 are flanked by basic residues, these cysteines are particularly reactive with electrophiles.

Multiple classes of compounds have been shown to activate Nrf2 and all share the feature of being thiol reactive or having metabolites that are thiol reactive (Linnewiel et al. 2009). Furthermore, the potencies of inducers parallels their reactivity with thiol groups (Dinkova-Kostova et al. 2001). Mass spectrometric identification of Keap1 adducts with various electrophiles have identified a handful of cysteines that are often alkylated (Luo et al. 2007; Kansanen et al. 2009). Three of these Keap1 cysteines (Cys151, Cys273 and Cys288) are required for suppression of Nrf2 *in vivo* (Yamamoto et al. 2008). In addition, using mutant Keap1 protein with various amino acid substitutions for Cys151, Eggler *et al.* (2009) reported that the molar volume of the residue at this position is positively correlated with the magnitude of response of an ARE-luciferase reporter, suggesting that a greater bulk of modification leads to increased interference with Nrf2 ubiquitylation.

Some insight into the roles played by individual cysteines was achieved by investigating the two homologues of Keap1 found in zebrafish (Kobayashi et al. 2009). Both homologues, Keap1a and Keap1b, regulate Nrf2 degradation but differ in their specificities for Nrf2 activators (Kobayashi et al. 2009). Keap1a possesses a cysteine equivalent to Cys273 in human Keap1 and is only responsive to the endogenous Nrf2 activators, prostaglandins 15d-PGJ_2 and PGA_2

(Kobayashi et al. 2009). Conversely, Keap1b, possesses a cysteine equivalent to Cys151 in human, and is responsive to numerous xenobiotics including sulforaphane, 1,2-napthoquinone andebselen (Kobayashi et al. 2009). Thus, it appears that Keap1 has multiple "sensing" cysteines capable of responding to different compounds and perhaps even discriminating between endogenous signalling compounds and xenobiotics. Indeed, an analysis of the cysteines modified *in vitro* by various agents supports this hypothesis since 15d-PGJ_2 and PGA_2 alkylate Cys273, whereas many dietary compounds alkylate Cys151 (Kansanen et al. 2009).

The current structural evidence for Keap1 suggests that Cys272 and Cys288 are in close proximity to the Kelch motif. As the Kelch motif appears to be involved in binding Nrf2, these cysteines residues may be positioned for triggering a shift in the structure of Keap causing'the latch to open'. Cys151, on the other hand, is far from this substrate binding region on the stem of the 'cherry' (BTB domain). Modification of Cys151 is therefore unlikely to interfere with binding of Keap1 to Nrf2 and may alternatively interfere with interactions between Keap1 and the Cullin3 ubiquitin ligase .

1.3.4. Regulation of Nrf2 and Keap1 via phosphorylation

Phosphorylation is thought to provide a limited contribution to Nrf2 stability and transcriptional activity (Sun et al. 2009). A number of kinases have been shown to phosphorylate Nrf2 including PKR-like endoplasmic reticulum kinase (PERK), protein kinase C, casein kinase-2, phosphatidylinositol 3-kinase, mitogen-activated protein kinase (MAPK) and p38 (Lee et al. 2001; Huang et al. 2002; Cullinan et al. 2003; Cullinan et al. 2004; Andreadi et al. 2006; Apopa et al. 2008). Phosphorylated residues include Ser40, Ser215, Ser408, Ser558, Thr559 and Ser577 (Huang et al. 2002; Sun et al. 2009).

Keap1 is also phosphorylated *in vivo* at the conserved Tyr141 which may be required for recruitment of Cullin3 (Jain et al. 2008). In addition, treatment with hydrogen peroxide resulted in the removal of this phosphate, suggesting that stress-induced dephosphorylation of Keap1 may be another sensory mechanism. In addition, modulation of nuclear export and import signals in Nrf2 and Keap1 by either phosphorylation or alkylation may also be important for controlling Nrf2 activity (Jain et al. 2005; Velichkova et al. 2005).

1.3.5. Nrf2 activators and anti-inflammation

A striking positive correlation exists between the anti-inflammatory activity and potency of Nrf2 activators in mouse macrophages and embryonic fibroblasts (Dinkova-Kostova et al. 2005; Liu et al. 2008). This correlation suggests the presence of a common target and/or mechanism of action.

There are at least three mechanisms by which Nrf2 activators can effect anti-inflammation. Firstly, through upregulation of anti-inflammatory targets of Nrf2 such as heme oxygenase-1 (HO-1) (Gong et al. 2002). Secondly, increased levels of Nrf2 may reduce the activity of the inflammatory transcription factor NF-κB by competing for the co-activator cAMP response element-binding protein (CBP) (Liu et al. 2008). And finally, by inhibiting NF-κB by covalently modifying cysteines present in its DNA-binding domain and/or the activation loop of the NF-κB activating protein, inhibitor of NF-κB kinase (IκK)-α, as has been documented for sulforaphane, xanthohumol and bardoxolone methyl (Heiss et al. 2001; Ahmad et al. 2006; Harikumar et al. 2009).

1.3.6. Phase I metabolism and AhR activation

Although phase I (oxidation) and phase II (conjugation) enzymes often work in concert to eliminate xenobiotics, they are regulated by different transcription factors. While phase II enzymes are regulated as part of the Nrf2 regulon, phase I enzymes are regulated by multiple transcription factors including the aryl-hydrocarbon receptor (AhR). The AhR is ligand activated, with a preference for planar aromatic compounds such as dioxin or benzo(a)pyrene, and directs transcription through its cognate binding element, the xenobiotic-responsive element (XRE) (Denison et al. 2003). Well described targets of the AhR include cytochrome P450 (CYP)-*1A1*, *CYP1A2*, and *CYP1B1*. The AhR also provides feed-forward activation of Nrf2 via XREs in the *Nrf2* promoter (Miao et al. 2005).

The AhR is also involved in endocrine regulation. The enzymes CYP1A1 and CYP1B1 are involved in estrogen metabolism (Dannan et al. 1986; Spink et al. 1992). Furthermore, activation of the AhR can interfere with estrogen receptor activity through competition for cofactors. An additional negative aspect to AhR activation is the potential of AhR targets to cause bioactivation of xenobiotics to harmful compounds (Shimada et al. 1996).

As the structural features required for inducing the AhR (planar aromatic) and Nrf2 (electrophilic) are not mutually exclusive it is possible for a single compound (i.e. planar aromatic and electrophilic) to activate both transcription factors. Due to the negative health consequences associated with exposure to AhR activators, compounds that activate Nrf2 without activating the AhR are predicted to confer greater health promoting benefits.

Importantly, the enzyme that I use for identifying Nrf2 activators in this work, quinone reductase (QR), is a target of both the AhR and Nrf2 (Favreau et al. 1991). In order to identify selective Nrf2 activators it is important to exclude AhR regulation as a possible means of QR induction.

1.3.7. The role of Nrf2 activators in chronic disease prevention

Though much remains to be resolved regarding the molecular dynamics of Nrf2 activation, it is clear that this transcription factor plays an essential role in protection against electrophile and oxidative stresses and therefore is expected to play a role in the development of chronic diseases in which such stresses are implicated. Indeed, Nrf2 activators or direct Nrf2 activation are protective in animal models of brain injury (Zhao et al. 2007), hypertension (Wu et al. 2004), colon cancer (Yuan et al. 2007), and cardiac hypertrophy (Li et al. 2009). Cell culture models have also demonstrated protection by Nrf2 activators against ultraviolet (UV)-A radiation (Kimura et al. 2009), cigarette smoke (Kode et al. 2008), glutamate excitotoxicity (Li et al. 2007), spinal cord injury (Liu et al. 2008), aflatoxin B_1 cytotoxicity (Pokharel et al. 2006) and cisplatin cytotoxicity (So et al. 2006).

In the case of protection in an rat model of cardiovascular disease, supplementation with broccoli sprouts, a rich source of the Nrf2 activator sulforaphane, also conferred protection to the offspring of female test animals regardless of the offspring diet suggesting that the modifications of gene expression effected by Nrf2 activators may have long-lasting, epigenetic effects (Noyan-Ashraf et al. 2006).

Several clinical trials are in progress examining the effect of the Nrf2 activators sulforaphane and bardoxolone methyl in clinical conditions where ROS stress or inflammation are involved such as chronic kidney failure in patients with diabetes or chronic obstructive

pulmonary disorder (Reata Pharmaceuticals 2012). Previous clinical trials with the compound oltipraz were not successful, however this compound was much less potent than sulforaphane or bardoxolone methyl (effective *in vitro* concentrations of 15 µM (oltipraz) vs. 0.2 µM (sulforaphane) or 0.002 µM (bardoxolone methyl)). Phase 2 trials of bardoxolone methyl showed that this compound effectively restores kidney function in diabetics with chronic kidney disease and is currently in phase 3 clinical trials (Pergola et al. 2011; Reata Pharmaceuticals 2012).

Although the results with bardoxolone methyl are promising, the results of sulforaphane-based interventions will also be of great interest. In contrast to bardoxolone methyl, which is a synthetic patented drug, sulforaphane is readily available through broccoli and other cruciferous vegetables. As sulforaphane is a benchmark for diet-based Nrf2 activation, the results of these trials will provide valuable evidence to support or refute the use of a dietary approach to reducing inflammation and oxidative stress for chronic disease prevention.

Serum concentrations of sulforaphane that are required for activity *in vitro* can be achieved relatively easy as its precursor, glucoraphanin, is abundant in broccoli sprouts (~300 µmol/g dry weight), has a high bioavailability (approximately 80%) and the concentrations required for activity are quite low (Fahey et al. 1997). The concentration of sulforaphane required to double activity of QR (CD) *in vitro* is approximately 0.2 µM. More modest increases in activity, such as a 25% or 50%, can be achieved at 0.05 or 0.1 µM. A dose of 40 g of broccoli sprouts (150 µmol of the sulforaphane precursor glucoraphanin) in humans leads to peak serum concentrations (including metabolites) greater than 2 µM (Clarke et al. 2011). In contrast, quercetin has a CD value of 13 µM, a concentration that is likely never achieved under an average diet. Consumption of a large portion of fried onions (340 g fresh weight) with 224 µmol (68 mg) equivalents of quercetin only led to an average peak plasma concentration of 0.74 µM (Hollman et al. 1997).

Another consideration is that the local exposure concentration to a xenobiotic may greatly exceed systemic concentration. It may be possible for lower exposures of an Nrf2 activator to cause an effect in these tissues and furthermore, as these same tissues are more prone to exposure to potentially harmful xenobiotics, may afford a higher relative level of protection against carcinogenesis in these tissues. Consistent with this hypothesis, cancers of the digestive tract

such as the stomach and colon appear to be the most effected by fruit and vegetable consumption (WCRF-AICR 2007).

1.4. Objectives

Despite the importance of the Nrf2-ARE axis in the dietary hormetic response, much remains to be learned regarding the diversity of Nrf2 activators, their mechanism of action, and their overall effects on the cell and organism. This study aimed to expand our understanding of the distribution and mechanism of action of Nrf2-activating phytochemicals by:

1) Identifying plant extracts that have potent QR-inducing activity, a proxy for Nrf2 induction.

2) Isolating the active components from active extracts using QR-bioassay-guided fractionation and identifying the purified compounds using UV spectrometry, NMR and mass spectrometry

3) Investigating the mechanism of action of the purified compounds by studying their effects on Keap1 (or models of Keap1 cysteines) and on transcript levels using qRT-PCR and RNA-seq.

Hypotheses to be tested:

1) Induction of the antioxidant enzyme QR by plant extracts will not be correlated with their direct antioxidant potential.

2) QR inducing activity will be due to induction of the Keap1-Nrf2-ARE axis caused by covalent modification of cysteine thiols of Keap1.

3) Treatment with QR inducing compounds will lead to changes in transcript levels of genes that are known to be controlled by Nrf2.

CHAPTER 2

SCREENING WESTERN CANADIAN PLANTS FOR QR INDUCING ACTIVITY

2.1. Introduction

As discussed in Chapter 1, activating Nrf2 through pharmacological or dietary means is a promising approach to prevent or delay diseases that involve inflammation or oxidative stress. In order to expand the number of lead compounds for drug development and provide informed dietary guidance with respect to activating Nrf2, a greater understanding of the distribution and potency of Nrf2 activators in plants is necessary.

2.1.1. The Canadian flora

Canada is home to over 3000 native plant species, 147 of which are endemic (WCMC 1994). To my knowledge, no screen examining the Canadian flora has been undertaken for Nrf2 activators. I focused on the Western Canadian flora because of the ready access to plant material and regional relevance.

2.1.2. QR induction as a guide for identifying Nrf2-activating extracts

Screening for Nrf2 activation directly using Western blots or electromobility shift assays is not practical for a large screen. Measuring changes in the level of a downstream target of Nrf2 such as the level of a transcript or protein can simplify the screening process. I chose to use the enzymatic activity of the Nrf2 target QR as a marker for Nrf2 activation.

QR is an enzyme that plays multiple protective roles in animal cells (reviewed in (Dinkova-Kostova et al. 2010)). QR prevents the redox-cycling of quinones and associated generation of reactive oxygen species by catalyzing the two-electron reduction of quinones using either NADH or NADPH. The corresponding hydroquinones can then be acted on by conjugating enzymes which halts the redox-cycling process. QR also possesses superoxide scavenging activity (Siegel et al. 2004) and prevents the degradation of the tumor suppressor p53 by acting as a gatekeeper for the 20S proteasome (Asher et al. 2005).

Many of the Nrf2 activators identified to date were isolated using QR induction as a guide (Fahey et al. 2004). Examples include isothiocyanates from broccoli, wasabi and watercress, curcumin from turmeric, resveratrol from grapes, and withanolides from tomatillo (Fahey et al. 2004). The 'Prochaska' assay is a commonly used method for quantifying QR activity. This protocol involves treating mouse Hepa-1c1c7 cells (grown in 96-well plates) with the compound or extract of interest and harvesting the cells after 24 or 48 h. Cells are lysed and QR activity and protein concentration are determined via chromogenic reactions. The QR activity of treated cells is compared to solvent-treated controls to determine the level of QR induction. Hepa-1c1c7 cells are used because of their high inducibility and similarity to hepatocytes (Hankinson 1979; De Long et al. 1986).

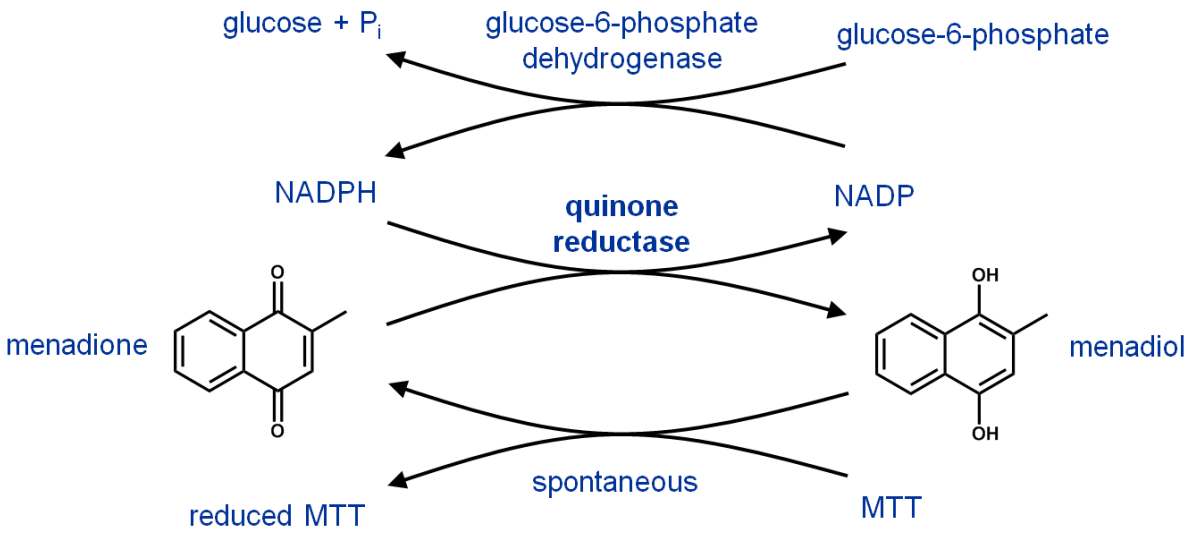

Figure 2-1. QR bioassay reaction scheme. Cell lysates are incubated with menadione, MTT and an NADPH regenerating system consisting of glucose-6-phosphate, NADP and glucose-6-phosphate dehydrogenase. Using NADPH, QR reduces menadione to menadiol. Menadiol then spontaneously reduces MTT. The concentration of reduced MTT is measured spectrophotometrically at 595 nm.

The chromogenic reaction that forms the basis of the 'Prochaska' assay is shown in Figure 2-1. QR catalyzes the reduction of menadione to menadiol which in turn reduces the dye 3-(4,5-dimethylthiazol-2-yl)-2,5-diphenyltetrazolium bromide (MTT). The level of reduced MTT is measured by absorbance at 595 nm. The other substrate for the QR catalyzed reaction, NADPH, is produced enzymatically using glucose-6-phosphate dehydrogenase and glucose-6-phosphate.

The protein concentration is determined for each lysate to correct for differential growth and variation in the number of cells plated per well.

2.1.3. Direct antioxidant activity vs. indirect antioxidant activity

Nrf2 activators are of interest because they increase the cellular capacity for dealing with oxidative stresses and resolving inflammation. As such Nrf2 activators have also been referred to as "indirect antioxidants" (Dinkova-Kostova et al. 2008). Conversely, direct antioxidants such as β-carotene, flavonoids, vitamins C and E that react directly with free radicals have also received attention as a means to combat oxidative stress. A primary difference is that direct antioxidants prevent redox signalling in general whereas Nrf2 activators activate an adaptive stress response that increases the ability to cope with the various stressors associated with redox signalling (Lee et al. 2003; Wu et al. 2011).

Although several studies have shown that high concentrations of antioxidants are protective *in vitro,* supplementation with antioxidants *in vivo* has largely failed as a means to prevent chronic disease (Bjelakovic et al. 2007). Several large intervention trials with direct antioxidants (vitamins C, E and beta-carotene) have shown that supplementation with relatively large doses have no effect on mortality from cancer or cardiovascular disease (Sesso et al. 2008; Lin et al. 2009) and that beta-carotene may increase lung cancer risk in smokers (Jeon et al. 2011). A recent study showed that daily supplementation with 400 IU of vitamin E and 1000 mg of vitamin C greatly reduced the benefit of exercise as judged by sensitivity to insulin (Ristow et al. 2009). Despite the lack of clinical evidence to support their use, direct antioxidants continue to be widely marketed.

Phytochemicals with direct antioxidant activity can possess additional biological activities. For instance, compounds such as quercetin and epigallocatechin-gallate are direct antioxidants as well as being Nrf2 activators. In fact, the ARE to which Nrf2 binds is so called because the first compounds known to activate it were phenolic antioxidants such as *t*-butylhydroquinone (Rushmore et al. 1990). However, as not all Nrf2 activators are antioxidants, the name ARE is misleading. The lesser-used name 'electrophile responsive element' is more accurate. Despite this, I have chosen to use ARE in this work due to its greater prevalence in the literature.

Despite their different modes of action, direct antioxidants and Nrf2 activators share a limited degree of structural similarity. Direct antioxidants require functional groups to stabilize the molecule following acceptance or donation of an electron. On the other hand, Nrf2 activators require functional groups that provide an electrophilic center that can modify cysteine residues of Keap1. Functional groups such as carbonyls or conjugated π-bonds can contribute in both situations. Therefore, although limited, there exists some rational for the hypothesis that extracts with potent direct antioxidant activity are more likely to activate Nrf2. To test this hypothesis I have chosen to assay the panel of extracts for direct antioxidant capacity and compare with QR induction, my proxy for Nrf2 activation.

Several methods to assay direct antioxidant activity involve a compound for which the visible light absorbance differs greatly between its radical and non-radical forms. Examples include the diphenylpicrylhydrazyl (DPPH) and 2,2'-azino-bis(3-ethylbenzothiazoline-6-sulphonic acid (ABTS) reagents. I have chosen to use the DPPH assay as it is compatible with the extraction solvent used for screening (methanol) and it is widely used (Cheng et al. 2006).

2.1.4. Selection of plant material for screening

Since closely related plants display similar phytochemical compositions, a variety of plant species is desirable to increase the effective number of compounds being screened. Availability and ecological status (i.e. endangered or abundant) are also important to consider. Plants with distributions limited to Western Canada were favored over widespread species.

Phytochemical variation occurs between different plant parts and between individuals of the same species. Therefore collecting the whole plant or multiple plant parts and using several individuals from different growing conditions ensures that the variety of compounds produced by a given species is represented in an extract.

2.1.5. Drying, grinding and extraction of plant material

Drying plants prior to extraction is essential for standardizing yields and facilitating extraction. To avoid decomposition of thermolabile compounds I have selected 37°C as a maximal temperature for drying. Compounds that rapidly decompose at or below 37°C are less desirable as they would also decompose in the human body.

The diversity of plant natural products provides a challenge when selecting a single solvent for extraction. Previous screens for bioactive plants have used extraction solvents with intermediate polarity such as methanol, ethanol or ethyl acetate which result in extracts enriched in compounds of intermediate polarity. This is beneficial as compounds with intermediate polarity possess functional groups required for bioactivity while being of low enough polarity to penetrate biological membranes. I chose methanol as an extraction solvent.

Filtered methanolic extracts are appropriate for chemical assays such as the DPPH assay (Cheng et al. 2006). However, biological assays cannot tolerate high concentrations of organic solvents. I have chosen to completely remove methanol and resuspend in dimethylsulfoxide (DMSO) for biological assays. Advantages to using DMSO include its relatively low toxicity (safe to use in most cell lines up to 1% v/v), its ability to dissolve a large range of compounds and the fact that it has very low volatility. Low volatility is desirable when resuspension volumes are small and the solution may be stored between use. To facilitate throughput, a specific volume of extract, rather than specific mass of dried extract was used during DMSO stock preparation.

2.2. Materials and methods

2.2.1. Preparation of extracts and samples for screening

Plant material was collected in the wild or purchased through plant suppliers or grocers. The location of harvest or source for each plant was recorded. Plants were identified by Nick Page, Jonathan Page or David Konkin. Plant tissue was cut into small pieces and dried at 37°C. Dried material was ground with a coffee grinder, screened at 0.5 mm and extracted with 8.3 mL methanol per g of plant material. Extraction was conducted in the dark with stirring for 24 h prior to vacuum filtration using Whatman #1 filter paper and Millipore Spin-X centrifugal filtration. One-mL of filtered extract was dried under vacuum at room temperature and resuspended in 50 µL or 30 µL of DMSO. A sample of filtered methanolic extract was used for the DPPH radical scavenging assay. Unless otherwise specified, chemicals were obtained from Sigma-Aldrich.

2.2.2. Cell culture

Hepa-1c1c7 cells (American type culture collection) were maintained in 75 cm^2 flasks using α-minimal essential medium without nucleosides containing Glutamax (Invitrogen)

supplemented with 10% charcoal-treated fetal bovine serum (FBS) (Spencer et al. 1990), 100 U/mL penicillin G and 100 µg/mL streptomycin in a humidified incubator at 37°C and 5% CO_2. Cells were subcultured at 70-80% confluency using trypsin-ethylenediaminetetraacetic acid (EDTA) solution. Early divisions of the culture (< 20 passages) were used for bioassays. Cultures were stored in liquid nitrogen with 5% DMSO.

2.2.3. QR bioassay

Hepa-1c1c7 cells were grown in 96-well plates at approximately 5000 cells per well in 200 µL medium. After 24 h the medium was replaced and dilutions of pure compounds or extracts dissolved in DMSO were added to the medium. The final concentration of DMSO was 0.1% (v/v). Dilutions were tested in duplicate. After 48 h the cells were rinsed with 200 µL of Dulbecco's phosphate buffered saline (D-PBS) and 50 µL of a solution containing 0.08% digitonin and 2 mM EDTA (pH 7.8) was added to each well. The solution was incubated for 10 min at 37°C followed by 10 min at room temperature with orbital shaking. Thirty-µL of lysate was used for the QR assay as previously described (Prochaska et al. 1988) and 20 µL was used for protein determination using bicinchoninic acid (Smith et al. 1985). Experimental QR activities were compared to the activities of DMSO treated controls. Concentrations required to double activity were determined by plotting the dose-response curve and identifying the concentration at which the curve intersected a two-fold increase in activity. QR measurements were discarded at concentrations that reduced protein content to less than 50% of the control value.

2.2.4. DPPH radical scavenging assay

The DPPH bioassay was adapted from the procedure used by Ursini *et al*. (1994). Using methanol, 8 or more two-fold serial dilutions were prepared from each methanolic extract. One-hundred-µL of 100 µM DPPH (Sigma-Aldrich) radical in methanol was added to 10 µL of each dilution in 96-well plates. After a 10 min incubation at room temperature the absorbance at 530 nm was measured. A separate dilution series of each extract prepared in methanol was prepared to correct for the absorbance of the extract at 530 nm. Ten-µL of methanol or 50 mM ascorbic acid in methanol was used to determine the assay start and endpoints, respectively. The inhibitory concentration required to reduce the radical concentration by 50% (IC_{50}) values were calculated by logarithmic regression.

2.3. Results and discussion

2.3.1. Optimization of the QR bioassay

The QR bioassay was validated using sulforaphane as a positive control. Several experimental parameters were examined in order to ensure robustness and reproducibility. A 48 h incubation with inducers led to greater intensity of response than a 24 h incubation. A longer incubation time may allow a greater accumulation of QR. Using fetal bovine serum treated with activated charcoal slightly reduced the basal level of induction (Figure 2-2). This may be due to the removal of Nrf2 activators such as cyclopentenone prostaglandins, J2-isoprostanes or nitric oxide (Kim et al. 2006; Gao et al. 2007; Liu et al. 2007). As plating 5000 cells per well did not substantially alter the intensity of response compared to 10000 cells per well (Figure 2-3), I used 5000 cells per well to allow more plates to be seeded from the same size starter culture. Although these preliminary experiments were not replicated and therefore statistical comparisons between conditions were not conducted, the findings are supported by previous work (Fahey et al. 2004).

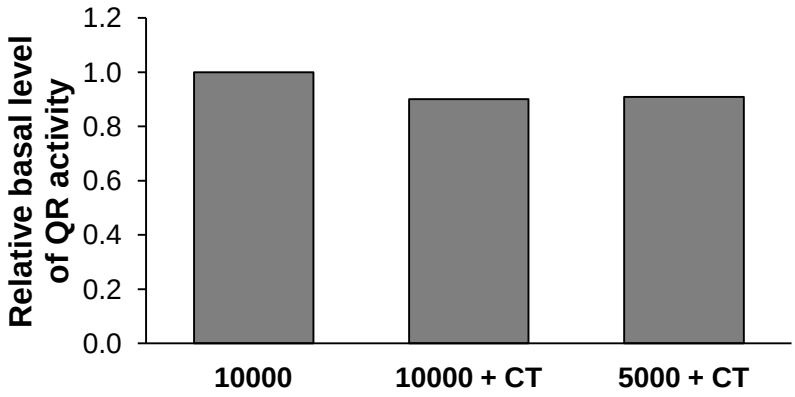

Figure 2-2. Effect of cell concentration and charcoal-treated FBS on basal QR activity. Relative basal QR activity of untreated Hepa-1c1c7 plated at 10000 or 5000 cells per well with (+ CT) or without charcoal-treated FBS in the culture medium. Results from a single experiment with 2 technical replicates.

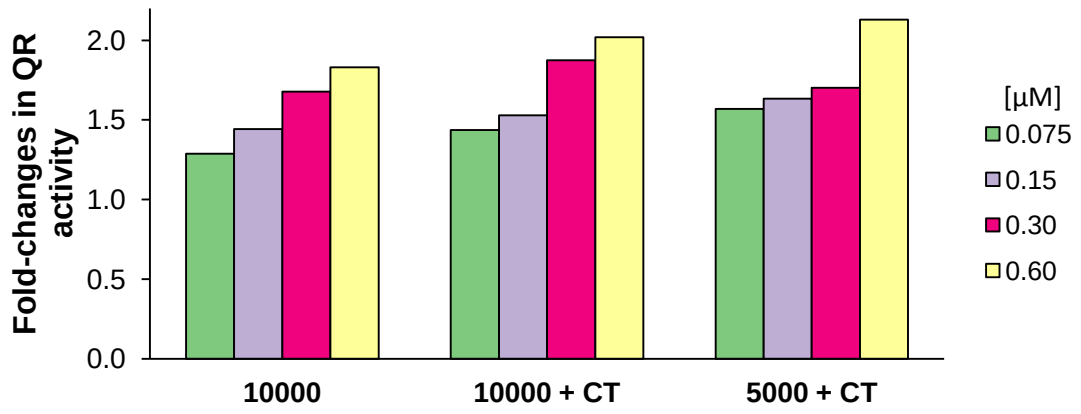

Figure 2-3. Effect of cell concentration and charcoal-treated FBS on QR induction. Fold-changes in QR activity of Hepa-1c1c7 cells in response to sulforaphane concentrations ranging from 0.0075 µM to 0.60 µM when plating different numbers of cells (10000 or 5000) and using charcoal-treated (+ CT) FBS in the culture medium. Results from a single experiment with 2 technical replicates.

The responsiveness of Hepa-1c1c7 cells declines with the number of passages (the number of times the culture is divided) (Fahey et al. 2004). Only cells that were passaged less than 20 times were used. I experimented with directly plating cells from frozen stocks but found that this resulted in a higher number of apoptotic cells and reduced responsiveness in the bioassay (data not shown). Allowing the cells to divide after thawing enriched the culture with healthy rapidly-dividing cells. In general, cells that were under stress displayed decreased inducibility in the QR bioassay due to an elevated QR baseline.

2.3.2. Procurement of plant material and extract preparation

Plant selection criteria included availability, abundance, dietary consumption, use as traditional medicine and the phylogenic relationship of the plant to the other plants in the screen. Many plants were collected in British Columbia by Nick Page, others I collected in Saskatchewan (Table A1). Extracts were prepared in a manner that facilitated a reasonable throughput using 6 g of dried material and an extract volume of 50 mL. To reduce degradation, extracts were stored in the dark at 4ºC.

2.3.3. QR bioassay screening results

Methanolic extracts from 162 plants were screened for QR induction. Six two-fold dilutions were tested for each extract at concentrations of 4, 2, 1, 0.5, 0.25, 0.125 or 2.4, 1.2, 0.6, 0.3, 0.15 mg/mL (mg of dried material used for extraction per mL of medium). Due to the viscosity of certain extract resuspensions used to prepare these dilutions, I increased the volume of DMSO used for dissolving the samples from 30 µL to 50 µL which resulted in the lower range of test concentrations for those samples (2.4 mg/mL and lower).

The greatest level of induction was often achieved at concentrations with measurable toxicity as judged by a decrease in the protein content of the well. Since I normalized for cell growth by comparing specific QR activity (activity per mass of protein present), I often found high induction levels at extract concentrations that reduced the protein concentration. These measurements were considered unreliable and results were discarded in cases where protein content dropped to less than 50% of the DMSO-treated controls.

Induction levels ranged from 0.34-fold (*Elaegnus commutata*, wolfwillow, leaves) to 2.97-fold (*Cicorium intibus*, chicory, roots). The maximal level of induction achieved at any concentration was used to index the extracts. The complete list of extracts sorted by maximal QR induction can be found in Table 2-1. The distribution of the maximal induction values are given in Figure 2-4.

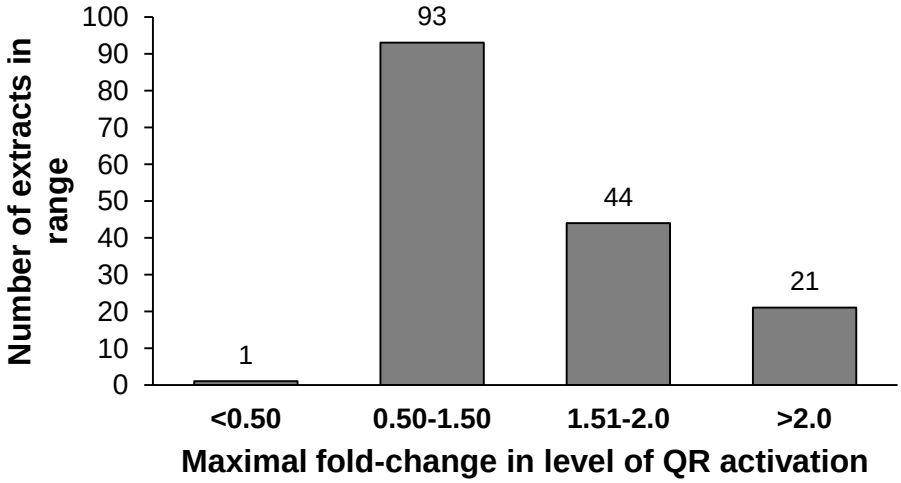

Figure 2-4. Distribution of maximal levels of QR induction of the 162 extracts tested.

Extracts are sorted by family in appendix table A1Several families of plants consistently showed elevated results.. These included the Umbelliferae, Compositae, Araliaceae and Grossulariaceae which possessed average maximal induction values of 1.87, 1.67, 1.65, and 1.52-fold, respectively. Conversely, the extracts prepared from members of the Ericaceae were nearly devoid of QR-inducing activity (average maximal induction of 0.98-fold), although fruit extracts of *Arctostaphylos uva-ursi* (kinnickinnick) and *Vaccinium myrtillus* (bilberry) were exceptions with maximal induction values of 1.65 and 1.51-fold.

Rosaceae was the best represented family with 22 extracts tested. In general Rosaceae extracts were weak inducers (average maximal induction of 1.25-fold). However, two Rosaceae extracts, *Sorbus americana* (American mountain-ash, fruit) and *Sorbus aucuparia* (European mountain-ash, fruit) stood out with maximal induction values of 2.32 and 2.15-fold, respectively. A chalcone glycoside has been reported from the fruits of the related species *Sorbus commixta* (Bhatt et al. 2009). Due to the similarity of this chalcone to the known QR inducer xanthohumol (Miranda et al. 2000), I suspect that related chalcones may be contributing to the QR induction by the *S. americana* and *S. aucuparia* extracts.

Families for which a limited number of extracts were prepared but showed promise included the Gentianaceae (*Centantaurium erytheae*, European centaury, maximal QR induction = 2.40-fold, and *Gentiana sceptrum*, king gentian, maximal QR induction = 2.18-fold) and Labiatae (*Scutellana lateriflora*, blue skull cap, max. QR = 2.24-fold, *Ocimum basilicum*, basil, maximal QR induction = 1.67-fold). A methanol extract of the Labiatae plant *Scutellaria baicalensis* has been previously shown to induce QR in Hepa-1c1c7 cells (Park et al. 1998). These authors did not subject the extract to bioassay-guided fractionation, rather they provided evidence that a major flavonoid from this plant, baicalin, possessed weak QR-inducing activity (CD value ~ 150 µM).

The two extracts of *A. latifolia* (yellow-sand verbena, roots or aerial tissues) produced considerable QR induction (maximal QR induction for roots = 2.52-fold, maximal QR induction of aerial parts = 1.76-fold), indicating that active compounds may be distributed throughout the plant.

Table 2-1. Summary of extract sources, results in QR a30nd DPPH assays and traditional use history.

Common name	Species and author	Family	Plant part	Max QR[a]	Conc. at max QR[b]	DPPH IC_{50}[c] (mg/mL)	Tradit-ional use[d]	Blood medicine[e]
wild chicory	*Cichorium intybus* L.	Compositae	roots	2.97	2.0	15.3	yes	no
celeriac	*Apium graveolens* var. *rapaceum*	Umbelliferae	roots	2.67	1.0	107	yes	no
yellow sand-verbena	*Abronia latifolia* Eschsch.	Nyctaginaceae	roots	2.52	0.3	75.2	no	
common tansy	*Tanacetum vulgare* L.	Compositae	flowers	2.51	0.3	2.28	yes	no
devil's club	*Oplopanax horridus* (Sm.) Miq.	Araliaceae	leaves and stems	2.45	2.0	4.08	yes	yes
European centaury	*Centaurium erythaea* Raf.	Gentianaceae	whole plant	2.40	1.2	10.8	no	
American mountain-ash	*Sorbus americana* Marsh.	Rosaceae	fruit	2.32	0.60	13.1	yes	yes
bitter root	*Lewisia rediviva* Pursh	Portulacaceae	roots	2.32	0.30	9.75	yes	yes
osha	*Ligusticum porteri* J.M. Coult. & Rose	Umbelliferae	roots	2.27	0.15	2.06	yes	no
blue skull cap	*Scutellana lateriflora* L.	Labiatae	leaves	2.24	2.0	1.15	yes	no
king gentian	*Gentiana sceptrum* Griseb.	Gentianaceae	leaves and stems	2.18	2.4	5.38	no	
European mountain-ash	*Sorbus aucuparia* L.	Rosaceae	fruit	2.15	0.30	3.73	yes	no
feverfew	*Tanacetum parthenium* (L.) Schultz-Bip.	Compositae	leaves and flowers	2.14	0.25	16.8	yes	no
cretan viper's-bugloss	*Echium creticum* L.	Boraginaceae	aerial parts	2.11	2.4	28.6	no	no
red-osier dogwood	*Cornus alba* L.	Cornaceae	fruit	2.09	2.4	5.3	yes	no
sheep sorrel	*Rumex acetosella* L.	Polygonaceae	leaves	2.08	4.0	42.7	yes	no
big sagebrush	*Artemisia tridentata* Nutt.	Compositae	aerial tissues	2.07	0.30	2.12	yes	no
pestle parsnip	*Lomatium nudicaule* (Pursh) Coult. & Rose	Umbelliferae	leaves	2.06	4.0	2.87	yes	no
osha	*Ligusticum porteri* J.M. Coult. & Rose	Umbelliferae	roots	2.04	0.30	3.86	yes	no
devil's club	*Oplopanax horridus* (Sm.) Miq.	Araliaceae	fruit	2.02	2.4	2.09	yes	yes
boneset	*Eupatorium perfoliatum* L.	Compositae	leaves and flowers	2.01	2.0	4.78	yes	no
bitter blend tea	Various	Various	various	1.99	0.30	6.83		
parsnip	*Pastinaca sativa* L.	Umbelliferae	roots	1.99	4.0	142	yes	no
gotu kola	*Centella asiatic* (L.) Urban	Umbelliferae	stems and leaves	1.92	0.60	2.91	no	
springbank clover	*Trifolium wormskioldii* Lehm.	Leguminosae	whole plant	1.91	1.2	9.22	yes	no
elecampane	*Inula helenium* L.	Compositae	n/a	1.85	0.15	21.8	yes	no
radish	*Raphanus sativus* L.	Cruciferae	root	1.85	4.0	27.2	no	
old man's beard	*Usnea* sp.	Parmeliaceae	lichen	1.84	0.60	115		
Siberian ginseng	*Eleutherococcus senticosus* (Rupr. & Maxim.) Maxim.	Araliaceae	roots	1.84	2.0	126	no	

soapberry	*Shepherdia canadensis* (L.) Nutt	Elaegnaceae	fruit	1.84	2.4	10.9	yes	no
echinacea	*Echinacea* sp.	Compositae	roots	1.81	2.4	5.92		
angled luffa	*Luffa acutangula* (L.) Roxb	Cucurbitaceae	skin of fruit	1.80	2.4	40.5	no	
echinacea	*Echinacea angustifolia* DC	Compositae	roots	1.80	2.4	2.43	yes	yes
stink currant	*Ribes bracteosum* Dougl. ex Hook	Grossulariaceae	fruit	1.78	2.4	10.3	yes	no
tai zi shen	*Pseudostellaria* sp.	Caryophyllaceae	n/a	1.78	2.4	326		
bitter gourd	*Momordica charantia* L.	Cucurbitaceae	fruit	1.77	1.2	117	no	
yellow sand-verbena	*Abronia latifolia* Eschsch.	Nyctaginaceae	aerial parts	1.76	1.2	2.41	no	
burdock	*Arctium minus* (Hill) Bernh.	Compositae	roots/rhizomes	1.75	0.5	4.79	yes	yes
american arnica	*Arnica chamissonis* Less.	Compositae	roots/rhizomes	1.74	2.0	13.9	no	
balsam root	*Balsamorhiza* sp.	Compositae	leaves and roots	1.72	0.6	5.24		
dijon mustard	*Brassica juncea* (L.) Czerniak	Cruciferae	seeds	1.72	0.5	15.9	yes	no
licorice	*Glycyrrhiza glabra* L.	Leguminosae	roots	1.72	4.0	29.1	yes	no
maria's swedish bitters	Various	Various	various	1.72	2.4	24.6		
chai hu	*Buplerum* sp.	Umbelliferae	n/a	1.71	1.2	34.8		
basil	*Ocimum basilicum* L.	Labiatae	leaves	1.67	4.0	23.1	no	
domestic plum	*Prunus* sp.	Rosaceae	fruit, no pit	1.67	2.4	26.2		
French artichoke	*Cynara scolymus* L.	Compositae	flesh	1.66	1.0	10.8	no	
cocoa	*Theobroma cacao* L.	Sterculiaceae	powder	1.65	2.4	4.72	no	
kinnikinick	*Arctostaphylos uva-ursi* (L.) Sprengel	Ericaceae	fruit	1.65	2.4	0.901	yes	yes
milk thistle	*Silybum marianum* (L.) Gaertn.	Compositae	seeds	1.65	4.0	37.8	no	
turmeric	*Curcuma longa* L.	Zingiberaceae	roots	1.64	1.0	2.16	no	
pestle parsnip	*Lomatium nudicaule* (Pursh) Coult. & Rose	Umbelliferae	whole plant	1.63	0.30	149	yes	no
wax currant	*Ribes cereum* Dougl.	Grossulariaceae	fruit	1.61	2.4	2.39	yes	no
licorice	*Glycyrrhiza glabra* L.	Leguminosae	roots	1.60	1.0	3.62	yes	no
cotoneaster	*Cotoneaster* sp.	Rosaceae	fruit	1.57	2.4	3.56		
ribgrass	*Plantago lanceolata* L.	Plantaginaceae	leaves	1.56	4.0	8.04	no	
bindweed	*Convolvulus* sp.	Convolvulaceae	seed	1.54	1.2	12.7		
chili pepper	*Capsicum annuum* L.	Solanaceae	fruit	1.54	2.4	13.2	yes	no
dandelion	*Taraxacum officinale* Weber ex Wigg.	Compositae	leaves	1.54	4.0	17.6	yes	yes
cough root	*Lomatium dissectum* (Nutt.) Mathias & Constance	Umbelliferae	roots	1.53	0.60	4.34	yes	yes
gymnema	*Gymnema sylvestre* (Retz.) Sm.	Asclepiadaceae	leaves	1.53	0.15	6.93	no	
ginseng	*Panax ginseng*	Araliaceae	n/a	1.53	0.60	199	no	
bilberry	*Vaccinium myrtillus* L.	Ericaceae	fruit	1.51	2.4	5.39	yes	no
elderberry	*Sambucus calliicarpa*	Caprifoliaceae	fruit	1.51	2.4	15.4	yes	no
red currant	*Ribes rubrum* L.	Grossulariaceae	fruit	1.51	2.4	38.8	yes	no

qu mai	*Dianthus* sp.	Caryophyllaceae	n/a	1.50	0.60	67.4		
crowberry	*Empetrum nigrum* L.	Empetraceae	fruit	1.49	0.60	1.31	yes	no
parsley	*Lomatium grayi* (Coult. & Rose) Coult. & Rose	Umbelliferae	leaves	1.49	4.0	26.1	no	
cascara	*Rhamnus purshiana* DC	Rhamnaceae	n/a	1.47	1.2	4.73	no	
chokecherry	*Prunus virginiana* L.	Rosaceae	fruit	1.45	2.4	22.1	yes	yes
red flowering currant	*Ribes sanguineum* Pursh	Grossulariaceae	fruit	1.44	2.4	0.73	no	
western snowberry	*Symphoricarpos occidentalis* Hook.	Caprifoliaceae	fruit	1.44	2.4	0.71	yes	no
wasabi	*Wasabia wasabi* (Siebold) Makino	Cruciferae	rhizomes	1.43	4.0	143	no	
wild sarsparilla	*Aralia nudicaulis* L.	Araliaceae	roots/rhizomes	1.43	0.50	118	yes	yes
nasturtium	*Tropaeolum* sp.	Tropaeolaceae	flowers	1.41	4.0	1.33		
creeping juniper	*Juniperus horizontalis* Moench	Cupressaceae	fruit	1.40	0.075	1.51	yes	no
entire-leaved gumweed	*Grindelia integrifolia* DC.	Compositae	flowers	1.39	1.2	11.9	no	
high-bush cranberry	*Viburnum* sp.	Caprifoliaceae	fruit	1.38	1.2	0.81		
horny goat weed	*Epimedium sagittatum* (Sieb. & Zucc.) Maxim.	Berberidaceae	leaves	1.38	0.30	0.811	no	
black hawthorn	*Crataegus douglasii* Lindley	Rosaceae	fruit	1.37	2.4	1.76	yes	no
jie geng	*Platycodon* sp.	Campanulaceae	n/a	1.37	0.075	71.6		
cherry	*Prunus* sp.	Rosaceae	fruit	1.36	2.4	65.1		
chokecherry	*Prunus virginiana* L.	Rosaceae	fruit	1.36	2.4	17.5	yes	yes
san qi	*Panax pseudoginseng*	Araliaceae	n/a	1.35	0.30	313	no	
wolf willow	*Elaegnus commutata* Bernh. ex Rydb.	Elaegnaceae	fruit	1.34	1.2	3.22	yes	no
ribwort	*Plantago lanceolata* L.	Plantaginaceae	leaves	1.33	2.4	2.61	no	
broccoli	*Brassica oleracea* L.	Cruciferae	sprouts	1.32	4.0	6.48	yes	no
grape	*Vitis vinifera* L.	Vitaceae	skin of fruit	1.31	2.4	3.11	no	
bacopa	*Bacopa* sp.	Scrophulariaceae	whole plant	1.30	0.15	0.11		
European bittersweet	*Solanum dulcamara* L.	Solanaceae	fruit	1.30	2.4	9.38	yes	no
bloodroot	*Sanguinaria canadensis* L.	Papaveraceae	roots	1.29	0.0094	8.93	yes	yes
lettuce	*Lactuca sativa* L.	Compositae	leaves	1.28	4.0	56.8	yes	no
hawthorn	*Crataegus* sp.	Rosaceae	fruit	1.27	2.4	4.74		
twisted stalk	*Streptopus* sp.	Liliaceae	fruit	1.27	2.4	117		
concord grape	*Vitis labrusca* L.	Vitaceae	fruit	1.25	2.4	76.3	yes	yes
red elderberry	*Sambucus racemosa* L.	Caprifoliaceae	fruit	1.25	2.4	13.9	yes	no
black gooseberry	*Ribes lacustre* (Pers.) Poir.	Grossulariaceae	fruit	1.24	2.4	3.65	yes	no
bunchberry	*Cornus canadensis* L.	Cornaceae	fruit	1.24	1.2	4.44	yes	no
nasturtium	*Tropaeolum* sp.	Tropaeolaceae	flowers	1.23	2.4	3.06		
carrot	*Daucus carota* L.	Umbelliferae	roots	1.22	4.0	19.6	yes	yes

false lily-of-the-valley	*Maianthemum dilatatum* (A. Wood) Nels. & J.F. Macbr.	Liliaceae	fruit	1.22	0.30	23.9	yes	yes
pokeweed	*Phytolacca americana* L.	Phytolaccaceae	fruit	1.22	0.60	1.43	yes	yes
mangosteen	*Garcinia mangostana* L.	Guttiferae	husks	1.20	0.075	0.861	no	
valerian	*Valeriana officinalis* L.	Valerianaceae	roots	1.18	0.25	18.6	no	
common snowberry	*Symphoricarpos albus* (L.) S.F. Blake	Caprifoliaceae	fruit	1.17	2.4	1.28	yes	no
himalaya blackberry	*Rubus discolor* Weihe & Nees	Rosaceae	fruit	1.17	0.15	1.56	no	
pispsissewa	*Chimaphila umbellata* (L.) W. Barton (Euras.)	Ericaceae	leaves	1.16	1.0	0.291	yes	yes
red huckleberry	*Vaccinium parvifolium* Sm.	Ericaceae	fruit	1.15	2.4	27.9	yes	no
bitter gourd	*Momordica charantia* L.	Cucurbitaceae	fruit	1.14	1.2	48.1	no	
wang bu liu xing	*Vaccaria hispanica* (Miller) Rauschert	Caryophyllaceae	seed	1.14	0.075	221	no	
goji	*Lycium* sp.	Solanaceae	fruit	1.12	2.4	14.8		
yellow gentian	*Gentiana lutea* L.	Gentianaceae	roots	1.12	0.50	37.2	no	
broccoli	*Brassica oleracea* L.	Cruciferae	crowns	1.10	10	15.9	yes	no
comfrey	*Symphytum offincinale* L.	Boraginaceae	roots	1.09	2.4	20.5	yes	no
Oregon grape	*Mahonia aquifolium* (Pursh) Nutt.	Berberidaceae	fruit	1.08	0.30	9.15	yes	yes
bitter cherry	*Prunus* sp.	Rosaceae	fruit	1.07	0.15	1.51		
passion flower	*Passiflora* sp.	Passifloraceae	flowers and leaves	1.06	2.4	5.34		
astragalus	*Astragalus* sp.	Leguminosae	roots	1.04	0.60	107		
nootka rose	*Rosa nutkana* Presl	Rosaceae	hip, no seeds	1.02	1.2	1.33	yes	no
black salsify	*Scorzonera hispanica*	Compositae	roots	1.01	0.019	8.79	no	
codonopsis	*Codonopsis* sp.	Campanulaceae	roots	1.00	0.60	105		
carolina rose	*Rosa carolina* L.	Rosaceae	hip	0.99	0.60	0.52	yes	no
cranberry	*Vaccinium oxycoccus* L.	Ericaceae	fruit	0.99	2.4	120	yes	no
irish moss	*Chondrus crispus* Stackhouse	Gigartinaceae	leaves	0.99	4.0	>120	no	
Oregon grape	*Mahonia aquifolium* (Pursh) Nutt.	Berberidaceae	bark	0.98	0.075	11.7	yes	yes
hop	*Humulus lupulus* L.	Cannabaceae	hop cones	0.97	0.15	1.06	yes	no
rhubarb	*Rheum rhabarbarum* L.	Polygonaceae	stems	0.97	0.50	5.87	no	
lady's leek	*Allium cernuum* Roth	Liliaceae	bulbs	0.95	0.50	85.1	yes	no
potato	*Solanum tuberosum* L.	Solanaceae	root, no skin	0.94	2.4	236	yes	no
wild sarsparilla	*Aralia nudicaulis* L.	Araliaceae	leaves	0.93	0.25	6.58	yes	yes
cranberry	*Vaccinium oxycoccus* L.	Ericaceae	fruit	0.92	0.075	8.15	yes	no
genistein soy complex	*Glycine max* (L.) Merr	Leguminosae	n/a	0.92	1.2	119	no	
iceberg lettuce	*Lactuca sativa* L.	Compositae	leaves	0.91	0.60	39.6	yes	no
red delicious apple	*Malus* sp.	Rosaceae	skin of fruit	0.90	1.2	5.74		
poracher root	*Pteridium aquilinium* (L.) Kuhn	Dennstaedtiaceae	roots	0.88	0.075	2.64	yes	yes

trailing blackberry	*Rubus ursinus* Cham. & Schlecht.	Rosaceae	fruit	0.88	0.15	0.88	yes	no
yellow dock	*Rumex crispus*L.	Polygonaceae	roots	0.88	0.60	1.24	yes	yes
vaccaria	*Vaccaria saponaria*	Caryophyllaceae	seed	0.86	0.15	204	no	
common wild rose	*Rosa woodsii* Lindl.	Rosaceae	hip	0.85	0.075	0.381	yes	yes
lingonberry	*Vaccinium vitis-idaea* L.	Ericaceae	fruit	0.84	0.075	5.66	no	
green tea	*Camellia sinesis* (L.) Kuntze	Theaceae	leaves	0.83	0.30	0.191	no	
high-bush cranberry	*Viburnum* sp.	Caprifoliaceae	fruit	0.83	0.075	1.92		
domestic blueberry	*Vaccinium corymbosum* L.	Ericaceae	fruit	0.82	2.4	5.58	yes	no
labrador tea	*Ledum groenlandicum* Oeder	Ericaceae	leaves	0.81	0.25	1.51	yes	yes
pin cherry	*Prunus pensylvanica* L. f.	Rosaceae	fruit	0.81	2.4	10.9	yes	yes
potato	*Solanum tuberosum* L.	Solanaceae	skin of root	0.79	0.30	34.9	yes	no
salal	*Gaultheria shallon* Pursh	Ericaceae	fruit	0.79	0.60	0.651	yes	no
calendula	*Calendula* sp.	Compositae	flowers	0.78	0.30	47.4		
salmon berry	*Rubus spectabilis* Pursh	Rosaceae	fruit	0.78	0.60	1.55	yes	no
blueberry	*Vaccinium* sp.	Ericaceae	fruit	0.77	0.15	2.65		
grape	*Vitis vinifera* L.	Vitaceae	fruit	0.77	0.60	4.83	no	
goldenrod	*Solidago virgaurea*	Compositae	n/a	0.74	0.075	5.65	yes	no
blueberry	*Vaccinium* sp.	Ericaceae	fruit	0.73	0.075	2.07		
yuan zhi	*Polygala* sp.	Polygalaceae	n/a	0.69	0.075	11.6		
arjuna	*Terminalia arjuna* (DC) Wight & Arn.	Combretaceae	bark	0.68	0.15	0.21	no	
saskatoon berry	*Amelanchier alnifolia* Nutt.	Rosaceae	fruit	0.67	2.4	4.12	yes	yes
blueberry	*Vaccinium* sp.	Ericaceae	fruit	0.65	0.60	2.21		
valley seed	*Bassia scoparia* (L.) Voss	Chenopodiaceae	seed	0.51	0.075	4.95	no	
wolf willow	*Elaegnus commutata* Bernh. ex Rydb.	Elaegnaceae	leaves	0.34	0.15	0.121	yes	no
antelope-brush	*Purshia tridentata* (Pursh) DC.	Rosaceae	aerial tissues	toxic	n/d	0.361	yes	no
ashwagandha	*Withania somnifera* (L.) Dunal	Solanaceae	roots	toxic	n/d	15.9	no	
elecampane	*Inula helenium* L.	Compositae	roots	toxic	n/d	31.1	yes	no
raspberry	*Rubus idaeus* L.	Rosaceae	fruit	n/t	n/t	4.04	yes	yes
thimbleberry	*Rubus parviflorus* Nutt.	Rosaceae	fruit	n/t	n/t	1.49	yes	

[a]indicates the highest QR induction value for the extract.
[b]indicates the concentration (mg of dried material used for extraction per mL of medium) at which Max QR was achieved.
[c] indicates the concentration requires to neutralize 50% of a 100 µM DPPH solution
[d]indicates whether traditional uses are reported for the species in Moerman (1998).
[e] indicates whether traditional use included the indication of a blood medicine.
n/a indicates that the plant part for source material was not provided.
n/d indicates that the value could not be determined.
n/t indicates that the plant was not included in the assay.

For extracts prepared from distinct parts of the plant, extracts prepared from roots or rhizomes (# = 36, average maximal QR induction of 1.61) tended to be more potent than from aerial parts (leaves, stems, or flowers, # = 35, average maximal QR induction of 1.48) or fruit/seeds (# = 71, average maximal QR induction of 1.27). As fruit often serve as a means of attracting seed dispersers fewer noxious compounds are expected in fruit compared to vegetative tissues.

Certain extracts, such as *Elaegnus commutata* (wolf-willow, leaves, maximal QR induction = 0.34-fold) appeared to decrease the activity of QR. Although it is out of the scope of this project, these extracts could potentially provide leads for Keap1-activating/Nrf2-suppressing compounds. Also, if shown to be selective for cancerous cells, the highly-toxic nature of extracts such as *Inula helenium* (elecampane), *Purshia tridentata* (antelope-brush), *Withania somnifera* (ashwaganda) or *Sanguinaria canadensis* (blood root) could provide anti-cancer leads.

From a review of the literature associated with many of the extracts with high QR activation it was noted that traditional use of 'blood medicine', medicines believed to purify or influence the blood, appeared frequently. Could this historical use be associated with the presence of Nrf2 activators and provide a basis for understanding their traditional use? To answer this question I investigated the traditional use of all screened extracts.

Of the 162 plant extracts screened for QR activation, 133 were prepared from plants identified to the species level and were considered in the analysis of traditional uses. Of these, 133 plants, 88 had documented traditional North American medicinal uses (Moerman 1998). Twenty-eight of these had an indication of 'blood medicine'. I considered substantial QR-inducing activity as greater than 1.5-fold induction. Thirty-six of the 88 plants (40.9 %) with use as traditional medicines had substantial QR-inducing activity. Nine of the 28 plants (32.1%) with use as 'blood medicine' had substantial QR-inducing activity. As this proportion is lower that that occurring for any traditional use, 'blood medicine' does not appear to be a reliable indicator of QR induction.

2.3.4. Potential improvements to the QR screen

Although this screen was highly successful at identifying plant extracts with QR-inducing activity several improvements are possible.

Basing the test concentrations on weight of the extract rather than the weight of dried plant material would provide a better comparator for intrastudy results and facilitate comparison with studies from other laboratories. I would also reduce the uppermost concentration tested to ensure complete dissolution and limit the viscosity of the solution.

The 316-fold range covered using six 3.16-fold dilutions was not wide enough to consistently capture non-toxic concentrations and necessitated additional testing. Using a slightly higher dilution ratio such as 5-fold would increase the range covered to 3125-fold to avoid repeat testing.

To avoid edge effects the outer perimeter of wells on each 96-well plate were plated but not used for the QR bioassay (Lundholt et al. 2003). I would consider testing for edge effects in this system if undertaking another large screen as the savings gained by using these wells would be substantial.

False-positives could result via gas-transfer of volatile compounds between wells. Volatile inducers such as allyl-isothiocyanate can cause induction in adjacent wells and even non-volatile inducers such as dimethyl-fumarate have been reported to cause induction in adjacent wells (Fahey et al. 2004). As I tested duplicates of each concentration beside each other, I would expect a difference between the two duplicates in cases where volatile transfer was a concern. I did not observe such a pattern.

False-negatives may have resulted due to instability or insolubility of active compounds in the extraction application solvent (DMSO). Adding surfactants or additional amphipathic molecules such as polyethylene glycol 400 may prevent such false-negatives but may also cause complications such as increased toxicity.

The extraction procedure may have caused false-negatives by preventing interactions between compartmentalized precursor compounds and enzyme(s) required for their activation. This may explain the lack of QR induction by broccoli, a well-known source of the Nrf2 activator sulforaphane. In nature, insect damage causes the mixing of cells containing glucoraphanin and myrosinase which results in the production of sulforaphane. Although, homogenizing material prior to drying may help with this type of scenario, it may cause unwanted degradation of other compounds.

Since each extract contained a cocktail of phytochemicals, it is possible that high toxicity caused by one group of compounds may have masked the presence of QR inducers. Dividing the extract prior to screening could reduce masking if toxic compounds are separated from the Nrf2 activators.

2.3.5. Screening extracts for direct antioxidant activity using the DPPH antioxidant assay

The DPPH IC_{50} value is reported for each extract in Table 2-1. The most potent antioxidant extracts are summarized in Table 2-2. Green tea and rose hips are known to have high antioxidant activity and were among the top eight extracts tested (Valcic et al. 1999; Gao et al. 2000).

Although antioxidants can vary in their reactivity with different radical species, the commonly used antioxidant assays for examining plant tissues, DPPH, ABTS, and ferric reducing antioxidant capacity (FRAP) consistently give similar relative results or ranking of plant extracts (Ozgen et al. 2006). Therefore I would expect a very similar potency ranking of extracts if a different antioxidant assay was conducted.

The DPPH assay IC_{50} values of each extract are plotted against their corresponding maximal QR induction values in Figure 2-5. I hypothesized that there would not be a correlation between direct antioxidant activity and the QR bioassay. There was no significant correlation ($y = 0.0002x$, $R^2 = 0.0006$, $p = 0.75$) therefore the null hypothesis was not rejected. Direct antioxidant activity should not be used as a predictor of QR-bioassay activity or indirect antioxidant activity.

2.4. Conclusions

A wide range of activity was noted in both the QR and DPPH assays, with the top QR-activating extracts providing leads for bioassay-guided fractionation. Neither traditional use as 'blood medicines' nor direct antioxidant activity were found to be useful predictors of QR-inducing activity.

Table 2-2. Extracts with the greatest antioxidant capacity.

Common name	Species and author	DPPH IC_{50}[a] (mg/mL)	Max QR[b]
bacopa	*Bacopa* sp.	0.110	1.30
wolf willow	*Elaegnus commutata* Bernh. ex Rydb.	0.121	0.34
green tea	*Camellia sinesis* (L.) Kuntze	0.191	0.83
arjuna	*Terminalia arjuna* (DC) Wight & Arn.	0.210	0.68
pipsissewa	*Chimaphila umbellata* (L.) W. Barton (Euras.)	0.291	1.16
antelope-brush	*Purshia tridentata* (Pursh) DC.	0.361	toxic
common wild rose	*Rosa woodsii* Lindl.	0.381	0.85
carolina rose	*Rosa carolina* L.	0.520	0.99

[a] indicates the concentration required to neutralize 50% of a 100 µM DPPH solution
[b]indicates the highest QR induction value for the extract.

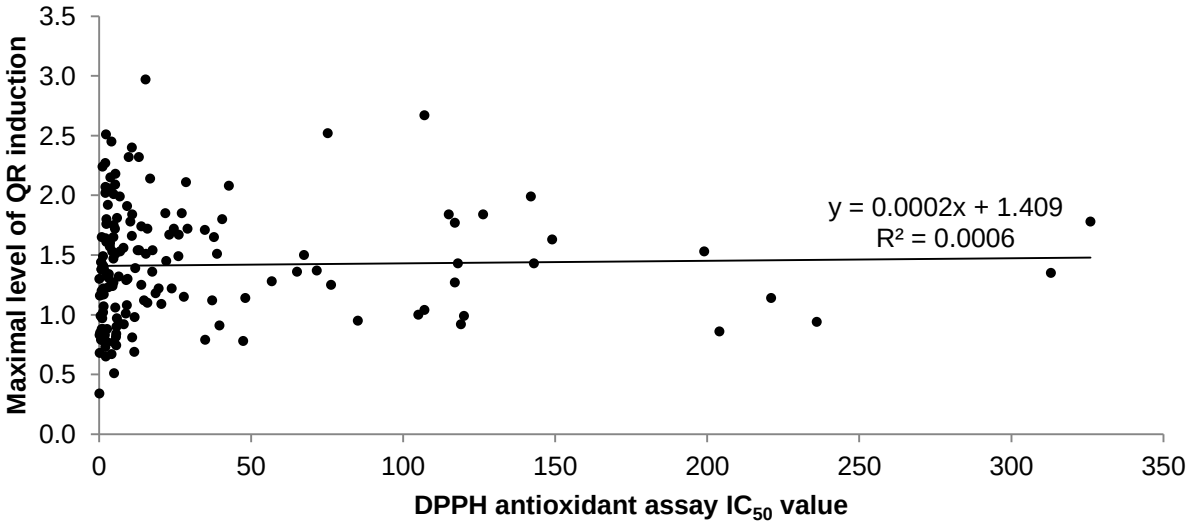

Figure 2-5. Comparison of maximal QR induction with DPPH assay IC_{50} values.

CHAPTER 3

ISOLATION AND IDENTIFICATION OF PUTATIVE NRF2 ACTIVATORS IN PLANT EXTRACTS

3.1. Introduction

Of the extracts identified as QR-inducing, the 21 extracts capable of doubling the activity of QR were considered the strongest leads for isolating Nrf2 activators. Five extracts (*Ligusticum porteri, Oplopanax horridus, Aralia nudicaulis, Abronia latifolia, Lewisia rediviva*) were selected for fractionation based on the amplitude of induction, concentration required for activity, use history, novelty of the plant and the fact that QR induction had not been shown for these plants at the time of initial investigation. Cannabinoids were also isolated from *Cannabis sativa* in order to investigate the roles of QR and Nrf2 in the reported protective effects of these compounds. Due to a lack of positive results, the fractionation of *L. rediviva* is not reported here.

3.1.1. *Ligusticum porteri*

Native to high altitude environments in western North America, *L. porteri* Coult. & Rose (Apiaceae) is a perennial forb with pinnately compound leaves and small white flowers (Terrell et al. 2009). Common names for *L. porteri* include ‘osha’ and ‘bear-root’. *L. porteri* roots have a long history of use by Native Americans, particularly the Tarahumara, for treating a wide variety of ailments including respiratory infections and inflammation (Appelt 1985; Linares et al. 1987). For the Tarahumara, the plant is closely associated with bears which reportedly dig up the root and rub it on their fur (Terrell et al. 2009).

Two methanolic extracts of *L. porteri* roots, prepared from different sources, were tested in preliminary screening. Although the supplier of the dried *L. porteri* attests to the authenticity of the material, I was not able to obtain a voucher specimen for this plant. Both extracts displayed high values for maximal induction of QR (2.27- and 2.04-fold). Members of the Apiaceae plant family produce several classes of bioactive phytochemicals including polyacetylenes, coumarins and phthalides and include several food plants such as carrots, celery and parsnip (Murphy et al. 2004; Zidorn et al. 2005; Beck et al. 2007). There were no reports of QR-inducing activity of the above classes of compounds at the time of initial investigation.

3.1.2. *Oplopanax horridus* and *Aralia nudicaulis* (Araliaceae)

O. horridus (Sm.) Torr. & Gray ex Miq. (devil's club, Araliaceae) is a thorny shrub abundant in riparian habitats ranging from Alaska through British Columbia to the north-western United States (NatureServeExplorer 2010). Throughout its range indigenous people consider it one of the most important medicinal plants (Smith 1983). Infusions of *O. horridus* bark have a history of use as a tonic, blood medicine, emetic, and purgative as well as a treatment of diabetes and tuberculosis (Smith 1983).

A. nudicaulis L. (wild sarsparilla, Araliaceae) is an understory shrub abundant throughout the North American boreal forest (Johnson et al. 1995). *A. nudicaulis* forms large networks of underground rhizomes that project single compound leaves at regular intervals. Traditional uses for the rhizome of this plant include tonic, blood medicine, dermatological aid, and cough medicine (Moerman 1998).

Like other members of the Araliaceae, *O. horridus* and *A. nudicaulis* are known to produce fatty acid-derived polyacetylenes (Hansen et al. 1986) and triterpene saponins (Ma et al. 1999). During the course of this work, Lee *et al.* (2009) reported that the QR inducing activity of a *Panax ginseng* extract was due to the polyacetylene, panaxytriol, and not saponins (ginsenosides) (Lee et al. 2009).

O. horridus was selected for fractionation based on positive results in the QR bioassay (2.45 and 2.02-fold maximal induction for extracts of stems/leaves and fruit, respectively). I chose to focus on the inner bark as this tissue was used widely for traditional medicine (Smith 1983) and was reported to be phytochemically rich (Kobaisy et al. 1997). In response to the success achieved with *O. horridus*, the rhizomes of *A. nudicaulis* (maximal QR induction of 1.43-fold in screening) were investigated to expand the panel of polyacetylenes and identify structure-activity relationships.

3.1.3. *Abronia latifolia*

A. latifolia Eschsch. (Nyctaginaceae), commonly called 'yellow sand-verbena', is a small prostrate perennial herb native to sandy locations along the Pacific coast from Vancouver Island, British Columbia south to San Miguel Island, California (Tillett 1967). The yellow color of *A. latifolia* flowers is unique amongst the 20 related *Abronia* species (Galloway 1975) and are visited by the endangered Myrtle's silverspot butterfly (*Speyeria zerene myrtleae*) (Launer et al. 1992). *A.*

latifolia produces long edible taproots (Hedrick 1972). Although to my knowledge no medicinal uses have been reported for this plant, the roots provided a substantial food source for several indigenous groups including the Chinook (Hedrick 1972), Klallam (Gunther 1973) and Makah (Gunther 1973). The taste of *A. latifolia* roots is said to be similar to sugar beets (Gunther 1973).

The only published study of the phytochemistry of *A. latifolia* focused on the flavonoid constituents of the aerial tissues and identified several known flavones and flavonols: hispidulin, luteolin, nepetin, quercetin, and axillarin, chrysosplenol D, and one novel C-methyl isoflavone, abronisoflavone (Wollenweber et al. 1993).

Methanolic extracts of roots or aerial tissues of *A. latifolia* showed a maximal QR induction of 2.52-fold and 1.76-fold in the preliminary screen, respectively. Due to the British Columbia government considering this plant as at-risk, I choose to cultivate the plant from wild seed rather than collect a large amount of wild plant material for extraction and fractionation.

3.1.4. *Cannabis sativa*

C. sativa L. (Cannabaceae) is a dioecious herb that has long been used for its fibre, seed, oil and psychotropic effects (Li 1973). Although indigenous to central and southern Asia, *C. sativa* is now cultivated around the world. Cannabinoids, such as cannabidiolic acid (CBDA) and Δ^9-tetrahydrocannabinolic acid (THCA) are produced in glandular trichomes which cover the female flowers.

Upon heating, CBDA and THCA decarboxylate to cannabidiol (CBD) and Δ^9-tetrahydrocannabinol (THC), respectively. THC, an agonist at mammalian cannabinoid receptors, is the primary component responsible for the psychotropic effects of cannabis (Pertwee 2008). CBD does not activate cannabinoid receptors although it may modulate the effects of THC by acting as an antagonist at these receptors (Mechoulam et al. 2007). CBD has garnered attention for its neuroprotective effects in animal models of ischemia and Alzheimer's disease (Hampson et al. 2000; Braida et al. 2003; Iuvone et al. 2004). However the mechanism(s) conferring this protection are not understood.

A methanolic extract of *C. sativa* was a weak inducer of QR (concentration required to increase activity of QR by 50% (C_{50} value) ~ 15 µg/mL). Despite the weak activity, I decided to investigate whether cannabinoids where responsible for QR activation, as QR (and Nrf2)

activation by cannabinoids could provide a basis for understanding the neuroprotective effects of cannabinoids in animal models.

3.1.5. Bioassay-guided fractionation techniques

Identifying active components by fractionation involves dividing the mixture of interest, assaying its parts for activity and repeating this process on the most active fraction(s) until pure constituents are isolated. A variety of chemical separation methods (solvent-solvent partitioning, chromatography, crystallization, precipitation) can be employed.

In practice, solvent-solvent partitioning is often selected for the initial separation as it quickly separates large quantities of material, is easily scaled up and is compatible with most compounds. Solvent-solvent partitioning separates compounds on the basis of differential solubility in two or more immiscible solvents. A solvent-solvent partitioning scheme that separates compounds into low polarity (high solubility in hexane), intermediate polarity (high solubility in chloroform) and high polarity (high solubility in water) is given in section 3.3.1.2. For the same reasons discussed in Chapter 2 regarding extraction solvent selection, the chloroform (intermediate polarity) fraction is typically enriched in bioactive compounds.

Chromatography involves separating compounds in a solvent passing over a stationary phase. Differential interactions with the stationary phase allow temporal separation of different compounds. Chromatography can easily separate a complex mixture into a large number of discrete fractions. For initial separations with crude fractions, liquid chromatography using low-pressure systems with self-packed columns or SPE (solid phase extraction) columns are time and solvent-efficient methods. The resolution of high performance liquid chromatography (HPLC) is advantageous during the final purification of individual compounds.

3.1.6. Bioassays used to guide isolation of Nrf2 activators

Two bioassays were used to guide the fractionation process: 1) the QR bioassay and 2) thiol-reactivity using mass spectrometric detection of glutathione-reactive compounds. QR bioassay-guided fractionation relies on the QR bioassay as described in Chapter 2. Although QR bioassay-guided fractionation is a reliable and proven method for identifying Nrf2 activators, the process is laborious. Since the thiol-reactive cysteines of Keap1 are thought to be the sensors regulating the abundance and transcriptional activity of Nrf2, screening for thiol-reactive

electrophiles is an alternative approach to identifying Nrf2 activators (Liu et al. 2005). Glutathione is a useful model of Keap1 thiols and is readily available, inexpensive and small (Liu et al. 2005). Compounds that react with glutathione *in vitro* can be identified by tandem mass spectrometry (MS) by looking for precursors of characteristic glutathione fragmentation products, such as precursors of mass-to-charge ratios (*m/z*) 130 or 272 under positive or negative ionization conditions, respectively (Dieckhaus et al. 2005). Not only is this approach much quicker than the QR bioassay (4 h vs. 4 days), but it also provides information regarding the structure of the reactive compound (*m/z* and UV characteristics) that can be used to guide isolation.

3.1.7. Identification of isolated QR inducers

An array of experiments including MS, ultraviolet-visible (UV-VIS) spectroscopy, infrared spectroscopy, nuclear magnetic resonance spectroscopy (NMR) as well as chromatographic retention time provide complimentary structural information of an unknown compound. In order to unequivocally determine the structure of an isolated compound it is necessary to either solve the structure using NMR spectroscopy or X-ray crystallography or show that it is identical to a standard (typically using HPLC retention time and UV-VIS absorbance or mass spectrum). As I am interested in novel compounds for which standards do not exist I have routinely completed NMR analyses of isolated compounds.

3.2. Materials and methods

3.2.1. General experimental procedures

Flash chromatography was conducted on a Sepacore system (Buchi) equipped with a C-630 UV monitor and a C-660 fraction collector. Unless otherwise specified, preparative HPLC was conducted on a preparative 1100 system (Agilent) equipped with a fraction collector and a Gemini-NX C_{18} column (Phenomenex, 250 × 21.2 mm, 5 µm). Reverse phase analytical HPLC was conducted on an Alliance system (Waters). Normal phase analytical HPLC was conducted on an 1100 system (Agilent). Volatile solvents were removed under vacuum using a rotavap with heating to 28°C. Unless otherwise indicated, NMR experiments were performed in deuterated chloroform ($CDCl_3$) using an AV500 spectrometer (Bruker). Optical rotations were determined on a 341 polarimeter (Perkin-Elmer). High-resolution mass spectra were acquired on either an API

Qstar XL (Applied Biosystems), Q-Tof Ultima Global (Waters) or 4800 matrix-assisted laser desorption ionization (MALDI) tandem time of flight (TOF/TOF) mass spectrometer (Applied Biosystems). Cell culture reagents were obtained from Invitrogen. Unless otherwise specified, chemicals were obtained from Sigma-Aldrich.

3.2.2. QR and cell viability assays

Cell culture and QR bioassays were conducted as described in Chapter 2 with the exception of the incorporation of the Calcein AM (Invitrogen) cell viability assay into the QR bioassay workflow in the place of the rinse step. Each well was incubated in the dark with 200 µL of 1.0 µM Calcein AM in D-PBS at 37°C for 20 min and cellular viability was determined by measuring fluorescence (485 nm excitation and 535 nm emission). DMSO treated controls were considered to be at 100% viability. A reference for 0% viability was determined by incubating two DMSO treated control wells with 70% ethanol for 20 min. The Calcein AM cell viability assay did not interfere with the subsequent QR assay (data not shown).

3.2.3. Detection of glutathione adducts by tandem MS

Detection of glutathione adducts by tandem MS was based on previously published procedures (Johnson et al. 2001; Liu et al. 2005). A methanolic extract or solution was added to an aqueous solution containing 1 mM reduced glutathione and 25 mM Tris-Cl, pH 8.0 to give a final concentration of 200 µM or 0.5 mg/mL of the small molecule or extract and 10% or less methanol (v/v). The solution was incubated at 37ºC for 90 min and analyzed on a 1100 HPLC (Agilent) interfaced to a Quattro LC (Micromass) quadrupole tandem mass spectrometer using an Xterra RP_{18} column (Waters, 2.1 × 100 mm, 3.5 µM), a flow rate of 0.2 mL/min and a gradient of 5% to 100% organic solvent/water with 0.1% formic acid over 25 min. Acetonitrile and methanol were used as the organic solvent during analyses in positive and negative mode, respectively. Mass spectrometer source settings follow: cone voltage 20 V, radiofrequency (RF) lens 0.5, extractor 2, capillary 3.00, source block 120ºC, desolvation temp 350ºC.

3.2.4. *L. porteri*

3.2.4.1. Thiol-reactivity based separation

Thirty-grams of dried *L. porteri* roots (Richter's Herbs) were extracted with 250 mL of methanol. The extract was concentrated under reduced pressure and water was added to 10% (v/v).

After defatting with hexane, the methanol-water extract was partitioned with chloroform and the chloroform fraction washed with aqueous 1% NaCl to remove tannins (Figure 3-1, found in section 3.3.1.2, pg. 55). The chloroform partition (2.4 g) was separated into 20 fractions by open column chromatography (silica gel, 30 g, 200-425 mesh) using a gradient of 5-100% acetone in hexane. Glutathione-based thiol trapping indicated that a major thiol-reactive compound was present in fractions 13 and 14. Coniferyl ferulate (**1**) was purified from these fractions by preparative reverse phase thin layer chromatography (TLC) (C_{18}, 20 × 20 cm, 500 µm) using a 1 : 1 mixture of chloroform : acetone, and further purified by semi-preparative HPLC using a gradient of 60-100 % methanol/water and a Sunfire Prep C_{18} column (Waters, 10 × 250 mm, 5 µm) on a modular HPLC (Waters) with manual collection.

coniferyl ferulate (1), UV (acetonitrile/H_2O) $\lambda_{max.}$ (nm) 219, 270, 300sh, 320; ^{1}H, ^{13}C and HMBC NMR data in agreement with previous analysis (Lu et al. 2004). HRESIMS *m/z* 379.1196 $[M + Na]^{+}$ (calculated for $C_{20}H_{20}O_6Na$, 379.1210).

3.2.4.2. QR bioassay-guided separation

Dried *L. porteri* roots (104 g) were extracted twice with 500 mL of methanol and partitioned according to the scheme given in Figure 3-1 (section 3.3.1.2, pg. 55). The chloroform fraction (2.7 g) was separated into six fractions by flash chromatography over a silica gel (200-425 mesh) column (26 × 460 mm) using a gradient of 5-100% acetone in hexane. Fraction 2 was most active in the QR bioassay and was separated by flash chromatography using a reversed-phase cartridge (Buchi, RP_{18}, 40-63 µm, 12 × 75 mm) and a gradient of 5-100% acetonitrile in water. Active subfraction F2-3 (110 mg) was purified by semi-preparative HPLC (Waters Sunfire 10 × 250 mm C_{18} column, isocratic, 70% methanol/water) and yielded (*Z*)-ligustilide as the major component. (*Z*)-Ligustilide (**2**) was identified based on UV and ^{1}H and ^{13}C NMR experiments as well as comparison with an authentic standard (Chromadex). *trans*-6,7-Dihydroxyligustilide (**3**) was purified from an aqueous solution of (*Z*)-ligustilide, that had been incubated at 60°C for 18 h, by semi-preparative HPLC (isocratic 70% methanol/water) and identified by comparison of UV, ^{1}H NMR and mass spectrometric data with published values (Pushan et al. 1984; Li et al. 2003). The presence of the two enantiomers **3a** and **3b** in the *trans*-dihydroxyligustilide (**3**) isolate was confirmed by chiral analytical HPLC (Regis Technologies 4.6 × 250 mm (R,R)-Whelk-O1 column, isocratic 95% hexane/5% isopropanol/0.1% acetic acid).

(*Z*)-ligustilide (2), UV (acetonitrile/H_2O) $\lambda_{max.}$ (nm) 280, 327 in agreement with previous report (Li et al. 2003); ^1H, and ^{13}C NMR data in agreement with previous analysis (Gijbels et al. 1982; Pushan et al. 1984). ESIMS+ *m/z* 191 $[M + H]^+$ (calculated for $C_{12}H_{15}O_2$, 191).

***trans*-dihydroxyligustilide (3)**, UV (Acetonitrile/H_2O) $\lambda_{max.}$ (nm) 280 in agreement with previous report (Li et al. 2003); ^1H, and ^{13}C and HBMC NMR data in agreement with previous analysis (Pushan et al. 1984). ESIMS+ *m/z* 225 $[M + H]^+$ (calculated for $C_{12}H_{17}O_4$, 225).

3.2.5. *O. horridus*

Flash chromatography was performed with a column (460 × 26 mm) packed with silica gel (EMD, 230-400 mesh). Semi-preparative HPLC separations were performed on a 1100 system using an Xterra C_{18} column (Waters, 100 × 7.8 mm, 5 µm) for isolation of falcarindiol from *P. sativa* or a Sunfire C_{18} column (Waters, 250 × 10 mm, 5 µm) for all other separations. Preparative chiral HPLC was conducted using a Chiracel OD column (Daicel, 500 × 50 mm, 20 µm). Analytical TLC was performed using silica gel and developed by hexane: ethyl acetate, 14:1. (*R*)-sulforaphane was purchased from LKT laboratories. Analytical chiral HPLC separations were performed on an 1100 system using a Lux Cellulose-1column (Phenomenex, 250 × 4.6 mm, 5 µm). Fetal bovine serum was obtained from Invitrogen or PAA Laboratories.

O. horridus stems were collected in October 2008 near Pemberton Valley, BC, Canada. Taxonomic identification was done by Nick Page (Rainforest Applied Ecology, Vancouver, Canada). This plant is abundant in the area of harvest and not considered at risk (NatureServeExplorer 2010). A voucher specimen is deposited in the Herbarium of the University of Saskatchewan (accession #180047). Parsnip roots (*P. sativa*) were purchased from a supermarket in Saskatoon, SK, Canada.

Dried *O. horridus* inner bark (296 g) was exhaustively extracted with methanol, and subjected to solvent-solvent partitioning as detailed in Figure 3-1 (section 3.3.2, pg. 57). The resulting residue (9 g) was separated by reverse phase flash chromatography (C_{18}, 230-400 mesh, EMD) using a gradient of 40-100% acetonitrile in water. Preliminary fractions were combined on the basis of analytical TLC to give eleven fractions (I-XI). Pure compounds were isolated from these fractions by semi-preparative HPLC using water/acetonitrile in the following compositions (% acetonitrile): compounds **4**, **5**, **6**, **7**, gradient (42.5-70%); compounds **8** and **9**, isocratic (62.5%); compound **10**, gradient (62.5-79%); compounds **11** and **12**, isocratic (82.5%). Additional

purification of compounds **8** and **9** was conducted by isocratic preparative HPLC (78% methanol/water (0.05%TFA)). Chiral preparative separation of **8** was performed using 10% isopropanol / 90% hexane as the eluent.

Isolation of falcarindiol from *P. sativa* and Mosher's ester preparation was conducted by Yuping Lu (Page lab). Mosher's esters were prepared directly with MTPA-Cl as previously described (Hoye et al. 2007).

falcarintriol (4): colorless oil; $[\alpha]^{25}_{D}$ +169 (*c* 0.29, $CHCl_3$); UV (MeCN/H_2O) λ_{max} 235, 248, 261 nm; ^{1}H, ^{13}C and HMBC NMR data in Table 3-1, ^{1}H and ^{13}C NMR data in agreement with previous report (Papajewski et al. 1998); HRESIMS *m/z* 313.1775 $[M + Na]^+$ (calculated for $C_{18}H_{26}NaO_3$, 313.1774).

oplopantriol (5): colorless oil; $[\alpha]^{25}_{D}$ +186 (*c* 0.15, $CHCl_3$); UV (MeCN/H_2O) λ_{max} 234, 247, 260 nm; ^{1}H, ^{13}C and HMBC NMR data in agreement with previous report (Kobaisy et al. 1997); HRESIMS *m/z* 315.1953 $[M + Na]^+$ (calculated for $C_{20}H_{26}NaO_3$, 315.1930).

falcarindiol-acetate (6): colorless oil; $[\alpha]^{25}_{D}$ +205 (*c* 0.44, $CHCl_3$); UV (MeCN/H_2O) λ_{max} 235, 248, 261 nm; ^{1}H and ^{13}C NMR data in agreement with previous report (Kobaisy et al. 1997); HRESIMS *m/z* 355.1884 $[M + Na]^+$ (calculated for $C_{20}H_{28}NaO_4$, 355.1879).

oplopandiol-acetate (7): colorless oil; $[\alpha]^{25}_{D}$ +129 (*c* 0.10, $CHCl_3$); UV (MeCN/H_2O) λ_{max} 234, 247, 260 nm; ^{1}H and ^{13}C NMR data in agreement with previous report (Kobaisy et al. 1997); HRESIMS *m/z* 357.2027 $[M + Na]^+$ (calculated for $C_{20}H_{30}NaO_4$, 357.2036).

(3*S*,8*S*)-falcarindiol (8a): colorless oil; $[\alpha]^{25}_{D}$ +322 (*c* 0.21, $CHCl_3$); UV (MeCN/H_2O) λ_{max} 235, 247, 261 nm; ^{1}H and ^{13}C NMR data in agreement with previous report (Kobaisy et al. 1997).

(3*R*,8*S*)-falcarindiol (8b): colorless oil; $[\alpha]^{25}_{D}$ +218 (*c* 0.21, $CHCl_3$); UV (MeCN/H_2O) λ_{max} 235, 247, 261 nm; ^{1}H and ^{13}C NMR data in agreement with previous report (Kobaisy et al. 1997).

oplopandiol (9): colorless oil; $[\alpha]^{25}_{D}$ +271 (*c* 2.4, $CHCl_3$); UV (MeCN/H_2O) λ_{max} 234. 247, 260 nm; ^{1}H and ^{13}C NMR data in agreement with previous report (Kobaisy et al. 1997); HRESIMS *m/z* 285.1827 $[M + Na]^+$ (calculated for $C_{17}H_{26}NaO_2$, 285.1825).

(16*R*)-falcariniol-acetate (10): colorless oil; $[\alpha]^{25}_{D}$ -27.3 (*c* 0.11, $CHCl_3$); UV (MeCN/H_2O) λ_{max} 233, 243, 257 nm; ^{1}H and ^{13}C NMR data in Table 3-1, ^{1}H spectrum in agreement with previous report (Kobayashi et al. 1977); HRESIMS *m/z* 339.1922 $[M + Na]^+$ (calculated for $C_{20}H_{28}NaO_3$, 339.1930).

Table 3-1. NMR spectroscopic data for falcarintriol (**4**) and (16*R*)-falcarinol-acetate (**10**)

	falcarintriol (**4**)			(16*R*)-falcarinol-acetate (**10**)	
position	δ_C, mult.	δ_H, (*J* in Hz)	HMBC[a]	δ_C, mult.	δ_H, (*J* in Hz)
1	63.1,CH_2[b]	3.63, t (6.7)	2, 3	64.7, CH_2	4.04, t (6.8)
2	32.7, CH_2	1.55, m	1, 3	25.9, CH_2	1.60, m
3	25.6, CH_2	1.30, m		29.3, CH_2[e]	1.30, m
4	28.8, CH_2[c]	1.30, m		29.2, CH_2[e]	1.30, m
5	29.2, CH_2[c]	1.30, m		29.2, CH_2[e]	1.30, m
6	29.3, CH_2[c]	1.30, m		29.0, CH_2[e]	1.30, m
7	29.0, CH_2[c]	1.30, m		28.6, CH_2[e]	1.30, m
8	27.6, CH_2	2.10, m	7, 9, 10, 11, 12	27.1, CH_2	2.01, m
9	134.4, CH	5.58, m	7, 8, 10, 11, 12	133.0, CH	5.49, m
10	127.9, CH	5.50, m	7, 8, 9, 11, 12	122.1, CH	5.36, m
11	58.7, CH_2	5.19, d (8.2)	9, 10, 12, 13, 14, 15	17.7, CH_2	3.01, d (7.0)
12	79.8, qC			74.4, qC[f]	
13	70.2, qC[d]			71.3, qC[f]	
14	68.8, qC[d]			64.1, qC[f]	
15	78.5, qC			80.2, qC[f]	
16	63.4, CH[b]	4.91, br d (5.2)	12, 13, 14, 15, 17, 18	63.5, CH	4.89, t (5.3)
17	135.9, CH	5.92, ddd (17.1, 10.2, 5.2)	15, 16	136.3, CH	5.92, ddd (17.1, 10.2, 5.3)
18a	117.1, CH_2	5.45, ddd (17.1, 1.5, 1.0)	15, 16, 17	116.9, CH_2	5.44, d (17.1)
18b		5.24, ddd (10.2, 1.2, 1.0)	15, 16		5.22, d (10.2)
CO				171.3, qC	
CO*CH*$_3$				21.0, CH_3	2.02, s

[a]HMBC correlations are from protons stated to the indicated carbon.
[a-f]assignments may be interchanged

(*E*)-nerolidol (11): colorless oil; ^{1}H and ^{13}C data in agreement with previous reports (Mattes et al. 1987; Blanc et al. 2005). HRESIMS *m/z* 245.1869 $[M + Na]^+$ (calculated for $C_{20}H_{26}NaO_3$, 245.1875).

(3*R*)-falcarinol (12): colorless oil; $[\alpha]^{25}_{D}$ -32 (*c* 0.15, $CHCl_3$); UV (MeCN/H_2O) λ_{max} 232.7, 244.4, 257.4 nm; ^{1}H and ^{13}C NMR spectra in agreement with previous report (Nitz et al. 1990); HRESIMS *m/z* 267.1716 $[M + Na]^+$ (calculated for $C_{17}H_{24}NaO$, 267.1719).

3.2.6. *A. nudicaulis*

A. nudicaulis rhizomes were collected near Saskatoon, SK, Canada, August 2009. GPS coordinates: N52.09536, W106.69521. A voucher specimen was deposited in the SASK herbarium, Department of Plant Sciences, University of Saskatchewan.

Fresh rhizomes (593 g) were dried at room temperature, ground and sifted through a 2.4 mm screen. The resulting 269 g of dried tissue was extracted with 9 L of methanol. The extract was concentrated to 150 mL under vacuum (25-28°C), water was added to 10% and the extract was extracted four times with an equal volume of hexane. The methanolic extract was diluted with water to give 75% water/25% methanol and was extracted four times with an equal volume of chloroform. An aqueous 1% NaCl solution was used to extract tannins from the chloroform partition. Solvents were then removed from each fraction under vacuum. The chloroform partition was subjected to flash chromatography (15 × 230 mm column packed with 200-425 mesh silica gel (Fisher), gradient of 10-100% ethyl acetate/hexane). Sixty-three fractions were collected and combined by the basis of TLC (Si gel with ratios of hexane : ethyl acetate from 1:1 to 1:4) and HPLC analysis to eight fractions (A through G). Following clean up on a Sep-pak Vac 20cc C_{18} cartridge (Waters), the major compound panaxydol (**14**) was isolated by preparative C_{18} HPLC (79% methanol/water, isocratic). Falcarinol (**13**) was isolated by preparative HPLC (86% methanol/H_2O, isocratic). Ginsenoyne D (**15**) was isolated by preparative HPLC (79% methanol/H_2O, isocratic) and repurified by semi-preparative HPLC (85% methanol/H_2O, isocratic). 1,2-dihydro-epoxyoplopandiol-acetate (**16**) was isolated by preparative HPLC (83% methanol, isocratic) and repurified by semi-preparative HPLC (79% acetonitrile/H_2O, isocratic). Falcarinol-acetate (**17**) was isolated by preparative HPLC (83% methanol/H_2O, isocratic) and repurified by semi-preparative HPLC (88% methanol/H_2O, isocratic). Polyacetylenes **18-22** were isolated using a gradient of 60-93% methanol/water. Falcarinolol (**23**) was isolated by preparative HPLC (73% methanol/H_2O, isocratic). For all purifications other than that of panaxydol (**14**), methanol was removed under vacuum and water was removed by lyophilisation. The HPLC eluate of panaxydol (**14**) was extracted with dichloromethane, dried with $MgSO_4$, and concentrated under vacuum.

falcarinol (13): colorless oil; $[\alpha]^{25}_D$ -27 (*c* 0.96, $CHCl_3$); UV (MeCN/H_2O) λ_{max} 233, 244, 257 nm; ^1H and ^{13}C NMR spectra in agreement with previous report (Nitz et al. 1990); HRESIMS *m/z* 267.1716 $[M + Na]^+$ (calculated for $C_{17}H_{24}NaO$, 267.1719) ESIMS *m/z* 244.1 $[M + H]^+$.

panaxydol (14): colorless oil; $[\alpha]^{25}_D$ -113 (*c* 0.13, $CHCl_3$); UV (MeCN/H_2O) λ_{max} 221, 232, 243, 257 nm; ^1H and ^{13}C NMR data in agreement with previous report (Lu et al. 1998); HRESIMS *m/z* 283.16507 $[M + Na]^+$ (calculated for $C_{17}H_{24}NaO_2$, 283.16685).

ginsenoyne D (15): colorless oil; $[\alpha]^{25}_{D}$ -24.6 (*c* 0.07, $CHCl_3$); UV (MeCN/H_2O) λ_{max} 221sh, 230, 242, 256 nm; ^{1}H and ^{13}C NMR data in agreement with previous report (Hirakura et al. 1991); ESIMS *m/z* 263.1 $[M + H]^+$ (calculated for $C_{17}H_{27}O_2$,263.2).

1,2-dihydroepoxyoplopandiol-acetate (16): colorless oil; $[\alpha]^{25}_{D}$ -1.5 (*c* 0.07, $CHCl_3$); UV (MeCN/H_2O) λ_{max} 234, 269, 285, 300, 318 nm; ^{1}H data presented in Table 3-2; HRESIMS *m/z* 343.18695 [M + Na]+ (calculated for $C_{19}H_{28}NaO_4$, 343.18798). ^{1}H, ^{13}C, and HMBC NMR spectra are provided in Appendix A.

falcarinol-acetate (17): colorless oil; $[\alpha]^{25}_{D}$ -2.9 (*c* 0.03, $CHCl_3$); UV (MeCN/H_2O) λ_{max} 233, 244, 259 nm; ^{1}H spectrum in agreement with previous report (Kobayashi et al. 1977) and spectra for compound isolated from *O. horridus* (**10**); HRESIMS m/z 339.18976 [M + Na]+ (calculated for $C_{20}H_{28}NaO_3$, 339.19307).

panaxyne (18): colorless oil; $[\alpha]^{25}_{D}$ +17 (*c* 0.24, acetone); UV (MeCN/H_2O) λ_{max} 221sh, 227, 244, 257 nm; ^{1}H and ^{13}C NMR data in agreement with previous report (Yang et al. 2008); HRESIMS *m/z* 243.13460 $[M + Na]^+$ (calculated for $C_{14}H_{20}NaO_2$, 243.13555).

epoxyfalcarindiol (19): colorless oil; $[\alpha]^{25}_{D}$ +26 (*c* 0.37, $CHCl_3$); UV (MeCN/H_2O) λ_{max} 221sh, 232, 244, 258 nm; ^{1}H and ^{13}C NMR data in agreement with previous report (Fujimoto et al. 1991); HRESIMS m/z 299.16168 $[M + Na]^+$ (calculated for $C_{17}H_{24}NaO_3$, 299.16177).

epoxyoplopandiol (20): colorless oil; $[\alpha]^{25}_{D}$ +48 (c 0.51, CHCl3); UV (MeCN/H2O) λmax 221sh, 231, 257, 285, 311sh nm; ^{1}H and ^{13}C NMR data in agreement with previous report (Yang et al. 2010); HRESIMS m/z 301.17740 $[M + Na]^+$ (calculated for $C_{17}H_{26}NaO_3$, 301.17742).

10-methoxyheptadeca-1-en-4,6-diyne-3,9-diol (21): colorless oil; $[\alpha]^{25}_{D}$ -22 (*c* 0.29, $CHCl_3$); UV (MeCN/H_2O) λ_{max} 231, 243, 257, 267, 282 nm; ^{1}H and ^{13}C NMR data in agreement with previous report (Yang et al. 2008); HRESIMS *m/z* 315.1742 $[M + Na]^+$ (calculated for $C_{18}H_{28}NaO_3$, 315.1936).

panaxydiol (22): colorless oil; $[\alpha]^{25}_{D}$ +4 (*c* 0.21, $CHCl_3$); UV (MeCN/H_2O) λ_{max} 215, 241, 254, 264, 285 nm; ^{1}H and ^{13}C NMR data in agreement with previous report (Schmiech et al. 2009); HRESIMS m/z 283.16640 $[M + Na]^+$ (calculated for $C_{17}H_{24}NaO_2$, 283.16685).

falcarinolol (23): colorless oil; $[\alpha]^{25}_{D}$ -30 (*c* 0.08, $CHCl_3$); UV (MeCN/H_2O) λ_{max} 233, 244, 259 nm; ^{1}H NMR data in agreement with previous report (Kobayashi et al. 1977), ^{1}H, ^{13}C and HMBC NMR data presented in Table 3-2; HRESIMS *m/z* 297.18120 $[M + Na]^+$ (calculated for $C_{18}H_{26}NaO_2$, 297.18250).

Table 3-2. NMR spectroscopic data for 1,2-dihydroepoxyoplopandiol-acetate (**16**) and falcarinolol (**23**)

	1,2-dihydroepoxyoplopandiol-acetate (**16**)	falcarinolol (**23**)		
position[i]	δ_H, (*J* in Hz)	δ_C, mult.	δ_H, (*J* in Hz)	HMBC[a]
1	3H, 1.03, t (7.5)	63.2, CH_2	3.65, t (6.7)	2, 3
2	2H,1.81, m	32.8, CH_2	1.58, m	1, 3, 4
3	1H, 5.34, t (6.5)	25.7, CH_2	1.35, m	
4		29.4, CH_2[e]	1.35, m	
5		29.3, CH_2[e]	1.35, m	
6		29.0, CH_2[e]	1.35, m	
7		28.9, CH_2[e]	1.35, m	
8	1H, 4.36, dd (7.5,5.0)	27.0, CH_2	2.03, m	7, 9, 10, 12
9	1H, 3.13, dd (7.5, 4.0)	133.1, CH	5.49, m	7, 8, 11
10	1H, 3.05, m	122.0, CH	5.36, m	8, 11, 12
11	1.64, m	17.7, CH_2	3.03, d (6.7)	7, 8, 9, 10, 12, 13, 14, 15
12	1.50, m	80.2, qC		
13	1.30, m	64.0, qC[f]		
14	1.30, m	71.2, qC[f]		
15	1.30, m	74.4, qC		
16	1.30, m	63.5, CH	4.91, br d (5.3)	13, 14, 15, 17, 18
17	3H, 0.88, t (6.5)	136.2, CH	5.95, ddd (17.0, 10.2, 5.3)	15, 16
18a		117.0, CH_2	0.99, t (17.0)	16, 17
18b			5.24, d (10.2)	16
CO*CH*$_3$				
8'-O*H*	3H, 2.1, d (5.0)			

[a]HMBC correlations are from protons stated to the indicated carbon.
[b-f]assignments may be interchanged

3.2.7. *A. latifolia*

A. latifolia seeds were provided by Nick Page of Rainforest Applied Ecology. Thirty-eight plants were grown in the NRC Saskatoon phytotron and greenhouse. A voucher specimen (accession #180331) was deposited in the SASK herbarium, Department of Plant Sciences, University of Saskatchewan.

Root material (171 g) was cut into small pieces and dried at room temperature with air. Dried *A. latifolia* roots (43.3 g) were ground, screened at 0.85 mm and extracted with methanol. Three different extractions of the roots were undertaken to examine the difference between frozen roots, fresh tap roots and fresh small roots. After the first extraction and examination of the extracts by analytical HPLC the roots were combined on the basis of their similarity and

extracted together for a total of five extractions using 3.2 L methanol. The methanolic extract was concentrated and subjected to solvent-solvent partitioning as shown in Figure 3-10.

The dicholormethane/chloroform partition was separated into 90 fractions by flash chromatography (26 × 460 mm column packed with 110 g of 230-400 mesh silica gel (Fisher), linear gradient of pure dichloromethane to pure methanol). Preliminary fractions were combined on the basis of UV absorption at 280 nm. Solvent was removed from a sample of each fraction and resuspended in DMSO at 10 mg/mL and tested in the QR bioassay. Fractions 1-3 (A-C) were separated on a Sep-pak Vac 12 cc 2g C_{18} SPE cartridge (Waters) using methanol/water as the eluent. The percentage of methanol used was 30 % to 100% in 10% steps for the combined fractions 1 and 2 and 40% to 100% in 20% steps for fraction 3. Fractions were combined on the basis of analytical HPLC and tested in the QR bioassay. From the three active fractions 16 compounds were isolated by preparative HPLC. The solvent was removed under reduced pressure and lyophilisation and compounds were resuspended in deuterated methanol (MeOD) for ^{1}H, j-mod ^{13}C, HMQC and HMBC NMR. Compounds were tested in the QR bioassay following the acquisition of NMR spectra.

2-(2,6-dihydroxyphenyl)-5-hydroxy-7-methoxy-6,8-dimethylchroman-4-one (**24**)**:** UV (acetonitrile/H_2O) $\lambda_{max.}$ (nm) 286; ^{1}H NMR (MeOD) δ 6.98 (1H, t, J = 8.2 Hz, H-4'), 6.35 (2H, d, J = 8.2 Hz, H-3', H-5'), 5.92 (1H, dd, J_1 = 14.2 Hz, J_2 = 2.9 Hz, H-2), 3.95 (1H, dd, J_1 = 17.4 Hz, J_2 = 14.2 Hz, H-3a), 3.72 (3H, s, OMe-7), 2.51 (1H, dd, J_1 = 17.4Hz, J_2 = 2.9 Hz, H-3b), 2.06 (3H, s, Me-8), 2.01 (3H, s, Me-6). ^{13}C NMR ($CDCl_3$) δ 201.4 (C, C-4), 166.2 (C, C-7), 160.8 (C, C-5), 160.4 (C, C-4), 158.5 (C, C-2', C-4'), 131.1 (CH, C-4'), 112.0 (C, C-1'), 111.3 (C, C-8), 110.6 (C, C-6), 108.2 (CH, C-3', C-5'), 105.8 (C, C-10), 73.80 (CH, C-2), 60.56 (CH_3, OMe-7), 41.21 (CH_2, C-3), 8.63(CH_3, Me-6), 8.00 (CH_3, Me-8). HRESIMS observed *m/z* 331.11703 $[M + H]^+$ (calculated for $C_{18}H_{19}O_6$, 331.11762). Spectra included in Appendix A.

compound (**25**)**:** UV (acetonitrile/H_2O) $\lambda_{max.}$ (nm) 291; ^{1}H NMR (MeOD) δ 6.98 (1H, t, J = 8.2 Hz, H-4'), 6.34 (2H, d, J = 8.2 Hz, H-3', H-5'), 6.12 (1H, s, H-6 or -8), 5.95 (1H, dd, J_1 = 14.1 Hz, J_2 = 3.0 Hz, H-2), 3.96 (1H, dd, J_1 = 17.4 Hz, J_2 = 14.2 Hz, H-3a), 3.84 (3H, s, OMe-7), 2.45 (1H, dd, J_1 = 17.4 Hz, J_2 = 3.0 Hz, H-3b), 1.95 (3H, s, Me-8 or 6), 2.01 (3H, s, Me-6). ^{13}C NMR ($CDCl_3$) δ 200.0 (C, C-4), 163.5* (C, C-7), 161.4*(C, C-5), 160.4* (C, C-4), 158.5 (C, C-2', C-4'), 131.2* (CH, C-4'), 112.0* (C, C-1'), 111.3* (C, C-6 or C-8), 108.2* (CH, C-3', C-5'), 103.6

(C, C-10), 91.80 (CH, C-6 or C-8), 73.92 (CH, C-2), 56.38 (CH_3, OMe-7), 40.84 (CH_2, C-3), 6.98 (CH_3, Me-6 or Me-8), * denotes signal inferred from HMBC spectrum. HRESIMS *m/z* 317.10104 $[M + H]^+$ (calculated for $C_{17}H_{17}O_6$, 317.10197). Spectra included in Appendix A.

boeravinone E (26), UV (acetonitrile/H_2O) $\lambda_{max.}$ (nm) 278, 302sh, 340sh; ^1H, ^{13}C and HBMC data in agreement with previous analysis (Lami et al. 1991). HRESIMS *m/z* 329.06689, $[M + H]^+$ (calculated for $C_{17}H_{13}O_{7,}$ 329.06557).

3.2.8. *C. sativa*

C. sativa 'Finola' hemp plants were grown in the NRC Saskatoon phytotron. Female flowers were dried at room temperature. Dried flowers (200 g) were extracted overnight with 1.5 L hexane, filtered and concentrated under vacuum at 40°C to give 14 g of residue. The residue (125 mg) was resuspended in 0.75 mL of methanol, filtered with a Spin-X centrifugal filter (Corning) loaded onto a Sep-Pak vac 2 g C_{18} SPE cartridge (Waters) and eluted with 4 column volumes of methanol. The SPE eluate was filtered by Spin-X filter and CBDA was isolated using preparative HPLC (83% Methanol/H_2O with 0.05% trifluoroacetic acid). The residue (378 mg) was heated at 120°C for 30 min resuspended in methanol and filtered on a Spin-X filter. CBD was isolated by preparative HPLC (80% Methanol/H_2O with 0.05% trifluoroacetic acid).

THCA was isolated from a colleagues' crude THCA-rich fraction by preparative HPLC (85% Methanol/H_2O with 0.05% trifluoroacetic acid). THC was isolated by preparative HPLC (88% Methanol/H_2O with 0.05% trifluoroacetic acid) from a portion of the THCA-rich fraction that was heated to 130ºC for 40 min.

Solvent was removed from HPLC eluates by rotary evaporation at 30°C and lyophilization. Cannabinoids were identified by LC-UV-MS, ^1H and ^{13}C NMR (Choi et al. 2004). Deuterated methanol was used as the solvent for NMR experiments.

3.3. Results and discussion

3.3.1. Isolation of the active components from the methanolic extract of *L. porteri* roots

Due to the potential advantages of using thiol-reactivity as a guide to isolating Nrf2 activators I decided to attempt this approach first. However, following the failure of this method I later turned to using QR bioassay-guided fractionation.

3.3.1.1. Fractionation of the *L. porteri* extract guided by tandem MS-based detection of thiol-reactive extract components

In order to efficiently use thiol-reactivity as a guide for isolation I conducted some preliminary experiments to select a positive control and optimize the detection method. A panel of known QR inducers including curcumin, resveratrol, sulforaphane and xanthohumol were used for optimization. A number of scanning methods were successful in detecting GSH-adducts. These included scanning for parents of *m/z* 272 or 306 in negative mode and parents of *m/z* 130 in positive mode. I chose to scan for parents of *m/z* 130 in positive mode due to a greater signal to noise ratio. Xanthohumol was selected for use as a positive control. Tuning of the mass spectrometer was optimized using the xanthohumol-GSH adduct and oxidized glutathione.

A preliminary screen of solvent-solvent partitions (data not shown) showed that the *L. porteri* chloroform partition was the most QR-active. Therefore, following extraction and solvent-solvent partitioning, I proceeded to fractionate the chloroform partition using silica gel column chromatography. Two fractions showed a prominent glutathione-adduct that corresponded well with the primary compound in those fractions. The compound involved was isolated and identified as coniferyl ferulate (**1**). However, this compound proved to have negligible activity in the QR bioassay (<1.2-fold at 100 µM). Although the reason for the lack of QR-inducing activity was unclear, this finding emphasized the fact that not all thiol-reactive compounds will be Nrf2 activators. The thiol reactivity-based screening approach was therefore abandoned and I returned to using QR bioassay-guided fractionation on a fresh extract.

3.3.1.2. Alkylphthalides are the primary QR inducers in *L. porteri* roots

Silica gel-based separation of a newly prepared chloroform partition of *L. porteri* led to the identification of QR-inducing activity in fractions that were less polar than the fractions that contained coniferyl ferulate (**1**) (Figure 3-1). This further confirmed that coniferyl ferulate was not

responsible for the extract's QR-inducing activity. When the most active fraction (B) was separated on a reverse phase SPE cartridge, I found that the most active subfraction (B-3) included compounds with UV spectra similar to phthalides, a group of compounds previously reported from Apiaceae plants (Beck et al. 2007). Purification of the eight major compounds from this fraction revealed that while seven of these eight compounds displayed QR-inducing activity, a single compound had much higher activity than the rest (CD value of ~ 0.3 μg/mL compared to CD values of ~ 3 μg/mL). Analysis by ^{1}H, ^{13}C, and HMBC NMR showed that the most active compound was an isomer of ligustilide (Figure 3-2). A nuclear overhauser effect (NOE) experiment revealed the (*Z*)-geometry of the alkyl chain, giving (*Z*)-ligustilide (**2**) (Beck et al. 2007).

As previously described (Cui et al. 2006), pure (*Z*)-ligustilide (**2**) was unstable and rapidly degraded if stored in an aqueous solution. Following HPLC isolation, I identified the major degradation product by NMR (^{1}H, ^{13}C, HMBC and NOE experiments) as *trans*-6,7-dihydroxyligustilide (**3**). *trans*-6,7-Dihydroxyligustilide (**3**) was found to be optically inactive indicating that this isolate was a racemic mixture containing equal amounts of the enantiomers senkyunolide I (6*S*,7*R*-geometry) and ligustilidiol (6*R*,7*S*-geometry).

trans-6,7-Dihydroxyligustilide (**3**) was also identified in a newly prepared methanolic extract of *L. porteri* roots. Given the spontaneous conversion of (*Z*)-ligustilide (**2**) to *trans*-6,7-dihydroxyligustilide (**3**) under storage conditions the origin of this compound in the plant may also be non-enzymatic.

The induction of QR by (*Z*)-ligustilide (**2**), *trans*-6,7-dihydroxyligustilide (**3**) and (*R*)-sulforaphane is shown in Figure 3-3. Both (*Z*)-ligustilide and the racemic mixture of *trans*-6,7-dihydroxyligustilide were relatively potent inducers of QR, with CD values of 2.0 μM and 2.2 μM, respectively.

Hepa-1c1c7 cells tolerated high concentrations of (*Z*)-ligustilide and *trans*-6,7-dihydroxyligustilide (Table 3-3). The concentrations required to reduce cell viability by 50% (IC_{50}) values for these two compounds were 64 μM, and over 100 μM, respectively. The ratio of the IC_{50} and CD values, referred to as the chemopreventive index (CI), indicates the margin between the desired effect and adverse toxicity. The CI values for (*Z*)-ligustilide and *trans*-6,7-dihydroxyligustilide were 32 and > 45, respectively, indicating a large therapeutic window.

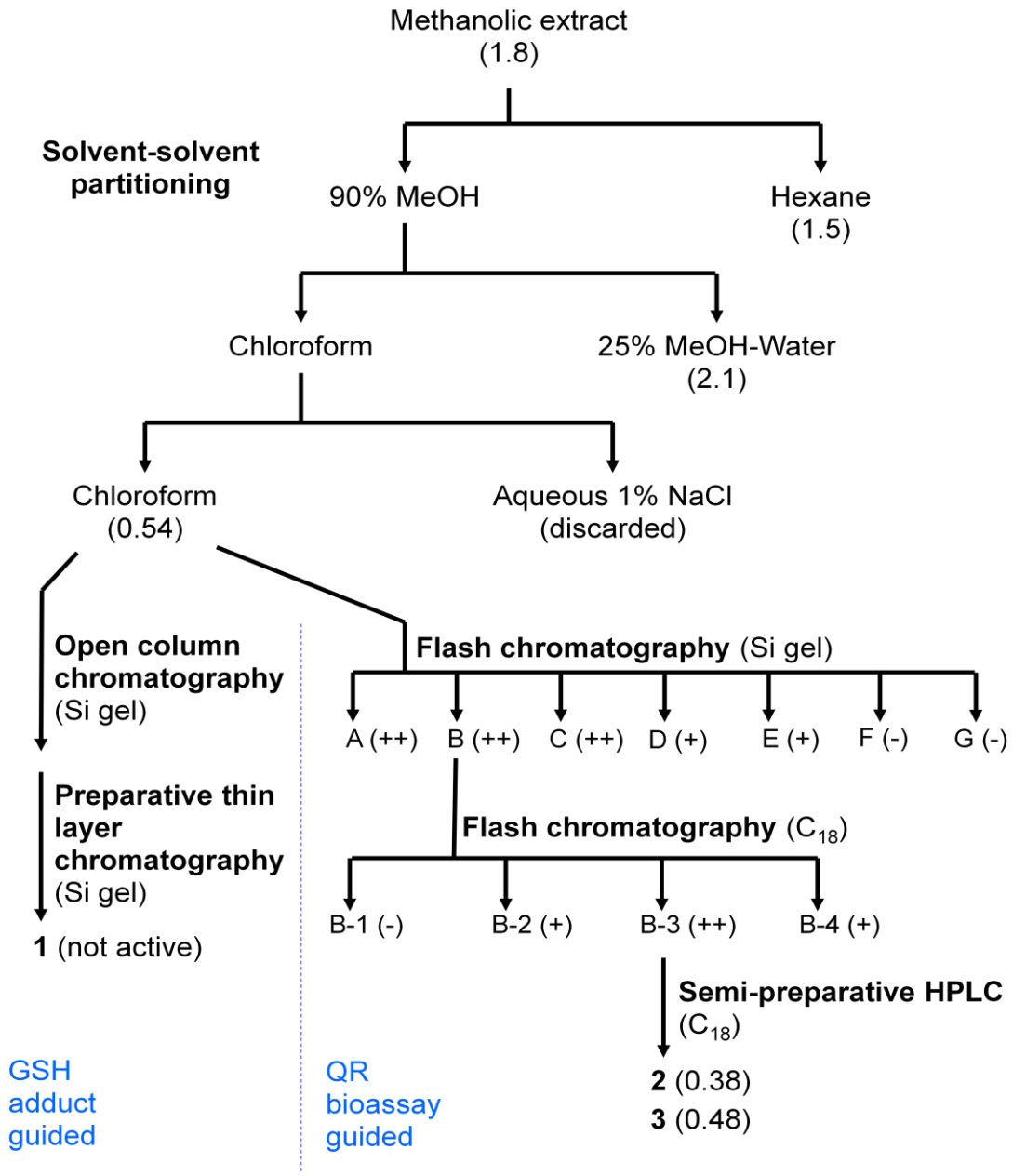

Figure 3-1. Separation scheme for methanol extracts of *L. porteri* roots. Concentrations required to double QR-activity (CD), µg/mL or relative activity (++ high activity, + moderate activity, low or no activity) are indicated in brackets.

Recent analysis of the pharmacokinetics of (*Z*)-ligustilide revealed that the (6*S*,7*R*) enantiomer of *trans*-6,7-dihydroxyligustilide (**3**), senkyunolide I is a metabolite of (*Z*)-ligustilide (Yan et al. 2008). Thus, the QR-inducing activity of senkyunolide I and related metabolites may contribute to the activity of (*Z*)-ligustilide *in vivo.*

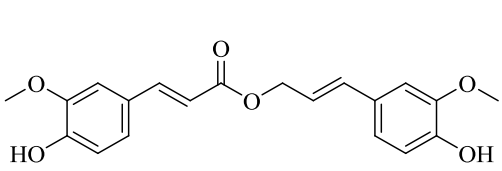

coniferyl ferulate **(1)**

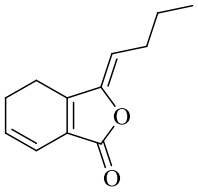

(*Z*)-ligustilide **(2)**

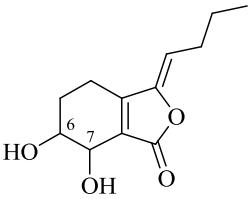

trans-6,7-dihydroxyligustilide **(3)**

Figure 3-2. Compounds isolated from *L. porteri.*

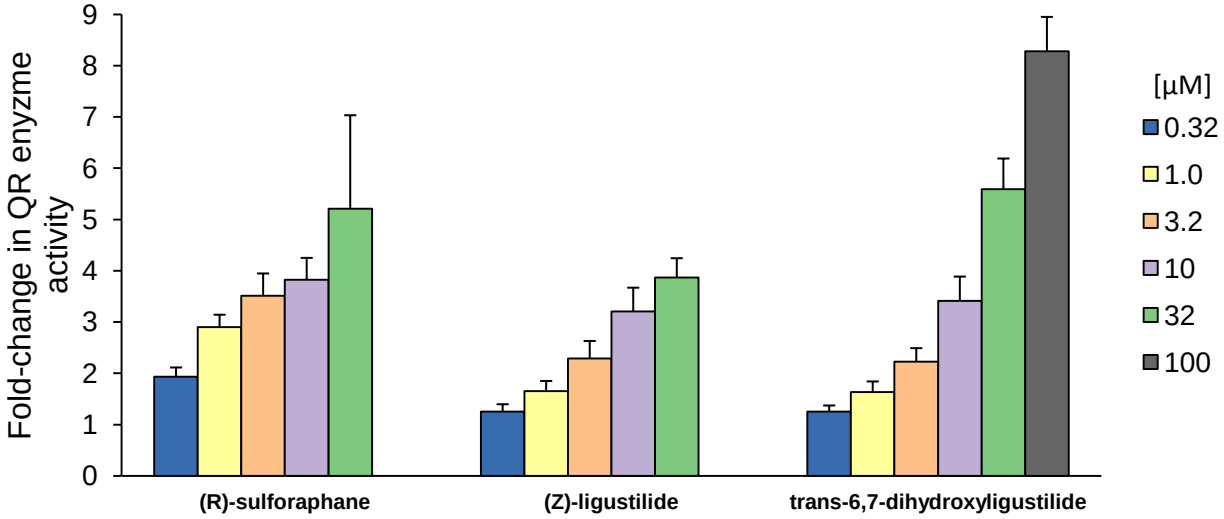

Figure 3-3. QR induction following exposure to *L. porteri* alkylphthalides. Hepa-1c1c7 cells were exposed to alkylphthalides for 48 h and QR activity was compared to solvent treated controls. (*R*)-sulforaphane was included as a positive control. Results are the mean of at least three experiments ± the standard deviation.

Table 3-3. Summary of bioassay results for *L. porteri* phthalides.

Compound	QR inducing activity CD[a] (µM)	Cell viability IC_{50}[b] (µM)	CI (IC_{50}/CD)
(*R*)-sulforaphane	0.36 ± 0.08	8.1 ± 2.5	23
(Z)-ligustilide **(2)**	2.0 ± 0.66	64 ± 8.9	32
trans-6,7-dihydroxyligustilide **(3)**	2.2 ± 0.90	> 100	> 45

[a] refers to the concentration required to double activity of the enzyme QR relative to DMSO treated controls.
[b] refers to the concentration required to reduce cell viability to 50% in Hepa-1c1c7 cells.

During this work, Dietz *et al*. (2008) reported that an extract of *Angelica sinensis*, a member of the Apiaceae used in traditional Chinese medicine (dang gui), was a strong inducer of QR. Bioassay-guided fractionation of this extract also led these investigators to (*Z*)-ligustilide and

senkyunolide I (6*S*,7*R*-dihydroxyligustilide) as the primary components responsible for QR-inducing activity.

3.3.2. C_{17}-type polyacetylenes from *O. horridus* are potent inducers of QR

Methanolic extracts of *O. horridus* stems or a sample that combined berries and leaves were active in the QR-bioassay screen (maximal QR induction of 2.02-fold at 2 mg/mL, and 2.45 fold at 2 mg/mL, respectively). I choose to use the extract of the inner stem bark for bioassay-guided fractionation because it was unclear whether the berries or leaves were responsible for activity in the combined extract and for the reason that the inner stem bark is the most commonly used part for traditional medicine (Moerman 1998).

Solvent-solvent partitioning led to an increase in activity in the chloroform partition (Figure 3-4). Flash chromatography of the chloroform-soluble fraction yielded several polyacetylene rich fractions (fractions C through J) with high QR-inducing activity. Pure polyacetylenes were isolated from these fractions by preparative HPLC (Figure 3-5).

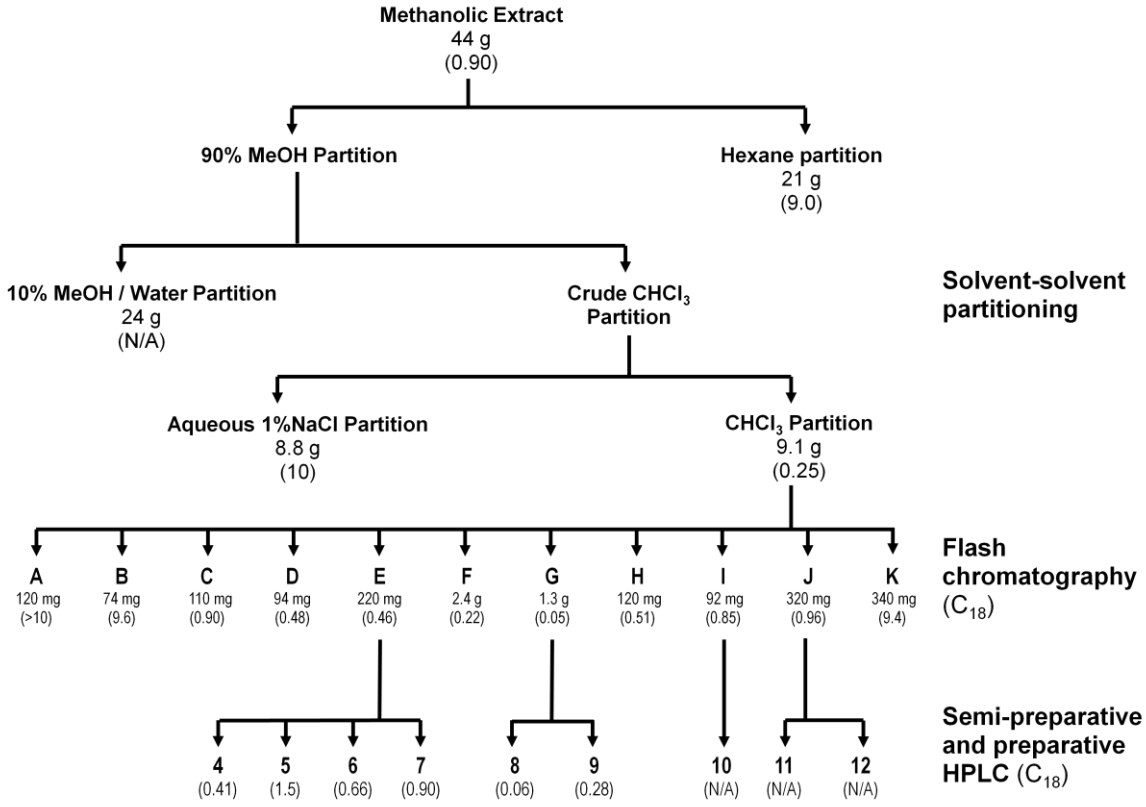

Figure 3-4. Separation scheme for methanol extract of *O. horridus* inner stem bark. Concentrations required to double QR-activity (CD values, µg/mL) are indicated in brackets.

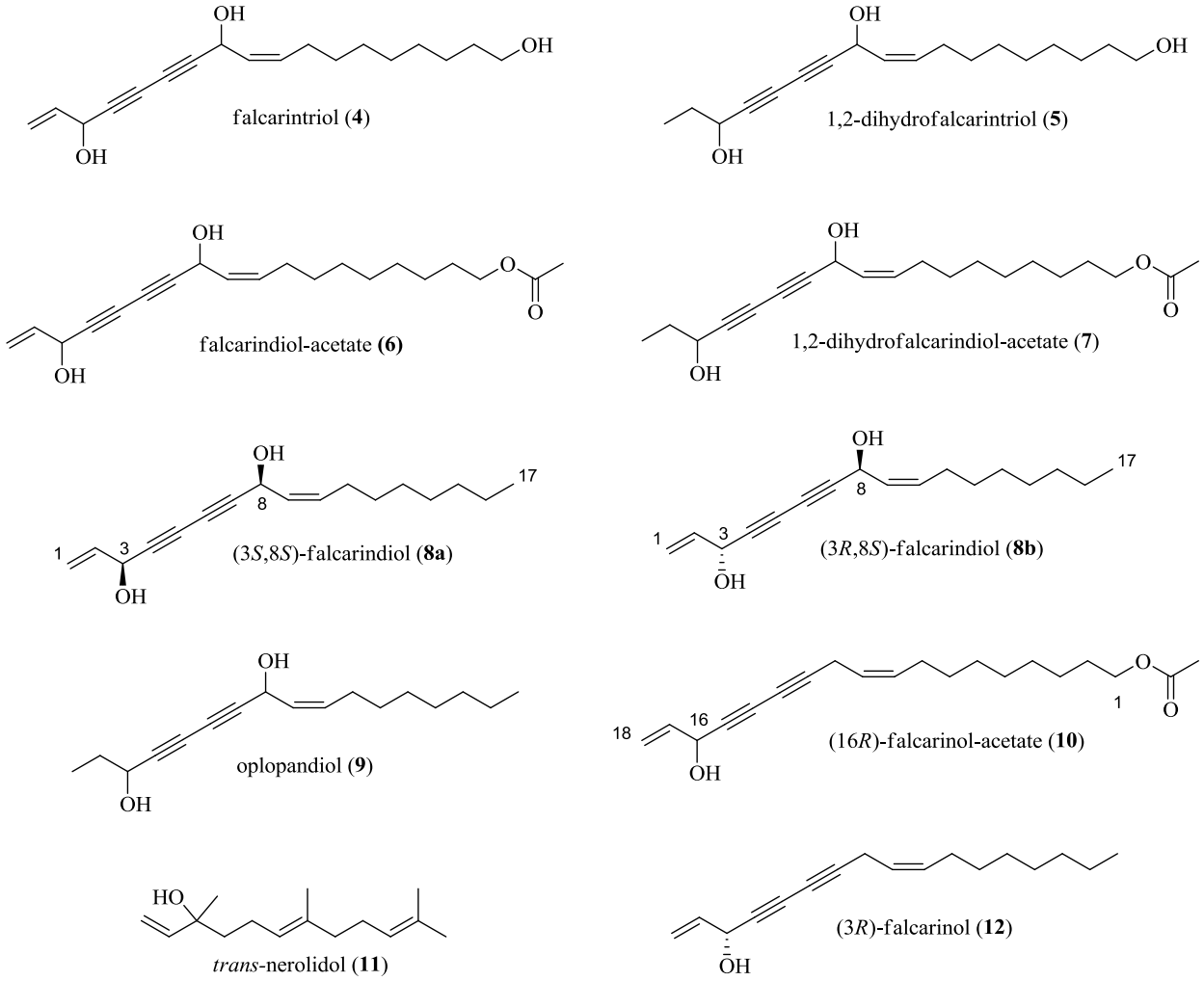

Figure 3-5. Compounds isolated from *O. horridus.*

^{1}H NMR, ^{13}C NMR, and MS spectra for compounds **4-9**, and **12** matched those of previously reported polyacetylenes from *O. horridus* (Kobaisy et al. 1997; Huang et al. 2010). However, the levorotary optical rotations of falcarinol (**12**) and falcarinol-acetate (**10**) were in contrast with the previously reported dextrorotary observations and indicated (*R*) rather than (*S*) configurations for these compounds (Larsen et al. 1970; Terada et al. 1989). As all previous polyacetylenes from *O. horridus* were assigned to have (3*S*) configurations, the observation of a (3*R*) configuration for falcarinol was puzzling. I used chiral HPLC to analyze the enantiopurity of falcarindiol-acetate (**6**), falcarindiol (**8**), oplopandiol (**9**) and falcarinol (**12**) to help resolve this discrepancy. Although only a single peak was detected for falcarindiol-acetate (**6**), oplopandiol (**9**)

and falcarinol (**12**), two stereoisomers of falcarindiol (**8**) were detected at a ~ 3:1 ratio. The less abundant falcarindiol stereoisomer (**8b**) displayed an equal retention time to (3*R*,8*S*)-falcarindiol isolated from *Pastinaca sativa* (parsnip). A colleague (Yuping Lu) had previously determined the *P. sativa* falcarindiol to have a (3*R*,8*S*) configuration by Mosher's ester analysis.

Purification of the falcarindiol stereoisomers by chiral HPLC led to the observation that both stereoisomers were strongly dextrorotary. Only two dextrorotary configurations of falcarindiol exist: (3*R*,8*S*) and (3*S*,8*S*) (Ratnayake et al. 2002). As the less abundant stereoisomer, **8b,** was already identified as (3*R*,8*S*), the configuration of the more abundant stereoisomer, **8a,** was assigned as (3*S*,8*S*).

Detailed NMR analysis provided further support for these configurational assignments. Each falcarindiol stereoisomer was analyzed by ^{1}H and ^{13}C NMR under identical conditions (concentration, solvent composition and NMR set-up). Although proton and carbon NMR spectra of the two stereoisomers of falcarindiol were nearly identical, an obvious difference was noted for the signals corresponding to the proton at position 3. This difference would only be expected for a pair of diastereomers and is therefore consistent with the assignments of (3*S*,8*S*) and (3*R*,8*S*).

My assignment of the more abundant *O. horridus* falcarindiol (**8a**) as (3*S*,8*S*) is compatible with the previous assignment by Kobaisy *et al.* (1997) of falcarindiol from *O. horridus* as (3*S*,8*S*). In addition, Yang *et al*. (2010) recently reported that *Oplopanax elatus* produces the same two diastereomers of falcarindiol and that the (3*S*,8*S*)-falcarindiol (**8a**) was the more abundant diastereomer.

Although the detection of falcarindiol (**8**) with a (3*R*,8*S*) configuration supports the idea that *O. horridus* produces hydroxylated polyacetylenes of both (3*R*) and (3*S*) configurations it does not fully explain the discrepancy between the present finding of (3*R*)-falcarinol (**12**) with the previous report of (3*S*)-falcarinol (Kobaisy et al. 1997). The possibility of distinct chemotypes of *O. horridus* warrants further inspection as these chemotypes could be useful for determining the enzymes(s) responsible for the (3*R*) configuration.

Most polyacetylenes isolated and tested from *O. horridus* were potent QR inducers (Figure 3-6) having CD values in the low µM to sub-µM range (Table 3.4). The central hydroxyl group (8-OH in falcarindiol (**8**)) appeared to be integral to the activity of these polyacetylenes because (16*R*)-falcarinol-acetate (**10**) and (3*R*)-falcarinol (**12**), which lacked this group, did not consistently

double QR activity, and only reached this induction level with a substantial reduction in cell viability. The terminal double bond appeared to be required for maximal QR inducing activity although compounds possessing the reduced terminus (1,2-dihydrofalcarintriol (**5**) and 1,2-dihydrofalcarindiol-acetate (**7**))also displayed less toxicity than the comparable compounds a 1,2 double bond (falcarintriol (**4**) and falcarindiol-acetate (6)). Given the relatively low CI values for these compounds these decreases may be a reasonable tradoff. Oplopandiol (**9**) had both potent QR inducing activity (CD = 1.2 µM) and relatively low impact on cell viability (IC_{50} = 14.2 µM) giving a CI of 12. The presence of an acetyl or hydroxyl group at the aliphatic terminus consistently reduced activity as well as toxicity.

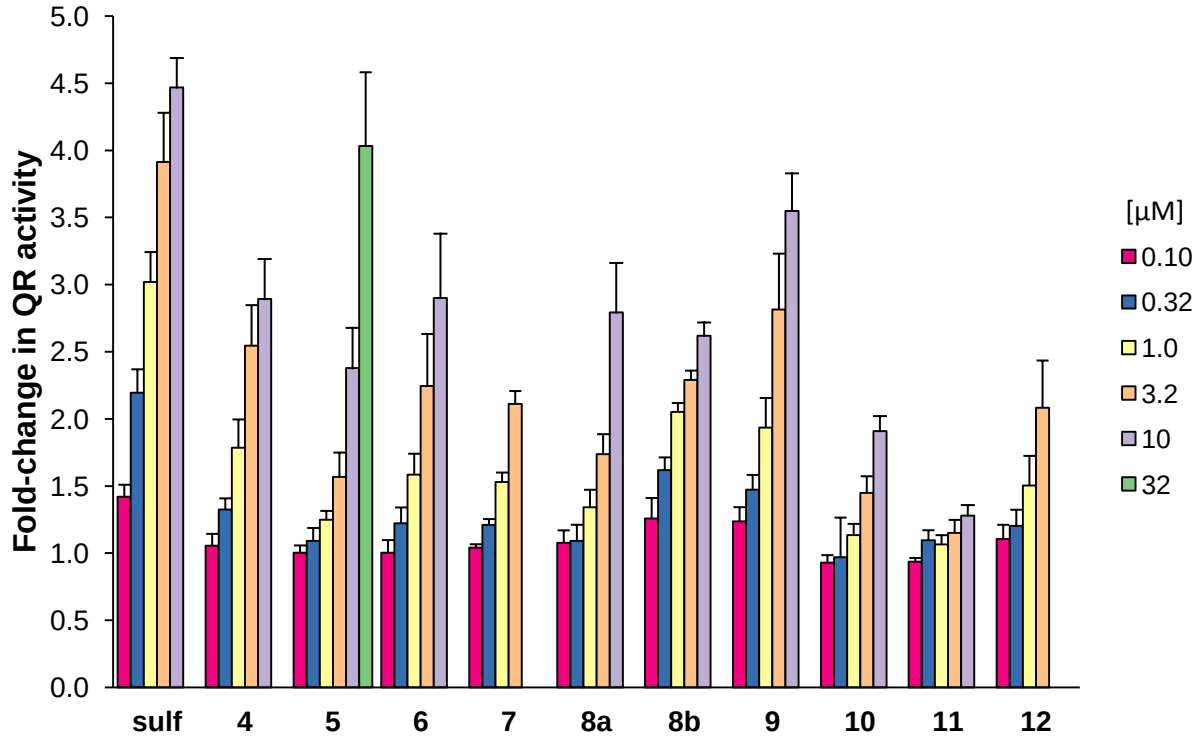

Figure 3-6. QR induction following exposure to *O. horridus* compounds. Hepa-1c1c7 cells were exposed to *O. horridus* compounds for 48 h and QR activity was compared to solvent treated controls. (*R*)-sulforaphane was included as a positive control. Results are the mean of at least three experiments ± the standard deviation.

The most potent inducer of QR from *O. horridus* was (3*S*,8*S*)-falcarindiol (**8a**). Strikingly, this diastereoisomer was approximately six times more potent than the (3*R*,8*S*) -falcarindiol (**8b**) diastereomer. The Nrf2-inducing activity of falcarindiol and a related polyacetylene panaxytriol was reported during the preparation of a manuscript of this work (Lee et al. 2009; Ohnuma et al.

2009). However, the former study did not report falcarindiol-configuration(s), nor the important difference in potency of the diastereomers.

The sesquiterpene (*E*)-nerolidol (**11**) was isolated and identified due to its abundance in a potent fraction (fraction J). Although previously shown to possess anti-inflammatory activity (Tung et al. 2008), (*E*)-nerolidol had no activity in the QR bioassay, nor did this compound display synergy when tested at a concentration of 10 µM with falcarindiol (**8**) or oplopandiol (**9**) (data not shown).

Table 3-4. Summary of bioassay results for *O. horridus* compounds.

Compound	QR inducing activity CD[a] (µM)	Cell viability IC_{50}[b] (µM)	CI IC_{50}/CD
(*R*)-sulforaphane	0.24 ± 0.05	21.2 ± 3.0	88
falcarintriol (**4**)	1.6 ± 0.8	15.4 ± 4.0	9.6
1,2-dihydrofalcarintriol (**5**)	6.7 ± 1.7	> 32	> 4.8
falcarindiol-acetate (**6**)	2.3 ± 1.0	18.4 ± 2.0	8.0
1,2-dihydrofalcarindiol-acetate (**7**)	12.4 ± 2.0	> 32	> 2.6
(3*S*,8*S*)-falcarindiol (**8a**)	0.85 ± 0.22	4.5 ±3.5	5.3
(3*R*,8*S*)-falcarindiol (**8b**)	4.8 ± 0.5	> 10	> 2.1
oplopandiol (**9**)	1.2 ± 0.4	14.2 ± 7.9	12
(16*R*)-falcarinol-acetate (**10**)	N/A[c]	14.2 ± 7.5	-
trans-nerolidol (**11**)	N/A[c]	>32	-
(3*R*)-falcarinol (**12**)	N/A[c]	5.2 ± 0.7	-

[a] refers to the concentration required to double activity of the enzyme QR relative to DMSO treated controls.
[b] refers to the concentration required to reduce cell viability to 50% in Hepa-1c1c7 cells.
[c] N/A indicates maximal magnitude of activation less than two-fold.

3.3.3. Additional polyacetylenes from *A. nudicaulis* further define polyacetylene structure-activity relationships

The goal of fractionation of the *A. nudicaulis* methanolic root extract was to identify additional QR-inducing C_{17}-type polyacetylenes and investigate structure-activity relationships. Therefore, in addition to pursuing the most active fractions, all abundant compounds with UV and mass spectra characteristic of C_{17}-type polyacetylenes were isolated. Fractionation of the *A. nudicaulis* extract is summarized in Figure 3-7.

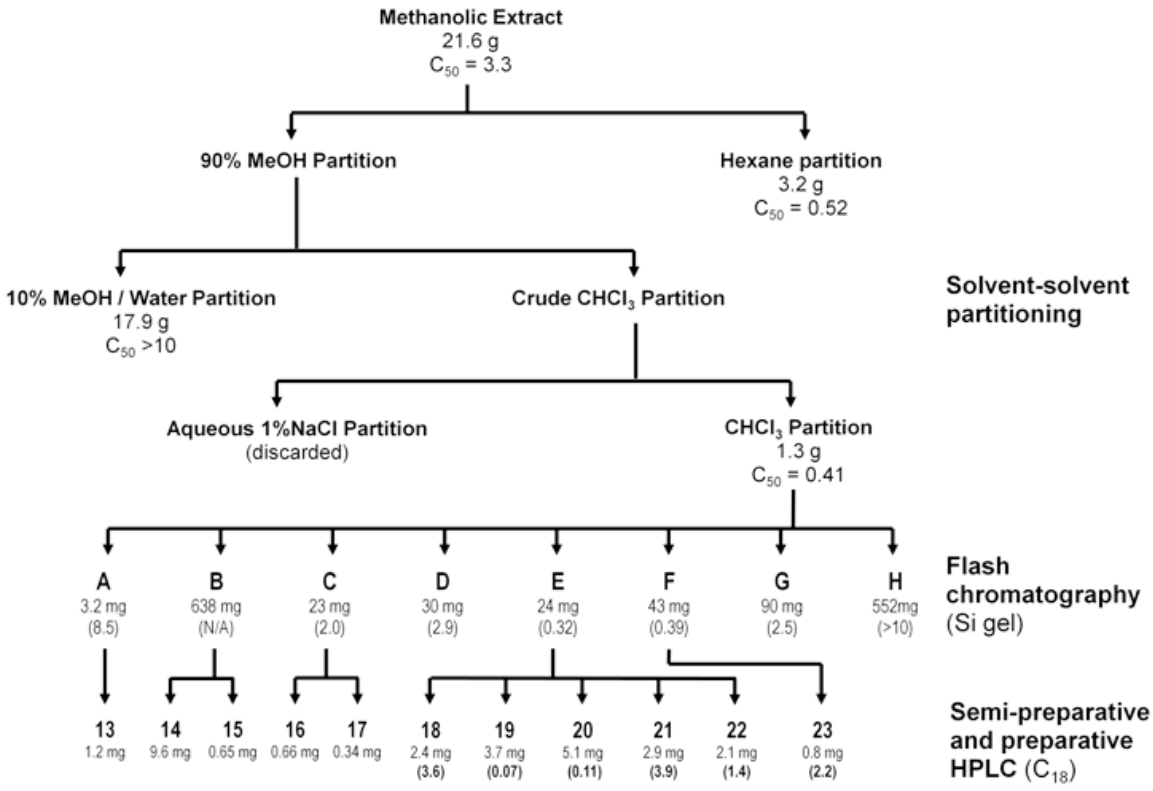

Figure 3-7. Separation scheme for methanol extract of *A. nudicaulis* roots. Concentrations required to double QR activity (CD) or concentration required to increase QR activity by 50% (C_{50}), are indicated in µg/mL in brackets.

As was the case for *O. horridus*, a multitude of bioactive C_{17}-type polyacetylenes were present in the chloroform partition of *A. nudicaulis.* Eleven of these were isolated and identified following silica gel flash chromatography, preparative reverse phase HPLC and semi-preparative reverse phase HPLC (Figure 3-8).

Although the structures of the polyacetylenes isolated from *A. nudicaulis* (Figure 3-8) closely resembled those from *O. horridus*, only two (falcarinol (**13**) and falcarinol-acetate (**17**)) of the 11 compounds identified were also isolated from *O. horridus.* Of the compounds isolated, one (epoxyoplopandiol (**20**)) was novel, none were previously described from this plant, and none were previously identified as QR inducers. One distinct feature of several of the *A. nudicaulis* polyacetylenes was an epoxide group (position 9,10 in panaxydol (**14**)).

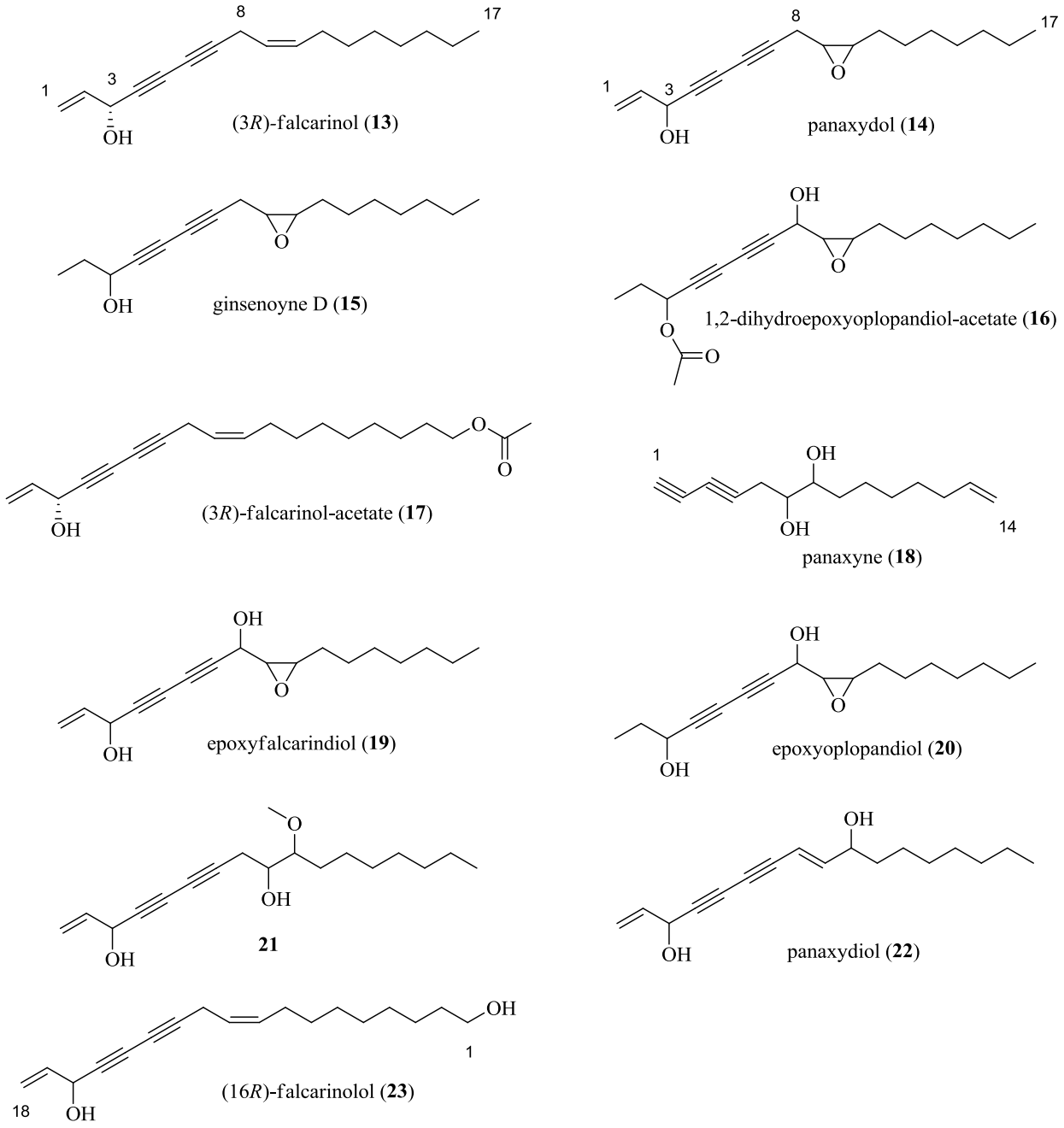

Figure 3-8. Compounds isolated from *A. nudicaulis.*

The most abundant polyacetylene was panaxydol (**14**). Lu *et al.* (1998) have reported the configuration of this compound isolated from *Panax ginseng*, to be (3*R*, 9*R*, 10*S*). The specific rotation of panaxydol (**14**) (-113) in deuterated chloroform was similar to that reported for the (3*R*, 9*R*, 10*S*) stereoisomer (-96.1) by Lu *et al.* (1998). As eight stereoisomers are possible for this compound and Araliaceae plants have been shown to produce polyacetylenes with both 3*R*

and 3*S* configurations, I am cautious about assigning a configuration to panaxydol on the basis of optical rotation alone. On the other hand, falcarinol isolated from *A. nudicaulis* (**13**) has only a single stereocenter and therefore levorotary (negative) optical rotation for this compound is enough to assign a (3*R*) configuration on the basis that it matches the report by Zheng et al. (1999) for (3*R*)-falcarinol. Similarly the levorotary optical rotations for falcarinol-acetate (**17**) and falcarinolol (**23**) imply an (*R*) configuration for these compounds. The configuration of the remaining polyacetylenes could not be deduced based on optical rotation due the presence of multiple stereocenters.

The QR bioassay results for purified *A. nudicaulis* polyacetylenes are presented in Figure 3-9 and a summary of bioassay results is presented in Table 3-5. The potency of epoxyfalcarindiol (**19**) (CD value of 0.41 µM) exceeded that of the most potent polyacetylene isolated from *O. horridus*, (3*S*,8*S*)-falcarindiol (**8a**) (CD value of 0.85 µM). The structure of epoxyfalcarindiol (**19**) differed from falcarindiol (**8**) by an epoxide in the place of a double bond in falcarindiol (**8**).

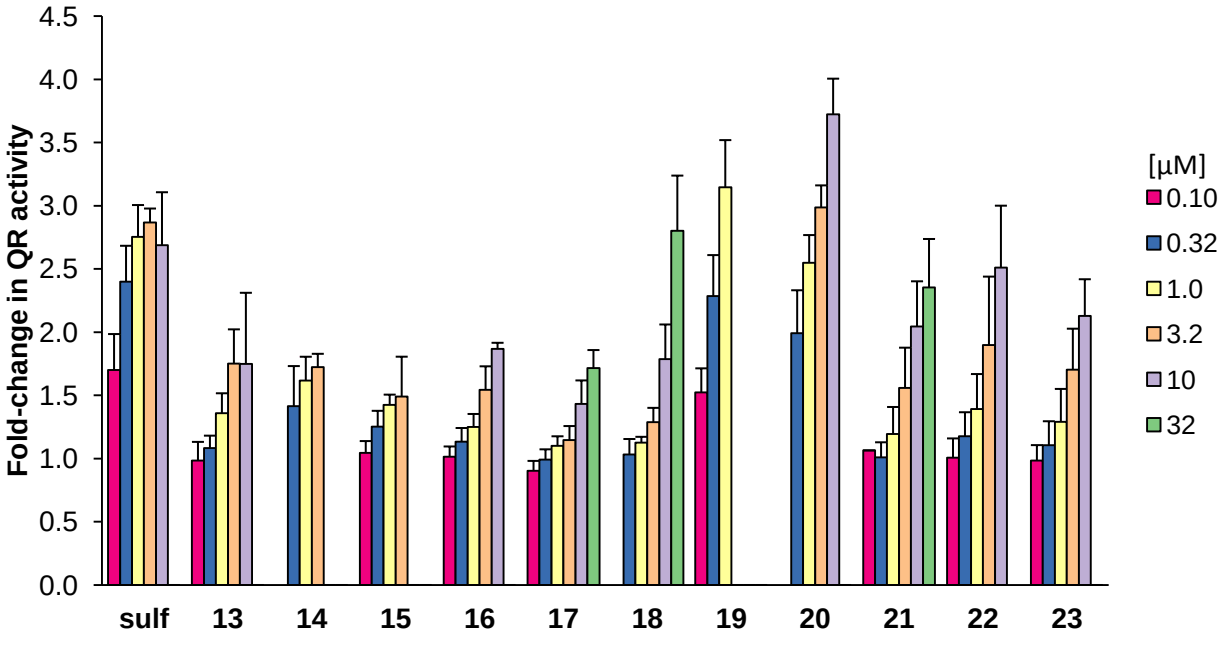

Figure 3-9. QR induction following exposure to *A. nudicaulis* polyacetylenes. Hepa-1c1c7 cells were exposed to *A. nudicaulis* polyacetylenes for 48 h and QR activity was compared to solvent treated controls. (*R*)-sulforaphane was included as a positive control. Results are the mean of at least three experiments ± the standard deviation.

Table 3-5. Summary of bioassay results for *A. nudicaulis* compounds.

Compound	QR inducing activity CD[a] (μM)	Cell viability IC_{50}[b] (μM)	CI IC_{50}/CD
(*R*)-sulforaphane	0.17 ± 0.08	5.8 ± 1.5	33.5
falcarinol (**13**)	N/A[c]	6.3 ± 0.6	-
panaxydol (**14**)	N/A[c]	2.6 ± 1.6	-
ginsenoyne D (**15**)	N/A[c]	3.1 ± 1.2	-
1,2-dihydroepoxyoplopandiol- acetate (**16**)	N/A[c]	16.1 ± 0.5	-
falcarinol-acetate (**17**)	N/A[c]	>32	-
panaxyne (**18**)	16.1 ± 7.3	74.2 ± 7.1	4.6
epoxyfalcarindiol (**19**)	0.24 ± 0.10	6.5 ± 1.3	27.2
epoxyoplopandiol (**20**)	0.41 ± 0.17	10.9 ± 1.7	26.5
21	13.2 ± 12.5	14.6 ± 5.3	1.1
panaxydiol (**22**)	5.3 ± 3.3	18.6 ± 13.1	3.5
falcarinolol (**23**)	7.8 ± 4.8	14.8 ± 1.1	1.9

[a] refers to the concentration required to double activity of the enzyme QR relative to DMSO treated controls.
[b] refers to the concentration required to reduce cell viability to 50% in Hepa-1c1c7 cells.
[c] N/A indicates maximal magnitude of activation less than two-fold.

Although the exact configuration was not determined for all of the compounds isolated, the same general correlations between structure and activity that were observed with *O. horridus* polyacetylenes were observed for the *A. nudicaulis* polyacetylenes. Table 3-6 summarizes the structure activity relationships of the *A. nudicaulis* and *O. horridus* polyacetylenes.

Maximal QR-inducing activity required the presence of a second hydroxyl group (position 8 in falcarindiol) flanking the conjugated triple bonds, a terminal alkene (1,2 position in falcarindiol), an epoxide group in place of the double bond (9,10 in falcarindiol) and lack of modification to the aliphatic terminus.

Information regarding the metabolism of falcarindiol-type polyacetylenes in humans is lacking but it is possible that the epoxylated compounds could be metabolites of their corresponding alkenes. As (3*S*,8*S*)-falcarindiol showed substantially increased QR-activity (six-fold greater) compared to (3*R*,8*S*)-falcarindiol, it would be interesting to compare stereoisomers of epoxyfalcarindiol (**19**) for activity. If the configuration of the 3-hydroxyl group of epoxyfalcarindiol (**19**) isolated in this study was (*R*), there exists the possibility that the (3*S*) stereoisomer may possess even higher activity. A six-fold increase in activity of epoxyfalcarindiol (**19**) would lead to a CD value of only 40 nM and would place it in a very select group of compounds with CD values in the tens of nM range.

Table 3-6. Summary of structure activity relationships amongst polyacetylenes isolated from *O. horridus* and *A. nudicaulis.*

	CD value[a]			IC_{50} value[b]		
	with	without	ratio	with	without	ratio
Hydroxyl group (position 8)						
8b v **12**	4.8	N/A	-	>10	5.2	>1.9
6 v **10**	2.3	N/A	-	18.4	14.2	1.2
19 v **14**	0.24	N/A	-	6.5	2.6	2.5
20 v **15**	0.41	N/A	-	10.9	3.1	3.5
Mean	*4.5*	*N/A*	-	*>11.5*	*6.3*	*2.4*
Terminal double bond (position 1)						
4 v **5**	1.6	6.7	**0.2**	15.4	>32	<0.5
6 v **7**	2.3	12.4	**0.2**	18.4	>32	<0.6
8a v **9**	0.85	1.2	**0.7**	4.5	14.2	0.3
14 v **15**	N/A	N/A	-	2.6	3.1	0.8
19 v **20**	0.24	0.41	**0.6**	6.5	10.9	0.6
Mean	*1.2*	*5.2*	***0.4***	*9.5*	*>18.4*	*<0.6*
Epoxide instead of double bond (position 9,10)						
19 v **8a**	0.24	0.85	**0.3**	6.5	4.5	1.4
20 v **9**	0.41	1.2	**0.3**	10.9	14.2	0.8
14 v **13**	N/A	N/A	-	2.6	6.3	0.4
Mean	*0.3*	*1.0*	***0.3***	*6.7*	*8.3*	*0.9*
Hydroxyl group (position 17/18)						
4 v **8a**	1.6	0.85	**1.9**	15.4	4.5	3.4
5 v **9**	6.7	1.2	**5.6**	>32	14.2	>2.3
23 v **13**	7.8	N/A	-	14.8	6.3	2.3
Mean	*4.2*	*1.0*	***4.0***	*20.7*	*8.3*	*2.7*
Acetate group (position 17)						
6 v **8a**	2.3	0.85	**2.7**	18.4	4.5	4.1
7 v **9**	12.4	1.2	**10.3**	>32	14.2	>2.3
Mean	*7.4*	*1.0*	***7.2***	*>25.2*	*9.4*	*>3.1*

[a] refers to the concentration required to double activity of the enzyme QR relative to DMSO treated controls.
[b] refers to the concentration required to reduce cell viability to 50% in Hepa-1c1c7 cells.
[c] indicates maximal magnitude of activation less than two-fold

3.3.4. QR-inducing flavonoids from the methanolic *A. latifolia* root extract

Disappointingly, the level of QR induction from greenhouse-grown *A. latifolia* plants (maximal induction of 1.1-fold for the root extract) was greatly reduced compared to the extracts from wild-grown material (2.52-, and 1.76-fold for root and aerial tissue extracts, respectively). Although the reasons for this are not clear, I suspect that a lack of ecological interactions in the

controlled growth environment led to decreased production of the active compounds. The production of many phytochemicals is reserved until elicited by wounding or other stimuli (Harborne 1999). This may decrease the associated metabolic expense of their production. Spraying the crop with jasmonic acid, a regulator of plant defense metabolism, could potentially overcome this deficiency in future studies (Gundlach et al. 1998).

I reasoned that, since there was still some activity, the compounds responsible for activity in the wild-grown material may still be present in low amounts and that bioassay-guided fractionation may yield interesting results. Indeed, following solvent-solvent partitioning of the root extract (Figure 3-10), I noted a substantial increase in the activity of the chloroform/dichloromethane partition (maximal induction of 1.7-fold).

During the solvent-solvent partitioning of the root extract I experimented with using the less toxic compound dichloromethane in place of chloroform. However, I found that chloroform had a greater capacity for extracting compounds in the polarity range of interest. The dichloromethane and chloroform partitions were combined.

Fractionation of the dichloromethane/chloroform partition using silica gel flash chromatography revealed that the least polar fractions (A, B and C) contained the active constituents. These fractions were subjected to a C_{18} SPE cartridge to remove very non-polar compounds and provide a crude separation of the remaining compounds prior to purification by semi-preparative C_{18} HPLC. Although the yields were low (0.59 - 1.94 mg), a total of 14 compounds were isolated. Due to the low yields of these compounds, NMR analysis following the QR bioassay would not be possible. Therefore I worked on solving the structures of the most abundant compounds and collected basic NMR spectra for the remaining compounds prior to completing the QR bioassay.

The first compound, identified on the basis of ^{1}H and ^{13}C, HMBC, heteronuclear multiple quantum coherence (HMQC) and NOE NMR experiments, was a novel C-methyl flavanone, **24**. Similar to the C-methyl isoflavone, abronisoflavone, that was previously isolated from this plant, **24** was also C-methylated. In addition to the C-methyl group at position 6, **24** also possessed a C-methyl at position 8. Although C-methyl flavonoids are uncommon, this is not the first report of a C-methyl flavanone (Wollenweber et al. 2000).

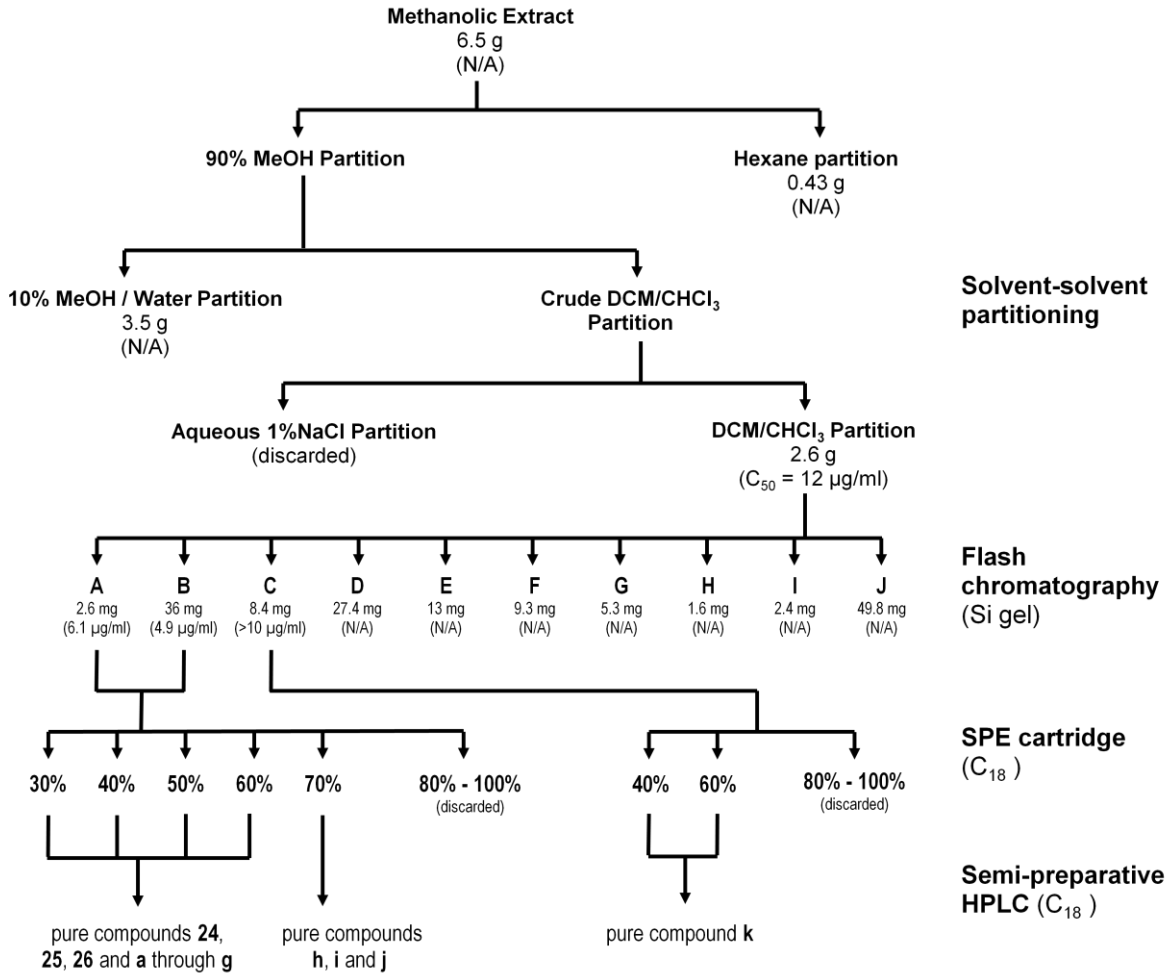

Figure 3-10. Separation scheme for methanol extract of *A. latifolia* roots. Concentrations required to double QR-activity (CD) or concentrations required to increase QR-activity by 50% (C_{50}) are indicated in brackets. For the SPE cartridge clean-up the percentage composition of the mobile phase (methanol/water) is provided for each fraction.

NMR spectra of the second compound, **25**, closely resembled **24** with the exceptions of missing a 3H singlet at ~2.0 ppm and a new 1H singlet at 6.12 ppm. When combined with accurate mass measurement, these observations indicated that this compound was lacking one of the C-methyl groups found in **24**. I did not attempt to confirm the position of this methyl group as this compound proved to be inactive (see below).

Of the 14 isolated compounds eight had similar NMR and UV spectra to compounds **24** and **25** consistent with these compounds also being flavanones. The structures of these compounds were not solved, however, on the basis of a lack of activity in the QR bioassay.

Unlike the flavanones **24** and **25**, which had a single rounded UV maximum at ~292 nm, five of the other compounds (**f**, **g**, **j**, **k** and **26)** isolated from the active fraction had a different absorbance spectrum with a peak at ~278 nm and shoulders at 300 nm and 340 nm. The most abundant of these compounds (1.43 mg) was identified as boeravinone E (**26**), a rotenone, on the basis of ^{1}H, ^{13}C and HMBC NMR experiments (Figure 3-11).

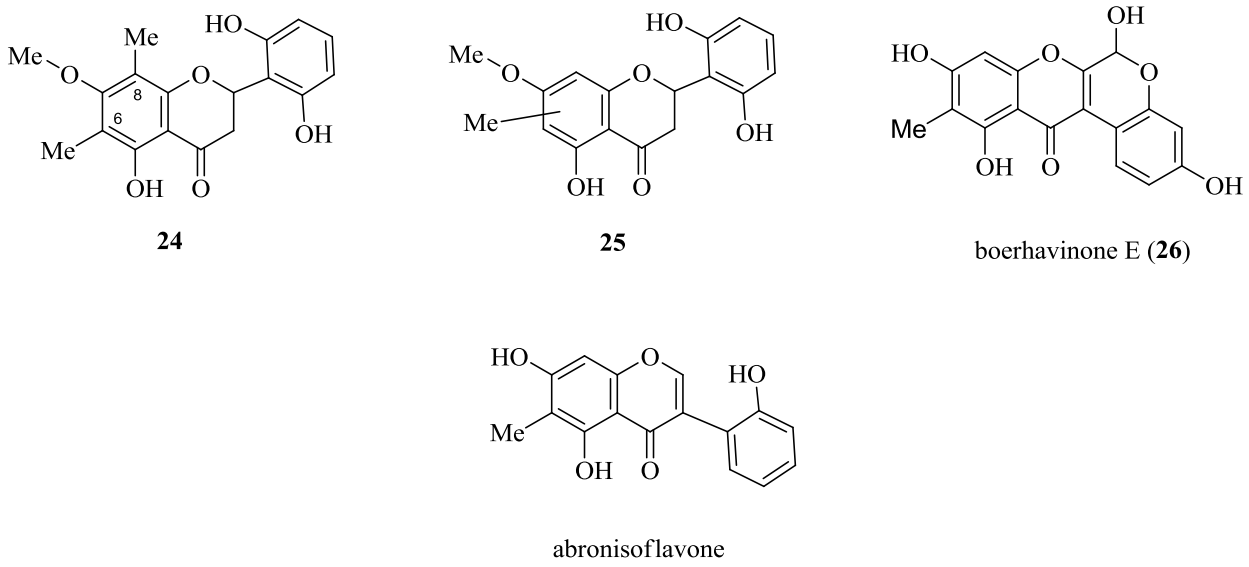

Figure 3-11. Compounds isolated from *A. latifolia*. Abronisoflavone was previously identified from *A. latifolia* (Wollenweber et al. 1993).

All 14 isolated compounds were assayed for QR-inducing activity (Figure 3-12). Only compound **k** caused an increase in QR activity greater than two-fold (CD value = 3.2 µg/mL or 10 µM (assuming mass of 324 Da)). Compound **f** was the next most active with a maximal level of induction of 1.9-fold achieved at 10 µg/ml. Both compounds **f** and **k** had UV absorbance spectra nearly identical to boeravinone E (**26**) indicating that these compounds possessed the same chromophore as boerhavinone E (**26**). NMR spectra for these compounds also shared the majority of signals with boerhavinone E (**26**) consistent with these compounds also being rotenones. However, similarly decorated isoflavones could have comparable UV and NMR spectra and I was unable to exclude such structural possibilities for compounds **f** and **k.**

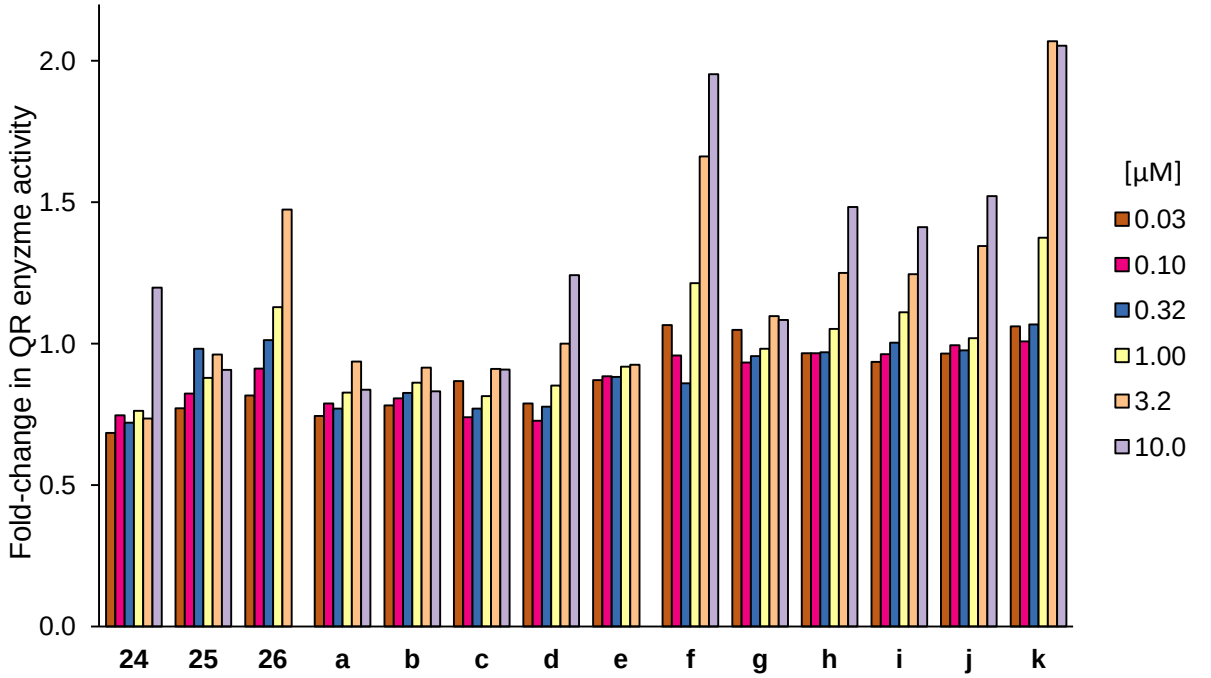

Figure 3-12. QR induction following exposure to *A. latifolia* compounds. Hepa-1c1c7 cells were exposed to *A. nudicaulis* polyacetylenes for 48 h and QR activity was compared to solvent treated controls. (*R*)-sulforaphane was included as a positive control. Results are the mean of a single experiment with two technical replicates.

Overall the spectral and QR data suggest that certain rotenones (and possibly isoflavones) are moderate QR inducers (10 μM is not groundbreaking), whereas C-methyl isoflavones such as **24** and **25** are very weak or inactive. These observations are consistent with the expected thiol-reactivity of these classes of flavonoids. Rotenones (boerhavinone E) or isoflavones (abronisoflavone) have an α,β-unsaturated carbonyl group that can act as a Michael addition acceptor whereas flavanones such as **24** and **25** do not.

Although many of the described Nrf2-activating flavonoids identified to date also possess a Michael acceptor functionality, it should be noted that flavonoids with ortho- or para-substituted hydroxyl groups can be oxidized to electrophilic quinones and may therefore modify Keap1 indirectly (Lee-Hilz et al. 2006). Additionally, several flavonoids are thought to activate QR through the aryl hydrocarbon receptor (Yannai et al. 1998). However, in this circumstance the lack of potency precludes further investigation into the mechanism of action of these compounds.

3.3.5. Induction of QR by cannabinoids from *C. sativa*

A methanolic extract of female 'Finola' hemp flowers was a weak inducer of QR in Hepa-1c1c7 cells (C_{50} ~ 15 µg/mL). Heat treatment of this extract converted a proportion of cannabinoids to their decarboxylated forms (data not shown) and resulted in greater QR induction (C_{50} ~7 µg/mL , CD ~ 15 µg/mL, maximal induction 2.8-fold) consistent with decarboxylated cannabinoids being the active components (Figure 3-13).

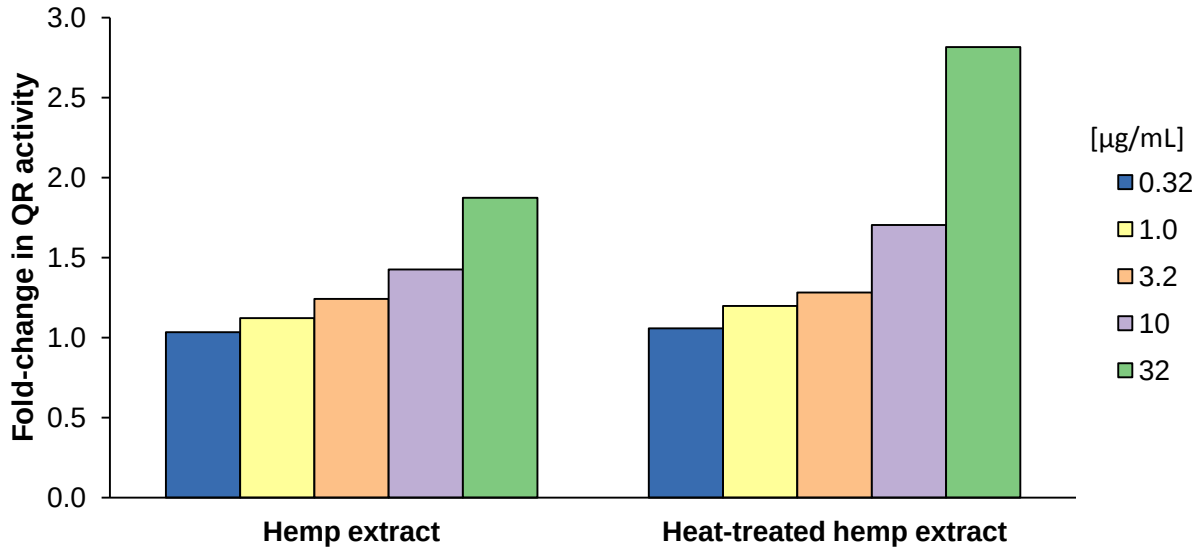

Figure 3-13. QR induction following exposure to hemp extracts. Hepa-1c1c7 cells were exposed to hemp extract for 48 h and QR activity was compared to solvent treated controls. The heated extract was exposed to 120ºC for 30 min to decarboxylate the acid forms of cannabinoids present in the extract. Result of a single experiment with two technical replicates.

To confirm whether cannabinoids were responsible for the QR-inducing activity of the hemp extract, I isolated the major cannabinoids CBDA and THCA and used heating followed by HPLC purification to isolate the corresponding decarboxylated cannabinoids CBD and THC (Figure 3-14). I found that it was much more efficient to heat crude extracts rather than purified CBDA or THCA when producing CBD and THC. Heating a dried 'Finola' extract at 120ºC for 30 min converted the majority of CBDA to CBD (data not shown).

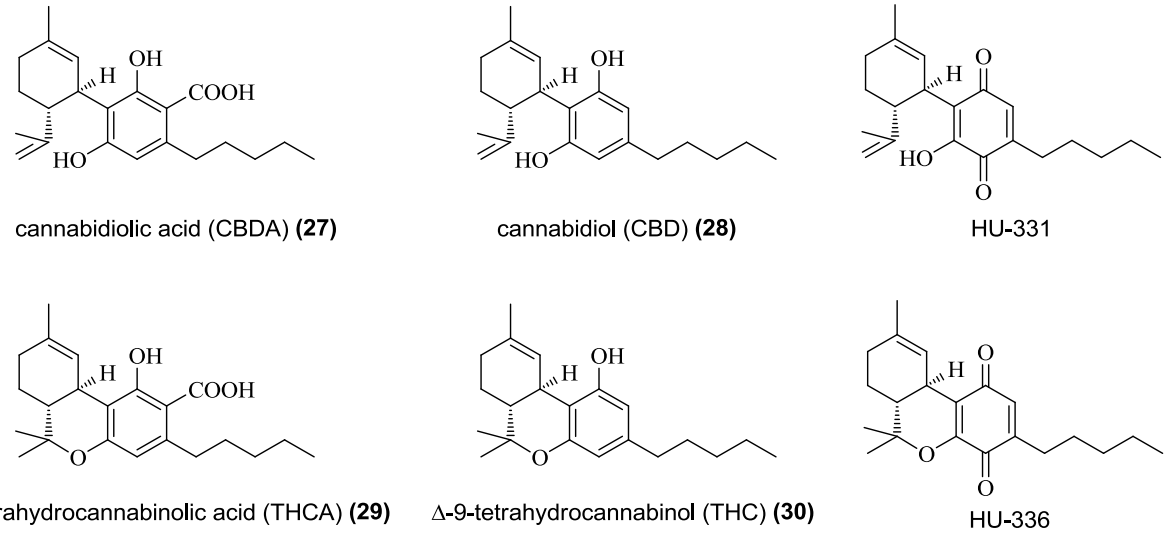

Figure 3-14. Compounds isolated from *C. sativa* and the derivatives HU-331 and HU-336.

The results of the QR bioassay for purified cannabinoids are given in Figure 3-15. A summary is provided in Table 3-7. All the cannabinoids tested displayed some degree of QR activation. CBDA and CBD treatment resulted in the greatest amplitude of QR activation at ~2.5-fold, whereas the maximal induction by THCA and THC was ~1.5-fold. In both cases the decarboxylated forms were more potent requiring approximately a tenth of the concentration of the carboxylated forms for maximal QR induction. CBD displayed a CD value of approximately 1.6 μM (0.63 μg/mL).

Although cannabinoid receptors are present in mouse liver (Osei-Hyiaman et al. 2008), current evidence does not suggest that cannabinoid receptors modulate the expression of QR by cannabinoids. Furthermore, CBD displays only very weak affinity for CB receptors compared to THC and was a much more effective QR inducer than THC. Therefore it is unlikely that cannabinoid receptors are mediating the activation of QR.

Since CBD and THC are not electrophilic, I would not expect these compounds to activate Nrf2 directly. Inclusion of the small thiol N-acetylcysteine in the culture medium failed to reduce the activity of CBD or THC. However, the phenolic moieties of CBD and THC can be oxidized to electrophilic quinones that would be expected to be highly thiol-reactive. Examples of non-electrophilic substances being oxidized to Nrf2-activating electrophiles are not uncommon and include carnosic acid, acetominophen and polyunsaturated fatty acids (Gao et al. 2007; Copple et al. 2008; Satoh et al. 2008).

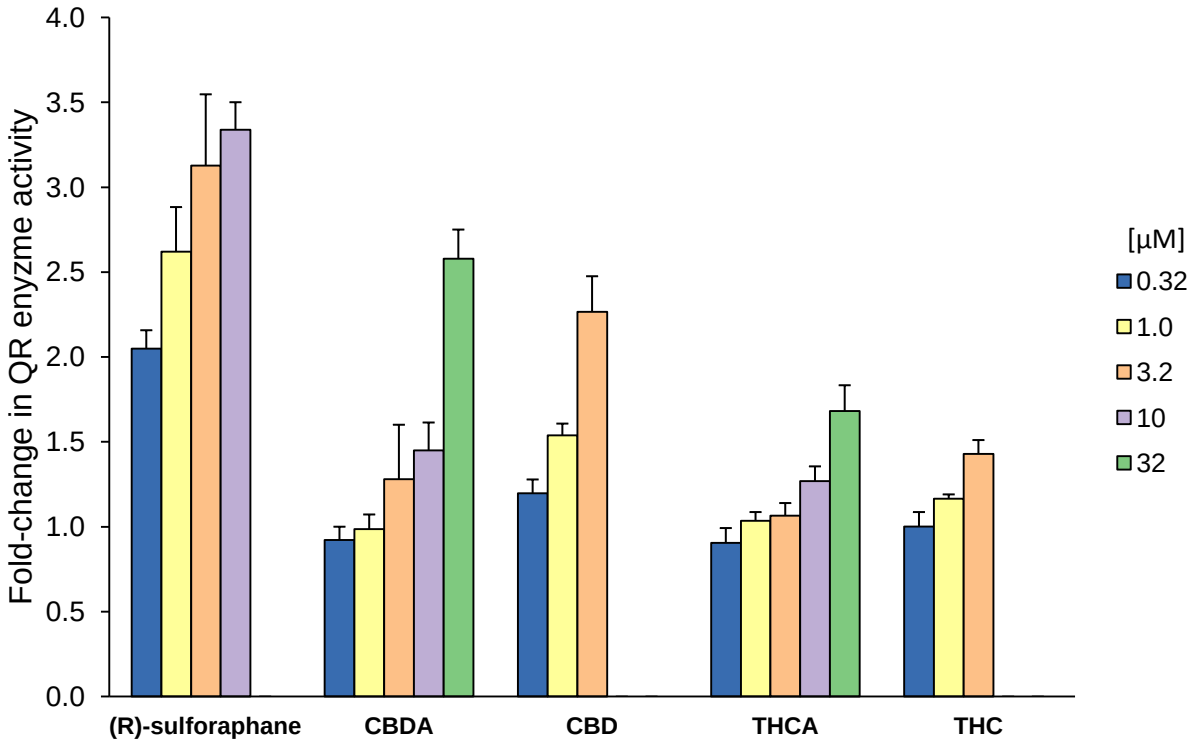

Figure 3-15. QR induction following exposure to cannabinoids. Hepa-1c1c7 cells were exposed to cannabinoids for 48 h and QR activity was compared to solvent treated controls. (*R*)-sulforaphane was included as a positive control. Results are the mean of at least three independent experiments ± the standard deviation.

Table 3-7. Summary of bioassay results for *C. sativa* cannabinoids and the positive control (*R*)-sulforaphane.

Compound	QR inducing activity CD (µM)	Cell viability IC_{50} (µM)	CI IC_{50}/CD
(*R*)-sulforaphane	0.27 ± 0.04	11.5 ± 3.8	42.6
27 CBDA	20.8 ± 1.0	29.9 ± 10.6	1.4
28 CBD	1.6 ± 0.8	4.8 ± 0.3	3.0
29 THCA	N/A[a]	63.2 ± 5.9	-
30 THC	N/A[a]	5.4 ± 0.3	-

[a] N/A indicates maximal magnitude of activation less than two-fold

Electrophilic metabolites of CBD, such as HU-331 (Figure 3-14) are produced via metabolism by CYP P450 3A enzymes *in vivo* (Bornheim et al. 1998) or *in vitro* under basic, oxidizing conditions (Kogan et al. 2004). Such derivatives of CBD form the colored basis of the 'Beam test' for marijuana (Mechoulam et al. 1968). HU-331 can inactivate CYP3A enzymes by

covalent modification, which is suspected to occur at cysteine residues (Bornheim et al. 1998; Yamaori et al. 2011).

In contrast to the electrophilic derivative of CBD (HU-331), the analogous derivative of THC (HU-336, Figure 3-14) requires stronger oxidizing conditions for production *in vitro* and does not appear to occur *in vivo*. The free hydroxyl in CBD appears to be required for the enzymatic production of HU-331 by CYP3A enzymes (Bornheim et al. 1993). The decreased tendency for THC to form electrophilic intermediates is consistent with the hypothesis that cannabinoids activate QR via reaction with Keap1 thiols (indirectly via electrophilic intermediates) because THC consistently displayed decreased activity in the QR bioassay compared to CBD.

3.4. Conclusions

Of the two methods used to guide fractionation of potential Nrf2 activators, the QR bioassay was the most reliable. The only compound isolated using thiol reactivity as a guide, coniferyl ferulate (**1**), proved to be inactive in the QR bioassay.

The prominence of the coniferyl ferulate-glutathione product in the thiol-screening assay highlights an important shortcoming of the thiol-reactivity-based approach. Thiol-reactive non-Nrf2-inducing compounds such as coniferyl ferulate may mask less abundant Nrf2 activators through shear abundance and by out-competing the less abundant compounds for the model thiol. Although nothing can be done regarding the abundance of non-active compounds, an excess of model thiol could ensure that all thiol-reactive compounds are represented in the thiol-screening assay. Even though I attempted to include an excess of glutathione in the reactions (2:1 molar ratio of glutathione to extract compounds based on an average molecular mass of 200 Da of compounds in the extract), I would include a larger excess of thiol in any future implementation of this approach.

A further disadvantage to using the thiol-screening assay to identify novel Nrf2-activating agents is that, since it is based on a single mechanism of action, compounds that act through novel mechanisms would be overlooked. Compounds that behave as prodrugs, that is compounds that require metabolic activation, would also be overlooked using this method in its current form.

One disadvantage of the QR bioassay is the variability inherent in the assay itself. For example, the dose-reponses for (*R*)-sulforaphane shown in Figures 3-6 and 3-8 differ in the maximal induction achieved. Cultures started from different stocks sometimes displayed differences in absolute magnitude of their responses. Importantly, the CD value was similar between the two groups of experiments. This result emphasizes the importance of including positive controls in the type of experiment so that results between different sets of experiments can be compared directly.

The variety of QR inducers isolated highlights the flexibility of the biological system(s) controlling QR activity. Aside from the cannabinoids, all of the active compounds isolated have electron-deficient centers that could potentially react with Keap1 thiols *in vivo*. For compounds such as rotenones, isoflavones and phthalides that possess conjugated unsaturated carbonyl groups (Michael acceptor functionalities) I expect that these functionalities, if any, would be involved in Keap1-adduction. In the case of the polyacetylenes the site of thiol-reactivity is less clear. The reactivity of polyacetylenes with model thiols and recombinant Keap1 are discussed in Chapter 4.

Although the QR bioassay has proven reliable for identifying Nrf2 activators, it does not predict with certainty that QR inducers are operating through Nrf2. Aside from monitoring Nrf2 nuclear translocation directly, confirming that the abundance of Nrf2 transcriptional targets is elevated and the abundance of AhR transcriptional targets is decreased can provide additional evidence to support to the hypothesis that these compounds activate QR via Nrf2. Such transcriptional studies are presented in Chapter 5.

The ecological functions that the above compounds serve in the plant are elusive. As all the compounds isolated were obtained from non-fruiting and non-flowering tissues, it seems unlikely that these compounds would serve the purpose of attracting seed dispersers or pollinators. I think the most reasonable putative functions are as anti-feedants, anti-microbials or allelochemicals (compounds that inhibit or interfere with adjacent plants). For instance, the polyacetylenes isolated from *O. horridus* were highly abundant in the inner stem bark. The outer bark of *O. horridus* displays a menacing array of spines. The selective pressure that led to the development of the spines of *O. horridus* may have also led to the production of these compounds in the inner stem bark. Also of note is the capability for polyacetylenes such as

falcarinol to cause contact dermatitis (Leonti et al. 2010) and contribute to the unpleasant taste of old carrots (Czepa et al. 2003). Perhaps the polyacetylenes work in concert with the spines to synergistically cause irritation to herbivores.

It is not necessary, however, for a given phytochemical to serve a single ecological role. Indeed, antifungal activities for falcarinol-type polyacetylenes have been reported as have allelochemical activities for more distantly related polyacetylenes (Stevens 1986; Olsson et al. 1996).

Multi-faceted advantages for phytochemical groups may aid in explaining the tremendous phytochemical diversity found in the world's flora. A given metabolite may at first provide an advantage under one set of conditions and later on provide a building block towards a metabolite that confers a complimentary advantage. Compounds or groups of compounds that have multiple ecological functions (and therefore multiple cellular targets) may be selected for on the basis of efficiency. However, specificity rather than promiscuity is usually preferred for drug candidates and investigational drugs. Examination of the cellular targets of a panel of QR inducers in mammalian cells is one of the goals of examining global changes in gene expression described in Chapter 5.

CHAPTER 4

THE MECHANISM OF ACTION OF ARALIACEAE POLYACETYLENES

4.1. Introduction

The data reported in Chapter 3 revealed the structures and potencies of numerous QR inducers. Thiol residues of Keap1 are thought to be the primary site of action for QR inducers that function through Nrf2 activation. Although the presence of electrophilic functionalities in the majority of these compounds are consistent with a mechanism of action involving modification of Keap1 and activation of Nrf2, additional mechanisms such as activation of AhR may be responsible for QR induction by these compounds. This chapter describes studies aimed at testing the hypothesis that the C_{17}-polyacetylenes isolated from *O. horridus* and *A. nudicaulis* induce QR by modifying the structure of Keap1. These studies include assays to test the thiol-reactivity of representative polyacetylenes using low molecular weight thiols and recombinant Keap1 as well as a study of the effects of polyacetylenes on the secondary structure of Keap1.

4.1.1. Low molecular weight model thiols

Detection of compounds that react with glutathione *in vitro* using electrospray ionization-tandem MS (ESI-MS/MS) was discussed in Chapter 3. In addition to glutathione, methyl thioglycolate and cysteine (Figure 4-1) have also been used to study thiol-reactivity *in vitro* (Beck et al. 1995; Johnson et al. 2001; Dieckhaus et al. 2005).

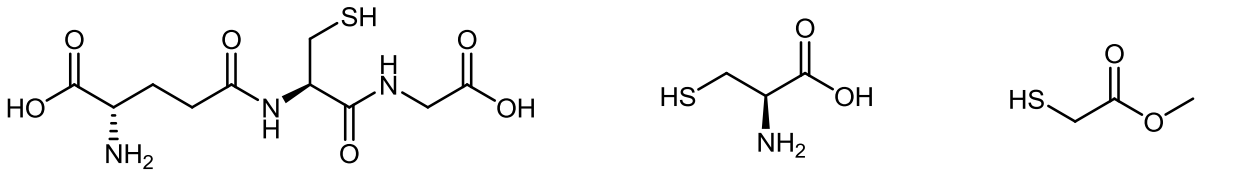

glutathione (*L*)-cysteine methyl thioglycolate

Figure 4-1. Structures of low molecular weight model thiols used to test thiol reactivity of QR inducers.

UV absorbance data and fragmentation patterns detected by MS can provide some structural information for the product of a QR activator and model thiol. However, NMR-based analysis can often provide an unequivocal solution for the product structure. Cysteine is a

preferred model thiol for NMR studies as it contributes a low number of signals to the product and therefore facilitates structure elucidation.

Although Keap1 possesses numerous cysteine residues, these residues vary in their reactivity with Nrf2 activators. The intrinsic pKa of cysteine in an average protein is about 9.1 meaning that, at physiological pH (7.0-7.4), the percentage ionization of these residues would be ~2% and that these residues would not be highly nucleophilic (Harris et al. 2002). The most reactive cysteines of Keap1 are flanked by basic amino acids that increase the effective pH environment leading to an increase in the nucleophilicity of the cysteine thiols by stabilization of the ionized state, the thiolate ion (Snyder et al. 1981). I have chosen to use a higher than physiological pH (8.0 or 10.0) when examining the reactivity of QR inducers with cysteine in order to emulate the reactivity of the most reactive Keap1 residues and provide greater reaction yields.

4.1.2. Keap1

Reactivity with model thiols may serve as a general indicator whether a Keap1-based mechanism of action is feasible. However, demonstrating reactivity with recombinant Keap1 will provide strong evidence for this mechanism of action. I have used MS to measure changes in the mass of Keap1 following incubation with QR inducers as a means of measuring the reactivity of these compounds with Keap1.

4.1.2.1. Production of recombinant Keap1 protein

Recombinant Keap1 is the most practical means to obtain Keap1 for biophysical studies. Several expression and purification systems have been reported for Keap1(Dinkova-Kostova et al. 2002; Dinkova-Kostova et al. 2005; Eggler et al. 2005; Hong et al. 2005). Expression hosts include *E. coli*, insect cells and human embryonic kidney-293 cells. Purification strategies have included ammonium sulphate precipitation, immobilized metal-affinity chromatography, and gel filtration. In general, Keap1 has been a difficult protein to purify. Using a low temperature during expression, minimal media and carefully controlling the pH of the harvest medium have been reported to increase the yield of Keap1 (Dinkova-Kostova et al. 2002; Dinkova-Kostova et al. 2005; Eggler et al. 2005; Hong et al. 2005).

4.1.2.2. MALDI-TOF-based detection of Keap1 adduction

Detecting changes in the mass of Keap1 resulting from covalent modification by small molecules is fundamentally different than detecting alkylation of small molecules. The molecular weight of a small molecule such as falcarindiol (260 Da) is small relative to that of Keap1 (70 kDa) and therefore requires a high resolution detector, such as one based on time-of-flight (TOF), for accurate measurement. Furthermore, ionization of large proteins is also subject to different constraints than small molecules. Although proteins can be easily ionized under electrospray conditions, a variety of charge states typically occur. These charge states can be useful when the protein being ionized is homogenous. However, when dealing with a protein population with varying degrees of modification (as may be the case when incubating with a small molecule) the deconvolution of this data becomes increasingly complex and impractical. MALDI is an ionization method used extensively in proteomics that involves laser excitation of a matrix that in turn ionizes the protein to be analyzed. In contrast to electrospray ionization, MALDI ionization typically yields singly-charged species and thereby simplifies interpretation. Therefore I have chosen to use MALDI-TOF for analysis of Keap1 modification by small molecules.

4.1.2.3. Circular dichroism-based detection of Keap1 modification

Nrf2 activators are thought to cause a conformational change in Keap1. Therefore, I have also examined changes in secondary structure of Keap1 in response to putative Nrf2 activators (falcarindiol stereoisomers) using circular dichroism spectroscopy (CD spectroscopy). CD spectroscopy involves measuring differences in absorption of left and right circularly polarized light over a range of wavelengths. Secondary structures such as α-helices and β-sheets display characteristic absorption patterns for circularly polarized light and therefore changes in the secondary structure of a protein can be calculated from changes in the protein's circular dichroism spectrum (Greenfield 2007).

4.2. Materials and methods

4.2.1. General experimental procedures

Cell culture reagents were obtained from Invitrogen. Unless otherwise specified, chemicals were obtained from Sigma-Aldrich. Sodium dodecylsulfate polyacrylamide gel electrophoresis (SDS-PAGE) was conducted according to Sambrook *et al* (1989).

4.2.2. Detecting reactivity of QR inducers with low molecular weight model thiols

Analytical scale reactions of QR inducers with low molecular weight model thiols followed the same procedure as described in Chapter 3 except where methyl thioglycolate or cysteine was used in place of glutathione and when conditions (pH, temp, incubation time) were altered as described.

For the preparative isolation of the major reaction product of oplopandiol (**16**) and cysteine, a 4 mL reaction consisting of 33 mM oplopandiol, 250 mM cysteine, 25 mM Tris-Cl, pH 10.0, and 40% (v/v) acetonitrile was incubated in the dark for 17 h at 30°C. The most abundant product, **31**, was isolated by isocratic (69% methanol/water) preparative HPLC on a preparative 1100 system (Agilent) equipped with a fraction collector, a flow rate of 12 mL/min and a Gemini-NX C_{18} column (Phenomenex, 250 × 21.20 mm, 5 µm particle size). Methanol was removed under vacuum with heating to 28°C. Water was removed by lyophilization. The structure of **31** was determined by ESI-MS and NMR (^{1}H, ^{13}C, HMBC and NOE) experiments in MeOD using a Bruker AV500 spectrometer.

4.2.3. Expression and purification of recombinant Keap1

Mouse Keap1 was codon optimized for expression in *E. coli* (NRC Saskatoon DNA technologies unit), Gateway™ cloned into the pHIS8GW vector (Invitrogen) and expressed in BL21 (DE3) pLysS *E. coli* cells grown in 4.8 L of lysogeny broth (LB) (Bertani 1951) at 15ºC using isopropyl β-D-1-thiogalactopyranoside (IPTG) induction (0.5 mM) for 24 h. The pH of the medium was adjusted to 8.0 by adding 48 mL of 1.0 M Tris base prior to collecting the cells by centrifugation. *E. coli* stocks were stored in 25% glycerol at -80 ºC.

Table 4-1. NMR spectroscopic data for the major cysteine-oplopandiol product (**31**)

position	δC	δH, (*J* in Hz)	HMBC[a]
1	10.0	1.02, t (7.5)	2, 3
2	31.8	1.73, m	1, 3, 4,
3	64.7	4.45, t (6.1)	1, 2, 4, 5, 6, 7
4	101.5		
5	81.6		
6	115.9	6.29, s	2, 3, 1', 8, 9, 11
7	149.4		
8	72.3	5.07, d (8.0)	6, 7, 9, 10
9	130.2		
10	134.8		
11	31.8	2.13, m	9, 10, 12
12	30.4[b]	1.3,m	
13	30.5[b]	1.3, m	
14	30.8[b]	1.3, m	
15	33.1	1.3, m	
16	23.8	1.3, m	
17	14.5	0.89, t (7.1)	15, 16
1'a	34.9	3.93, dd (14.4, 2.7)	7, 3'
1'b		2.97, dd (14.4, 10.5)	7, 2', 3'
2'	55.0	3.65, dd (10.5, 2.7)	1'
3'	172.5		

[a]HMBC correlations are from protons stated to the indicated carbon
[b]Assignments may be interchanged

Purification technique #1: Cells were resuspended in lysis buffer (50 mM Tris-Cl, pH 8.0, 250 mM NaCl, 2.5 mM imidazole, 10% glycerol, 10 mM β-mercaptoethanol, and protease inhibitors (1:160 dilution, Calbiochem, Protease Inhibitor set III)) and lysed by French press. A solution of denatured *E. coli* proteins was added to the lysate to compete for binding to GroEL as described by Rohman *et al.* (2000). His-tagged Keap1 was purified by immobilized metal affinity chromatography on a column of Talon resin (Clontech Laboratories) according to manufacturer's batch protocol using wash buffer consisting of 50 mM Tris-Cl, pH 8.0, 250 mM NaCl, 2.5 mM imidazole, 10% glycerol, 10 mM β-mecaptoethanol, and elution buffer consisting of 50 mM Tris-Cl, pH 8.0, 250 mM NaCl, 150 mM imidazole, 10% glycerol, and 10 mM β-mecaptoethanol. Adenosine triphosphate (ATP) was added to 10 mM and the lysate was incubated at 37ºC for 20 min with shaking prior to loading on the Talon column. Further purification of the protein was performed by gel filtration on an AKTA FPLC using a Superdex 200 10/300 GL column (GE Healthcare), running buffer consisting of 50 mM Tris-Cl, pH 8.0, 100 mM NaCl, and 10 mM β-mercaptoethanol.

Purification technique #2: Cells were resuspended in a solution of 100 mM Tris-Cl pH 8.4, 200 mM dithiothreitol (DTT), 100 mM EDTA, a small amount of lysoyzme (~5 mg) and protease inhibitors (1:160 dilution, Calbiochem, Protease Inhibitor set III) and lysed by sonication (on ice, two cycles of 24 repetitions of 5 seconds on, 6 seconds off, microtip, setting 4.5, Heat Systems Sonicator Ultrasonic Processor XL). Lysate was loaded onto an open column of 35 g Sephadex G-50 and eluted with buffer A (25 mM Tris-Cl buffer, pH 8.0, containing 5 mM EDTA). Fractions with protein content (as judged by UV absorbance at 280 nm) were combined, ammonium sulphate was added to a concentration of 300 mM and the lysate was frozen overnight at -80ºC. After thawing the solution on ice, the precipitate was collected by centrifugation (20,000 g for 20 min) and resolubilized in buffer B (25 mM Tris-Cl buffer, pH 8.0, containing 10 mM DTT and 5 mM EDTA). Insoluble material was removed by centrifugation (3220 g for 30 min) and the solution was desalted using a PD-10 column (GE Healthcare) equilibrated with buffer A, ammonium sulphate was added to a concentration of 300 mM and the solution was frozen overnight at -80ºC. The precipitate was collected by centrifugation (10000 g for 20 min), resolubilized in buffer B and the insoluble material was removed by centrifugation (14000 g for 5 min). The crude Keap1 lysate was then subjected to Talon purifcation as described in 'Purification technique #1' without the inclusion of the ATP incubation or denatured *E. coli* protein.

Protein concentration was determined using the Bradford assay. Purified protein was stored at -80ºC in buffer A with 10% glycerol. Prior to subsequent analysis, frozen Keap1 was thawed on ice and buffer was exchanged using a Zeba 7K MWKO desalting column (Thermo Scientific).

4.2.4. Mass spectrometric studies with recombinant Keap1

Purified Keap1 (4.1 µM or 3 µM) was incubated with the small molecule of interest in 25 mM Tris-Cl buffer, pH 8.0 for 90 min at room temperature or 37ºC. The reactions with varying ratios of Keap1 to small molecule also included, 200 µM tris(2-carboxyethyl)phosphine. Half a µL of matrix consisting of sinapinic acid dissolved in 50% acetonitrile/water with 0.1% trifluoroacetic acid was spotted and dried on a MALDI plate. Sample (0.5 µL) was then added to the spot, an additional 0.5 µL of matrix was added, mixed with the sample and dried at room temperature. One-thousand laser shots were acquired per spectrum on an Applied Biosystems 4800 MALDI-TOF/TOF operating in linear mode.

4.2.5. Circular dichroism studies with recombinant Keap1

Purified Keap1 (3 μM) was incubated with 9 μM of the small molecule of interest in 20 mM Tris-Cl buffer, pH 8.0, for 90 min at 37ºC. Data were acquired over the range of 195 nm to 260 nm at 0.5 nm intervals using a 0.5 mm pathlength quartz cuvette on an Applied Photophysics π*-180 instrument. Each experiment was performed in duplicate. Six spectra were acquired per replicate. Secondary structure was calculated using CDNN software.

4.3. Results and discussion

4.3.1. Investigations of QR inducer reactivity with model thiols

To investigate whether select QR inducers act by modifying Keap1 thiols, I have tested their reactivity with model thiols *in vitro*. Certain phthalides, polyacetylenes and alkamides (isolated from *Echinacea* by a colleague, Yuping Lu) display thiol-reactivity *in vitro*. Here I specifically describe the outcome of studies with the polyacetylenes falcarindiol and oplopandiol. Due to the publication of a thorough description of the nature of the phthalide (ligustilide) reaction (Dietz et al. 2008; Schinkovitz et al. 2008), I don't report my studies of phthalide reactivity.

4.3.1.1. C_{17}-type polyacetylenes are reactive with model thiols

As judged by MS, racemic falcarindiol reacted with glutathione or cysteine to give two products (not considering stereoisomers) of approximately equal abundance with HPLC elution times intermediate to that of the model thiol or falcarindiol. The mass of these products (568 m/z under positive ionization for the glutathione adduct for example) was consistent with an addition reaction (mass of glutathione is 307, falcarindiol is 260). A major change in UV absorbance of the product suggested that there was a modification to the conjugated triple bonds. As shown in Figure 4-2 the amount of product increased as the pH of the reaction was increased from 7.5 to 11.5. This curve parallels the expected thiol deprotonation curve for glutathione shown in blue (pKa = 9.12 (The Merck Index)).

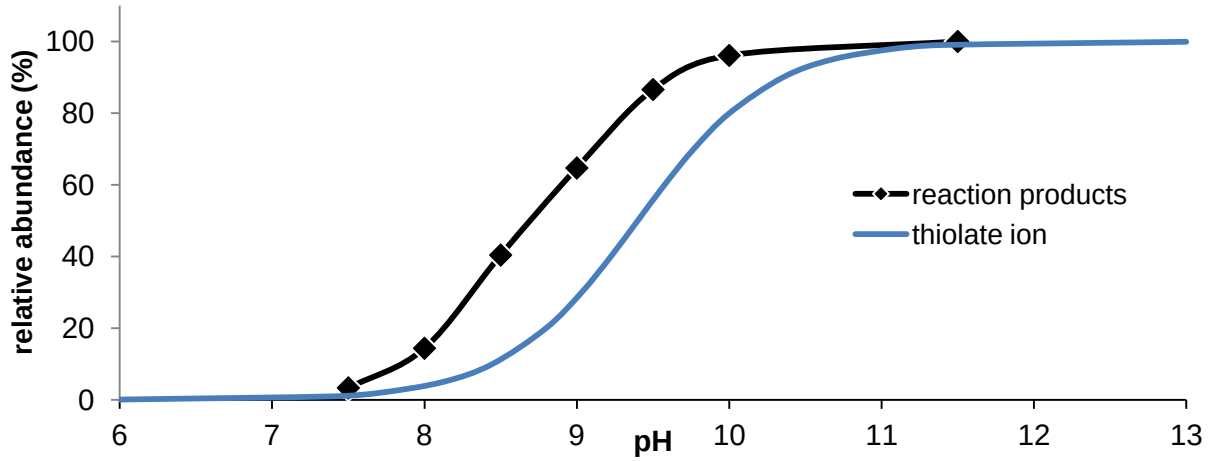

Figure 4-2. Relationship between reaction pH and yield of major products from reaction between falcarindiol and cysteine. Measured by integration of mass spectrogram peak area at m/z 568. The theoretical titration curve for the glutathione thiol is also presented for comparison (The Merck Index).

4.3.1.2. Trends of reactivity

Thiol reactivity is known to parallel Nrf2 activator potency (Kensler et al. 2010). However, strong electrophiles are not desirable for pharmacological interventions as they quickly react with less nucleophilic functionalities such as hydroxyls and amines resulting in low specificity for Keap1. Therefore, moderately weak electrophiles that selectively modify Keap1 are expected to have the greatest ratio of efficacy to adverse effects.

One of the structure-activity trends observed for C_{17}-type polyacetylenes was that the terminal double bond present in falcarindiol and absent in oplopandiol appeared to be required for maximal QR-inducing activity. In contrast to falcarindiol, the two major products formed from the reaction of oplopandiol with model thiols were not equally abundant. The more abundant product was present at roughly the same level as one of the major products of the falcarindiol reaction. Therefore I suspected that the double bond was playing a role in the reactivity of the nearest triple bond and that the major product would be one in which the reaction took place near the existing double bond in oplopandiol.

4.3.1.3. Structure of the major product of the oplopandiol-cysteine reaction

In order to determine the exact structure of the major product of the oplopandiol and a model thiol reaction I prepared a large scale reaction of oplopandiol and cysteine and isolated the major product by preparative HPLC. The structure of the major product is shown in Figure 4-3.

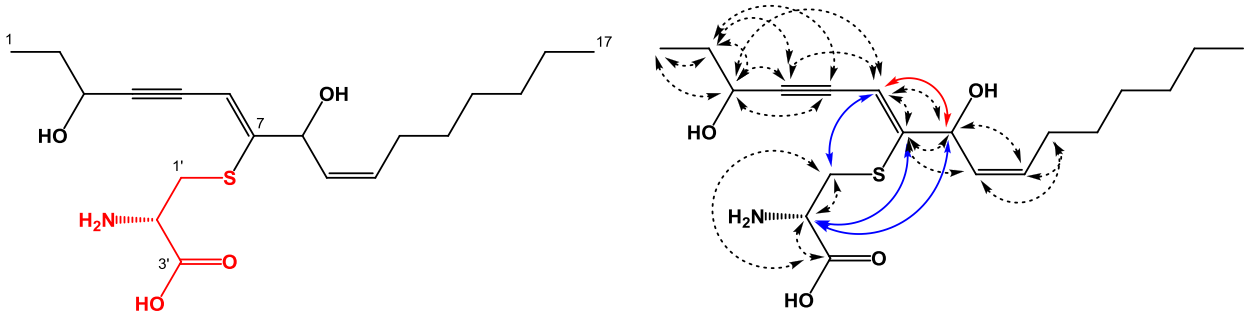

Figure 4-3. Structure of the major product (**31**) of a reaction between oplopandiol (**16**) and cysteine (shown in red in the representation on the left). On the right, HMBC correlations are indicated by dashed and blue arrows and an NOE critical to the assignment of the double bond configuration is represented in red.

The product structure revealed that addition was occurring at position 7 of oplopandiol (**16**). Consistent with a (*Z*) configuration about the new double bond an NOE was observed between the H-6 and H-8 protons. The preference for the attack of the cysteine thiol at the triple bond proximal to the double bond may explain why only one product predominates the reaction of 1,2-dihyrofalcarindiol with cysteine whereas two products in roughly equal yield predominated the reaction of falcarindiol with cysteine and why C_{17}-type polyacetylenes that possess the terminal double bond are more potent QR inducers.

Although alkynes do not typically undergo facile addition with thiols, an adjacent hydroxyl group can greatly accelerate this process (See Waters et al. 2000). Therefore, the lack of the C-8 hydroxyl in falcarinol may explain its reduced QR-inducing activity relative to falcarindiol. It is also conceivable that the presence of two reactive centres, as found in falcarindiol-type polyacetylenes, is required for most effective modification of Keap1. However, upon examination of reactions of falcarindiol (**1**) with cysteine or glutathione by LC-UV-MS/MS no bi-addition products were observed suggesting that the first reaction may impede the second by steric hindrance or as a result of a change in electophilicity of the alkyne. This lack of a result should not be taken as a strong indication that bi-addition would not take place *in vivo*, as a second thiol-reaction with Keap1 could be intramolecular. Intramolecular reactions can be more favorable than intermolecular reactions due to the reactive constituents being held in proximity. A better test for falcarindiol bi-addition products would include a model thiol with two reactive thiols such as the short peptide Lys-Cys-Lys-Cys-Lys.

4.3.2 Keap1 reactivity studies

4.3.2.1. Keap1 expression and purification

As reported in the literature, yields of recombinantly expressed mouse Keap1 in *E. coli* were low. Optimizing codon usage for expression in *E. coli* and lowering the temperature of the culture to 14ºC during expression increased the levels of soluble Keap1 such that accumulation of soluble protein in induced culture could be observed by eye on a Coomassie blue stained SDS-PAGE gel.

I initially used Talon purification (a form of immobilized metal affinity chromatography) to purify Keap1. However, I consistently co-purified another protein with an apparent molecular weight slightly lower than Keap1. The co-purifying protein was identified with the help of the NRC Saskatoon MS group as the large subunit of bacterial chaperone GroEL. The identity of the the other protein as Keap1 was also confirmed by MS of digested protein. Co-purifying GroEL is a commonly encountered problem during purification of overexpressed foreign proteins in *E. coli* (Thain et al. 1996; Rohman et al. 2000). GroEL is a multimeric protein that catalyzes protein folding. Proteins with an exposed hydrophobic region associate with a hydrophobic region of GroEL. Then, a conformational change in GroEL forces the misfolded protein into a more hydrophilic environment causing the hydrophobic area of the misfolded protein to be buried within the protein. The protein is then released and GroEL is reset via ATP hydrolysis.

I employed two methods to eliminate co-purification of GroEL with Keap1. The first involved incubating the cell lysate with denatured *E. coli* proteins to compete for GroEL binding. The second involved adding ATP to the lysate prior to loading on the Talon column. Together, these approaches considerably reduced the amount of co-purifying GroEL but did not eliminate it completely. Furthermore, there were still several other contaminating proteins present in my preparation. Therefore I used gel filtration to further purify the Keap1 protein. However, due to the similar size of the contaminant, I was unable to resolve the two proteins completely and the yield of Keap1 with satisfactory purity was very low (24 µg from 3.3 L of culture or 7.3 µg/L of culture). Although this amount of Keap1 allowed me to do some preliminary MS studies, I calculated that I needed at least 100 µg for circular dichroism spectroscopy studies and therefore I decided to try another approach for purifying Keap1.

Aside from immobilized metal affinity chromatography, precipitation has also been used to purify Keap1(Dinkova-Kostova et al. 2002). In the absence of DTT, Keap1 precipitates at a relatively low ammonium sulphate concentration of 300 mM. However, a reducing agent such as DTT is required to maintain solubility of Keap1 during cell lysis. Therefore I removed DTT from the lysate by gel filtration prior to adding ammonium sulphate. Precipitation offered a reasonably good purification step and avoided co-purification of GroEL (Figure 4-4). In order to get satisfactory purity I completed two rounds of precipitation followed by Talon purification. This strategy improved yields of Keap1 (226 µg from 4.8 L of culture or 47 µg/L of culture).

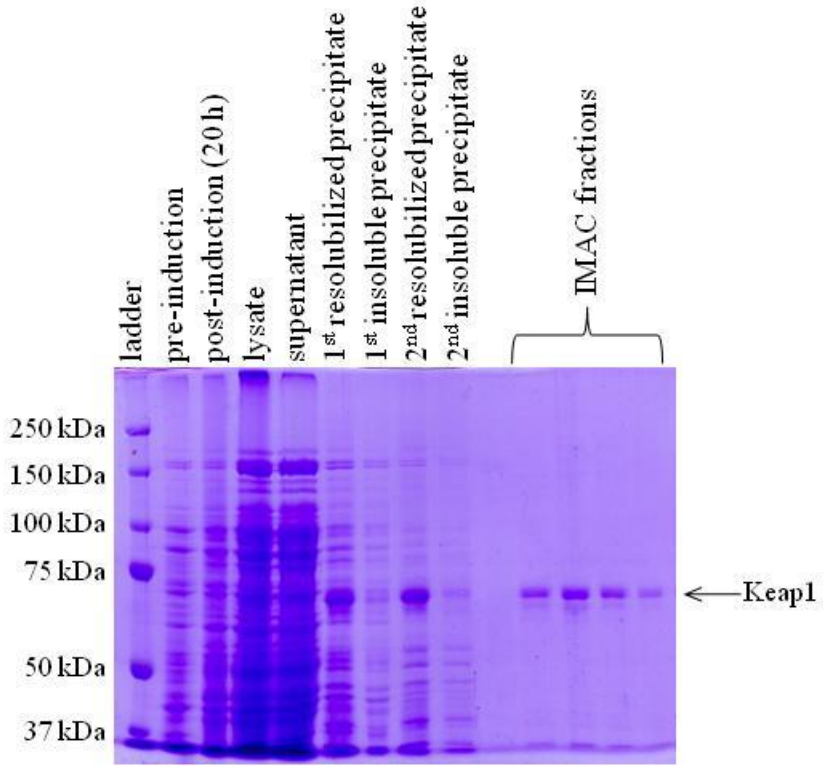

Figure 4-4. Purification of recombinant Keap1 expressed in *E. coli*. Two rounds of ammonium sulphate precipitation were followed by Talon purification. SDS-PAGE gel (10%)stained with Coomassie brilliant blue.

4.3.2.2. Mass spectrometric studies

Initial analysis of Keap1 by MALDI-TOF MS revealed that the ionization efficiency/signal strength of Keap1 was very low compared to the positive control, bovine serum albumin (BSA). I experimented with several different spotting techniques and found that a

'sandwich' method in which I deposited Keap1 onto a spot of matrix and then covered it with an additional spot of matrix greatly improved signal strength.

Incubations with the two falcarindiol stereoisomers revealed that both stereoisomers modify Keap1 and that greater ratios of falcarindiol to Keap1 resulted in a greater number of modifications (Figure 4-5). The ability to covalently modify Keap1 *in vitro* is consistent with the hypothesis that the falcarindiol stereoisomers and related polyacetylenes activate QR expression by modifying Keap1 cysteines.

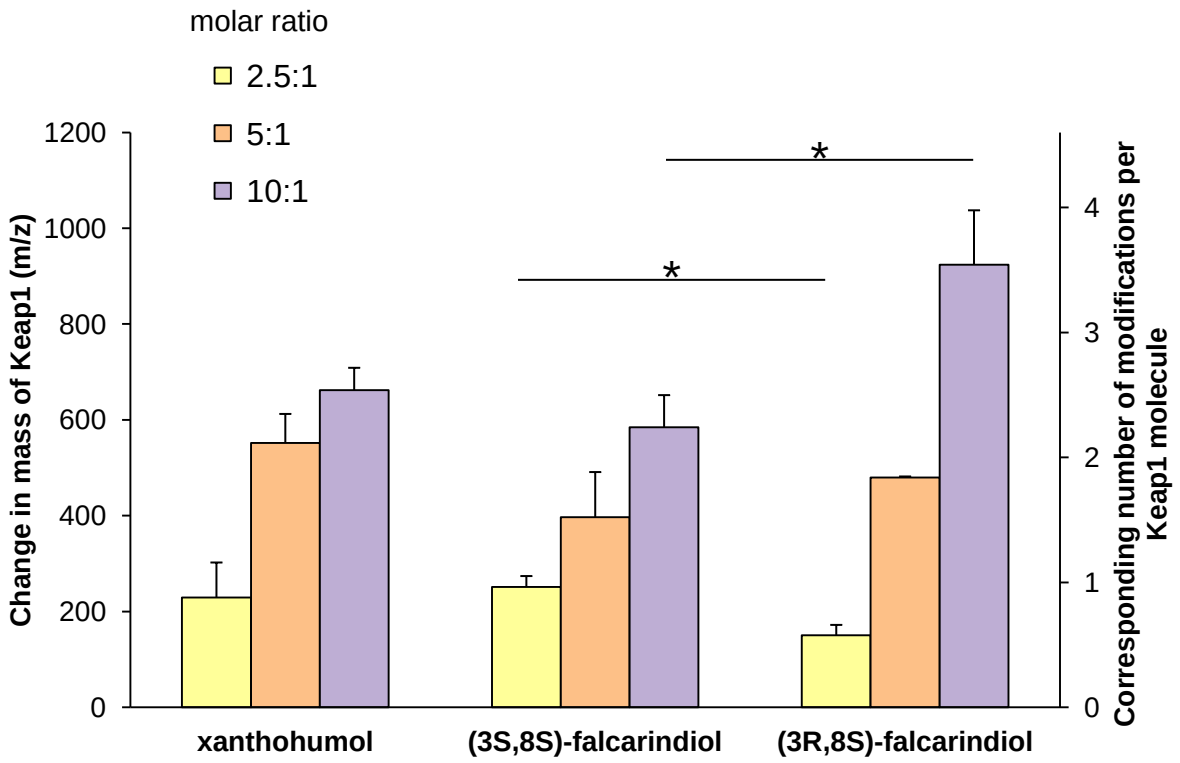

Figure 4-5. Changes in the mass of recombinant Keap1 following incubation with differing concentration of xanthohumol, (3*R*,8*S*)-falcarindiol, or (3*S*,8*S*)-falcarindiol. Measured by MALDI-TOF MS after a 90 min incubation at room temperature. The right axis indicates the corresponding number of modifications based on the molecular weights of xanthohumol (354.4) and falcarindiol (260.2). Results are the mean of six technical replicates ± standard deviation. Asterisks and hash indicate a significant differences ($p < 0.05$, student's *t*-test)

At a 2.5:1 ratio of falcarindiol to Keap1, the (3*S*,8*S*)-falcarindiol stereoisomer resulted in a significantly greater average increase in mass (251 Da) than the (3*R*,8*S*)-falcarindiol (151 Da).

As the mass of falcarindiol is 260 Da, these increases in the mass of Keap1 correspond to roughly a single modification or 0.6 modifications of Keap1 for the (3*S*,8*S*)-falcarindiol, and (3*R*,8*S*)-falcarindiol stereoisomers, respectively. The increased propensity for (3*S*,8*S*)-falcarindiol to react with Keap1 at low ratios of small molecule to Keap1 are consistent with the higher QR-inducing potency of (3*S*,8*S*)-falcarindiol and provides support for a mechanism of action involving modification of Keap1 cysteines. At higher ratios (5:1 or 10:1) of small molecule to Keap1, greater increases in mass were observed and in contrast to the lowest ratio (2.5:1), the (3*R*,8*S*)-falcarindiol stereoisomer caused a significantly greater change in mass than the (3*S*,8*S*)-falcarindiol stereoisomer (924 Da or 585 Da, equivalent to 3.6 or 2.0 modifications, respectively). Although it is unclear what concentration Keap1 is present at *in vivo*, I expect that the initial one or two reactions are the most important and that the reactivity at low ratios of falcarindiol to Keap1 are the most relevant.

In order to shed light on whether the falcarindiol stereoisomers differed in the rates at which they alkylated Keap1, I performed a small time course with the two compounds. I used a low ratio of falcarindiol to Keap1 (3:1) based on the prediction that the first alkylations of Keap1 are more important *in vivo*.

As shown in Figure 4-6, both (3*R*,8*S*)-falcarindiol and (3*S*,8*S*)-falcarindiol caused time-dependent increases in the mass of Keap1. The differences between the two stereoisomers were not significant ($p > 0.05$, student's *t*-test). Therefore it seems unlikely that a difference in the reaction rate of the two stereoisomers with Keap1 is responsible for the differences in their QR-activating potencies.

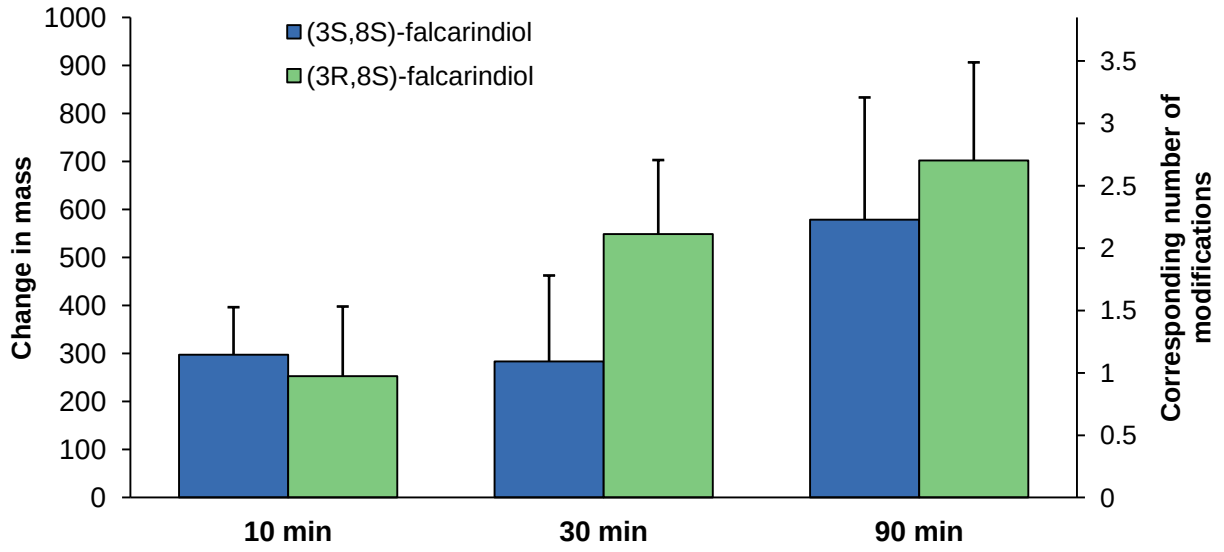

Figure 4-6. Changes in the mass of recombinant Keap1 over time following incubation with (3*R*,8*S*)-falcarindiol or (3*S*,8*S*)-falcarindiol. Reactions consisted of a 3:1 molar ratio of small molecule to Keap1 and were measured by MALDI-TOF MS after a 90 min incubation at 37ºC. The right axis indicates the corresponding number of modifications based on the molecular weight of falcarindiol (260.2). Results are the mean of six technical replicates ± standard deviation.

4.3.2.3. Falcarindiol stereoisomers differentially affect the secondary structure of Keap1 as judged by circular dichroism spectroscopy.

An alternative hypothesis for the difference in QR-activating potency of the falcarindiol stereoisomers is that the two compounds differentially affect the conformation of Keap1. Therefore I used circular dichroism spectroscopy to measure changes in secondary structure in response to treatment with the two falcarindiol stereoisomers. I again used a low ratio of falcarindiol to Keap1 (3:1). The resulting spectra and data deconvolution are provided in Figure 4-7 and Table 4-2 respectively.

The two stereoisomers caused opposing shifts to the circular dichroism spectrum of Keap1. For (3*R*,8*S*)-falcarindiol-treated Keap1 these changes corresponded to an increase in alpha-helix, a decrease in antiparallel and parallel beta-sheets and increases in β-turns and random coil with the inverse effect on each secondary structure occurring for (3*S*,8*S*)-falcarindiol. These findings are consistent with a mechanism of action for both stereoisomers involving changes in the secondary structure of Keap1 and suggests that the difference in QR induction of the falcarindiol

stereoisomers may stem from differences in the way that they alter the secondary structure of Keap1.

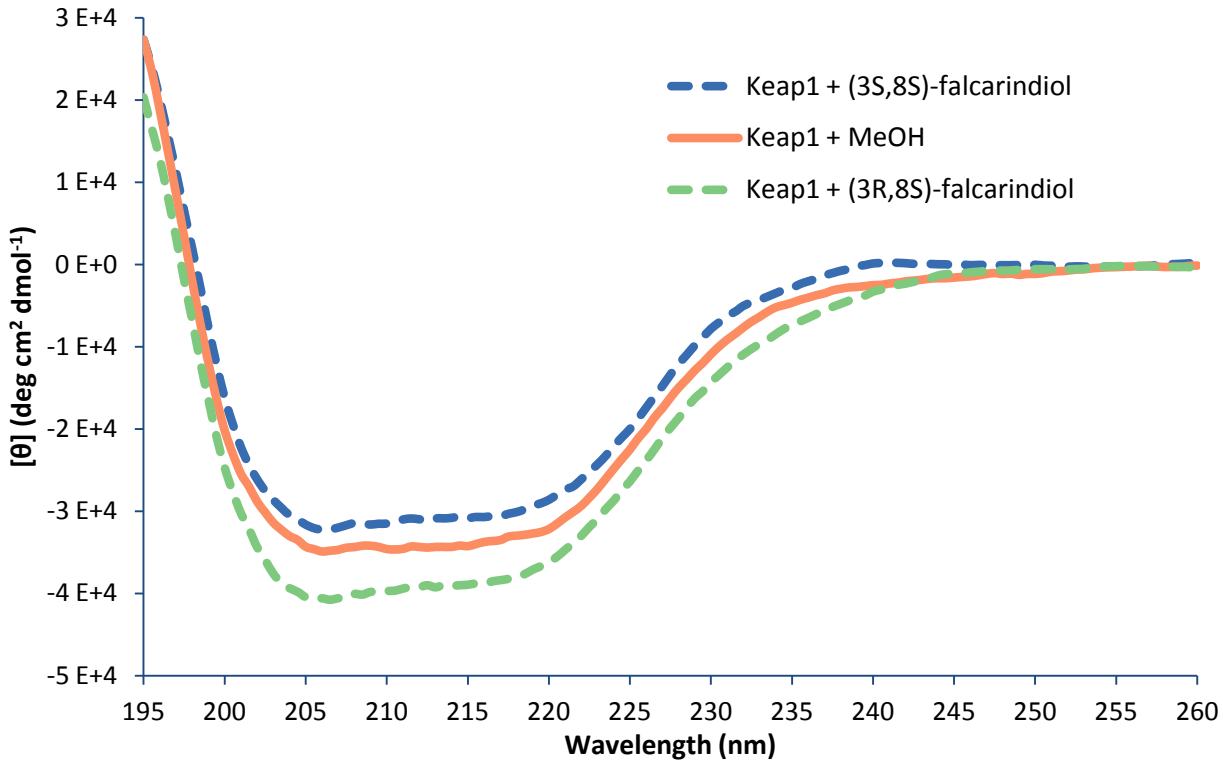

Figure 4-7. Changes in the circular dichroism spectrum of Keap1following incubation with (3*R*,8*S*)-falcarindiol or (3*S*,8*S*)-falcarindiol. Keap1 (3µM) was incubated with a falcarindiol stereoisomer (9 µM) or solvent (MeOH) at 37ºC for 90 min. Data are the mean of duplicate samples.

Table 4-2. Changes in secondary structure of recombinant Keap1 following exposure to (3R,8S)-falcarindiol or (3S,8S)-falcarindiol at a molar ratio of 3:1 for 90 min at 37ºC. Circular dichroism data was deconvoluted with CDNN.

	Solvent control	(3*R*,8*S*)-falcarindiol-treated	(3*S*,8*S*)-falcarindiol-treated	(3*R*,8*S*)-Fd change	(3*S*,8*S*)-Fd change
α-Helix	11.3	11.7	11.0	0.4	-0.3
Antiparallel β-sheet	30.6	28.5	31.9	-2.1	1.3
Parallel β-sheet	5.4	5.2	5.4	-0.2	0.0
β-Turn	20.4	20.9	20.2	0.5	-0.2
Random coil	33.8	34.5	33.5	0.8	-0.3
Total sum	101.4	100.8	102.0	-0.7	0.6

4.4. Conclusions

In summary, the polyacetylenes oplopandiol and falcarindiol form covalent adducts with low molecular weight model thiols and recombinant Keap1 *in vitro.* The reaction between falcarindiol-type polyacetylenes and cysteine occurs at the outer carbons of the triple bonds (positions 4 and 7) of these molecules. As judged by circular dichroism spectroscopy the resulting changes in secondary structure of Keap1 differs for the two stereoisomers of falcarindiol. These results provides support for the hypothesis that (3*S*,8*S*)-falcarindiol and (3*R*,8*S*)-falcarindiol activate QR by increasing the stability of Nrf2 by covalently modifying cysteine residues of its negative regulator Keap1 and offer an explanation for their differences in activity.

CHAPTER 5

THE EFFECTS ON TRANSCRIPTION OF QR INDUCERS

5.1. Introduction

QR inducers have received much attention due to their potential health benefits. Examples include sulforaphane, curcumin, xanthohumol and resveratrol. These compounds activate QR through the Keap1-Nrf2-ARE signalling pathway and therefore also increase the expression of other Nrf2-regulated cytoprotective genes. Additionally, these compounds modulate other signalling pathways including those mediated by NF-κB, FOXOs, and AhR. Understanding the breadth of changes that occur in the cell in response to potential health promoting compounds is essential for understanding the positive and negative consequences that may result from their use. Here I report changes in gene expression that result from exposure to QR inducers. The goals of these studies were to confirm whether QR inducers activate the transcription of additional Nrf2 targets and to investigate whether other transcriptional pathways are affected by these compounds. I have focused these studies on (*Z*)-ligustilide, cannabidiol and select polyacetylenes due to their potency and prevalence in food and drug plants.

5.1.1. Measuring changes in gene expression as an indicator of Nrf2 activation and off-target effects

The enzyme QR has served as a useful marker for activation of Nrf2 in numerous studies (Favreau et al. 1991). Although the reductive approach of examining the induction of this single Nrf2 target is useful from a screening point of view, it does not provide insight into the wide-ranging effects of exposure to a given xenobiotic. Identifying changes in expression of Nrf2 targets as well as other transcription factors such as AhR could provide evidence to support the hypothesis that these compounds induce QR via Nrf2 and indicate whether other signal transduction pathways are affected.

Among the types of information used to identify the effects of a xenobiotic (i.e. changes in transcription factor binding, transcription, translation, protein abundance, posttranslational modification of proteins), I have focused on transcript levels. Nrf2 is a transcription factor and changes in transcription are a primary means by which cells adapt and respond to changes in the environment.

The importance of transcription in cell regulation (development, homeostasis) is reflected by the large proportion of genes that encode transcription factors. It is estimated that the human genome encodes around 1400 transcription factors representing 5% of all genes (Vaquerizas et al. 2009). Epigenetic changes may also manifest through changes in transcription.

Although posttranscriptional stability also affects transcript levels, changes in transcription can, in general, be inferred from changes in the abundances of transcripts. For example, using, lipopolysaccharide (LPS) treated mouse bone marrow-derived dendritic cells, Rabani *et al.* (2011) found that the majority of temporal changes in RNA levels were determined by changes in transcription rates.

Quantitative real-time reverse-transcriptase polymerase chain reaction (qRT-PCR) can be used to determine relative changes in a small number of transcripts. Conversely, a more complete picture of global changes in transcription can be achieved using RNA sequencing (RNA-seq).

5.1.1. qRT-PCR

qRT-PCR is the current standard for quantifying a single transcript. Transcripts are reverse transcribed to complimentary DNAs (cDNAs) which are then subjected to PCR-based amplification under conditions that allow real-time quantification of the product. Primers define the region to be amplified. The number of cycles required to reach a threshold is directly related to the amount of starting material and, by comparison with a constitutively expressed transcript, relative changes in abundance between treatment groups can be determined. qRT-PCR is limited, however, by the requirement of designing and validating primers for each individual transcript to be measured and is not practical for examining large numbers of transcripts.

5.1.2. Transcriptomics and RNA-seq

Transcriptomics is the study of all RNAs within a cell. Transcriptomic analyses yield a global perspective of the changes in transcript abundance that occur in response to a treatment. Techniques that allow global analysis of mRNA levels include microarrays, serial analysis of gene expression (SAGE) and RNA-seq. Microarrays have a rich history of use and offer a relatively inexpensive way to look at widespread changes in gene expression. However, microarrays require *a priori* transcript information and suffer from a limited dynamic range due to their reliance on hybridization. SAGE provides a digital snapshot of transcript levels by sequencing small tags

derived from mRNAs and comparing the number of tags sequenced for each transcript. Due to the practical limitations of Sanger-based sequencing, SAGE was originally designed to facilitate transcript abundance measurements using a minimal amount of sequencing by only sequencing a short portion (i.e. 9 bp) of each transcript (Velculescu et al. 1995). However, the development of next-generation high-throughput sequencing technologies (i.e. Illumina Genome Analyzer) has allowed for more thorough analyses such as RNA-seq. RNA-seq involves sequencing fragments of cDNA derived from isolated RNA on a massive scale (Wang et al. 2009). Read lengths currently range from 25 - 800 bp depending on the technology used. Mapping of these short reads to the genome provides a digital reading of gene expression and allows *de novo* discovery of transcribed regions, novel transcriptional start sites and splice isoforms. As RNA-seq has no practical upper quantification limit, its dynamic range is only limited by the number of reads and has displayed linearity over five orders of magnitude (Mortazavi et al. 2008). The major limitations of RNA-seq are cost and the need for sophisticated data analysis.

I used RNA-seq to analyze global changes in gene expression in Hepa-1c1c7 cells in response to the QR inducers (*Z*)-ligustilide, (3*S*,8*S*)-falcarindiol and (3*R*,8*S*)-falcarindiol, 6-isovaleylumbelliferone (6-IVU), (*R*)-sulforaphane, and xanthohumol (Figure 5-1). (*Z*)-ligustilide, (3*S*,8*S*)-falcarindiol and (3*R*,8*S*)-falcarindiol were considered the most interesting QR-inducers isolated from my work. 6-IVU, isolated by a colleague, was unique amongst coumarins isolated from celeriac (*Apium graveolens* var. *rapaceum*) in that it possessed marked QR-inducing activity (CD value = 5 μM) that correlated with another unique feature, the presence of an isovaleryl decoration. (*R*)-Sulforaphane and xanthohumol are two of the most studied Nrf2 activators and were included for comparison.

qRT-PCR was used to validate the results of RNA-seq studies. I have used the transcriptomic data generated by these studies to investigate the following questions: 1) is increased QR activity due to increased transcription? 2) Do these QR inducers activate Nrf2 and increase transcription of other Nrf2 targets? 3) Is AhR or NF-κB activated by these QR inducers? 4) Do the falcarindiol stereoisomers differ in effects on transcription? 5) Are any additional transcriptional pathways affected by these compounds at the concentration required to induce QR?

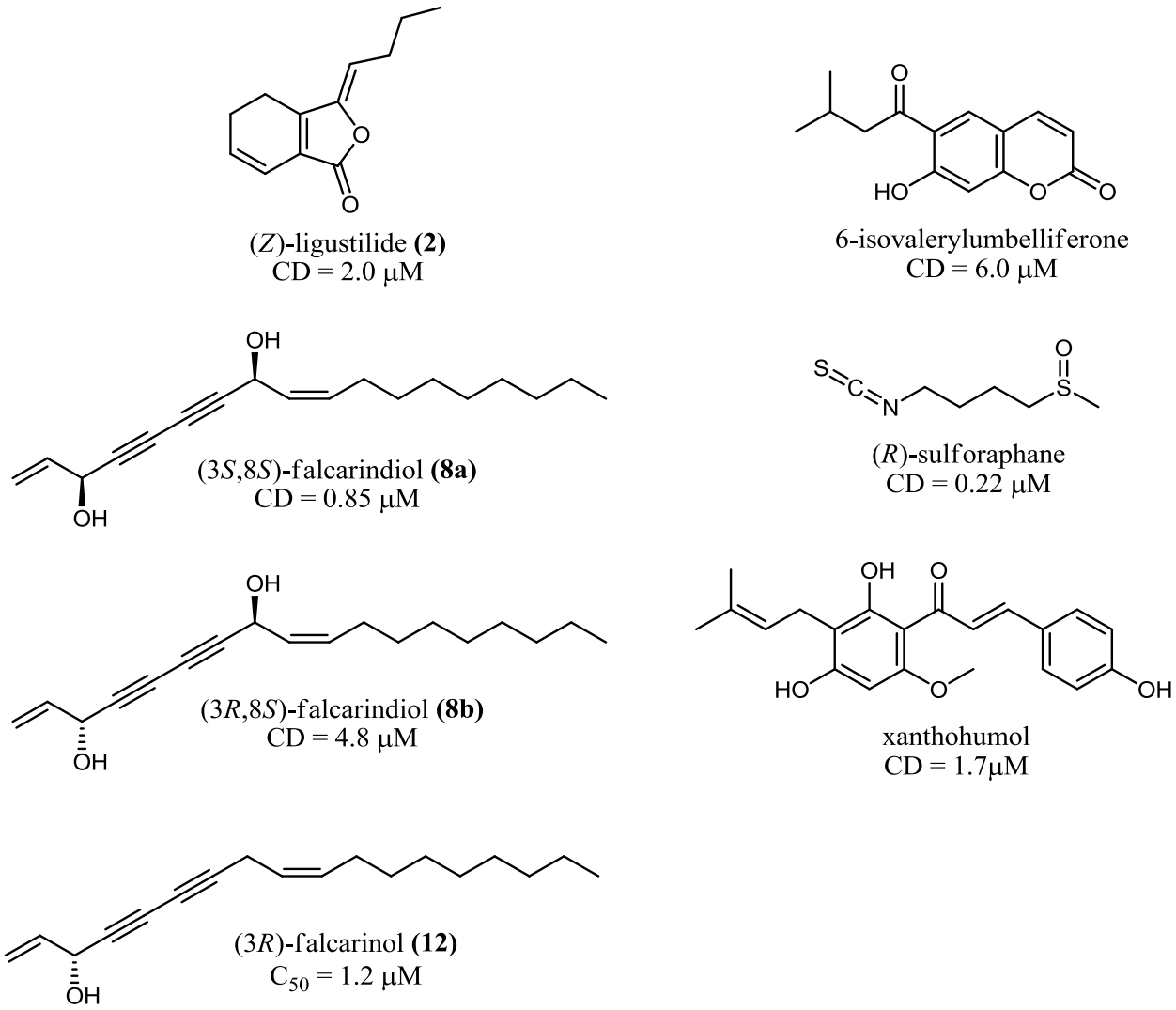

Figure 5-1. Compounds used to treat cells in RNA-seq analysis and their respective CD or C_{50} values.

5.2. Materials and methods

5.2.1. General experimental procedures

Cell culture reagents were obtained from Invitrogen. Unless otherwise specified, chemicals were obtained from Sigma-Aldrich.

5.2.2. RNA collection and cDNA synthesis for qRT-PCR and RNA-seq

Hepa-1c1c7 cells (ATCC) were grown in a humidified atmosphere composed of 5% CO_2 / 95% air at 37°C in a 225 cm^2 flask to 80 % confluency and plated in 6-well plates at 250,000 cells and 2.5 mL medium per well. After 24 h the medium was replaced and test compounds added such

that the final concentration of DMSO in the medium was 0.1%. After a further 12 h the medium was removed and RNA was harvested using a QIAGEN RNeasy kit according to manufacturer's instructions including an on-column DNAse I digest. Cells from three biological replicates were pooled during RNA isolation. RNA was quantified using a Nanodrop (Thermo Scientific). RNA integrity was determined using an Agilent 2100 Bioanalyzer and PicoRNA plate.

For qRT-PCR analysis, cDNA was synthesised from 0.5 µg of total RNA using a Qiagen Quantitect cDNA synthesis kit according to manufacturer's instructions using the supplied mix of oligo-dT and random primers with an extension time of 30 min. cDNA for RNA-seq was synthesized from 10 µg of total RNA using the Illumina mRNA-seq sample prep kit according to manufacturer's instructions.

5.2.3. RNA-seq

5.2.3.1. Sequencing summary

Single-ended 36 bp reads were acquired on an Illumina GII_x Genome Analyzer using one lane per cDNA sample. One lane per flow-cell was dedicated to the PhiX control DNA. Bases were called using Bustard (1.3) and the PhiX control was used for base-call calibration. Reads were mapped to the mouse genome (NCBI Mouse build 37.61) using Bowtie (v0.12.7) and splice junctions identified *de novo* using Tophat (v1.2.0) with default parameters (Appendix B). Differential expression and splicing was determined using Cufflinks/Cuffcompare/Cuffdiff (v0.9.3) with quartile normalization and bias correction.

5.2.3.2. Online analysis tools

For the subsequent web-based analyses, Ensembl gene IDs or Entrez gene IDs for the genes with differential expression in the ranges of > 1.5-fold and/or < 0.67-fold and mean reads mapped per kilobase of gene per million reads mapped (RPKM) values greater than one were submitted. Where applicable results with p values greater than 0.001 were excluded.

5.2.3.2.1. Identification of transcription factor regulation by target gene signature analysis

Target gene signature analysis was conducted using the TFacts.org web service with default parameters (Essaghir et al. 2010) (http://www.tfacts.org/TFactS-new/TFactS-v2/index1.html). Both up- and down-regulated genes were included.

5.2.3.2.2. Detection of over-represented gene ontology terms, pathway-based sets and neighbor-based sets

Over-representation analyses were conducted using the ConsensusPathDatabase-mouse web service (http://cpdb.molgen.mpg.de/MCPDB). Network neighborhood-based sets were limited to one-next neighbor.

5.2.4. qRT-PCR

qRT-PCR was conducted on an StepOnePlus instrument (Applied Biosystems) using SYBR green master mix (Applied Biosystems) with a final volume of 20 µL. The concentration of each primer was 1.0 µM . Primer efficiency was validated using four two-fold dilutions of an arbitrarily chosen cDNA. *β-Glucuronidase* was used as the normalizing gene. The primer sequences are provided in Table 5-1.

Table 5-1. Primers used for qRT-PCR.

Gene	Forward primer 5'-3'	Reverse primer 5'-3'
QR	CGACAACGGTCCTTTCCAGA	GCAGGATGCCACTCTGAATC
HO-1	CAAGCCGAGAATGCTGAGTTCATG	ACTGGGTTCTGCTTGTTGCGCT
CYP1A1	GACCCTTACAAGTATTTGGTCGTG	GGTATCCAGAGCCAGTAACCTC
β-GLUCURONIDASE	TGCTCTGAAACCCGCCGCAT	GGGCCCCCAGGTCTGCATCA

5.3. Results and discussion

5.3.1. Cell treatment and RNA isolation for qRT-PCR and RNA-seq

The mouse hepatoma cell line Hepa-1c1c7 has been used extensively for studies of induction of xenobiotic metabolism. The availability and history of use of this cell line were major factors considered when choosing to use this cell line for transcript level analyses. Primary (human) cell lines may provide more relevant results with respect to exposure of normal human tissues, however, the lack of availability and variability between cell lines would have impaired the ability to reproduce the data or draw direct comparisons with other studies (Goyak et al. 2008). It is important to note the potential discrepancy in transcriptional behaviour of this cell line compared to native human hepatocytes that may be a result of, differences in the level of differentiation and the genetic instability of cancer cells, the donor animal species (mouse vs. human), and the lack of

physiological interactions in a monoculture compared to *in vivo*. A whole animal (mouse) model was considered, but my familiarity with the Hepa-1c1c7 cell line and its proven responsiveness to the compounds of interest, combined with the ease at which I could perform the experiments with this cell line, prevailed.

For the most part, the concentrations of each test compound were chosen to be slightly higher than the concentration required to double activity of QR (see Section 3.3). The number of cells plated and level of confluency during exposure were chosen to mirror that which was optimized in the QR bioassay (see Section 2.3.1).

The time frame for treatment (12 h) for mRNA analyses was substantially shorter than the treatment time used in the QR bioassay (48 h). Since I chose concentrations for exposure that were minimal and closest to physiological relevance I wanted to maximize the amount of time for changes in transcript levels to manifest. A transcriptional study examining the response of dendritic cells (mouse and human) to a variety of immune activators showed that certain groups of transcripts peaked as early as 30 min, while others peaked as late as 8 or 12 h (Amit et al. 2009). Using a later time point may allow non-linear or secondary responses to be observed. For example, where the increased transcription of a transcription factor results in increased expression of the targets of the second transcription factor. This may provide a better picture of the ultimate changes in transcription resulting from a treatment.

A commercial kit (Qiagen RNeasy) was chosen for RNA isolation. Although the optional DNAse digest was conducted there is still a possibility that some minor degree of DNA contamination could exist in the sample. Any low level DNA contamination would have a greatest effect on the quantification of low abundance transcripts and may also contribute to reads mapping to “non-transcribed” regions of the genome during RNA-seq analysis.

Isolated RNA was of utmost quality as judged by Agilent 2100 Bioanalyzer with resulting RNA integrity numbers (RIN) of 9.9-10. An RIN of 10 represents a state where no degradation has occurred.

5.3.2. RNA-seq

5.3.2.1. Sequencing

The Illumina platform was selected due to its sequencing capacity and availability (NRC Saskatoon). Single-end, 36 bp reads were considered sufficient for examining differential expression in mouse as the sequenced genome was available for this animal and therefore *de novo* transcript assembly was not required.

Table 5-2. Number of RNA-seq reads passing quality restrictions.

Treatment	Number of reads
1st RNA-seq experiment	
DMSO	16,995,319
(3*S*,8*S*)-falcarindiol (1 μM)	19,128,690
(3*R*,8*S*)-falcarindiol (1 μM)	16,129,902
(*R*)-sulforphane (1 μM)	17,323,370
(*Z*)-ligustilide (10 μM)	268,231
6-isovaleryl-umbelliferone (10 μM)	3,417,980
xanthohumol (5 μM)	109,911
2nd RNA-seq experiment	
DMSO	21,830,250
(3*R*,8*S*)-falcarindiol (10 μM)	22,891,773
(3*R*)-falcarinol (2 μM)	13,411,510
(*Z*)-ligustilide (10 μM)	11,693,528
6-isovaleryl-umbelliferone (10 μM)	35,302,747
xanthohumol (5 μM)	47,695
mean	*13,734,685*

Approximately 14 million high-quality reads were obtained per sample (Table 5-2). However, three of the original samples (ligustilide (10 μM), 6-isovaleryl-umbelliferone (10 μM), xanthohumol (5.0 μM)) yielded low numbers of quality reads. The three unsuccessful samples were later re-run along with three additional samples that were collected according to the same procedure as the first set (an additional DMSO control, 10 μM (3*R*,8*S*)-falcarindiol, 2.0 μM falcarinol). These were needed to fill out the remaining lanes on the flow cell. Unfortunately the second xanthohumol run was also unsuccessful. The few reads that were collected for the

xanthohumol experiments were subjected to bioinformatics analysis but did not yield meaningful data.

5.3.2.2. RNA-seq data processing

Sequence analysis was carried out using the Bowtie/Tophat/Cufflinks workflow jointly developed between UC Berkeley, the University of Maryland and Caltech (Langmead et al. 2009; Trapnell et al. 2010). This workflow uses a Burrows-Wheeler index when mapping which results in high performance and a low memory footprint. Additionally, this software can correct for biases inherent to RNA-seq experiments and has a high level of community support, including support at NRC Saskatoon.

5.3.2.3. Bias corrections

Despite the power of RNA-seq, the technique is not without limits. During preparation for RNA-seq (cDNA production, fragmentation, amplification) both positional and sequence specific biases are created. For instance, amongst a collection of random primers certain primer sequences appear to be favored by reverse transcriptases leading to a non-random distribution of cDNA fragments and inaccurate calculations of differential expression (Oshlack et al. 2009). Detecting primer biases and normalizing the data based on these biases is a recent improvement to the Tophat software (v1.2.0) and was implemented during analysis.

Another bias affecting analysis of differentially expressed genes arises from the way that transcripts are quantified in RNA-seq. Transcript abundance is expressed as RPKM. As a result of changes in the abundance of other transcripts, the relative proportion of a given transcript to the total pool can change without a change in the absolute level of this transcript. Highly expressed transcripts have the greatest effect on the relative proportions of other transcripts. For example, consider a highly expressed gene that makes up 50% of the transcript population. If the abundance of this transcript increases as a result of a treatment the RPKM values for unaffected transcripts would proportionately decrease although their absolute levels were unaffected. Quartile normalization allows the use of only the lowest expressed 75% of loci in calculating the RPKM denominator and thereby decreases the bias introduced by changes in high abundance transcript levels (Bullard et al. 2010). It is important to note that RPKM values obtained using this normalization will be higher than those obtained without it as the denominator will be smaller.

5.3.2.4. Analysis parameters

As the default parameters for RNA-seq using Bowtie/Cufflinks/Tophat have been optimized for mammalian analysis, these setting were left unaltered. A maximum of two mismatches were allowed per alignment. Allowing mismatches during sequence alignment is important due to the possibility of errors inherent in the study design and due to biological variability. Experimental errors include those introduced during the reverse transcription step (approximately 1 in 20,000) or due to sequencing inaccuracy (Roberts et al. 1988). Differences due to biological variability include those resulting from genomic changes in the cancer cell line and from RNA-DNA differences that arise from RNA-editing or unknown processes (Li et al. 2011).

Although differential expression data exist for each transcript, and several transcripts were often identified per gene, I have reserved analysis and interpretation to the gene-level expression data for the sake of simplicity and manageability.

5.3.2.5. General observations

Of the 35556 genes and putative genes annotated in the NCBI Mouse genome annotation ~ 14000 were consistently detected by RNA-seq (Table 5-3). The significantly lower number of genes with transcript level data (Grubbs's test, $p < 0.05$) for the (*Z*)-ligustilide treatment set correlate with the lower amount of quality reads that were produced from that sample (see Table 5-2, Grubb's test, $p < 0.05$).

Table 5-3. Number of genes with RNA-seq transcript level data per treatment.

Treatment	Number of genes with expression data
(3*S*,8*S*)-falcarindiol (1μM)	13,852
(3*R*,8*S*)-falcarindiol (1 μM)	13,933
(3*R*,8*S*)-falcarindiol (10 μM)	14,022
(3*R*)-falcarinol (2 μM)	13,878
(*R*)-sulforphane (1μM)	13,898
6-isovaleryl-umbelliferone (10 μM)	13,962
(*Z*)-ligustilide (10 μM)	12,958
mean	*13,786*

A breakdown of the distribution of global RPKM values is given in Figure 5-2. The median and mean RPKM values were 63.2 and 220.8, which translates into median and mean transcript coverage of approximately 32- and 109-fold, respectively (based on 36 bp-read length, not corrected for quartile normalization). Ferritin, an iron-binding protein was the most abundant transcript with an average RPKM of 27,284. Amongst the 50 most abundant transcripts, as judged by RPKM, 10 coded for ribosomal proteins, 10 coded for enzymes involved in primary metabolism and cellular respiration, five coded for translation factors and five coded for structural or scaffold proteins. Of the top 50 most highly expressed transcripts six were of unknown function or predicted pseudogenes. Genes with transcript abundance less than one RPKM were excluded from subsequent analysis as their abundance estimations were considered unreliable. Filtering of data to remove RPKMs <1 reduced the mean number of genes with transcription information from 13,786 to 13,069.

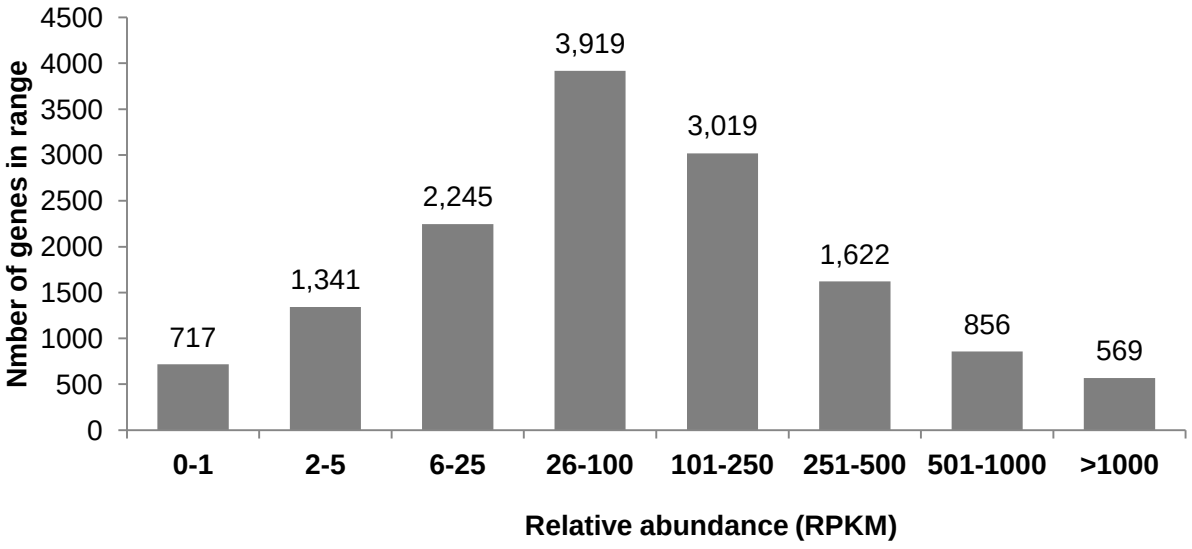

Figure 5-2. Distribution of average genic RPKM values.

5.3.2.6. Relative changes in gene expression level per treatment

The distribution of differential expression for each treatment group is provided in Figure 5-3. In general, treatments using higher concentrations (10 μM vs. 1 μM) resulted in greater overall perturbations of transcript levels as demonstrated by increases in the proportion of genes with differential expression (> 1.5 or < 0.5 in Figure 5-3). (3*R*,8*S*)-Falcarindiol was the only compound to be tested at more that one concentration (1 μM and 10 μM). Not surprisingly, the treatment at 10

μM resulted in a larger perturbation of transcript levels. Remarkably, the more potent QR-inducing stereoisomer, (3*S*,8*S*)-falcarindiol resulted in a lower degree of global changes than (3*R*,8*S*)-falcarindiol ($p < 0.001$, chi-square test of goodness of fit). With 1 μM (3*S*,8*S*)-falcarindiol 11% of transcripts fell outside of the 0.5-1.5-fold change range, while 19% of transcripts were outside of this range for 1 μM (3*R*,8*S*)-falcarindiol suggesting that (3*R*,8*S*)-falcarindiol has greater widespread effects on transcript levels. One μM (3*S*,8*S*)-falcarindiol also resulted in fewer transcript levels increasing to greater than 1.5-fold compared to (*R*)-sulforaphane (4% vs. 11%) which was tested at the same concentration (1 μM).

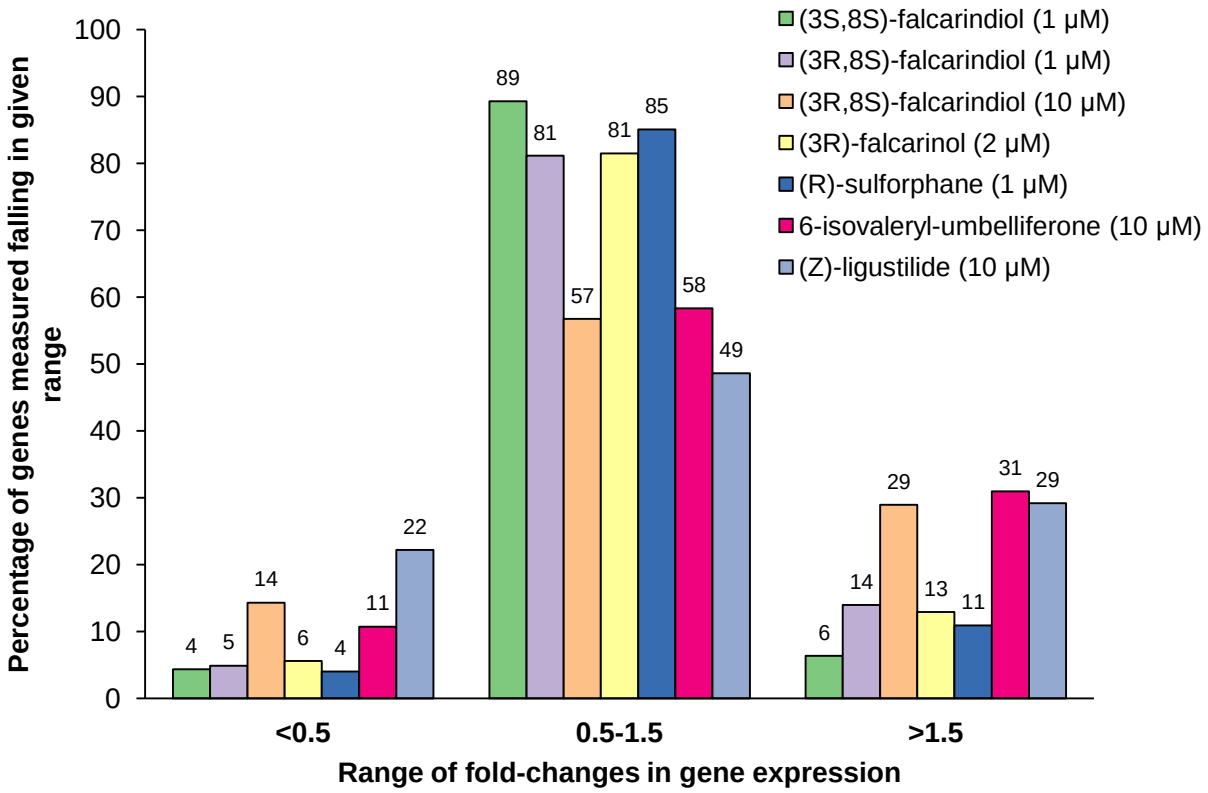

Figure 5-3. Distribution of fold-changes for all genes detected in response to treatment. Hepa-1c1c7 cells were exposed to the indicated compounds for 12 h and transcript levels were measured by RNA-seq. Due to rounding total percentage for each treatment may not equal 100.

5.3.2.7. Induction of QR enzymatic activity is correlated with increased transcript abundance

The levels of induction of QR activity determined by bioassay and QR transcript levels determined by RNA-seq and qRT-PCR are provided in Figure 5-4. In every case except for (*Z*)-

ligustilide, the fold difference in transcript level of QR after 12 h was closely correlated with enzyme activity after 48 h, consistent with transcriptional regulation of QR enzyme activity. Transcript levels in the (*Z*)-ligustilide treatment increased as judged by both RNA-seq and qRT-PCR but did not correlate with enzymatic activity to the same degree as the other treatments. It is unclear whether this difference is do to variability in measurement.. Due to the difference in sampling time points between transcript (12 h) and enzyme activity (48 h), it is possible that QR induction by (*Z*)-ligustilide is delayed compared to the other treatments. As (*Z*)-ligustilide induces phase I enzyme expression (see below), it is possible that a phase I enzyme-dependent metabolite of (*Z*)-ligustilide may mediate the full induction of QR through Nrf2 and confer this delay.

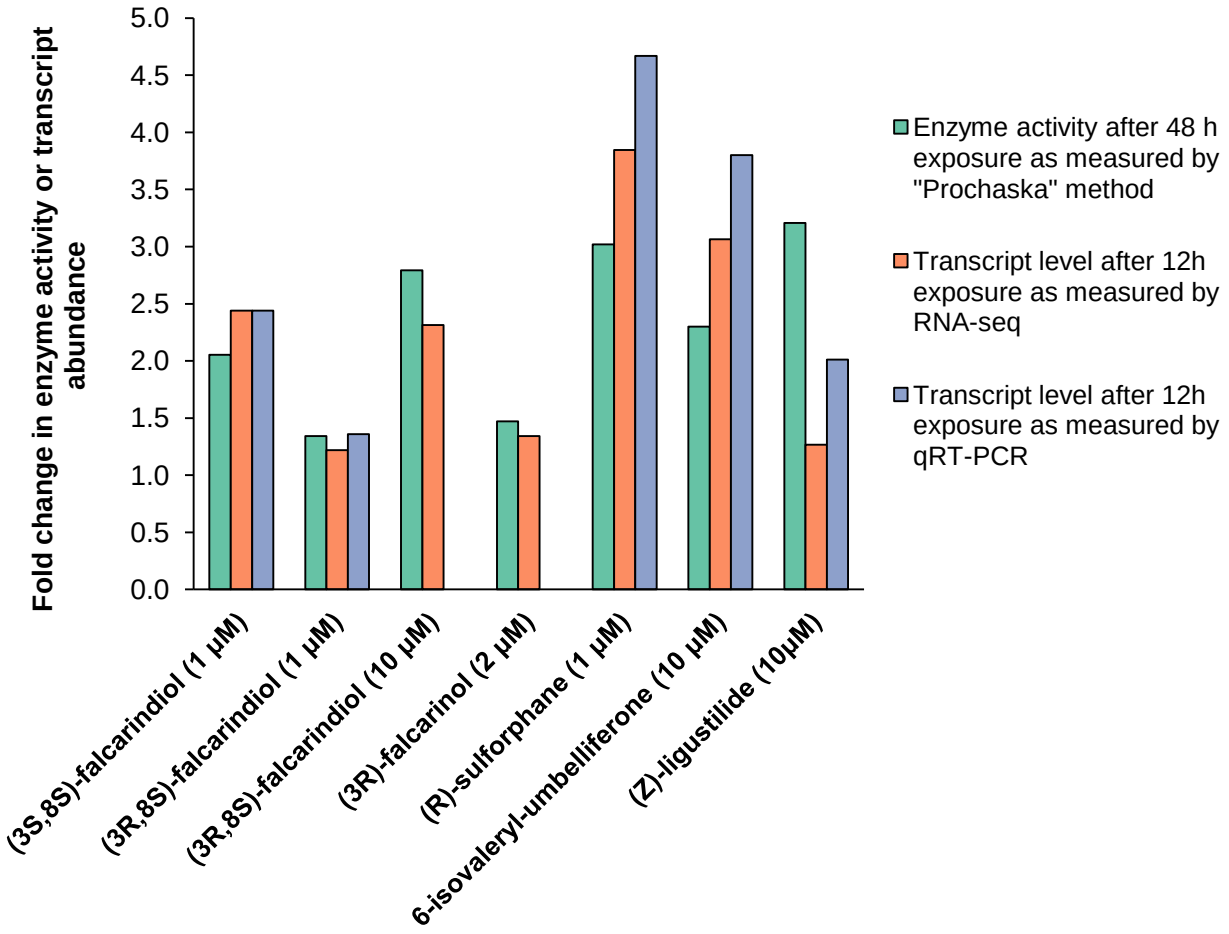

Figure 5-4. Comparison of QR enzyme activity (48 h) and transcript levels (12 h) in Hepa-1c1c7 cells after exposure to the indicated compounds. QR enzyme activity is the mean of two technical replicates. qRT-PCR

results are the mean of two technical replicates. RNA-seq results are from a single replicate of three pooled samples.

5.3.2.8. Effects of treatments on transcription of Nrf2 targets

A summary of transcript level changes for the most commonly used Nrf2 marker genes can be found in Table 5-4. In general, the compounds tested at concentrations that resulted in substantial QR induction (measured in the QR bioassay) caused induction of transcriptional markers for Nrf2 activity (1 µM (3*S*,8*S*)-falcarindiol, 10 µM (3*R*,8*S*)-falcarindiol, 1 µM (*R*)-sulforaphane, 10 µM 6-IVU, and 10 µM (*Z*)-ligustilide) whereas the treatments that did not produce a substantial activation of QR did not share this level of marker induction (1 µM (3*R*,8*S*)-falcarindiol and 2 µM (3*R*)-falcarinol). These findings are consistent with a mechanism of action of 1 µM (3*S*,8*S*)-falcarindiol, 10 µM (3*R*,8*S*)-falcarindiol, 1 µM (*R*)-sulforaphane, 10 µM 6-IVU, and 10 µM (*Z*)-ligustilide involving increased Nrf2-directed transcription. A comparison between 1 µM (3*S*,8*S*)-falcarindiol and 1 µM (*R*)-sulforaphane showed that 1 µM (*R*)-sulforaphane caused a greater increase in the levels of these transcripts at the same concentration, consistent with (*R*)-sulforaphane having greater activity in the QR-bioassay. The results for (*Z*)-ligustilide were unclear as two of the genes showed high levels of induction whereas the other three were more or less unchanged.

Table 5-4. Fold-changes in transcript levels of Nrf2 target genes. Hepa-1c1c7 cells were exposed to the indicated compounds for 12 h and transcript levels were measured by RNA-seq.

Description	**(3*S*,8*S*)-falcarindiol (1 µM)**	**(3*R*,8*S*)-falcarindiol (1µM)**	**(3*R*,8*S*)-falcarindiol (10 µM)**	**(3*R*)-falcarinol (2 µM)**	**(*R*)-sulforphane (1 µM)**	**6-isovaleryl-umbelliferone (10 µM)**	**(*Z*)-ligustilide (10 µM)**
QR	**2.4** (2.5)	1.2 (1.4)	**2.3**	1.3	**3.8** (4.7)	**3.1** (3.8)	1.3 (2.0)
HO-1	**2.0** (2.8)	1.4 (1.2)	**9.1**	**2.0**	**3.2** (3.8)	**2.3** (1.8)	**3.8** (2.2)
GLUTAMATE-CYSTEINE LIGASE-C	1.5	1.1	1.2	1.2	1.7	1.3	1.2
GLUTAMATE-CYSTEINE LIGASE-M	1.6	0.8	1.9	0.9	**2.6**	1.5	**5.4**
GLUTATHIONE S-TRANSFERASE, A3	**2.2**	1.0	1.9	1.2	**3.4**	1.5	0.9
mean	***1.9***	***1.1***	***3.3***	***1.3***	***3.0***	***1.9***	***2.5***

Parentheses denote values obtained from qRT-PCR analysis

Table 5-5 provides an expanded summary of Nrf2 targets for which Nrf2 regulation is not as well characterized as those used in Table 5-4. In addition to regulation by Nrf2, I would expect that the regulation of the gene listed in Tables 5-4 and 5-5 to be mediated by other co-operative or competitive factors. Even in a simplistic case where several genes are regulated by a single specific transcription factor, the number of binding elements and the degree of consensus for the specific transcription factor, as well as general transcription factors (e.g. TATA-binding protein (TBP), TFIIB, TFIID), can result in unique expression levels for each gene. Additionally, accessibility of the promoter region (Berger 2007), mRNA processing efficiency (Furger et al. 2002), and posttranscriptional stability (Lai 2002) will contribute to the variability of transcript abundance reported in Tables 5-3 and 5-4. The *HO-1* gene is an example of an Nrf2 target under complex regulation. At least four transcription factors (Nrf2, NF-κB, activator protein-1, and heat shock factor-1) regulate *HO-1* transcription (Alam et al. 2007). Additionally, the protein Bach1 represses Nrf2-mediated transcription through competitive binding to regulatory elements. One of the substrates for HO-1, heme, binds to and inhibits Bach1 from associating with the *HO-1* promoter.

For comparison I have also included the proportion of all genes measured that were substantially upregulated (greater than 1.5-fold) in each treatment group at the bottom of Table 5-5. (*R*)-sulforaphane (1 µM) treatment upregulated 17 of 28 (61%) of the Nrf2 targets compared to 7.8% of all transcripts measured. (3*S*,8*S*)-falcarindiol (1 µM) upregulated 10 of 28 (36%) of Nrf2-targets compared to 3.5% of all transcripts measured. These changes for (*R*)-sulforaphane and (3*S*,8*S*)-falcarindiol were statistically significant (Pearson's chi-square test, ($p < 0.01$) and provide support for the hypothesis that these compounds cause QR induction by activating Nrf2. In marked contrast to the 1 µM (3*S*,8*S*)-falcarindiol treatment, 1 µM (3*R*,8*S*)-falcarindiol treatment only upregulated a single Nrf2 target (3.6%) compared to 11.3% of all genes. As this concentration of (3*R*,8*S*)-falcarindiol did not greatly induce QR enzyme activity it is not surprising that Nrf2 targets were not activated. Conversely, a higher concentration of (3*R*,8*S*)-falcarindiol (10 µM) substantially increased the transcript levels of 15 of the 28 Nrf2-targets (54%) compared to 26% of all transcripts which was statistically significant ($p < 0.01$). This transcriptional signature is consistent with Nrf2 activation but less supportive than that of (3*S*,8*S*)-falcarindiol (1 µM) or (*R*)-sulforaphane (1 µM).

(*Z*)-ligustilide (10 µM) and 6-IVU (10 µM) also showed upregulation of a high proportion (39% and 36%, respectively) of the Nrf2 target genes listed in Table 5-5. However, this proportion did not greatly exceed the global proportion of upregulated genes (28% and 27%, respectively). Similarly, (3*R*)-falcarinol (2 µM) treatment also increased transcript levels for a higher proportion of Nrf2 targets (14%) than all targets (8%). This information is consistent with Nrf2 activation by these compounds but was not statistically significant (p values > 0.01).

Amongst the targets summarized in Table 5-5, *QR*, *HO-1*, *GLUTATHIONE SYNTHETASE*, *GLUTATHIONE S-TRANSFERASE-ALPHA-3* and *KEAP1* were the only targets that showed increases of greater than three-fold in any of the treatment conditions. Epoxide hydrolase 1, leukotriene A4 dehydrogenase, cullin 3, ring-box 1 and Maf G showed very little induction or were down-regulated in all of the treatment conditions.

5.3.2.9. Effects on transcription of AhR targets

AhR is the other primary transcription factor involved in regulating the expression of QR. Comparing the expression of additional AhR targets can provide an indication of whether this transcription factor was responsible for, or contributed to QR induction. Changes in transcript levels of AhR targets are summarized in Table 5-6. RPKM plots highlighting the Nrf2 and AhR targets summarized in Tables 5-5 and 5-6 can be found in Figure 5-5.

Consistent with AhR activation, 6-IVU (10 µM) caused a three-fold or greater increase in the transcript levels of all five AhR. (*Z*)-ligustilide (10 µM), (3*R*,8*S*)-falcarindiol (10 µM), and to a lesser extent, (*R*)-sulforaphane (1 µM), (3*R*,8*S*)-falcarindiol (1 µM), and (3*R*)-falcarinol (2 µM) also displayed upregulation of these targets, consistent with moderate to modest activation of the AhR receptor. AhR activation for sulforaphane was previously reported (Anwar-Mohamed et al. 2009).

(3*S*,8*S*)-falcarindiol (1 µM) was the only compound that completely lacked an AhR signature. Excluding the possibility of AhR-mediated QR activation provides support for an Nrf2-based mechanism for (3*S*,8*S*)-falcarindiol.

Table 5-5. Expanded list of fold-changes in transcript levels of Nrf2 target genes. Hepa-1c1c7 cells were exposed to the indicated compounds for 12 h and transcript levels were measured by RNA-seq.

Description	ENSEMBL identifier	(3*S*,8*S*)-falcarindiol (1µM)	(3*R*,8*S*)-falcarindiol (1µM)	(3*R*,8*S*)-falcarindiol (10µM)	(3*R*)-falcarinol (2 µM)	(*R*)-sulforphane (1µM)	6-IVU (10µM)	(*Z*)-ligustilide (10µM)	Reference for Nrf2-regulation
Oxidant metabolism and sequestration									
QR	ENSMUSG00000003849	**2.44**	1.22	**2.31**	1.34	3.85	**3.06**	1.27	(Ross et al. 2000)
CATALASE	ENSMUSG00000027187	1.31	1.13	**2.77**	1.33	1.56	1.60	1.54	(Otieno et al. 2000; Cho et al. 2005)
SUPEROXIDE DISMUTASE 1	ENSMUSG00000022982	1.18	1.05	1.32	0.83	1.53	1.83	1.44	(Otieno et al. 2000)
FERRITIN HEAVY CHAIN	ENSMUSG00000024661	1.16	1.11	1.81	1.40	1.45	**2.16**	**2.57**	(Pietsch et al. 2003; Cho et al. 2005)
EPOXIDE HYDROLASE 1	ENSMUSG00000038776	1.02	1.00	1.18	1.07	1.32	1.07	0.99	(Thimmulappa et al. 2002)
SULFIREDOXIN 1	ENSMUSG00000032802	1.41	1.31	**2.61**	1.65	1.74	**2.12**	**3.36**	(Bae et al. 2011)
Small molecule antioxidant production and reduction									
HO-1	ENSMUSG00000005413	1.96	1.36	**9.15**	**2.03**	**3.19**	**2.26**	**3.81**	(Shan et al. 2006)
THIOREDOXIN 1	ENSMUSG00000028367	1.09	0.70	0.69	0.51	1.02	0.53	0.43	(Kim et al. 2001)
THIOREDOXIN REDUCTASE 1	ENSMUSG00000020250	1.34	1.08	1.46	0.94	1.89	1.17	1.06	(Reisman et al. 2009)
GLUTAMATE-CYSTEINE LIGASE, CATALYTIC SUBUNIT	ENSMUSG00000032350	1.46	1.13	1.25	1.16	1.72	1.33	1.20	(Reisman et al. 2009)
GLUTAMATE-CYSTEINE LIGASE, MODIFIER SUBUNIT	ENSMUSG00000028124	1.55	0.83	1.85	0.91	**2.60**	1.52	**5.41**	(Reisman et al. 2009)
GLUTATHIONE SYNTHETASE	ENSMUSG00000027610	1.07	1.59	**11.53**	1.40	1.98	1.26	1.34	(Lee et al. 2005)
GLUTATHIONE REDUCTASE	ENSMUSG00000031584	1.59	1.01	**2.15**	1.41	**2.29**	0.73	0.82	(Ansher et al. 1986)

Table 5-5 cont.

Description	ENSEMBL identifier	(3*S*,8*S*)-falcarindiol (1 µM)	(3*R*,8*S*)-falcarindiol (1 µM)	(3*R*,8*S*)-falcarindiol (10 µM)	(3*R*)-falcarinol (2 µM)	(*R*)-sulforphane (1 µM)	6-IVU (10 µM)	(*Z*)-ligustilide (10 µM)	Reference for Nrf2-regulation
Conjugating and detoxification enzymes									
GLUTATHIONE S-TRANSFERASE, A3	ENSMUSG00000025934	**2.21**	0.97	1.88	1.25	**3.42**	1.46	0.85	(Jowsey et al. 2003; Malhotra et al. 2010)
UDP GLUCURONOSYLTRANSFERASE 2B34	ENSMUSG00000029260	1.59	0.83	0.59	0.85	1.59	0.46	0.38	(Reisman et al. 2009)
AFLATOXIN ALDEHYDE REDUCTASE	ENSMUSG00000028743	0.81	1.22	**2.06**	1.26	1.13	1.40	1.99	(Thimmulappa et al. 2002)
LEUKOTRIENE A4 DEHYDROGENASE	ENSMUSG00000015889	1.11	1.00	0.99	1.10	1.06	0.91	0.94	(Primiano et al. 1998)
MULTIDRUG RESISTANCE PROTEIN 1	ENSMUSG00000040584	0.96	0.76	0.49	0.55	0.91	0.93	0.63	(Song et al. 2009)
MULTIDRUG RESISTANCE PROTEIN 2	ENSMUSG00000025194	1.13	0.94	0.95	1.53	1.05	0.77	0.87	(Vollrath et al. 2006)
Production of reducing equivalents - pentose phosphate pathway									
HEXOSE-6-PHOSPHATE DEHYDROGENASE	ENSMUSG00000028980	0.97	1.47	**2.27**	1.00	1.36	**2.45**	1.70	(Reisman et al. 2009)
GLUCOSE-6-PHOSPHATE DEHYDROGENASE 2	ENSMUSG00000089992	1.75	1.35	1.66	1.08	**2.23**	1.10	0.94	(Wu et al. 2011)
GLUCOSE-6-PHOSPHATE DEHYDROGENASE X-LINKED	ENSMUSG00000031400	1.52	1.23	**2.03**	1.80	**2.61**	1.23	1.53	(Wu et al. 2011)
PHOSPHOGLUCONATE DEHYDROGENASE	ENSMUSG00000028961	1.76	1.47	**3.65**	1.46	**2.71**	1.82	**2.58**	(Thimmulappa et al. 2002)
Signal transduction									
KEAP1	ENSMUSG00000003308	0.96	1.26	**3.37**	1.46	1.54	**2.02**	1.95	(Lee et al. 2007)
SEQUESTOSOME 1	ENSMUSG00000015837	1.51	1.19	1.93	1.33	1.69	1.43	1.04	(Copple et al. 2010)
CULLIN 3	ENSMUSG00000004364	1.06	0.66	0.30	0.61	0.81	0.48	0.19	(Kaspar et al. 2010)
RING-BOX 1	ENSMUSG00000022400	1.01	0.80	0.71	0.85	0.76	0.88	0.47	(Kaspar et al. 2010)
MAF G	ENSMUSG00000025138	0.82	1.02	1.05	1.02	0.85	1.36	1.65	(Katsuoka et al. 2005)
Number of Nrf2-targets upregulated (>1.5-fold)		10	1	15	4	17	10	11	
Proportion of 28 Nrf2 targets upregulated (%)		**35.7**	**3.6**	**53.6**	**14.3**	**60.7**	**35.7**	**39.3**	
Proportion of genes with >1.5-fold expression globally (%)		3.5	11.3	26.0	8.4	7.8	27.7	26.9	
P value (calculated using Pearson's chi-square test, * indicates significance (p < 0.01))		**2.03E-08***	**9.66E-01**	**1.72E-03***	**2.05E-01**	**1.36E-12***	**2.38E-01**	**1.08E-01**	

Table 5-6. Fold-changes in transcript levels for AhR target genes. Hepa-1c1c7 cells were exposed to the indicated compounds for 12 h and transcript levels were measured by RNA-seq

Gene	(3*S*,8*S*)-falcarindiol (1 μM)	(3*R*,8*S*)-falcarindiol (1 μM)	(3*R*,8*S*)-falcarindiol (10 μM)	(3*R*)-falcarinol (2 μM)	(*R*)-sulforphane (1 μM)	6-isovaleryl-umbelliferone (10 μM)	(*Z*)-ligustilide (10 μM)
CYP1A1	0.9 (0.8)	1.1 (0.7)	1.2 (1.4)	1.4 (1.6)	1.3 (1.6)	**6.7** (7.5)	1.6 (1.4)
CYP1A2	1.0	1.7	**5.3**	1.7	**2.1**	**23.7**	**3.4**
CYP1B1	0.4	0.7	1.2	1.2	1.3	**3.6**	**2.4**
CYP2S1	1.2	1.4	1.4	1.1	1.5	**3.2**	2.1
C-MYC	1.1	1.3	**2.7**	1.5	1.3	**3.1**	**3.8**
mean	***0.9***	***1.2***	***2.4***	***1.4***	***1.5***	***8.1***	***2.7***

Parentheses denote values obtained from qRT-PCR analysis

6-IVU and (*Z*)-ligustilide are similar to known AhR ligands in that they are planar, aromatic and relatively non-polar with moderate molecular weights (190 and 246 Da respectively). Likewise, the polyacetylenes tested here have some similarity to an endogenous AhR ligand lipoxin A_4, an oxidized fatty acid derivative (Schaldach et al. 1999). However, the lack of induction of AhR at the 1 μM concentration for the polyacetylenes is consistent with these compounds being weak ligands for the AhR and is encouraging with respect to the beneficial potential of these compounds.

5.3.2.10. Computational analysis of transcriptional patterns resulting from exposure to QR inducers

Given the prior knowledge of QR induction, manual analysis of activation of Nrf2 and AhR was warranted. However, detailed analysis of all known transcription factors on a manual basis is prohibitively time consuming. I exploited available tools to expedite the identification of trends in the data. I used the database at Tfacts.org to search for transcriptional signatures (patterns of transcriptional regulation) of a wide range of transcription factors. Also, functional consequences of exposure to the test compounds were investigated by looking for enrichment of gene ontology (GO) terms, biochemical pathways and groups of interacting proteins (neighbor-based sets). Finally, I used principal component analysis (PCA) to compare the global effects on

transcription amongst the treatment groups. 5.3.2.11. Analysis of transcription factor binding signatures.

Tfacts (Essaghir et al. 2010) was used to look for transcriptional signatures indicative of transcription factor involvement. This service takes a list of up or down regulated genes and cross-references it with a database of known transcription factor targets (transcriptional signatures) to identify candidate transcription factors. A summary of the top hits for each treatment are provided in Table 5-7 in order of declining statistical likelihood.

Nrf2 was identified in all the treatments except that of (3*R*,8*S*)-falcarindiol (1 µM), and was one of the top three hits for both (3*S*,8*S*)-falcarindiol (1 µM) and (*R*)-sulforaphane (1 µM). This outcome is in accord with my prior manual analysis that supported Nrf2 activation by these compounds.

Although the TFACTs database does not appear to include the AhR, the aryl hydrocarbon receptor nuclear translocator (ARNT) was among the transcription factors identified in the 6-IVU treatment. AhR activity is dependent on formation of a complex with ARNT which functions as a transcriptional co-activator. Although ARNT may form complexes with other transcription factors such as hypoxia inducible factor (HIF)-α, ARNT transcriptional activation is often synonymous with AhR transcriptional activation and therefore the identification of this transcription factor as being activated by 6-IVU is consistent with my manual analysis that supported AhR activation by 6-IVU.

5.3.2.11. Over-representation of gene ontology, pathway and neighbour-based sets

ConsensusPathDB **(**CPDB) is a meta-database of protein interactions and annotations (Kamburov et al. 2011). Using lists of up and down regulated genes for each treatment group I queried CPDB to look for over-representation of GO terms, pathway-based sets and neighbour-based sets.

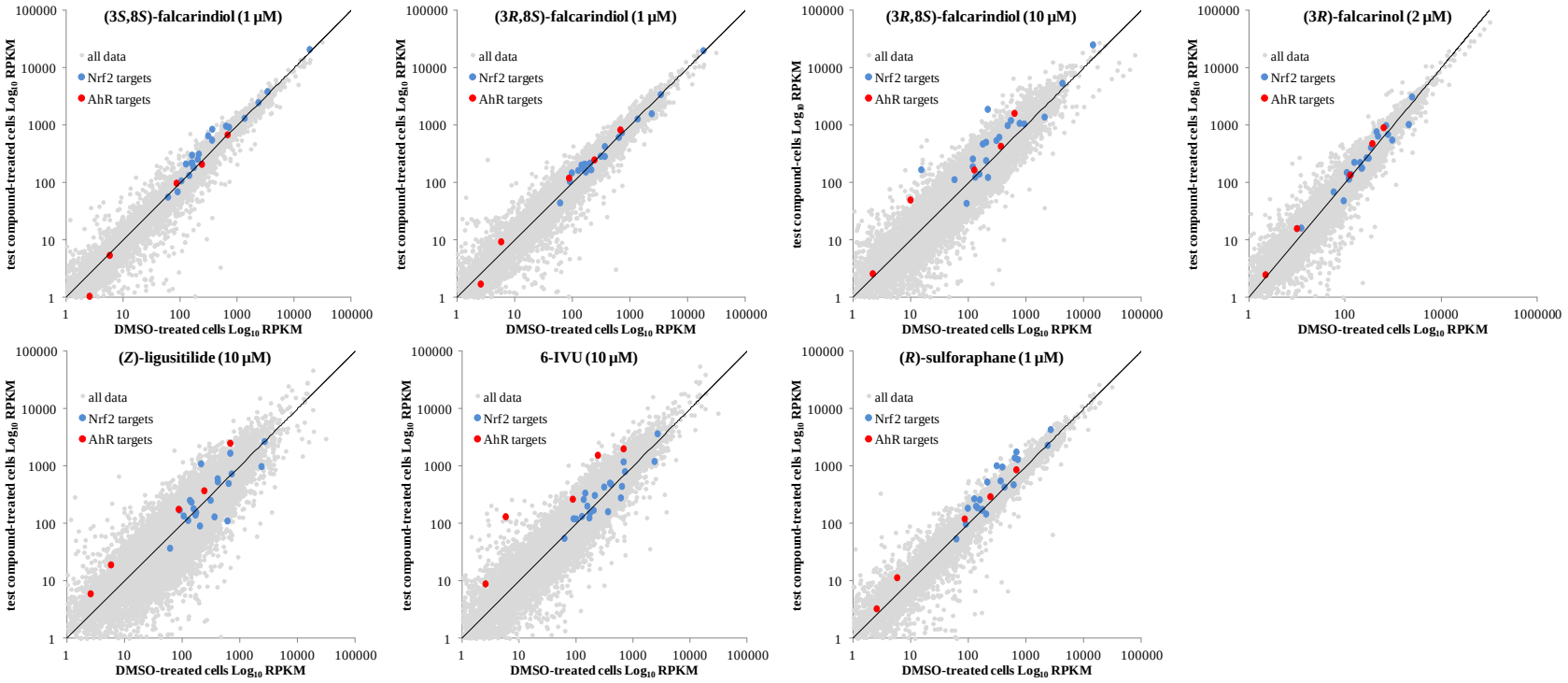

Figure 5-5. RPKM plots for treated vs. DMSO-treated cells. Dots on the left and right side of the line correspond to up and down regulated transcripts respectively. The Nrf2 and AhR targets listed in tables 5-4 and 5-5 are highlighted in blue and red respectively.

GO annotations are an attempt to provide a consistent set of terms describing the biological process, molecular function and cellular component with which a gene product is associated. These annotations are divided into levels with level 1 being the most general. Here, I only report enrichment of GO terms at level 3. I found levels 1 and 2 to be vague to provide useful information. This analysis is summarized in Table 5-8.

Pathway-based sets and neighbor-based sets represent groups of genes involved in the same biochemical pathway or that are known to interact, respectively. Tables 5-8 and B-1 (appendix) summarize the highest ranking sets for the two analyses.

Consistent with Nrf2 activation both (3*S*,8*S*)-falcarindiol (1 µM) and (*R*)-sulforaphane (1 µM) treatments showed enrichment in the GO terms 'response to oxidative stress' and 'pigment metabolic process' (heme metabolism is in part regulated by Nrf2 through regulation of HO-1). Additionally, (*R*)-sulforaphane treatment showed enrichment in glutamate-cysteine ligase complex and response to nitrosative stress. Terms associated with cell cycle regulation were well represented in the polyacetylene treatments while annotations involving regulation of metabolic processes were well represented in both (3R,8S)-falcarindiol treatments, the 6-IVU (10 µM) and (Z)-ligustilide (10 µM) treatments.

Pathway-based sets that were over-represented in the (3*S*,8*S*)-falcarindiol (1 µM) and (*R*)-sulforaphane (1 µM) treatments such as glutathione metabolism and the pentose phosphate pathway are consistent with Nrf2 activation. The (3*R*,8*S*)-falcarindiol (10 µM) treatment was associated with many pathways involved in translation. Both (3*S*,8*S*)-falcarindiol (1 µM) and (3*R*)-falcarinol (2 µM) treatments were commonly associated with transcript processing pathways. Finally, the 6-IVU (10 µM) and (*Z*)-ligustilide (10 µM) treatments showed a high number of associations with toll-like receptor (TLR), NF-κB, and nerve growth factor signalling.

Table 5-7. Filtered list of transcription factors signatures. Determined using TFACTS.org

(3*S*,8*S*)-falcarindiol (1 μM)	(3*R*,8*S*)-falcarindiol (1 μM)	(3*R*,8*S*)-falcarindiol (10 μM)	(3*R*)-falcarinol (2 μM)	(*R*)-sulforphane (1 μM)	6-isovaleryl-umbelliferone (10 μM)	(*Z*)-ligustilide (10 μM)
SP1	P53	ESR1	P53	WT1	FLI1	SMAD
NRF2	FOXO1	SREBP	FLI1	EGR1	WT1	FLI1
SRF	SREBP	FOXO3	NFKB1	NRF2	SMAD	SMAD3
RARB	ATF1	SMAD	TFAP2A	JUN	ESR1	STAT3
FLI1	CREB	STAT	BRCA1	RELA	SREBP	FOXO3
ESR1	ESR1	PPARD	AR	SMAD	ELK1	ESR1
JUN	ELK1	JUND	RELA	AP1	CREB	ELK1
GLI	RARB	GLI1	USF1	TBP	RARA	JUN
SREBP	FOXO3	STAT3	GLI1	GLI1	SMAD3	SREBP
NFKB1	BRCA1	CREB	NFKB	PPARG	JUN	AR
USF2	SRF	HIF1A	ATF4	JUND	HIF1A	NFKB
TCF/BETA-CATENIN	ATF4	JUN	CREB1	GLI2	JUND	JUND
TFAP2A	STAT5B	RELA	FOXO3	USF1	E2F	WT1
ETV4	GLI1	NFKB	CEBPA	FLI1	PPARD	RELA
EGR1	AR	AR	STAT	PPARD	SMAD7	TBP
ETS1	EGR1	NRF2	JUN	FOS	GLI1	E2F
STAT3	RARA	JUNB	HIF1A	P53	ETV4	ID1
HIF1A	STAT5A	SMAD3	PPARG	NFKB1	STAT5	FOXO4
USF1	HIF	ELK1	RARB	CREB	STAT1	PPARD
SMAD	HIF1A	RARA	ATF1	NFIA	HIF	HIF1A
RARA	PPARG	STAT5	WT1	NFKB	SRF	SRF
AP1	STAT	ATF4	PPARD	STAT5B	BRCA1	BRCA1
STAT	USF1	TBP	FOXO	HIF1A	REL	RARA
CREB	CEBPA	HIF	GLI2	NOTCH/ RBP-J	ID1	PPARG
TBP	TFAP2A	PPARG	ELK1	JUNB	FOS	E2F1
GLI1	STAT5	GATA1	SMAD	AR	STAT5B	STAT1
ATF1	FLI1	BRCA1	FOS	SMAD3	ATF4	MYBL2
RELA	NOTCH/ RBP-J	E2F1	LEF1	CEBPA	NFIC	NFIC
CREB1	GLI2	FOS	RARA	STAT1	JUNB	SMAD4
NFKB	USF2	LXR	USF2	HIF	SMAD4	JUNB
P53	RELA	FLI1	ESR1	STAT5A	PPARG	MYB
SPI1	ETS2	E2F	EGR1	FOXO	ATF6	GLI1
GLI2	JUND	ATF1	NRF2	NFIC	ARNT	PAX6
SP3	STAT1	PPARA	JUNB	SREBP	STAT5A	HIF
FOXO1	NFIC	MYBL2	SMAD3	RARB	RARB	CREB
FOXO	ETS1	NFAT1	E2F	RARA	PPARA	STAT5
	JUN	LEF1	NOTCH/ RBP-J	ESR1	PAX6	STAT5B
	SPI1	NFIA	STAT5	ETS1	RARG	ATF2
	RXR/RAR	PAX6	RXR/RAR	FOXO1	CREM	ATF1
	STAT3	RARB	JUND	USF2	GATA1	STAT5A
	FOS	ATF2	STAT3	TFAP2A	LEF1	FOS
	ETS	STAT1	SREBP	STAT3	BCL6	TCFAP2A
	SP3	TCFAP2A	SP3	FOXO3	NFIA	ATF4
	POU2F1	ETV4	FOXO1	STAT5	MYBL2	ETS
	AP1	SMAD4	ETV4	SPI1	NFAT1	ETV4
	NFKB1	NFIC	CREB	CREB1	POU5F1	PPARA
		WT1	TBP	STAT	NRF2	NRF2
		ETS	NFIA	ATF1	ATF2	CREM
		POU2F1	ETS1	POU2F1	E2F4	POU2F1
		CEBPB	ATF2	HNF4A	FOXA1	E2F4
			AP1	SP3	E2F1	REST
			NFIC		FOXA2	RARB

Table 5-8. Over-represented gene ontology sets.

(3*S*,8*S*)-falcarindiol (1 μM)	(3*R*,8*S*)-falcarindiol (1 μM)	(3*R*,8*S*)-falcarindiol (10 μM)	(3*R*)-falcarinol (2 μM)	(*R*)-sulforphane (1 μM)	6-isovaleryl-umbelliferone (10 μM)	(*Z*)-ligustilide (10 μM)
Negative regulation of cell cycle process	Negative regulation of nitrogen compound metabolic process	Cytoplasm	Negative regulation of cell cycle process	**Response to oxidative stress**	Transcription factor binding	Transcription factor binding
Mitotic metaphase/anaphase transition	DNA binding	Intracellular membrane-bounded organelle	Mitotic metaphase/anaphase transition	Peptide metabolic process	Negative regulation of nitrogen compound metabolic process	Negative regulation of nitrogen compound metabolic process
Vitamin transport	Regulation of nitrogen compound metabolic process	Cytoplasmic part	Negative regulation of cell cycle	**Glutamate-cysteine ligase complex**	Regulation of nitrogen compound metabolic process	Negative regulation of biosynthetic process
Response to oxidative stress	Regulation of cellular metabolic process	Cellular macromolecule metabolic process	DNA binding	Cell junction assembly	Negative regulation of biosynthetic process	Macromolecule biosynthetic process
Pigment catabolic process	Negative regulation of biosynthetic process	Nuclear part	Microtubule	Microtubule-based movement	Regulation of macromolecule metabolic process	Regulation of macromolecule metabolic process
Negative regulation of cell cycle	Regulation of macromolecule metabolic process	Intracellular non-membrane-bounded organelle	Intracellular non-membrane-bounded organelle	Negative regulation of cell cycle process	Regulation of cellular metabolic process	Negative regulation of cellular metabolic process
Regulation of cell cycle process	Negative regulation of cellular metabolic process	Purine nucleotide binding	Cell junction assembly	Transcription factor binding	Regulation of biosynthetic process	Regulation of nitrogen compound metabolic process
Regulation of female receptivity	Regulation of primary metabolic process	Ribonucleotide binding	Gene expression	**Pigment catabolic process**	Regulation of primary metabolic process	DNA binding
Kinetochore	Regulation of metabolic process	RNA binding	Developmental growth involved in morphogenesis	**Response to nitrosative stress**	DNA binding	Regulation of biosynthetic process
	Regulation of biosynthetic process	Ligase activity, forming carbon-nitrogen bonds	Regulation of nitrogen compound metabolic process	Vitamin transport	Macromolecule biosynthetic process	Enzyme binding
	Negative regulation of macromolecule metabolic process	Protein metabolic process	Macromolecule biosynthetic process		Negative regulation of cellular metabolic process	Cell junction assembly

Table 5.8 cont.

(3*S*,8*S*)-falcarindiol (1 μM)	(3*R*,8*S*)-falcarindiol (1 μM)	(3*R*,8*S*)-falcarindiol (10 μM)	(3*R*)-falcarinol (2 μM)	(*R*)-sulforphane (1 μM)	6-isovaleryl-umbelliferone (10 μM)	(*Z*)-ligustilide (10 μM)
	Oxidoreductase activity, acting on the CH-NH group of donors	Ribosome	Cerebellar Purkinje cell layer development		Gene expression	Regulation of cellular metabolic process
	Gene expression	Macromolecule catabolic process			Negative regulation of cell cycle process	Gene expression
	Macromolecule biosynthetic process	Intracellular organelle lumen			Transcription coactivator activity	Post-embryonic camera-type eye development
	Cell junction assembly	Intracellular transport			Cellular macromolecule metabolic process	Flotillin complex
	Adenosine deaminase activity	Mitotic cell cycle			Regulation of cell shape	Negative regulation of macromolecule metabolic process
	Specific transcriptional repressor activity	Hydrolase activity, acting on acid anhydrides			Negative regulation of macromolecule metabolic process	Regulation of primary metabolic process
	Regulation of signaling pathway	Protein localization			Regulation of metabolic process	Cell leading edge
	Microtubule	Protein transport			Cell junction assembly	Specific RNA polymerase II transcription factor activity
	Maintenance of location in cell	Cell cycle phase			Flotillin complex	Transforming growth factor-beta production
	Regulation of cell cycle	Macromolecule modification			Cell leading edge	Transcription factor complex
	Transcription factor binding	Energy derivation by oxidation of organic compounds			Regulation of signaling pathway	Positive regulation of nitrogen compound metabolic process
	Embryonic heart tube development	Generation of precursor metabolites and energy			Nucleobase, nucleoside, nucleotide and nucleic acid metabolic process	Negative regulation of cell cycle process
		Cellular macromolecule localization			Specific RNA polymerase II transcription factor activity	Regulation of metabolic process
		Cellular catabolic process			Regulation of signaling process	Microtubule

Table 5-9. Over-represented pathway-based sets.

(3S,8S)-falcarindiol (1 µM)	**(3R,8S)-falcarindiol (1 µM)**	**(3R,8S)-falcarindiol (10 µM)**	**(3R)-falcarinol (2 µM)**	**(R)-sulforphane (1 µM)**	**6-isovaleryl-umbelliferone (10 µM)**	**(Z)-ligustilide (10 µM)**
Metabolism of carbohydrates	Gap junction trafficking and regulation	Metabolism of proteins	Transport of Mature mRNA Derived from an Intronless Transcript	**Pentose phosphate pathway (hexose monophosphate shunt)**	TRAF6 mediated induction of NFkB and MAP kinases upon TLR7/8 or 9 activation	Signalling by NGF
Regulation of Glucokinase by Glucokinase Regulatory Protein	Gap junction degradation	Gene Expression	Transport of Mature mRNAs Derived from Intronless Transcripts	**Glutathione metabolism - *Mus musculus* (mouse)**	MyD88 dependent cascade initiated on endosome	Toll Like Receptor TLR1:TLR2 Cascade
Glucose transport	Acute myeloid leukemia - *Mus musculus* (mouse)	SRP-dependent cotranslational protein targeting to membrane	Transport of the SLBP independent Mature mRNA	**Glutathione synthesis**	Toll Like Receptor 7/8 Cascade	MyD88:Mal cascade initiated on plasma membrane
Hexose transport	Gap junction trafficking	Translation	Transport of the SLBP Dependant Mature mRNA	**Pentose phosphate pathway - *Mus musculus* (mouse)**	Toll Like Receptor 9 Cascade	Toll Like Receptor 4 Cascade
Transport of the SLBP independent Mature mRNA	Resolution of AP sites via the multiple-nucleotide patch replacement pathway	GTP hydrolysis and joining of the 60S ribosomal subunit	Regulation of Glucokinase by Glucokinase Regulatory Protein	**Glutathione conjugation**	Activated TLR4 signalling	TRAF6 mediated induction of NFkB and MAP kinases upon TLR7/8 or 9 activation
Transport of the SLBP Dependant Mature mRNA	Removal of DNA patch containing abasic residue	Eukaryotic Translation Termination	Glucose transport	Insulin effects increased synthesis of Xylulose-5-Phosphate	Toll Receptor Cascades	MyD88 dependent cascade initiated on endosome
Transport of Mature mRNA Derived from an Intronless Transcript	Gap junction - *Mus musculus* (mouse)	Formation of a pool of free 40S subunits	Hexose transport	Vitamin C (ascorbate) metabolism	Toll Like Receptor 3 Cascade	Toll Like Receptor 7/8 Cascade
Transport of Mature mRNAs Derived from Intronless Transcripts	Signalling by NGF	Cap-dependent Translation Initiation	snRNP Assembly	Gap junction - *Mus musculus* (mouse)	Signalling by NGF	Toll Like Receptor 9 Cascade
snRNP Assembly	C6 deamination of adenosine	Eukaryotic Translation Initiation	Metabolism of non-coding RNA	Prefoldin mediated transfer of substrater to CCT/TriC	Toll Like Receptor TLR1:TLR2 Cascade	Activated TLR4 signalling
Metabolism of non-coding RNA	Formation of editosomes by ADAR proteins	L13a-mediated translational silencing of Ceruloplasmin expression	Transport of Mature Transcript to Cytoplasm	Post-chaperonin tubulin folding pathway	MyD88:Mal cascade initiated on plasma membrane	Toll Like Receptor TLR6:TLR2 Cascade

Table 5.9 cont.

(3S,8S)-falcarindiol (1 µM)	(3R,8S)-falcarindiol (1 µM)	(3R,8S)-falcarindiol (10 µM)	(3R)-falcarinol (2 µM)	(R)-sulforphane (1 µM)	6-isovaleryl-umbelliferone (10 µM)	(Z)-ligustilide (10 µM)
Transport of Mature mRNA derived from an Intron-Containing Transcript	mRNA Editing: A to I Conversion	3, -UTR-mediated translational regulation	Transport of Mature mRNA derived from an Intron-Containing Transcript	Acute myeloid leukemia - *Mus musculus* (mouse)	MyD88-independent cascade initiated on plasma membrane	Toll Like Receptor 2 Cascade
Transport of Mature Transcript to Cytoplasm	NGF signalling via TRKA from the plasma membrane	Peptide chain elongation	Metabolism of RNA	RNA Polymerase III Transcription Termination	Toll Like Receptor 4 (TLR4) Cascade	Toll Receptor Cascades
Metabolism of RNA	Adherens junction - *Mus musculus* (mouse)	Eukaryotic Translation Elongation	Processing of Capped Intron-Containing Pre-mRNA	Cooperation of Prefoldin and TriC/CCT in actin and tubulin folding	NFkB and MAP kinases activation mediated by TLR4 signaling repertoire	NGF signalling via TRKA from the plasma membrane
Transmembrane transport of small molecules	Integrin alphaIIb beta3 signaling	Cell Cycle	TRAF6 mediated NF-kB activation	Chaperonin-mediated protein folding	TRAF6 Mediated Induction of proinflammatory cytokines	NFkB and MAP kinases activation mediated by TLR4 signaling repertoire
SLC-mediated transmembrane transport	Resolution of Abasic Sites (AP sites)	Cell Cycle, Mitotic	mRNA Processing	Metabolism of carbohydrates	Toll Like Receptor TLR6:TLR2 Cascade	TRAF6 Mediated Induction of proinflammatory cytokines
Pentose phosphate pathway (hexose monophosphate shunt)	Base Excision Repair	Ribosome - *Mus musculus* (mouse)	Metabolism of carbohydrates	Adherens junction - *Mus musculus* (mouse)	Toll Like Receptor 2 Cascade	MyD88-independent cascade initiated on plasma membrane
Pentose phosphate pathway - *Mus musculus* (mouse)	Prostate cancer - *Mus musculus* (mouse)	Ubiquitin mediated proteolysis - *Mus musculus* (mouse)	Formation and Maturation of mRNA Transcript	NF-kB is activated and signals survival	NGF signalling via TRKA from the plasma membrane	PI3K/AKT signalling
mRNA Processing	Focal adhesion - *Mus musculus* (mouse)	Metabolism	Gene Expression	Acute myeloid leukemia - *Mus musculus* (mouse)	Prostate cancer - *Mus musculus* (mouse)	
Formation and Maturation of mRNA Transcript	Formation of annular gap junctions	The citric acid (TCA) cycle and respiratory electron transport	human TAK1 activates NFkB by phosphorylation and activation of IKKs complex	Endometrial cancer - *Mus musculus* (mouse)	Toll Like Receptor 3 (TLR3) Cascade	
Processing of Capped Intron-Containing Pre-mRNA	Pathways in cancer - *Mus musculus* (mouse)	Mitotic M-M/G1 phases	Viral dsRNA:TLR3:TRIF Complex Activates RIP1	Signaling by EGFR	Post-chaperonin tubulin folding pathway	
Vitamin C (ascorbate) metabolism	ErbB signaling pathway - *Mus musculus* (mouse)	Ribosomal scanning and start codon recognition	NF-kB is activated and signals survival	ErbB signaling pathway - *Mus musculus* (mouse)	EGFR downregulation	
Glutathione metabolism - *Mus musculus* (mouse)	p130Cas linkage to MAPK signaling for integrins	p53 signaling pathway - *Mus musculus* (mouse)	human TAK1 activates NFkB by phosphorylation and activation of IKKs	Pathways in cancer - *Mus musculus* (mouse)	Endocytosis - *Mus musculus*	

Detection of over-representation of neighbor-based sets (Figure B-1) centered around glutathione synthesis (GSHB-glutathione synthetase and GSH0-gamma-glutamyl-cysteine synthase regulatory subunit) in the sulforaphane (1 µM) treatment is consistent with Nrf2 activation. The detection of an over-represented neighbor-based set centered around IKK-B in the 6-IVU (10 µM) and (*Z*)-ligustilide (10 µM) was in agreement with the enrichment of NF-κB and TLR signalling pathways detected in the pathway-based analysis. Also, detection of a set centered around ARNT in response to 6-IVU (10 µM) is consistent with activation of the AhR by this compound.

5.3.2.12. Principal components analysis

Principal components analysis (PCA) is a method used to detect patterns in highly dimensional data. PCA relies on calculating metrics to represent the degree that each variable accounts for differences amongst sample sets. In other words, PCA can reduce complex sample sets (gene expression data for 14000 genes under a range of conditions) to single points by simplifying the variability amongst samples to principal components that are represented by chart axes. I chose to use PCA to look for trends amongst the RNA-seq data and as a means to verify differences between the falcarindiol stereoisomers. The results of this analysis are shown in Figure 5-6. Table 5-10 is a summary of the statistics associated with this analysis.

As a verification of the computational outcome, I completed an analysis of a subset of the data (946 genes beginning with the letter A). The outcome of this subset (not shown) followed a nearly identical pattern to that of the whole set.

Principal components 1 and 2 accounted for 46% and 20% of the variance between sample groups. On the basis of these principal components the gene expression patterns of (3*R*,8*S*)-falcarindiol (1 µM) and (3*S*,8*S*)-falcarindiol (1 µM) were both more alike (*R*)-sulforaphane (1 µM) than they were each other. This finding provides support for the hypothesis that the two falcarindiol stereoisomers display different pharmacological effects. The grouping of 6-IVU (10 µM) and (*Z*)-ligustilide (10 µM) when plotted on principal components 1 and 2 was in agreement with the high level of similarity that was observed between these two treatments in the TFACTS and CPDB analysis mentioned above. Principal components 3 and 4 accounted for 15% and 9% of

the variance between sample groups and captured similarities between the (3*R*,8*S*)-falcarindiol (1 µM), (3*R*,8*S*)-falcarindiol (10 µM), (3*S*,8*S*)-falcarindiol (1 µM) and (*R*)-sulforaphane (1 µM).

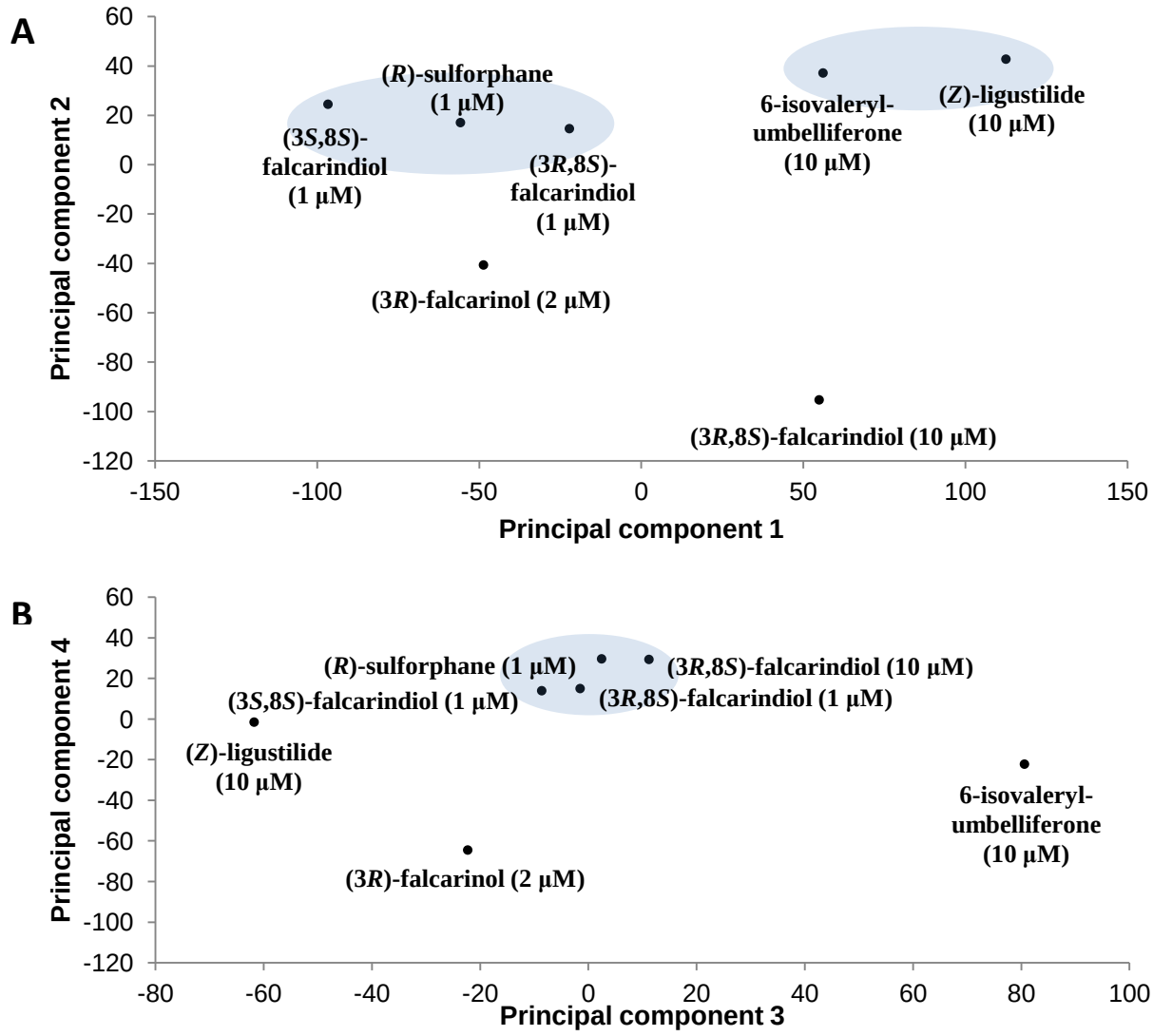

Figure 5-6. Principal components analysis of differential gene expression patterns. Treatments groups are plotted on A) principal components 1 and 2, and B) principal components 3 and 4. Calculated using R.

Table 5-10. Summary statistics for PCA analysis of differential gene expression patterns.

	PC1	PC2	PC3	PC4	PC5	PC6
Standard deviation	75.4257	50.0795	42.8448	33.69789	26.20258	23.15927
Proportion of variance	0.4591	0.2024	0.1482	0.09164	0.05541	0.04329
Cumulative proportion of variance	0.4591	0.6615	0.8097	0.90131	0.95671	1

5.3.2.13. Follow-up on computational studies

Upon completing the above computational analyses some trends in the data were apparent. (3*S*,8*S*)-falcarindiol and (3*R*,8*S*)-falcarindiol differ substantially in their global effects on transcription. Aside from the differences in Nrf2 activation, (3*R*,8*S*)-falcarindiol treatment appeared to cause changes associated with cellular metabolism. This was based on the over-representation of GO terms associated with metabolic processes and the presence of many transcription factors involved in metabolism in the TFACTs analysis for the (3*R*,8*S*)-falcarindiol treatments. This signature was common to (3*R*,8*S*)-falcarindiol (10 µM), 6-IVU (10 µM) and (*Z*)-ligustilide (10 µM) treatments and appeared to be captured to a degree in principal component 1 of the PCA. Also of interest, was the activation of NF-κB associated signalling pathways. Transcription factors associated with these pathways were detected for all of the treatments by TFACTS analysis but for the other analyses these pathways were particularly enriched in the (*Z*)-ligustilide, 6-IVU and falcarinol treatments. Therefore I decided to look further into the regulation of metabolism with particular focus on lipid homeostasis as well as NF-κB signalling.

5.3.2.14. Regulators of lipid homeostasis

Sterol-responsive element binding proteins (SREBPs) are basic-helix-loop-helix transcription factors that regulate lipid metabolism reviewed in Eberle et al. (2004). Three SREBP isoforms SREBP-1a, SREBP-1c, and SREBP-2 have been identified in mammals. SREBP-1a and -1c are derived from alternate transcriptional start sites of the SREBP-1 gene and differ in their transactivation domains.

In the transcriptional signature analysis (TFACTS), SREBP was one of the top three hits in response to both 1 µM and 10 µM (3*R*,8*S*)-falcarindiol, and was also identified in the 1 µM (3*S*,8*S*)-falcarindiol, (3*R*)-falcarinol (2 µM), (*Z*)-ligustilide (10 µM) and 6-IVU (10 µM) treatments. TFACTS does not distinguish between SREBP isoforms. Consistent with SREBP activation, GO terms associated with metabolic processes were over-represented in both (3*R*,8*S*)-falcarindiol treatments and the (*Z*)-ligustilide (10 µM) and 6-IVU (10 µM) treatments.

A summary of transcript level changes of SREBP-1 and -2 targets and regulators is provided in Table 5-11. Most of these targets were identified by microarray analysis of overexpression and deletion lines and validated using an additional technique (i.e. qRT-PCR) (Horton et al. 2003). On average the transcript levels of these targets were increased with (3*R*,8*S*)-falcarindiol (1 µM), (3*R*,8*S*)-falcarindiol (10 µM), (*Z*)-ligustilide (10 µM) and 6-IVU (10 µM) treatments. The genes that were subjected to the largest and most consistent changes were acetoacetyl-CoA synthetase, the LDL-receptor, fatty acid synthase and ABC1 which is known to be negatively regulated by SREBP-2 (Zeng et al. 2004; Tamehiro et al. 2007).

SREBPs share a level of identity with Nrf2 as both are basic helix-loop-helix transcriptions factors. Could it be that Keap1 regulates SREBPs via ubiquitylation and that the small molecules tested also interfere with this process? Interestingly the mouse *SREBP-1* gene possesses an ETGD sequence in the N-terminus which is very similar to the ETGE / ESGE sequences recognized by Keap1 for two of its known substrates, Nrf2 and phosphoglycerate mutase family member 5 (PGAM5), respectively (Lo et al. 2006; Tong et al. 2006). However, the literature suggests that Nrf2 is involved in down-regulating SREBP mediated transcription (Tanaka et al. 2008; Zhang et al. 2010) which reduces the likelihood of this mechanism of action. Upon further investigation, it was revealed that the *SREBP-1* and *SREBP-2* transcripts are themselves upregulated suggesting that activation of *SREBP* transcription was secondary to activation of another transcription factor (or other means of increasing transcript levels) rather than a mechanism involving changes in the stability or transcriptional activity of the SREBP proteins.

Table 5-11. Transcript levels of validated SREBP-1 and SREBP-2 targets and regulators. Hepa-1c1c7 cells were exposed to the indicated compounds for 12 h and transcript levels were measured by RNA-seq.

Description	**ENSEMBL identifier**	(3S,8S)-falcarindiol (1 μM)	(3R,8S)-falcarindiol (1 μM)	(3R,8S)-falcarindiol (10 μM)	(3R)-falcarinol (2 μM)	(R)-sulforphane (1 μM)	6-isovaleryl-umbelliferone (10 μM)	(Z)-ligustilide (10 μM)
Targets								
ACETOACETYL-COA SYNTHETASE	ENSMUSG00000029482	0.95	1.22	1.94	1.16	1.21	1.77	2.03
ATP CITRATE LYASE	ENSMUSG00000020917	0.78	1.09	1.01	0.90	1.09	1.45	0.58
7-DEHYDROCHOLESTEROL REDUCTASE	ENSMUSG00000058454	0.61	1.14	1.07	0.78	0.63	0.67	0.75
FARNESYL DIPHOSPHATE SYNTHETASE	ENSMUSG00000059743	0.91	0.85	1.32	1.13	0.89	1.31	0.90
HMG-CO A REDUCTASE	ENSMUSG00000021670	0.98	1.61	1.10	1.33	1.34	1.16	1.11
LOW DENSITY LIPOPROTEIN RECEPTOR	ENSMUSG00000032193	1.18	1.43	1.72	1.03	1.34	1.73	1.68
CYTOCHROME P450, FAMILY 51 (CYP51)	ENSMUSG00000001467	0.91	0.68	0.51	0.77	0.87	0.55	0.31
FATTY ACID SYNTHASE	ENSMUSG00000025153	1.05	1.78	2.22	1.53	1.14	2.68	4.19
ATP-BINDING CASSETTE, SUB-FAMILY A, MEMBER 1 (ABCA1) (DOWN-REGULATION, INVERSE USED IN CALCULATING MEAN)	ENSMUSG00000015243	1.00	0.84	0.60	0.88	0.73	0.71	0.59
Mean		***0.93***	***1.22***	***1.39***	***1.09***	***1.10***	***1.41***	***1.47***
Regulators								
STEROL REGULATORY ELEMENT BINDING FACTOR 1 (SREBP1)	ENSMUSG00000020538	0.81	1.45	2.30	1.25	1.20	2.29	2.98
STEROL REGULATORY ELEMENT BINDING FACTOR 2 (SREBP2)	ENSMUSG00000022463	1.02	1.51	2.39	1.28	1.22	2.15	2.62
ESTROGEN RECEPTOR 1 (ESR1)	ENSMUSG00000019768	1.24	1.73	1.63	1.66	1.72	2.91	3.23
FORKHEAD BOX O3 (FOXO3)	ENSMUSG00000048756	0.93	1.38	1.91	1.34	1.07	2.25	3.28

Numerous transcriptional regulators of SREBPs have been documented. These include the liver X receptor / retinoid X receptor, ROR-alpha, the cannabininoid-1 receptor (CB_1), the estrogen receptor-1 (ESR-1) and hepatocyte nuclear factor-4a (Sampath et al. 2004; Wang et al. 2006). Furthermore, the SREBP-1c isoform directs it's own transcription in a positive feedback loop (Horton et al. 2003).

TFACTS analysis had highlighted ESR-1 and a transcriptional regulator of ESR-1, FOXO3, as being active in the same treatments that produced an SREBP signature. Examination of the RNA-seq data revealed that the transcript levels of these transcription factors were elevated and correlated with that of SREBPs and their targets. Therefore, it is feasible that a transcriptional cascade of FOXO3, ESR-1, SREBPs and their targets may occur in the presence of (3*R*,8*S*)-falcarindiol, (*Z*)-ligustilide or 6-IVU. However, a mechanism responsible for activation of FOXO3 under these conditions is not clear. Indeed, it is difficult to draw any conclusions regarding the mechanism(s) underlying these gene expression changes without further study.

5.3.2.15. NF-κB

As a central transcription factor mediating the expression of inflammatory genes, the effects of NF-κB activation are antagonistic to those of Nrf2 activation. Certain Nrf2 activators decrease activation of NF-κB by directly modifying cysteines of either the DNA-binding domain of the NF-κB subunit RelA, the catalytic cysteines of IKK or through other means such as causing competition for mutual co-factors such as CBP. A summary of the expression patterns of NF-κB targets genes are provided in Table 5-12.

The overall pattern of expression of NF-κB target genes was downregulation for the two most convincing Nrf2 activators in the screen, (3*S*,8*S*)-falcarindiol (1 µM) and (*R*)-sulforaphane (1 µM) and upregulation for 6-IVU (10 µM) and (*Z*)-ligustilide (10 µM). Interestingly, the pattern of NF-κB activation was similar to that of AhR activation with 6-IVU (10 µM) and (Z)-ligustilide (10 µM) appearing to be the most potent inducers of both systems. As the AhR is involved in NF-κB mediated inflammatory gene expression during exposure to lipopolysaccharide (Wu et al. 2011) it would be interesting to determine whether AhR activation is also involved in NF-κB mediated transcription under these conditions.

Table 5-12. Fold-changes in transcript levels of NF-κB targets. Hepa-1c1c7 cells were exposed to the indicated compounds for 12 h and transcript levels were measured by RNA-seq.

	ENSEMBL identifier	(3S,8S)-falcarindiol (1 μM)	(3R,8S)-falcarindiol (1 μM)	(3R,8S)-falcarindiol (10 μM)	(3R)-falcarinol (1 μM)	(R)-sulforphane (1 μM)	6-isovaleryl-umbelliferone (10 μM)	(*Z*)-ligustilide (10 μM)
CASPASE 4	ENSMUSG00000033538	1.21	1.19	0.55	0.91	1.08	1.02	0.34
CHEMOKINE LIGAND 2	ENSMUSG00000058427	0.43	1.09	0.37	0.26	0.66	2.80	2.43
TELOMERASE REVERSE TRANSCRIPTASE	ENSMUSG00000021611	0.44	1.54	1.16	0.55	0.91	0.97	0.62
ADP-RIBOSYLATION FACTOR RELATED PROTEIN 1	ENSMUSG00000038671	0.89	0.90	0.75	0.75	0.98	0.84	0.92
CHEMOKINE (C-X-C MOTIF) LIGAND 1	ENSMUSG00000029380	0.64	0.93	1.34	2.04	0.77	0.66	0.46
PROTEIN PHOSPHATASE 2A, REGULATORY SUBUNIT B (PR 53)	ENSMUSG00000039515	0.53	0.93	1.33	0.78	0.69	0.69	0.91
IMMEDIATE EARLY RESPONSE 3	ENSMUSG00000003541	0.64	0.89	1.75	1.47	0.56	1.75	1.04
TRANSFORMATION RELATED PROTEIN 53 (P53)	ENSMUSG00000059552	0.81	1.04	1.71	1.08	0.87	1.84	1.76
E74-LIKE FACTOR 3	ENSMUSG00000003051	0.75	1.19	1.32	1.11	0.65	1.23	0.88
MATRIX METALLOPEPTIDASE 3	ENSMUSG00000043613	0.77	0.84	0.43	0.72	1.02	0.79	0.32
MYELOCYTOMATOSIS ONCOGENE C-MYC	ENSMUSG00000022346	1.05	1.28	2.68	1.51	1.33	3.08	3.85
SUPEROXIDE DISMUTASE 2, SOD2	ENSMUSG00000006818	0.85	0.82	1.17	0.73	0.91	1.24	1.20
Mean		*0.75*	*1.05*	*1.21*	*0.99*	*0.87*	*1.41*	*1.23*

5.3.3. qRT-PCR validation of RNA-seq results

I used qRT-PCR to validate the RNA-seq results. Using validated primers and six targets a total of 32 qRT-PCR quantifications were performed. The correlation of these results with the RNA-seq results is provided in Figure 5-7. There was a general agreement between the two sets of data (slope = 1.06, R^2 = 0.82).

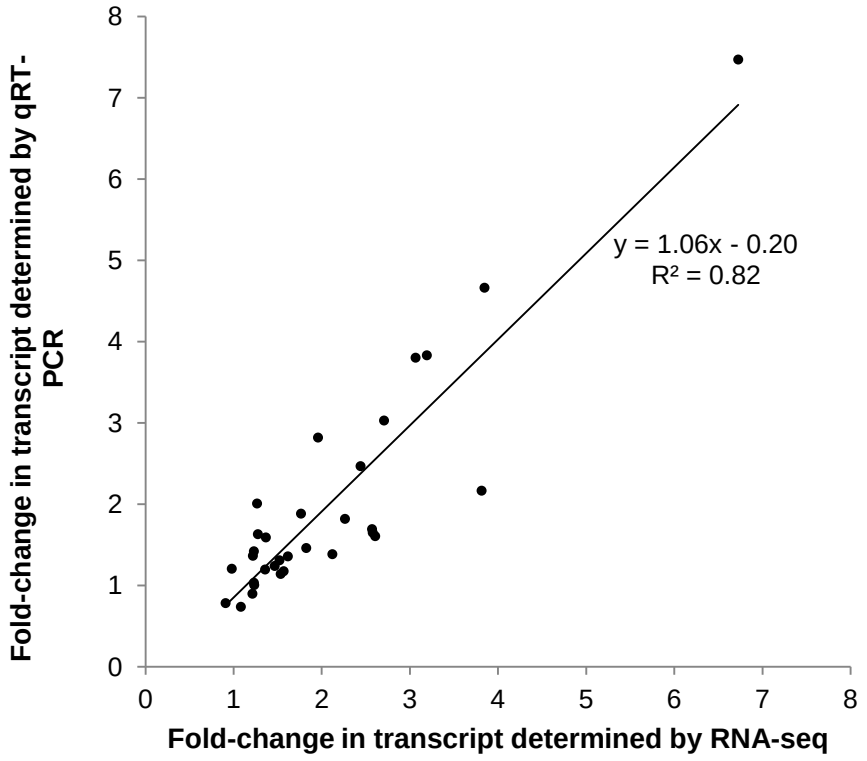

Figure 5-7. Correlation between fold-changes in transcript levels determined by RNA-seq and qRT-PCR.

5.3.4. Transcriptional investigation of QR induction by cannabidiol

Although CBD was not included in the RNA-seq analysis, I was interested to investigate whether the induction of QR by this compound was being mediated by Nrf2 and/or AhR. Using qRT-PCR, I examined the changes in the transcript levels of the Nrf2 targets (*QR* and *HO-1*) and AhR target (*CYP1A1*).

Changes in the transcript levels of *QR*, *HO-1* and *CYP1A1* following 12 h of exposure to CBD are shown in Figure 5-8. The level of QR transcript induction measured at 12 h (2.0) was

similar to that of the enzyme induction measured at 48 h consistent with a transcriptional control mechanism. Induction of HO-1 is consistent with activation of Nrf2 while induction of *CYP1A1* is suggestive of activation of AhR. Thus it appears that CBD may activate QR through both the Nrf2 and AhR pathways and lead to induction of both phase I and II of xenobiotic metabolism.

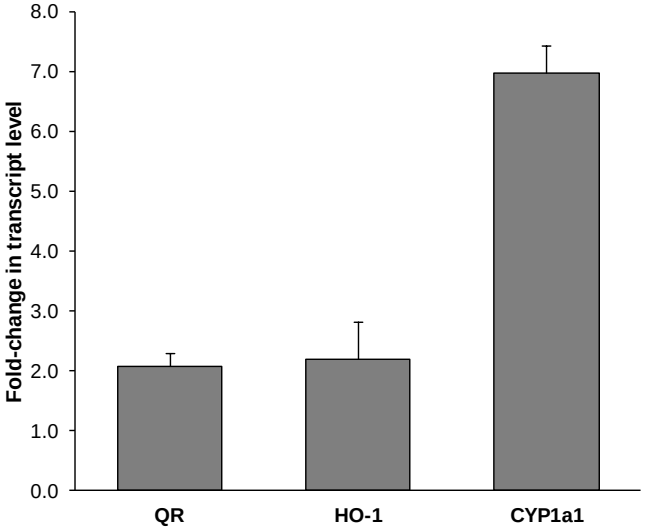

Figure 5-8. Changes in tranascript levels of *QR*, *HO-1* and *CYP1A1* following exposure to CBD. Hepa-1c1c7 cells were exposed to the indicated compounds for 12 h and transcript levels were measured by qRT-PCR. Values are the mean of three experiments ± the standard deviation.

5.4. Conclusions

Transcriptional analysis by RNA-seq and qRT-PCR provide further support for Nrf2 activation by (3*S*,8*S*)-falcarindiol. The transcriptional analyses also strongly support Nrf2 activation by (*R*)-sulforaphane and to a lesser extent by (3*R*,8*S*)-falcarindiol, 6-IVU, (*Z*)-ligustilide and CBD. AhR appears to be moderately activated by (3*R*,8*S*)-falcarindiol, (*Z*)-ligustilide and (*R*)-sulforaphane, and strongly activated by 6-IVU and CBD.

In addition to varying in their propensities for activating Nrf2, the two falcarindiol stereoisomers also differ in their specificity for this transcription factor, with (3*R*,8*S*)-falcarindiol having greater promiscuity. Several of the compounds ((3*R*,8*S*)-falcarindiol 6-IVU and (*Z*)-ligustilide) appeared to cause changes in metabolism and lipid homeostasis although the mechanism(s) involved remain unclear.

CHAPTER 6

GENERAL DISCUSSION

6.1. General conclusions

Screening of plant extracts for QR induction provided a large number of lead extracts and an overall indication of the prevalence of QR inducers in Western Canadian plants. The direct antioxidant activity of these extracts did not correlate with QR-inducing activity. Therefore direct antioxidant activity should not be used as an indicator of QR-inducing activity (indirect antioxidant activity). Based on findings of the bioassay guided fractionation, I suggest that phthalides and C_{17}-polyacetylenes may confer QR-inducing activity within the uninvestigated extracts of the Apiaceae and Araliaceae such as pestle parsnip and Siberian ginseng.

Taken as a whole, the results of the screening, isolation, biochemical and genomic experiments provide strong evidence for activation of Nrf2 by C_{17}-polyacetylenes, in particular (3*S*,8*S*)-falcarindiol, and support a mechanism of action involving modification of Keap1 cysteines. The results with the falcarindiol stereoisomers also underscore the impact that a difference in configuration can have on biological activity. Not only was this difference responsible for the substantially different effects these compounds had on the structure of Keap1 and QR-induction, but also the differences in their global effects on transcription.

These studies support the involvement of both Nrf2 and AhR in the induction of QR by (3*R*,8*S*)-falcarindiol, (*Z*)-ligustilide, CBD, (*R*)-sulforaphane, and 6-IVU. AhR appears to be moderately activated by (3*R*,8*S*)-falcarindiol, (*Z*)-ligustilide and (*R*)-sulforaphane, and strongly activated by 6-IVU and CBD. The widespread effects on transcription caused by (3*R*,8*S*)-falcarindiol, 6-IVU, (*Z*)-ligustilide indicate that other signal transduction pathways, such as those involved in lipid homeostasis, are also likely affected. Even the most specific Nrf2 activator isolated here, (3*S*,8*S*)-falcarindiol, appears to affect additional signal transduction pathways (e.g. cell cycle regulation). Given the abundance of cellular thiols, including those in enzyme active sites, I suspect that it will be difficult to find thiol-reactive Nrf2 activators that are devoid of off-target effects.

6.2. Technical and methodological considerations

As demonstrated by compounds such as (*Z*)-ligustilide and 6-IVU, the activation of the AhR can also contribute to QR induction and reduce the reliability of QR as a marker for Nrf2 activation. For this reason I would consider using an ARE-luciferase screen or similar reporter with minimal interference from alternative signal transduction pathways in future studies. Cell lines related to Hepa-1c1c7 with impaired AhR signalling could also be used to screen out QR inducers that act via AhR, although false negatives in cases where metabolic activation is required for Nrf2 activation could be problematic.

Following the isolation of falcarindiol and other QR-inducing polyacetylenes from *O. horridus* I looked to the related plant *A. nudicaulis* to identify additional QR-inducing polyacetylenes. This approach was quite successful as I was able to isolate several distinct polyacetylenes including the highly potent epoxyfalcarindiol.

Additional direct evidence for Nrf2 activation could be provided by examining changes in the cellular abundance and localization of Nrf2 by Western blot or subcellular localization. Unfortunately the Western blots I performed for this purpose were equivocal due to the lack of specificity of the Nrf2 antibody. An antibody with greater specificity is desirable to allow Western blots in future studies.

6.3. Physiological implications

Coping with exposure to xenobiotics is an important aspect of human biology. Intriguingly, the stresses associated with xenobiotic exposure are similar to stresses associated with redox stress and inflammation, namely, electrophilic and oxidative stresses. Therefore it is not that surprising that the response to these stresses is mediated by a common pathway through Nrf2.

As a signalling system that antagonizes inflammation and redox signalling, activation of Nrf2 is not without compromise. Inflammation and redox signalling are crucial for innate and acquired immunity as well as a multitude of regulatory pathways. Therefore, it makes sense that Nrf2 is inducible. It can offer protection against acute toxicity and provide negative feedback for redox signalling in times of need while a low baseline allows the greatest sensitivity for redox

signalling in the absence of stressors. This system is in general highly effective – diseases associated with inflammation and redox stress do not typically manifest until later in life. Having a higher basal level of Nrf2-directed transcription may provide increased protection against chronic diseases, but may come at other costs (i.e. decreased immunity) and therefore reduced fitness. It would be interesting to investigate whether there is an inverse correlation between susceptibility to infection and chronic disease incidence. As chronic diseases are greater contributors to death and disability than infectious diseases in industrialized nations, Nrf2 activators – whether dietary or pharmaceutical – remain an attractive intervention.

Although it is apparent that many compounds can activate Nrf2 at some concentration, few compounds have been shown to strongly activate Nrf2 at concentrations that are typically obtained through fruit and vegetable consumption. The compounds isolated in this research are no exception. Although these compounds are present in food plants it is doubtful that the concentrations achieved through their daily consumption ever surpass the CD value obtained in the QR bioassay. For instance, drinking 900 mL (containing 12 mg of falcarinol) of carrot juice only led to plasma falcarinol concentrations of ~10 nM (Haraldsdóttir et al. 2002), much lower than the CD value of the most potent polyacetylene isolated in this work (epoxyfalcarindiol (**26**), 240 nM). However, we must consider that there are typically several related compounds present and that more than one compound is active. There is also the possibility that more than one class of Nrf2 activator is present in a given plant. For instance (*Z*)-ligustilide (phthalide), (3*R*,8*S*)-falcarindiol (polyacetylene), and 6-IVU (coumarin) are present in the plant celeriac (*Apium graveolens* var. *rapaceum*, Apiaceae). Synergism between classes of Nrf2 activators is also possible. Then again, I did not encounter any great reduction in QR-induction during my fractionations which is consistent with a lack of synergy between components of those extracts.

Another consideration with respect to dosage is the impact of local exposure. For example, concentrations greater than those achieved in plasma are expected locally for epithelia of the digestive tract following ingestion or the lung following inhalation due to the lack of metabolism or dilution of the active compounds at the area of first exposure (Olsson et al. 2011). Therefore the high nM or low µM concentrations that are required for activity in the QR bioassay may be achieved in these areas despite lower plasma concentrations. For instance, after smoking a

cannabis cigarette containing 19 mg equivalents of CBD, CBD plasma levels decreased from 320 nM to 6 nM over 4 h (Agurell et al. 1986). While these concentrations are still much lower than the 2.0 µM CD value, the initial levels of exposure in the lung epithelia would be expected to be much higher and may come close to the CD value for this compound. In cases where local exposure is much greater than systemic exposure a greater localized effect is expected. Consistently, the digestive tract and lung are the tissues in which increased fruit and vegetable consumption appear to have the greatest protective effect against cancer (WHO 2003).

6.4. Safety

The presence of many of the compounds identified here in everyday foods provides a sense of safety surrounding their consumption. This is bolstered by the evidence supporting the health benefits of fruit and vegetable consumption. Despite this evidence, I suggest that adverse effects from overconsumption of a given phytochemical are not only possible but simply a matter of dosage.

The ability to cause stress by reacting with cellular thiols is inherent in Keap1-modifying Nrf2 activators. This property also underlies the hormetic nature of their dose responses. At low concentrations, they produce protection whereas at high levels, which overwhelm adaptive cellular defences, toxicity occurs. While this may be unlikely at the low doses of these compounds that occur in food plants it remains a major consideration with respect to consuming concentrated doses.

Although it appears that many of the aforementioned compounds activate Nrf2, it is apparent that additional signalling pathways are also affected. In particular, the effects on lipid homeostasis genes are potentially alarming and warrant further investigation. Furthermore, it is possible that these compounds affect signalling pathways (e.g. endocrine signalling) as reflected in the gene expression data collected from Hepa-1c1c7 cells. The isoflavone and estrogen receptor agonist genistein provides an example of endocrine disruption by an Nrf2 activator (Kuiper et al. 1998; Yannai et al. 1998).

I must also advise caution if considering using any of the plants used in this study for medicinal purposes. Just because something is natural does not mean it is safe. Nor does the

presence of potentially beneficial compounds exclude the potential for detrimental compounds to be present. For example, falcarindiol can be found along with the highly toxic polyacetylene, oenanthotoxin in *Oenanthe fistulosa* (Appendino et al. 2009). Although the fact that some of these plants have traditional uses suggests that they do not exhibit high toxicity, they have not been subjected to rigorous toxicological studies. Unfortunately, these types of body system effects cannot be predicted by the study of an individual cell type such as Hepa-1c1c7.

6.5. Implications for traditional medicine

Despite having less toxicological documentation, using non-food plants for Nrf2 activation may be advantageous as non-food plants may contain higher concentrations of Nrf2 activators than food plants. Because many Nrf2 activators are distasteful, they may have been bred out of food crops. Also, the number of plants used as food is relatively small and food plants mainly belong to a handful of plant families. Therefore, expanding use to non-food plants allows a much larger natural pharmacopeia. Additionally, many plants that are rich phytochemical sources are simply not useful as foods. Take for example the C_{17}- polyacetylenes. Judging by HPLC, these compounds comprise the majority of compounds present in extracts from the inner stem bark of *O. horridus*, which is not used as a food, while being only a minor component of carrot root extracts.

The finding that many extracts of plants used in traditional medicine activate QR and confirmation of the presence of Nrf2 activators in some of these samples is an important finding with respect to understanding their traditional use. Nrf2 activation could provide some rationale for uses such as treating diseases linked to inflammation and oxidative stress. For other indications such as tuberculosis, a connection to Nrf2 activation is not apparent. Although demonstrating a biological activity for these traditional medicines does not confirm their efficacy it does provide some basis for understanding whether their use is justified.

6.6. Future directions

Screening for QR-inducing extracts provided more leads than could be followed up. Compositae plants figured prominently amongst the top inducers. Yuping Lu (Page lab) and I have shown that unique polyacetylenes are responsible for QR-induction in these plants (data not

shown) however, we have not investigated which signal transduction pathways are involved. Also, I am interested in isolating the active compounds from members of the Grossulariaceae as this family consistently displayed QR-inducing activity in the screen and includes a number of food plants (currants, gooseberries).

Only limited pharmacokinetic (absorption, distribution, metabolism and exception) data exist for the most promising Nrf2-activator classes identified here, the phthalides and C_{17}-polyacteylenes. Improving our understanding of the pharmacokinetics of these compounds would be useful in accessing dose requirements for further studies *in vivo* and understanding the physiological relevance of their exposure.

The basic phytochemical information gained as part of this work contributes to our knowledge of the structures, distribution and abundance of phytochemicals. This information could be useful for cataloguing the phytochemicals present in foods and herbal medicines and their abundances. Combining this information with detailed cohort studies on nutrition may provide insight into the impact that these compounds have on human health.

APPENDIX A

ADDITIONAL INFORMATION FOR PLANT MATERIAL

Table A1. Additional details for plant material used for QR bioassay screening

Common name	Species and Author	Family	Max QR[a]	Extractor	Additional notes	Date Collected
san qi	*Panax pseudoginseng* Wall.	Araliaceae	1.35	D. Konkin	Botanicum Herbs - 5260	Nov-05
ren shen -ginseng	*Panax ginseng* L.	Araliaceae	1.53	D. Konkin	Botanicum Herbs - 5090	Nov-05
siberian ginseng	*Eleutherococcus senticosus* (Rupr. & Maxim.) Maxim.	Araliaceae	1.84	Eric Bol	Richter's H2864	
wild sarsparilla	*Aralia nudicaulis* L.	Araliaceae	1.43	Eric Bol		
wild sarsparilla	*Aralia nudicaulis* L.	Araliaceae	0.93	Eric Bol		
devil's club	*Oplopanax horridus* (Sm.) Miq.	Araliaceae	2.45	Eric Bol	BC	
devil's club	*Oplopanax horridus* (Sm.) Miq.	Araliaceae	2.02	D. Konkin	BC	
gymnema	*Gymnema sylvestre* (Retz.) Sm.	Asclepiadaceae	1.53	D. Konkin	Source Naturals	Nov-05
Oregon grape	*Mahonia aquifolium* (Pursh) Nutt.	Berberidaceae	0.98	D. Konkin	Purchased in Vancouver	Nov-05
Oregon grape	*Mahonia aquifolium* (Pursh) Nutt.	Berberidaceae	1.08	Eric Bol		Jul-05
horny goat weed	*Epimedium sagittatum* (Sieb. & Zucc.) Maxim.	Berberidaceae	1.38	D. Konkin	Planetary Formulas	Nov-05
cretan viper's-bugloss	*Echium creticum* L.	Boraginaceae	2.11	D. Konkin		Jan-06
comfrey	*Symphytum offincinale* L.	Boraginaceae	1.09	D. Konkin	Purchased in Vancouver	Nov-05
codonopsis	*Codonopsis* sp.	Campanulaceae	1.00	D. Konkin	Planetary Formulas	Nov-05
jie geng	*Platycodon* sp.	Campanulaceae	1.37	D. Konkin	Botanicum Herbs - 7310	Nov-05
hop	*Humulus lupulus* L.	Cannabaceae	0.97	D. Konkin	Purchased in Saskatoon	Nov-05
high-bush cranberry	*Viburnum* sp.	Caprifoliaceae	1.38	D. Konkin	Jasper	Aug-05
elderberry	*Sambucus calliicarpa*	Caprifoliaceae	1.51	Eric Bol		
high-bush cranberry	*Viburnum sp*	Caprifoliaceae	0.83	D. Konkin		
common snowberry	*Symphoricarpos albus* (L.) S.F. Blake	Caprifoliaceae	1.17	D. Konkin	BC	Sep-05
western snowberry	*Symphoricarpos occidentalis* Hook.	Caprifoliaceae	1.44	D. Konkin	Saskatoon, SK	Sep-05
red elderberry	*Sambucus racemosa* L.	Caprifoliaceae	1.25	D. Konkin		
tai zi shen	*Pseudostellaria* sp.	Caryophyllaceae	1.78	D. Konkin	Botanicum Herbs - 5093	Nov-05
wang bu liu xing	*Vaccaria hispanica* (Miller) Rauschert	Caryophyllaceae	1.14	D. Konkin	Botanicum Herbs - 5620	Nov-05
vaccaria	*Vaccaria saponaria*	Caryophyllaceae	0.86	D. Konkin	Wild	Nov-05
qu mai	*Dianthus* sp.	Caryophyllaceae	1.50	D. Konkin	Botanicum Herbs - 8950	Nov-05
valley seed	*Bassia scoparia* (L.) Voss	Chenopodiaceae	0.51	D. Konkin	Wild	Nov-05
arjuna	*Terminalia arjuna* (DC) Wight & Arn.	Combretaceae	0.68	D. Konkin	Planetary Formulas	Nov-05
lettuce	*Lactuca sativa* L.	Compositae	1.28	Eric Bol		

calendula	*Calendula* sp.	Compositae	0.78	D. Konkin	Wild	Nov-05
iceberg lettuce	*Lactuca sativa L.*	Compositae	0.91	D. Konkin	Grocery Store in S'toon	Dec-05
milk thistle	*Silybum marianum* (L.) Gaertn.	Compositae	1.65	Eric Bol		
elecampane	*Inula helenium* L.	Compositae	1.85	D. Konkin	Purchased in Vancouver	Nov-05
dandelion	*Taraxacum officinale* Weber ex Wigg.	Compositae	1.54	Eric Bol	Vancouver, BC	
feverfew	*Tanacetum parthenium* (L.) Schultz-Bip.	Compositae	2.00	Eric Bol		
wild chicory	*Cichorium intybus* L.	Compositae	2.97	Eric Bol		
american arnica	*Arnica chamissonis* Less.	Compositae	1.74	Eric Bol		
French artichoke	*Cynara scolymus* L.	Compositae	1.66	Eric Bol		
black salsify	*Scorzonera hispanica*	Compositae	1.01	D. Konkin		
echinacea	*Echinacea* sp.	Compositae	1.81	D. Konkin	Purchased in Vancouver	Nov-05
goldenrod	*Solidago virgaurea*	Compositae	0.74	D. Konkin	Purchased in Vancouver	Nov-05
burdock	*Arctium minus* (Hill) Bernh.	Compositae	1.75	D. Konkin	Kamsack, SK (DK)	
boneset	*Eupatorium perfoliatum* L.	Compositae	2.01	Eric Bol		
big sagebrush	*Artemisia tridentata* Nutt.	Compositae	2.07	D. Konkin		
balsam root	*Balsamorhiza sp.*	Compositae	1.72	D. Konkin		
echinacea	*Echinacea angustifolia* DC	Compositae	1.80	D. Konkin		
entire-leaved gumweed	*Grindelia integrifolia* DC.	Compositae	1.39	D. Konkin		
elecampane	*Inula helenium* L.	Compositae	toxic	D. Konkin		
common tansy	*Tanacetum vulgare* L.	Compositae	2.51	D. Konkin		
bindweed	*Convolvulus* sp.	Convolvulaceae	1.54	D. Konkin	Wild	Nov-05
red-osier dogwood	*Cornus alba* L.	Cornaceae	2.09	Eric Bol	Vancouver, BC	
bunchberry	*Cornus canadensis* L.	Cornaceae	1.24	D. Konkin	Coquitlam watershed	Sep-05
wasabi	*Wasabia wasabi* (Siebold) Makino	Cruciferae	1.43	Eric Bol		
radish	*Raphanus sativus* L.	Cruciferae	1.85	Eric Bol		
broccoli	*Brassica oleracea* L.	Cruciferae	1.10	Eric Bol		
dijon mustard	*Brassica juncea* (L.) Czerniak	Cruciferae	1.72	Eric Bol		
broccoli	*Brassica oleracea* L.	Cruciferae	1.32	Eric Bol		
bitter gourd	*Momordica charantia* L.	Cucurbitaceae	1.77	Eric Bol	Purchased dried	
bitter gourd	*Momordica charantia* L.	Cucurbitaceae	1.14	D. Konkin	Purchased fresh	
angled luffa	*Luffa acutangula* (L.) Roxb	Cucurbitaceae	1.80	Eric Bol	Purchased	Jul-2005
creeping juniper	*Juniperus horizontalis* Moench	Cupressaceae	1.40	D. Konkin	Saskatoon, SK	Sep-05
poracher root	*Pteridium aquilinium* (L.) Kuhn	Dennstaedtiaceae	0.88	D. Konkin		
wolf willow	*Elaegnus commutata* Bernh. ex Rydb.	Elaegnaceae	1.34	D. Konkin	Saskatoon, SK	Nov-05
soapberry	*Shepherdia canadensis* (L.) Nutt	Elaegnaceae	1.84	Eric Bol	Near Lilloet BC	
wolf willow	*Elaegnus commutata* Bernh. ex Rydb.	Elaegnaceae	0.34	D. Konkin	Saskatoon, SK	Nov-05
crowberry	*Empetrum nigrum* L.	Empetraceae	0.99	D. Konkin		

cranberry	*Vaccinium oxycoccus* L.	Ericaceae	0.92	Eric Bol		
red huckleberry	*Vaccinium parvifolium* Sm.	Ericaceae	1.15	Eric Bol		
cranberry	*Vaccinium oxycoccus* L.	Ericaceae	0.99	D. Konkin	No Name Frozen Cranberries	Mar-06
lingonberry	*Vaccinium vitis-idaea* L.	Ericaceae	0.84	D. Konkin	Jasper	Aug-05
domestic blueberry	*Vaccinium corymbosum* L.	Ericaceae	0.82	D. Konkin	Surrey, BC	Sep-05
bilberry	*Vaccinium myrtillus* L.	Ericaceae	1.51	Eric Bol	Richter's H1410-050	
blueberry	*Vaccinium* sp.	Ericaceae	0.77	D. Konkin	Strathcona, BC	
blueberry	*Vaccinium* sp.	Ericaceae	0.65	D. Konkin	Strathcona, BC	
blueberry	*Vaccinium* sp.	Ericaceae	0.73	D. Konkin	Strathcona, BC	
labrador tea	*Ledum groenlandicum* Oeder	Ericaceae	0.81	Eric Bol	Jasper	Aug-05
kinnikinick	*Arctostaphylos uva-ursi* (L.) Sprengel	Ericaceae	1.65	D. Konkin	UBC campus	Aug-05
salal	*Gaultheria shallon* Pursh	Ericaceae	0.79	Eric Bol	UBC campus	Jul-05
pispsissewa	*Chimaphila umbellata* (L.) W. Barton (Euras.)	Ericaceae	1.16	Eric Bol	Richter's H4489	
yellow gentian	*Gentiana lutea* L.	Gentianaceae	1.12	Eric Bol	Richter's H2820	
European centaury	*Centaurium erythaea* Raf.	Gentianaceae	2.40	D. Konkin		
king gentian	*Gentiana sceptrum* Griseb.	Gentianaceae	2.18	D. Konkin		
irish moss	*Chondrus crispus* Stackhouse	Gigartinaceae	0.99	D. Konkin	North Cap PEI	Jun-05
red currant	*Ribes rubrum* L.	Grossulariaceae	1.51	Eric Bol		
stink currant	*Ribes bracteosum* Dougl. ex Hook	Grossulariaceae	1.78	D. Konkin	Nossom Cr. Port Moody BC	Sep-05
black gooseberry	*Ribes lacustre* (Pers.) Poir.	Grossulariaceae	1.24	D. Konkin	Jasper	Aug-05
wax currant	*Ribes cereum* Dougl.	Grossulariaceae	1.61	Eric Bol		
red flowering currant	*Ribes sanguineum* Pursh	Grossulariaceae	1.44	Eric Bol	Page Farm, Courtenay, BC	
mangosteen	*Garcinia mangostana* L.	Guttiferae	1.20	Eric Bol		
basil	*Ocimum basilicum* L.	Labiatae	1.67	Eric Bol		
blue skull cap	*Scutellana lateriflora* L.	Labiatae	2.24	Eric Bol	Richter's H5360	
astragalus	*Astragalus* sp.	Leguminosae	1.04	D. Konkin	Planetary Formulas	Nov-05
genistein soy complex	*Glycine max* (L.) Merr	Leguminosae	0.92	D. Konkin	Source Naturals	Nov-05
licorice	*Glycyrrhiza glabra* L.	Leguminosae	1.72	D. Konkin	Fresh, purchased by Jon Page	
licorice	*Glycyrrhiza glabra* L.	Leguminosae	1.60	Eric Bol	Richter's H3701-100	
springbank clover	*Trifolium wormskioldii* Lehm.	Leguminosae	1.91	D. Konkin		
lady's leek	*Allium cernuum* Roth	Liliaceae	0.95	D. Konkin		Sep-05
false lily-of-the-valley	*Maianthemum dilatatum* (A. Wood) Nels. & J.F. Macbr.	Liliaceae	1.22	D. Konkin		
twisted stalk	*Streptopus sp.*	Liliaceae	1.27	D. Konkin		

yellow sand-verbena	*Abronia latifolia* Eschsch.	Nyctaginaceae	1.76	D. Konkin	Goose Spit dunes, Comox BC	
yellow sand-verbena	*Abronia latifolia* Eschsch.	Nyctaginaceae	2.52	D. Konkin		
bloodroot	*Sanguinaria canadensis* L.	Papaveraceae	1.29	Eric Bol	Richter's H1450	
old man's beard	*Usnea* sp.	Parmeliaceae	1.84	D. Konkin		
passion flower	*Passiflora* sp.	Passifloraceae	1.06	D. Konkin	Eclectic Institute	Nov-05
pokeweed	*Phytolacca americana* L.	Phytolaccaceae	1.22	Eric Bol		
ribgrass/ribwort plantain	*Plantago lanceolata* L.	Plantaginaceae	1.56	Eric Bol		
ribwort	*Plantago lanceolata* L.	Plantaginaceae	1.33	D. Konkin	Purchased in Vancouver, BC	Nov-05
yuan zhi	*Polygala* sp.	Polygalaceae	0.69	D. Konkin	Botanicum Herbs - 8510	Nov-05
sheep sorrel	*Rumex acetosella* L.	Polygonaceae	2.08	Eric Bol		
rhubarb	*Rheum rhabarbarum* L.	Polygonaceae	0.97	Eric Bol		
yellow dock	*Rumex crispus*L.	Polygonaceae	0.88	D. Konkin	Purchased in Vancouver, BC	Nov-05
bitter root	*Lewisia sp.*	Portulacaceae	2.32	D. Konkin		
cascara	*Rhamnus purshiana* DC	Rhamnaceae	1.47	D. Konkin	Purchased in Vancouver, BC	Nov-05
cherry	*Prunus* sp.	Rosaceae	1.36	D. Konkin		
domestic plum	*Prunus* sp.	Rosaceae	1.67	D. Konkin	Lillooet, BC	Aug-05
chokecherry	*Prunus virginiana* L.	Rosaceae	1.45	D. Konkin		
chokecherry	*Prunus virginiana* L.	Rosaceae	1.36	Eric Bol	Lilooet, BC	Jul-05
American mountain-ash	*Sorbus americana* Marsh.	Rosaceae	2.32	D. Konkin	U of S campus, SK	Sep-05
pin cherry	*Prunus pensylvanica* L. f.	Rosaceae	0.81	Eric Bol	Jasper	Aug-05
red delicious apple	*Malus* sp.	Rosaceae	0.90	Eric Bol		
hawthorn	*Crataegus sp*	Rosaceae	1.27	D. Konkin	Osoyous, BC	Aug-05
saskatoon berry	*Amelanchier alnifolia* Nutt.	Rosaceae	0.67	Eric Bol		
European mountain-ash	*Sorbus aucuparia* L.	Rosaceae	2.15	D. Konkin	Lilloet Valley BC	Sep-05
cotoneaster	*Cotoneaster* sp.	Rosaceae	1.57	D. Konkin	Saskatoon, SK	Nov-05
black hawthorn	*Crataegus douglasii* Lindley	Rosaceae	1.37	D. Konkin	Tynehead Regional Park Surrey, BC	Aug-05
himalaya blackberry	*Rubus discolor* Weihe & Nees	Rosaceae	1.17	D. Konkin	Strathcona Park Vancouver, BC	Sep-05
salmon berry	*Rubus spectabilis* Pursh	Rosaceae	0.78	Eric Bol		
bitter cherry	*Prunus* sp.	Rosaceae	1.07	D. Konkin		

nootka rose	*Rosa nutkana* Presl	Rosaceae	1.02	D. Konkin		
trailing blackberry	*Rubus ursinus* Cham. & Schlecht.	Rosaceae	0.88	Eric Bol		
carolina rose	*Rosa carolina* L.	Rosaceae	0.99	Eric Bol	PEI	
common wild rose	*Rosa woodsii* Lindl.	Rosaceae	0.85	D. Konkin	Saskatoon, SK	Sep-05
antelope-brush	*Purshia tridentata* (Pursh) DC.	Rosaceae	toxic	D. Konkin		
bacopa	*Bacopa* sp.	Scrophulariaceae	1.30	D. Konkin	Planetary Formulas	Nov-05
potato	*Solanum tuberosum* L.	Solanaceae	0.94	D. Konkin	Purchased in Saskatoon	Nov-05

[a]indicates the highest QR induction value for the extract.
n/d indicates that the value could not be determined.

APPENDIX B

SPECTROSCOPIC INFORMATION FOR NOVEL COMPOUNDS

David; 22195
ANUD-Cp-Cf-2-2
1H, CDCl3
June 04, 2010

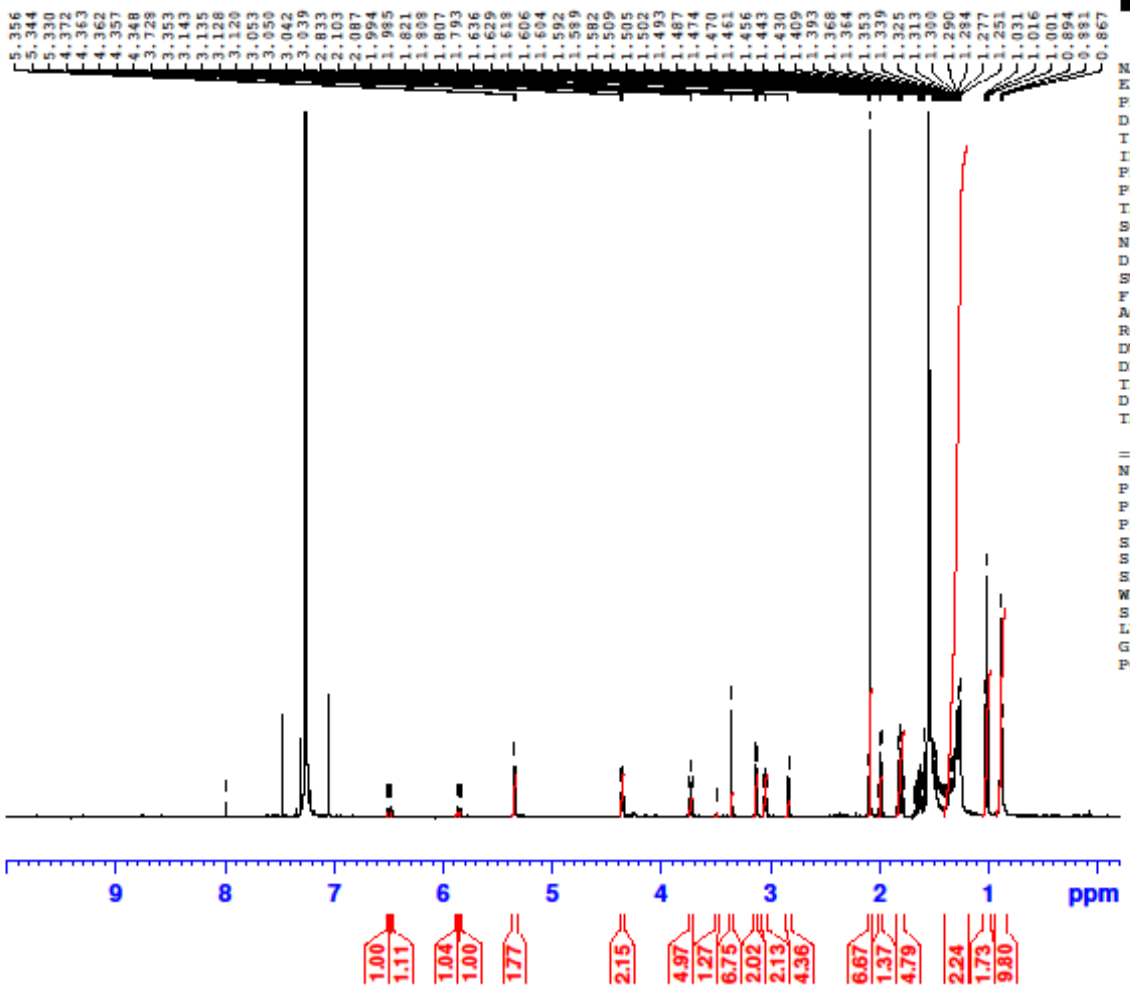

BRUKER

NAME	David22195
EXPNO	1
PROCNO	1
Date_	20100604
Time	8.57
INSTRUM	Spect
PROBHD	5 mm CPTXI 1H-
PULPROG	zg30
TD	65536
SOLVENT	CDCl3
NS	32
DS	2
SWH	10330.578 Hz
FIDRES	0.157632 Hz
AQ	3.1719923 sec
RG	575
DW	48.400 usec
DE	30.00 usec
TE	300.0 K
D1	1.00000000 sec
TD0	1
======== CHANNEL f1 ========	
NUC1	1H
P1	8.00 usec
PL1	5.20 dB
PL1W	7.81334925 W
SFO1	500.1330885 MHz
SI	32768
SF	500.1300130 MHz
WDW	EM
SSB	0
LB	0.30 Hz
GB	0
PC	1.00

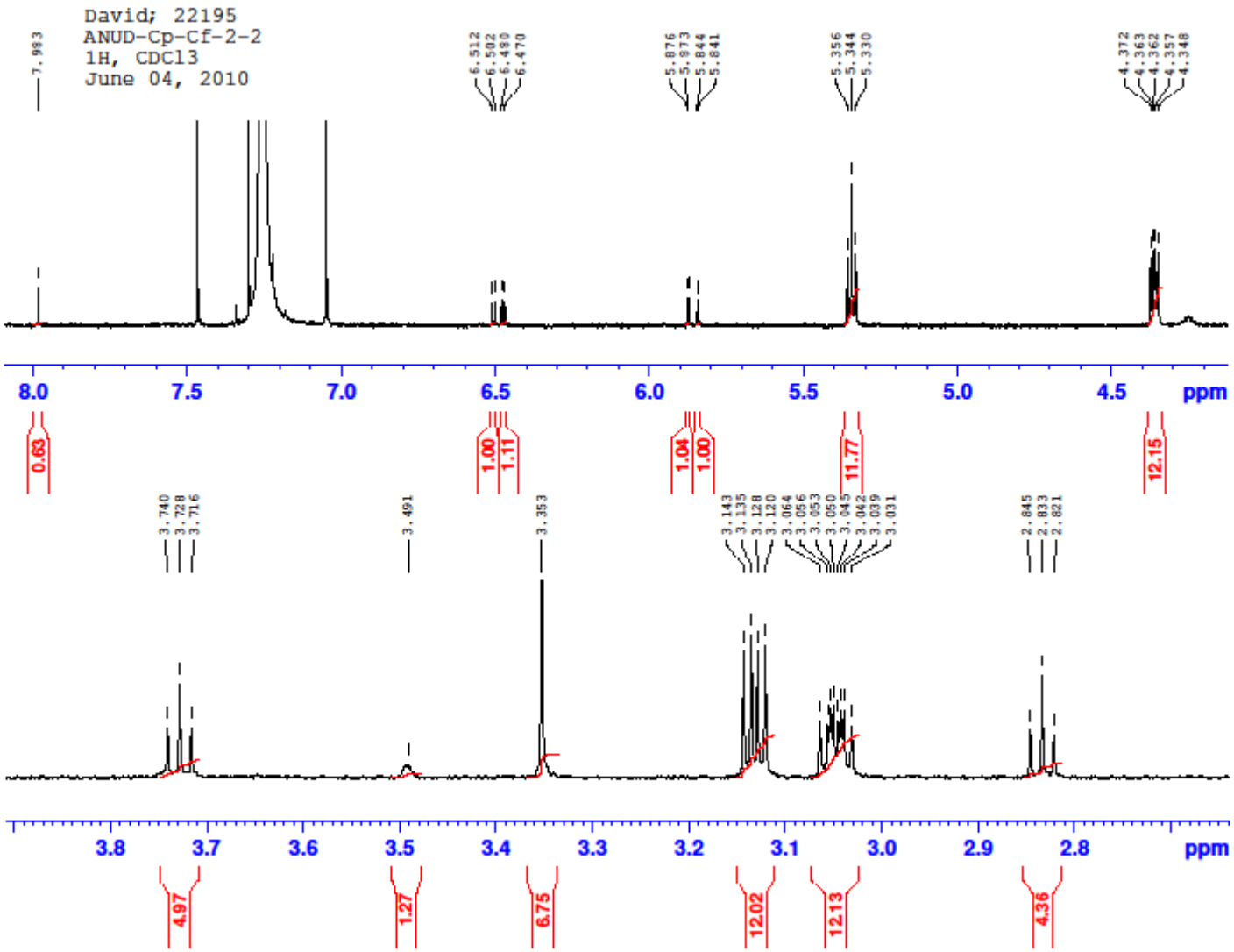
David; 22195
ANUD-Cp-Cf-2-2
1H, CDCl3
June 04, 2010
7.983
6.512
6.502
6.480
6.470
5.876
5.873
5.844
5.841
5.356
5.344
5.330
4.372
4.363
4.362
4.357
4.348
8.0
7.5
7.0
6.5
6.0
5.5
5.0
4.5
ppm
0.63
1.00
1.11
1.04
1.00
11.77
12.15
3.740
3.728
3.716
3.491
3.353
3.143
3.135
3.128
3.120
3.064
3.056
3.053
3.050
3.045
3.042
3.039
3.031
2.845
2.833
2.821
3.8
3.7
3.6
3.5
3.4
3.3
3.2
3.1
3.0
2.9
2.8
ppm
4.97
1.27
6.75
12.02
12.13
4.36

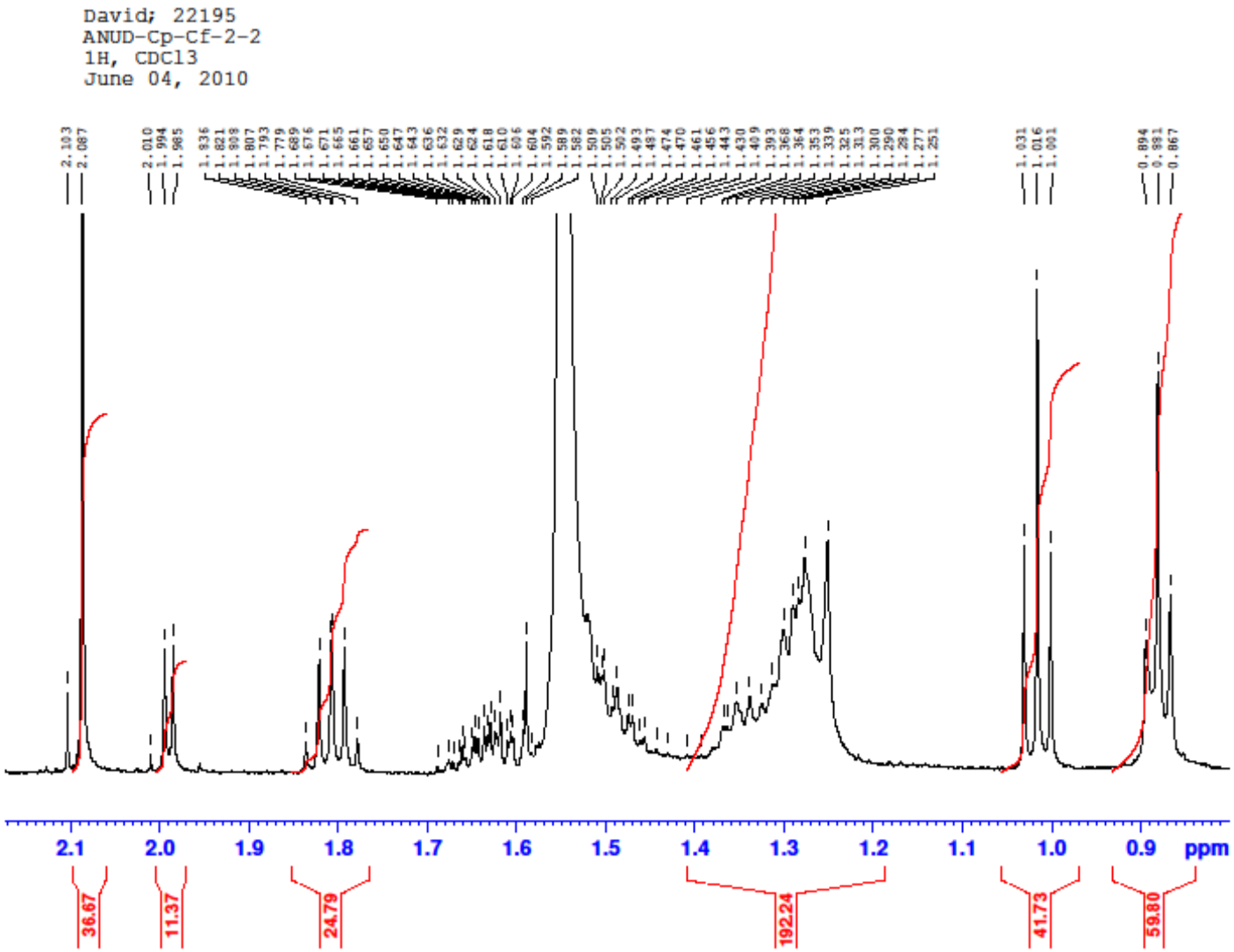
David; 22195
ANUD-Cp-Cf-2-2
1H, CDCl3
June 04, 2010
2.103
2.087
2.010
1.994
1.985
1.836
1.821
1.808
1.807
1.793
1.779
1.689
1.676
1.671
1.665
1.661
1.657
1.650
1.647
1.643
1.636
1.632
1.629
1.624
1.618
1.610
1.606
1.604
1.592
1.589
1.582
1.509
1.505
1.502
1.493
1.487
1.474
1.470
1.461
1.456
1.443
1.430
1.409
1.393
1.368
1.364
1.353
1.339
1.325
1.313
1.300
1.290
1.284
1.277
1.251
1.031
1.016
1.001
0.894
0.881
0.867
2.1
2.0
1.9
1.8
1.7
1.6
1.5
1.4
1.3
1.2
1.1
1.0
0.9
ppm
36.67
11.37
24.79
192.24
41.73
59.80

David; 22195
ANUD-Cp-Cf-2-2
13C, CDCl3
July 09, 2010

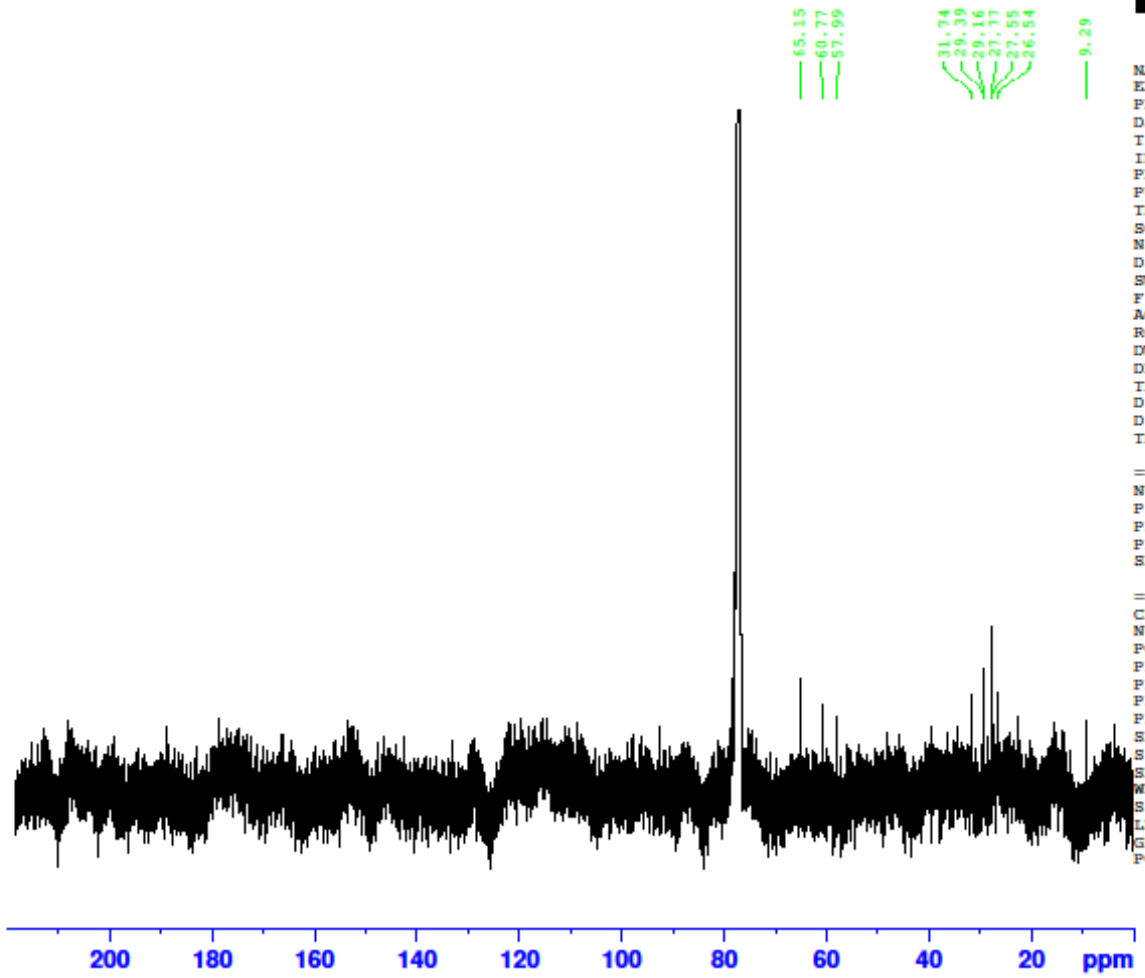

BRUKER

NAME	David22195
EXPNO	21
PROCNO	1
Date_	20100712
Time	7.51
INSTRUM	Spect
PROBHD	5 mm CPTXI 1H-
PULPROG	zgdc
TD	32768
SOLVENT	CDCl3
NS	141312
DS	2
SWH	29761.904 Hz
FIDRES	0.908261 Hz
AQ	0.5505524 sec
RG	2050
DW	16.800 usec
DE	30.00 usec
TE	300.0 K
D1	1.00000000 sec
D11	0.03000000 sec
TD0	1
======== CHANNEL f1 ========	
NUC1	13C
P1	13.10 usec
PL1	-1.50 dB
PL1W	106.44401550 W
SFO1	125.7703643 MHz
======== CHANNEL f2 ========	
CPDPRG2	waltz16
NUC2	1H
PCPD2	80.00 usec
PL2	5.20 dB
PL12	25.20 dB
PL2W	7.81334925 W
PL12W	0.07813348 W
SFO2	500.1320005 MHz
SI	32768
SF	125.7577890 MHz
WDW	EM
SSB	0
LB	1.00 Hz
GB	0
PC	1.40

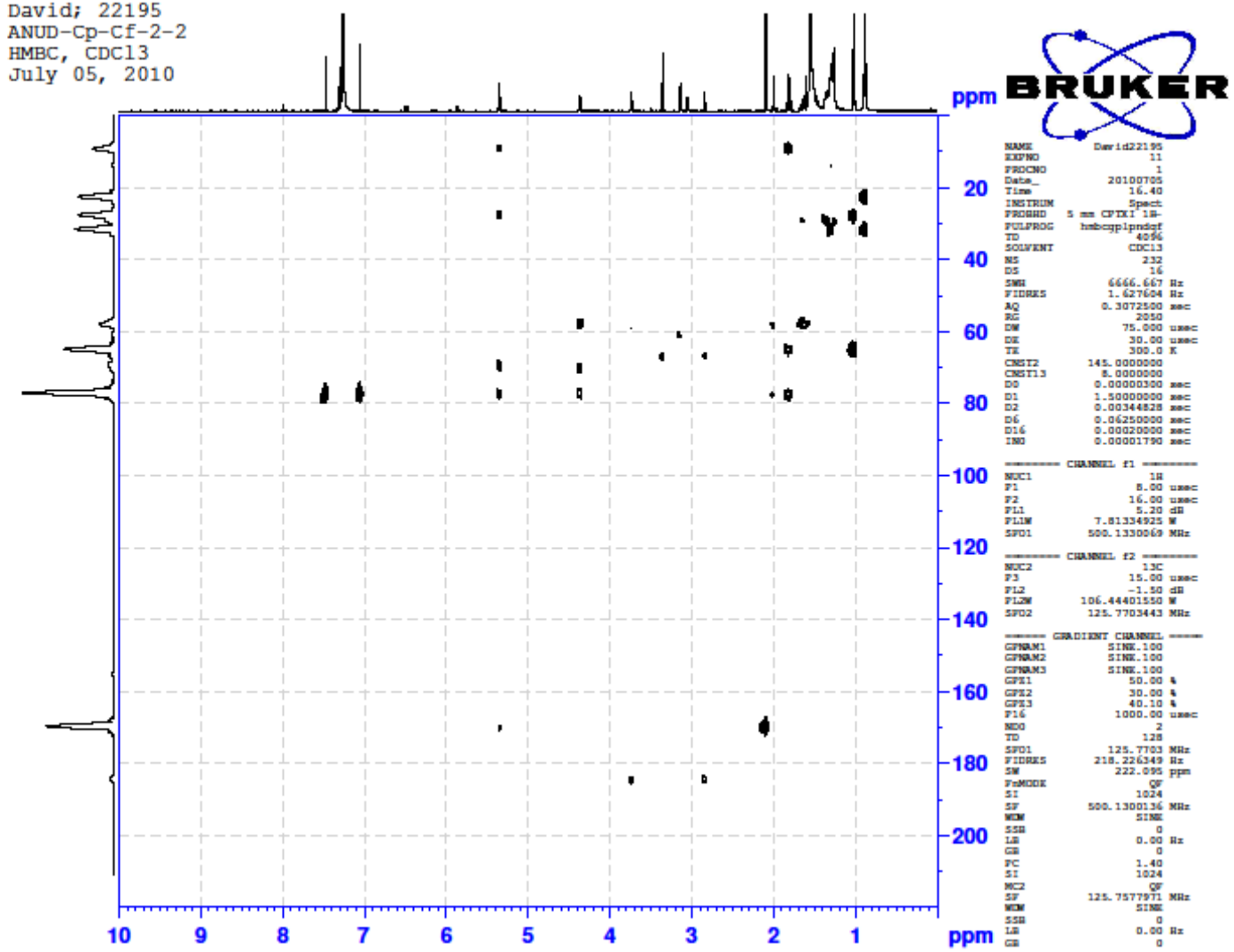
David; 22195
ANUD-Cp-Cf-2-2
HMBC, CDCl3
July 05, 2010
ppm
20
40
60
80
100
120
140
160
180
200
10
9
8
7
6
5
4
3
2
1
ppm
BRUKER
NAME David22195
EXPNO 11
PROCNO 1
Date_ 20100705
Time 16.40
INSTRUM Spect
PROBHD 5 mm CPTXI 1H-
PULPROG hmbcgplpndqf
TD 4096
SOLVENT CDCl3
NS 232
DS 16
SWH 6666.667 Hz
FIDRES 1.627604 Hz
AQ 0.3072500 sec
RG 2050
DW 75.000 usec
DE 30.00 usec
TE 300.0 K
CNST2 145.0000000
CNST13 8.0000000
D0 0.00000300 sec
D1 1.50000000 sec
D2 0.00344828 sec
D6 0.06250000 sec
D16 0.00020000 sec
IN0 0.00001790 sec
======== CHANNEL f1 ========
NUC1 1H
P1 8.00 usec
P2 16.00 usec
PL1 5.20 dB
PL1W 7.81334925 W
SFO1 500.1330069 MHz
======== CHANNEL f2 ========
NUC2 13C
P3 15.00 usec
PL2 -1.50 dB
PL2W 106.44401550 W
SFO2 125.7703443 MHz
====== GRADIENT CHANNEL =====
GPNAM1 SINE.100
GPNAM2 SINE.100
GPNAM3 SINE.100
GPZ1 50.00 %
GPZ2 30.00 %
GPZ3 40.10 %
P16 1000.00 usec
NDO 2
TD 128
SFO1 125.7703 MHz
FIDRES 218.226349 Hz
SW 222.095 ppm
FnMODE QF
SI 1024
SF 500.1300136 MHz
WDW SINE
SSB 0
LB 0.00 Hz
GB 0
PC 1.40
SI 1024
MC2 QF
SF 125.7577971 MHz
WDW SINE
SSB 0
LB 0.00 Hz
GB 0

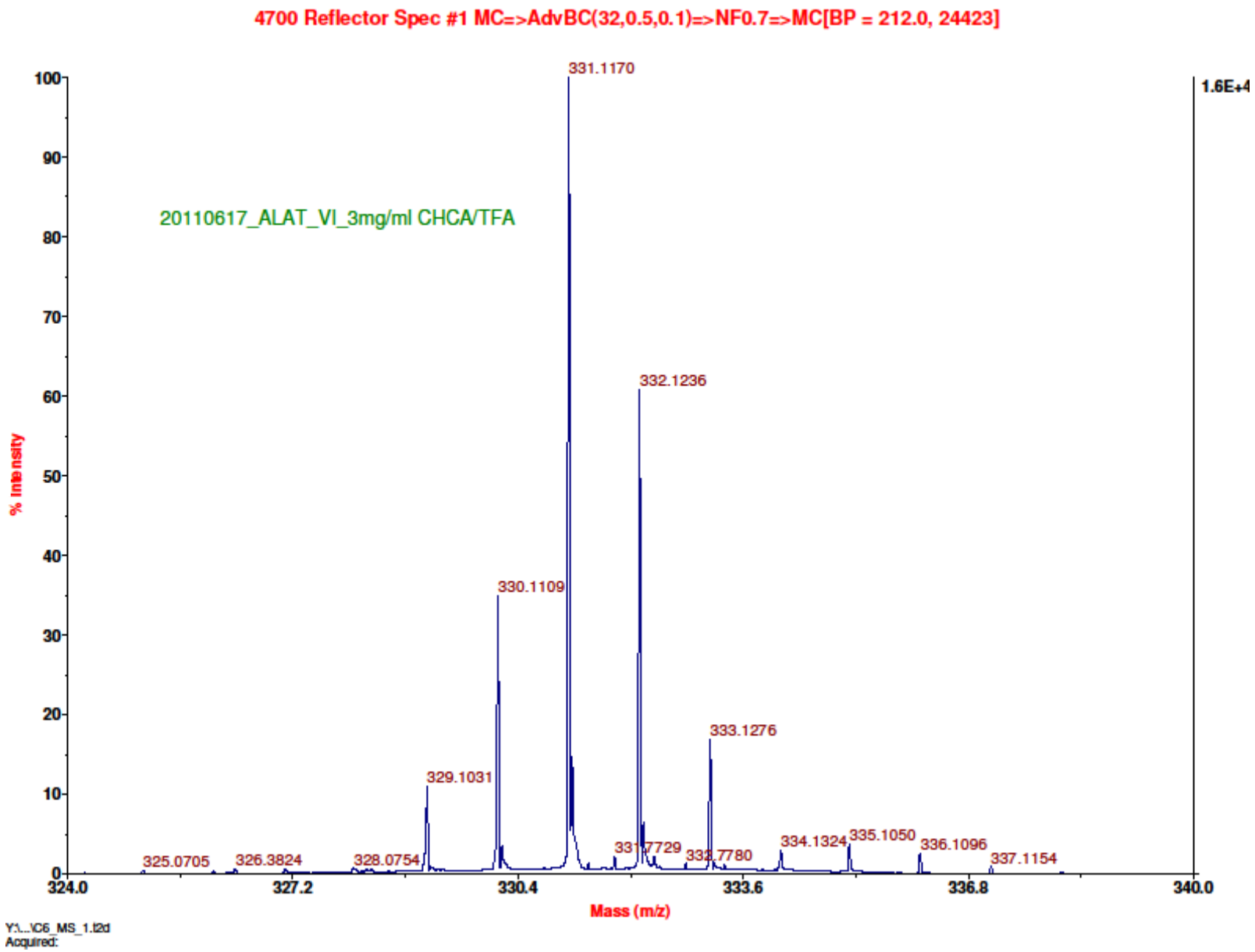
4700 Reflector Spec #1 MC=>AdvBC(32,0.5,0.1)=>NF0.7=>MC[BP = 212.0, 24423]
20110617_ALAT_VI_3mg/ml CHCA/TFA
% Intensity
Mass (m/z)
1.6E+4
331.1170
332.1236
330.1109
333.1276
329.1031
325.0705
326.3824
328.0754
334.1324
335.1050
336.1096
337.1154
Y:\...\C6_MS_1.t2d
Acquired:

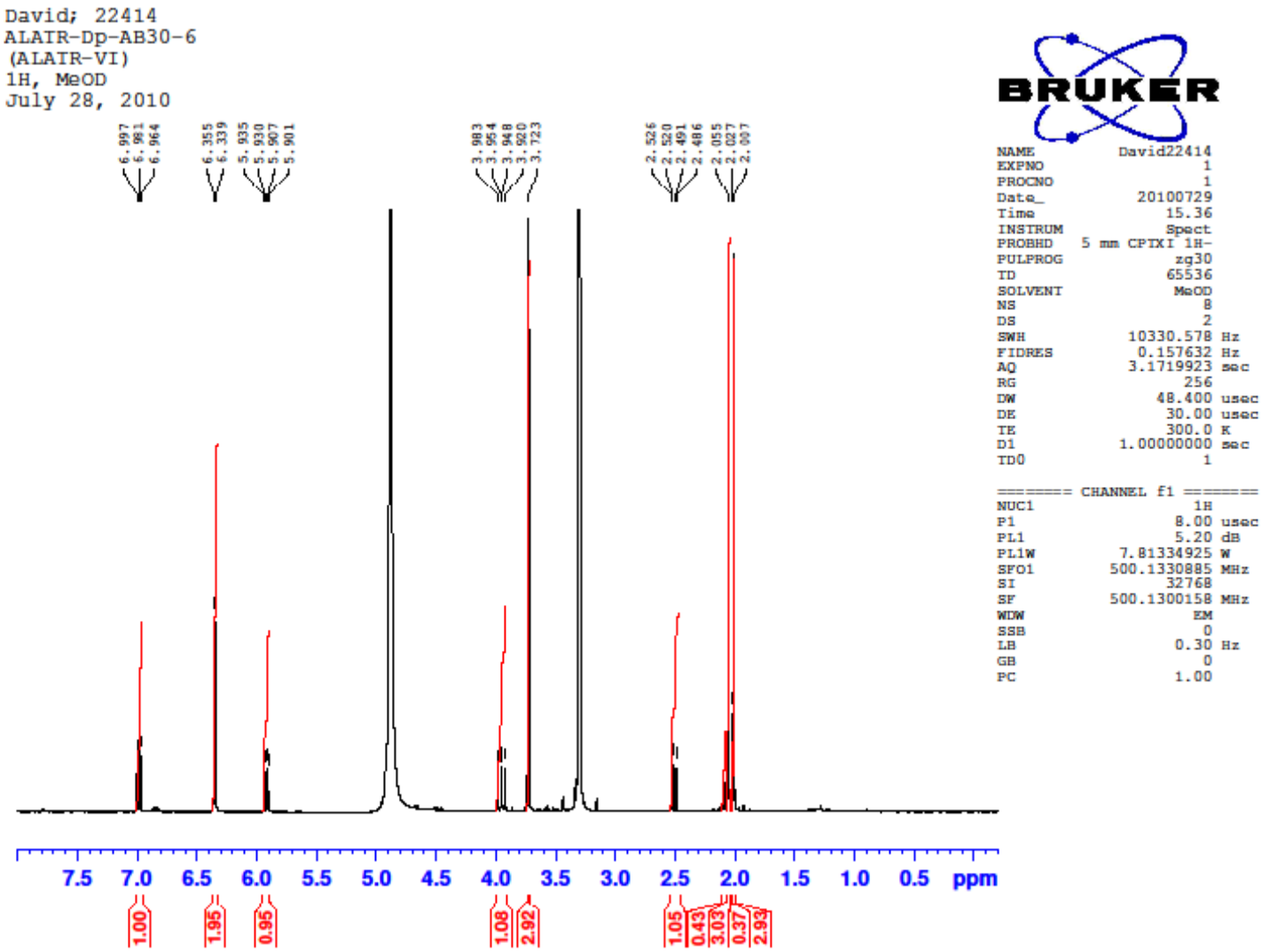

BRUKER

NAME	David22414
EXPNO	1
PROCNO	1
Date_	20100729
Time	15.36
INSTRUM	Spect
PROBHD	5 mm CPTXI 1H-
PULPROG	zg30
TD	65536
SOLVENT	MeOD
NS	8
DS	2
SWH	10330.578 Hz
FIDRES	0.157632 Hz
AQ	3.1719923 sec
RG	256
DW	48.400 usec
DE	30.00 usec
TE	300.0 K
D1	1.00000000 sec
TD0	1
======== CHANNEL f1 ========	
NUC1	1H
P1	8.00 usec
PL1	5.20 dB
PL1W	7.81334925 W
SFO1	500.1330885 MHz
SI	32768
SF	500.1300158 MHz
WDW	EM
SSB	0
LB	0.30 Hz
GB	0
PC	1.00

1H?

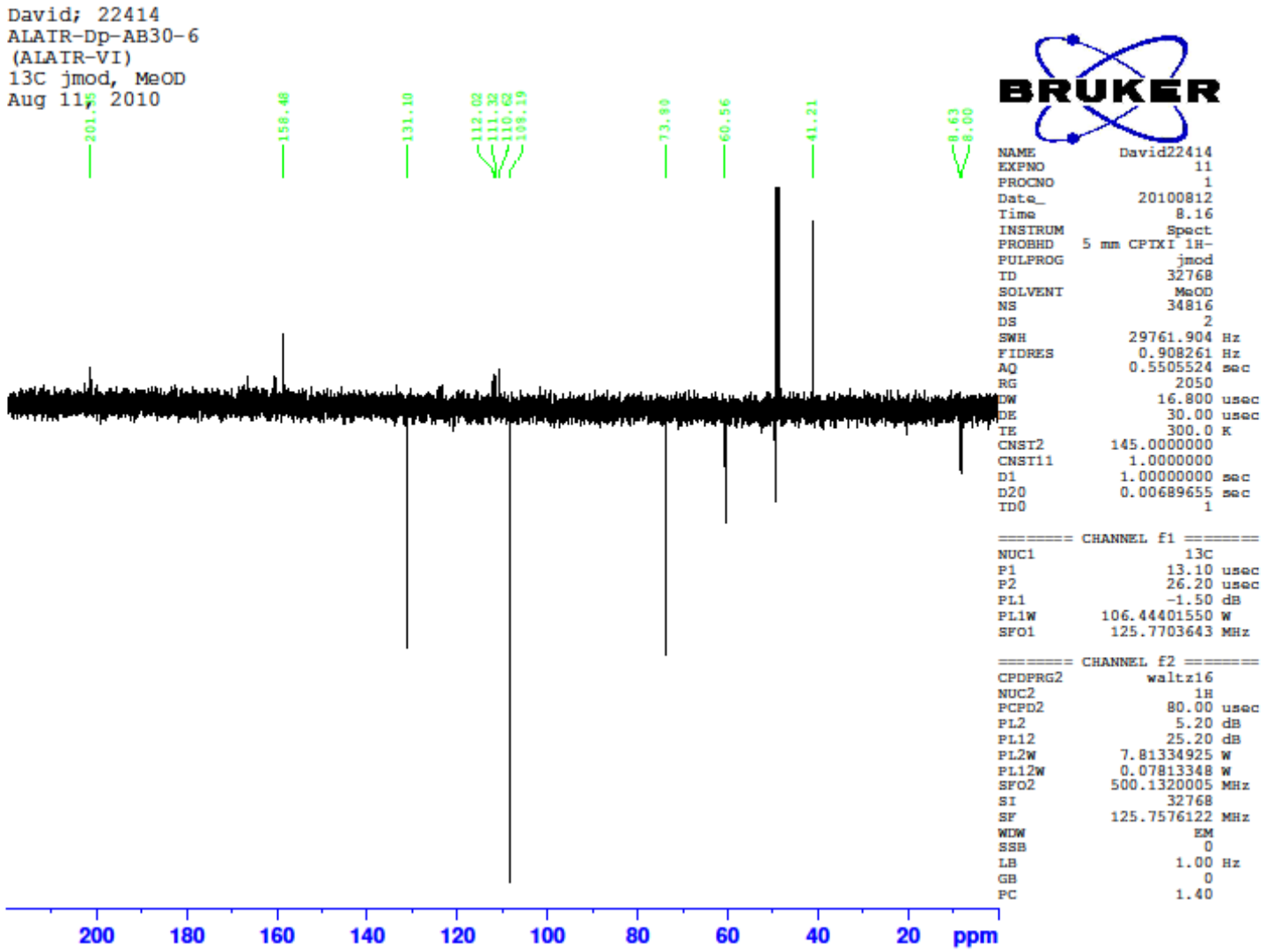

NAME	David22414
EXPNO	11
PROCNO	1
Date_	20100812
Time	8.16
INSTRUM	Spect
PROBHD	5 mm CPTXI 1H-
PULPROG	jmod
TD	32768
SOLVENT	MeOD
NS	34816
DS	2
SWH	29761.904 Hz
FIDRES	0.908261 Hz
AQ	0.5505524 sec
RG	2050
DW	16.800 usec
DE	30.00 usec
TE	300.0 K
CNST2	145.0000000
CNST11	1.0000000
D1	1.00000000 sec
D20	0.00689655 sec
TD0	1
======== CHANNEL f1 ========	
NUC1	13C
P1	13.10 usec
P2	26.20 usec
PL1	-1.50 dB
PL1W	106.44401550 W
SFO1	125.7703643 MHz
======== CHANNEL f2 ========	
CPDPRG2	waltz16
NUC2	1H
PCPD2	80.00 usec
PL2	5.20 dB
PL12	25.20 dB
PL2W	7.81334925 W
PL12W	0.07813348 W
SFO2	500.1320005 MHz
SI	32768
SF	125.7576122 MHz
WDW	EM
SSB	0
LB	1.00 Hz
GB	0
PC	1.40

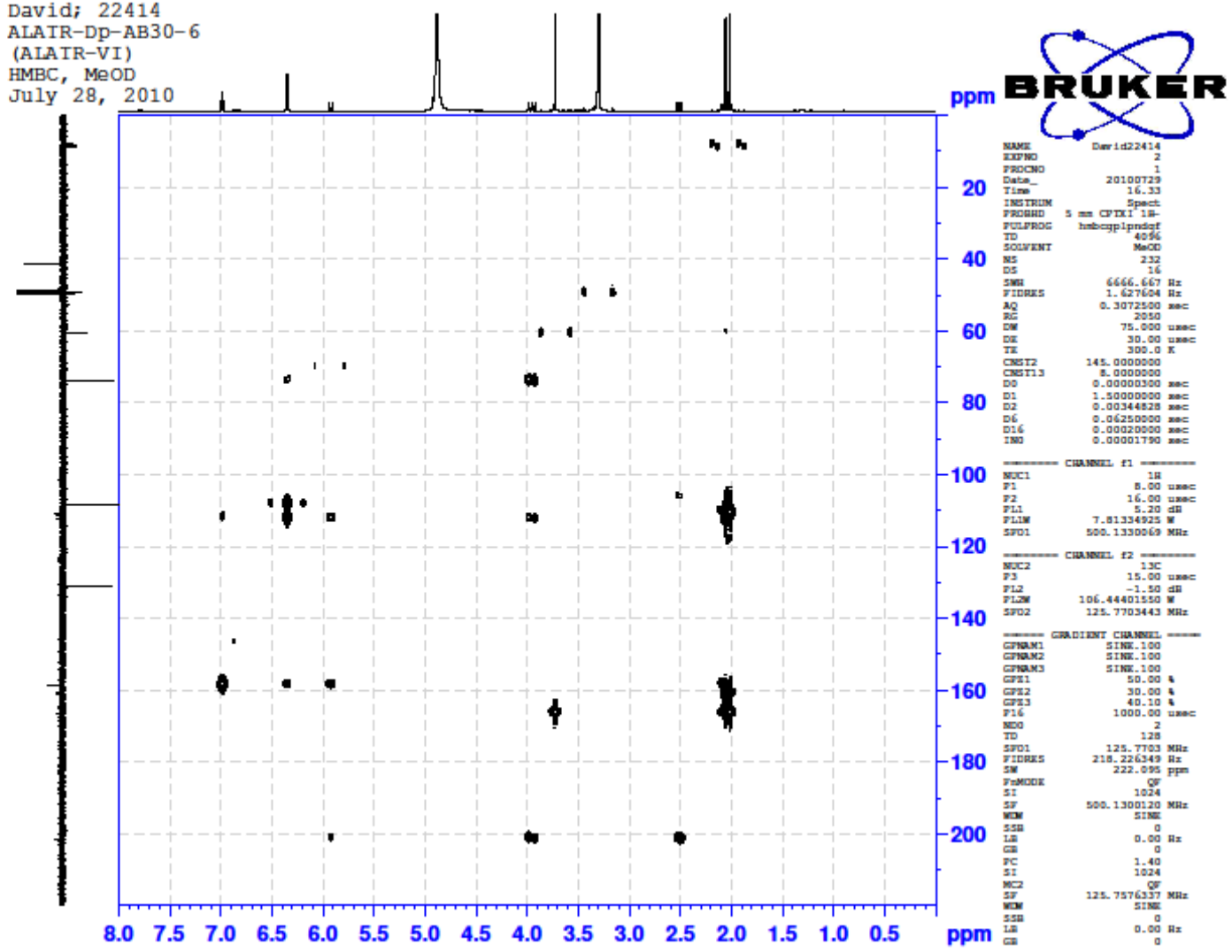
David; 22414
ALAIR-Dp-AB30-6
(ALAIR-VI)
HMBC, MeOD
July 28, 2010
ppm
8.0 7.5 7.0 6.5 6.0 5.5 5.0 4.5 4.0 3.5 3.0 2.5 2.0 1.5 1.0 0.5
ppm
20 40 60 80 100 120 140 160 180 200
BRUKER
NAME David22414
EXPNO 2
PROCNO 1
Date_ 20100729
Time 16.33
INSTRUM Spect
PROBHD 5 mm CPTXI 1H-
PULPROG hmbcgplpndqf
TD 4096
SOLVENT MeOD
NS 232
DS 16
SWH 6666.667 Hz
FIDRES 1.627604 Hz
AQ 0.3072500 sec
RG 2050
DW 75.000 usec
DE 30.00 usec
TE 300.0 K
CNST2 145.0000000
CNST13 8.0000000
D0 0.00000300 sec
D1 1.50000000 sec
D2 0.00344828 sec
D6 0.06250000 sec
D16 0.00020000 sec
IN0 0.00001790 sec
======== CHANNEL f1 ========
NUC1 1H
P1 8.00 usec
P2 16.00 usec
PL1 5.20 dB
PL1W 7.81334925 W
SFO1 500.1330069 MHz
======== CHANNEL f2 ========
NUC2 13C
P3 15.00 usec
PL2 -1.50 dB
PL2W 106.44401550 W
SFO2 125.7703443 MHz
====== GRADIENT CHANNEL =====
GPNAM1 SINE.100
GPNAM2 SINE.100
GPNAM3 SINE.100
GPZ1 50.00 %
GPZ2 30.00 %
GPZ3 40.10 %
P16 1000.00 usec
NDO 2
TD 128
SFO1 125.7703 MHz
FIDRES 218.226349 Hz
SW 222.095 ppm
FnMODE QF
SI 1024
SF 500.1300120 MHz
WDW SINE
SSB 0
LB 0.00 Hz
GB 0
PC 1.40
SI 1024
MC2 QF
SF 125.7576337 MHz
WDW SINE
SSB 0
LB 0.00 Hz
GB 0

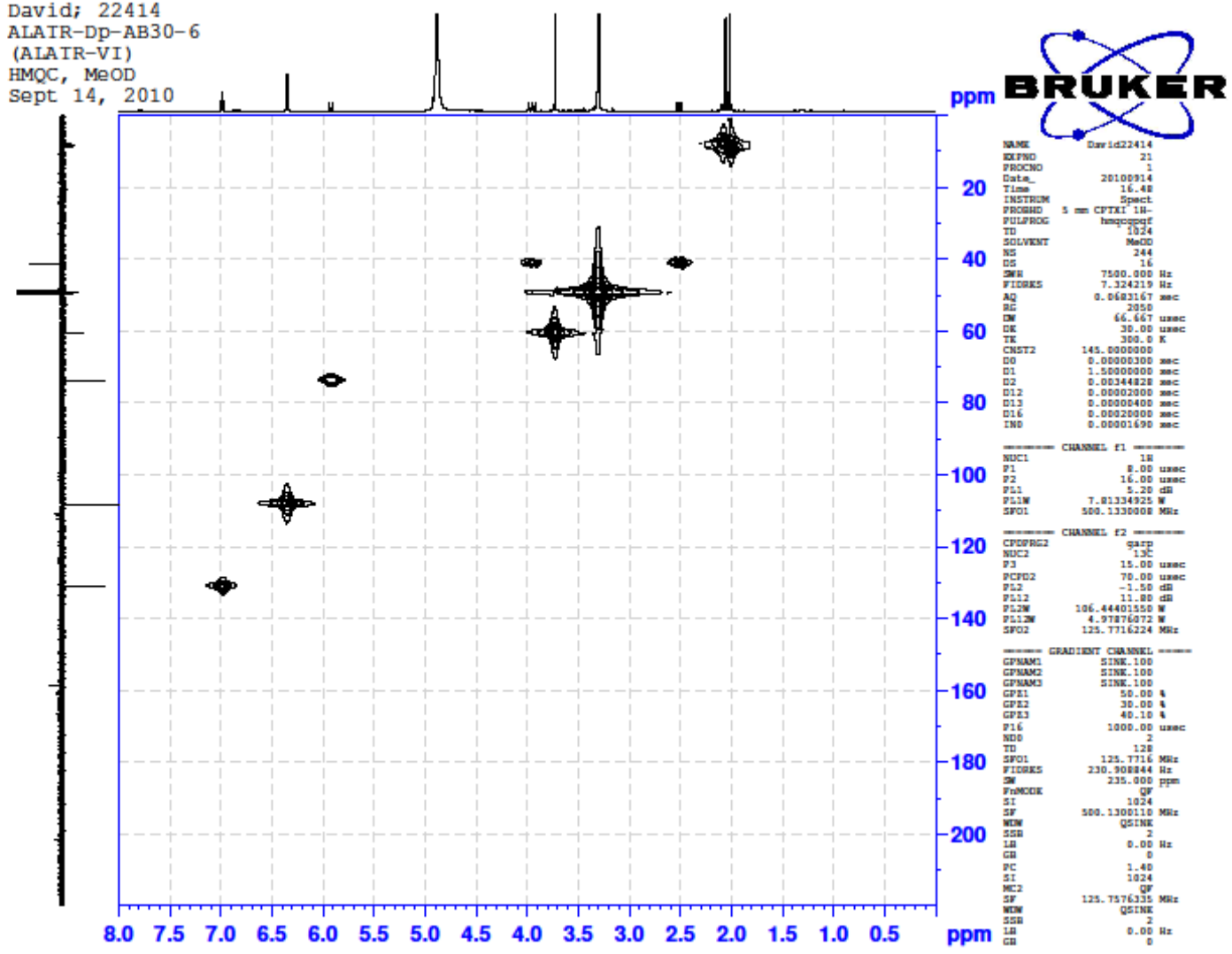
David; 22414
ALAIR-Dp-AB30-6
(ALAIR-VI)
HMQC, MeOD
Sept 14, 2010
ppm
20
40
60
80
100
120
140
160
180
200
8.0 7.5 7.0 6.5 6.0 5.5 5.0 4.5 4.0 3.5 3.0 2.5 2.0 1.5 1.0 0.5
ppm
BRUKER
NAME David22414
EXPNO 21
PROCNO 1
Date_ 20100914
Time 16.48
INSTRUM Spect
PROBHD 5 mm CPTXI 1H-
PULPROG hmqcgpqf
TD 1024
SOLVENT MeOD
NS 244
DS 16
SWH 7500.000 Hz
FIDRES 7.324219 Hz
AQ 0.0683167 sec
RG 2050
DW 66.667 usec
DE 30.00 usec
TE 300.0 K
CNST2 145.0000000
D0 0.00000300 sec
D1 1.50000000 sec
D2 0.00344828 sec
D12 0.00002000 sec
D13 0.00000400 sec
D16 0.00020000 sec
IN0 0.00001690 sec
CHANNEL f1
NUC1 1H
P1 8.00 usec
P2 16.00 usec
PL1 5.20 dB
PL1W 7.81334925 W
SFO1 500.1330008 MHz
CHANNEL f2
CPDPRG2 garp
NUC2 13C
P3 15.00 usec
PCPD2 70.00 usec
PL2 -1.50 dB
PL12 11.80 dB
PL2W 106.44401550 W
PL12W 4.97876072 W
SFO2 125.7716224 MHz
GRADIENT CHANNEL
GPNAM1 SINE.100
GPNAM2 SINE.100
GPNAM3 SINE.100
GPZ1 50.00 %
GPZ2 30.00 %
GPZ3 40.10 %
P16 1000.00 usec
ND0 2
TD 128
SFO1 125.7716 MHz
FIDRES 230.908844 Hz
SW 235.000 ppm
FnMODE QF
SI 1024
SF 500.1300110 MHz
WDW QSINE
SSB 2
LB 0.00 Hz
GB 0
PC 1.40
SI 1024
MC2 QF
SF 125.7576335 MHz
WDW QSINE
SSB 2
LB 0.00 Hz
GB 0

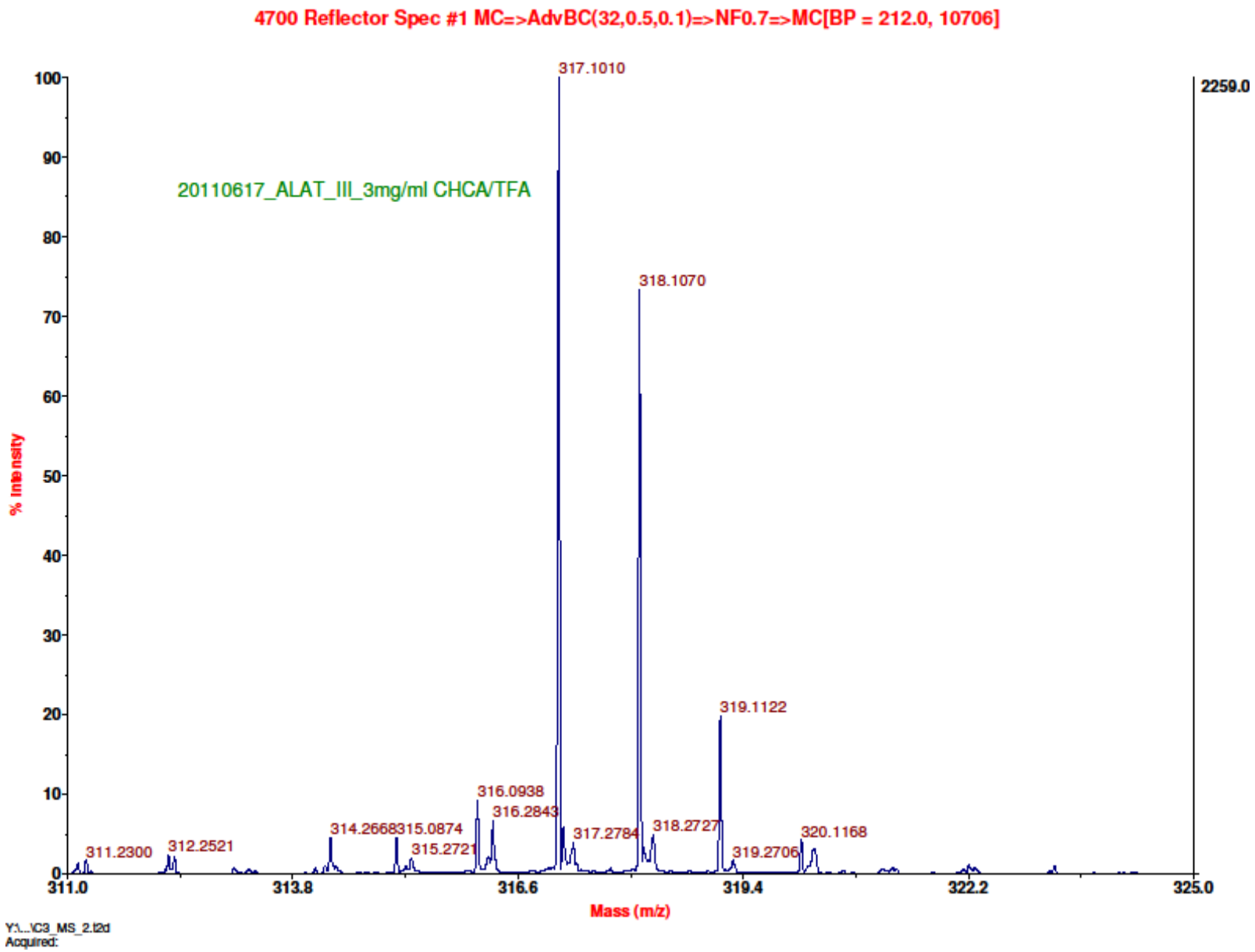
4700 Reflector Spec #1 MC=>AdvBC(32,0.5,0.1)=>NF0.7=>MC[BP = 212.0, 10706]
20110617_ALAT_III_3mg/ml CHCA/TFA
317.1010
318.1070
319.1122
316.0938
316.2843
314.2668
315.0874
315.2721
317.2784
318.2727
319.2706
320.1168
311.2300
312.2521
2259.0
% Intensity
Mass (m/z)
311.0
313.8
316.6
319.4
322.2
325.0
Y:\...\C3_MS_2.t2d
Acquired:

David; 22413
ALAIR-Dp-AB30-3
(ALAIR-III)
1H, MeOD
July 28, 2010

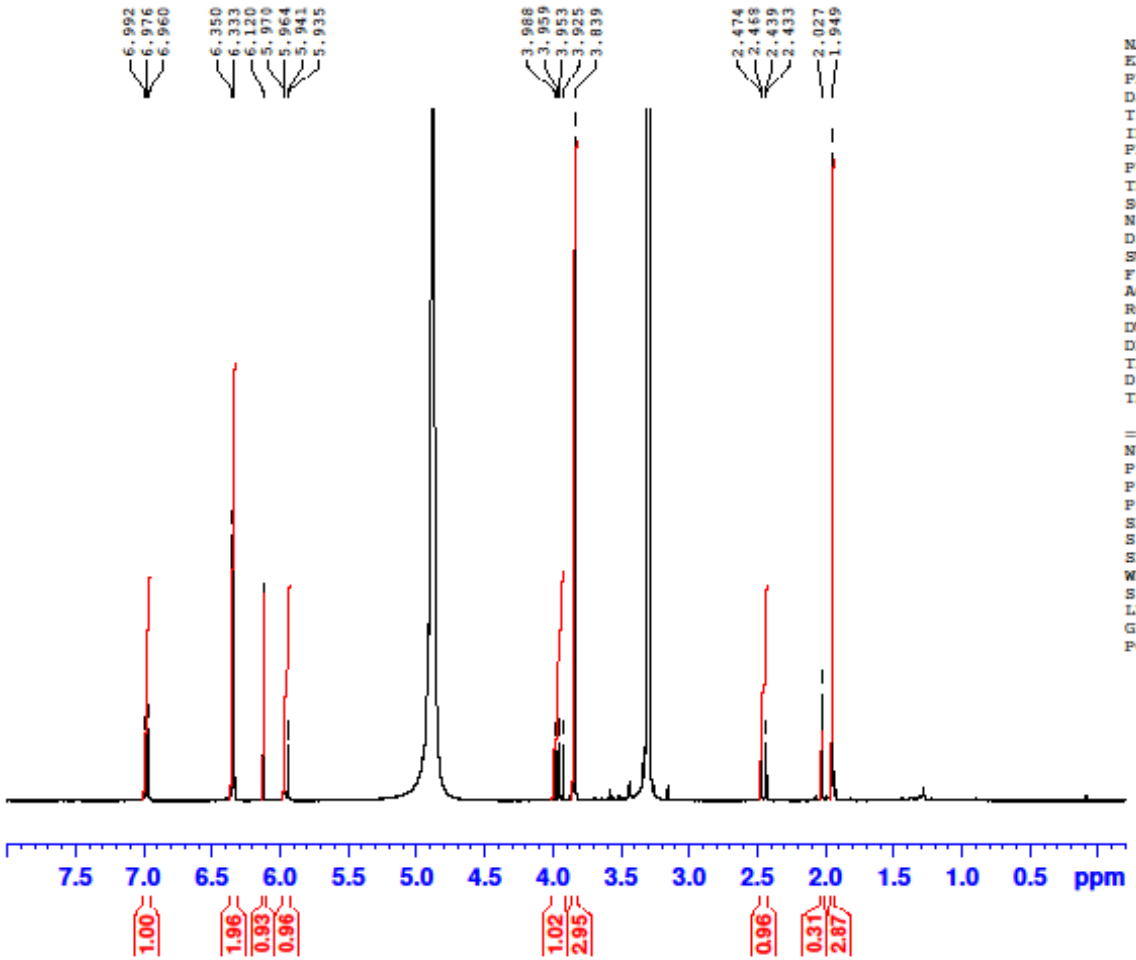

NAME	David22413	
EXPNO	1	
PROCNO	1	
Date_	20100729	
Time	15.31	
INSTRUM	Spect	
PROBHD	5 mm CPTXI 1H-	
PULPROG	zg30	
TD	65536	
SOLVENT	MeOD	
NS	8	
DS	2	
SWH	10330.578	Hz
FIDRES	0.157632	Hz
AQ	3.1719923	sec
RG	228	
DW	48.400	usec
DE	30.00	usec
TE	300.0	K
D1	1.00000000	sec
TD0	1	
======== CHANNEL f1 ========		
NUC1	1H	
P1	8.00	usec
PL1	5.20	dB
PL1W	7.81334925	W
SFO1	500.1330885	MHz
SI	32768	
SF	500.1300158	MHz
WDW	EM	
SSB	0	
LB	0.30	Hz
GB	0	
PC	1.00	

David; 22413
ALATR-Dp-AB30-3
(ALATR-III)
13C jmod, MeOD
Aug 10, 2010

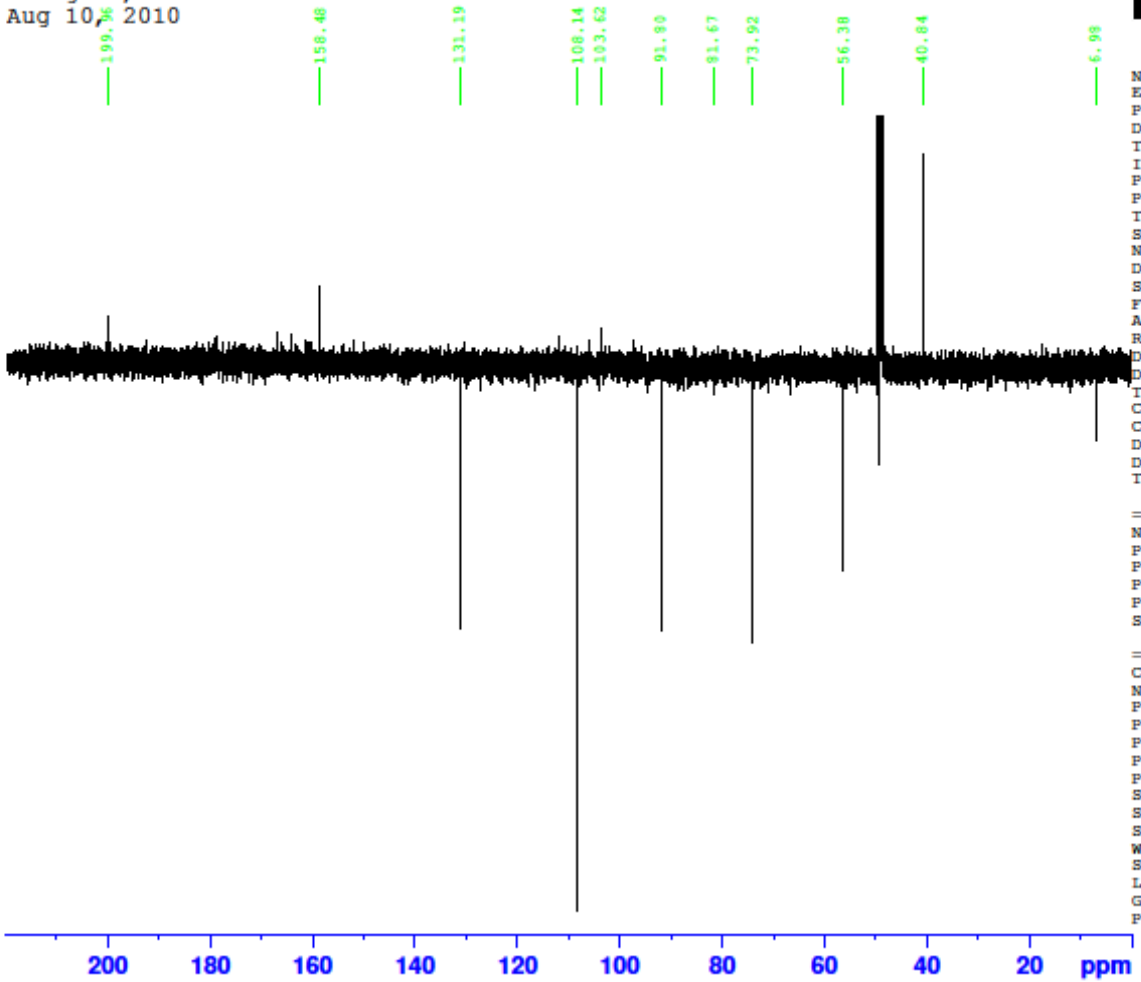

NAME	David22413
EXPNO	21
PROCNO	1
Date_	20100811
Time	8.13
INSTRUM	Spect
PROBHD	5 mm CPTXI 1H-
PULPROG	jmod
TD	32768
SOLVENT	MeOD
NS	34816
DS	2
SWH	29761.904 Hz
FIDRES	0.908261 Hz
AQ	0.5505524 sec
RG	2050
DW	16.800 usec
DE	30.00 usec
TE	300.0 K
CNST2	145.0000000
CNST11	1.0000000
D1	1.00000000 sec
D20	0.00689655 sec
TD0	1
======== CHANNEL f1 ========	
NUC1	13C
P1	13.10 usec
P2	26.20 usec
PL1	-1.50 dB
PL1W	106.44401550 W
SFO1	125.7703643 MHz
======== CHANNEL f2 ========	
CPDPRG2	waltz16
NUC2	1H
PCPD2	80.00 usec
PL2	5.20 dB
PL12	25.20 dB
PL2W	7.81334925 W
PL12W	0.07813348 W
SFO2	500.1320005 MHz
SI	32768
SF	125.7576122 MHz
WDW	EM
SSB	0
LB	1.00 Hz
GB	0
PC	1.40

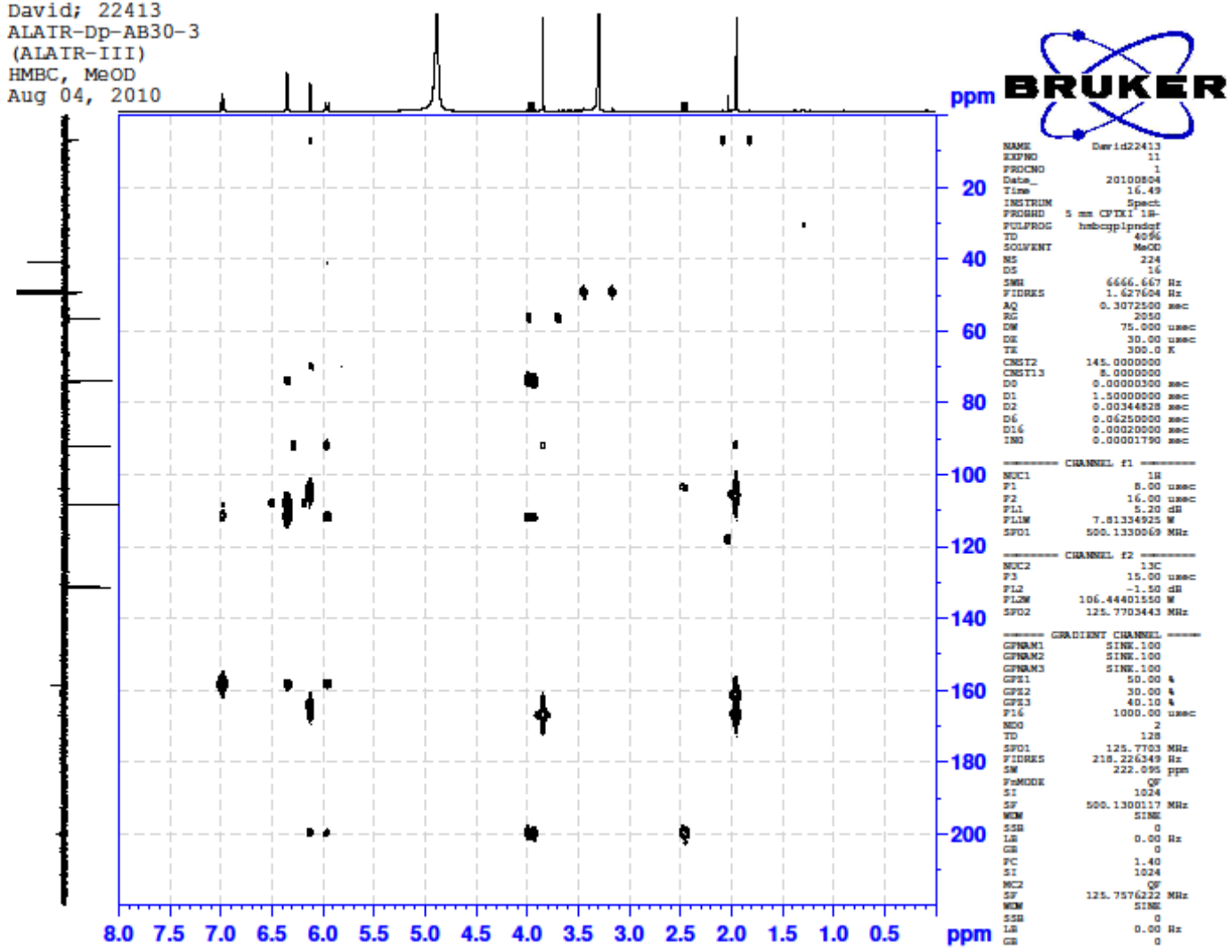

BRUKER

NAME	David22413
EXPNO	11
PROCNO	1
Date_	20100804
Time	16.49
INSTRUM	Spect
PROBHD	5 mm CPTXI 1H-
PULPROG	hmbcgplpndqf
TD	4096
SOLVENT	MeOD
NS	224
DS	16
SWH	6666.667 Hz
FIDRES	1.627604 Hz
AQ	0.3072500 sec
RG	2050
DW	75.000 usec
DE	30.00 usec
TE	300.0 K
CNST2	145.0000000
CNST13	8.0000000
D0	0.00000300 sec
D1	1.50000000 sec
D2	0.00344828 sec
D6	0.06250000 sec
D16	0.00020000 sec
IN0	0.00001790 sec
======== CHANNEL f1 ========	
NUC1	1H
P1	8.00 usec
P2	16.00 usec
PL1	5.20 dB
PL1W	7.81334925 W
SFO1	500.1330069 MHz
======== CHANNEL f2 ========	
NUC2	13C
P3	15.00 usec
PL2	-1.50 dB
PL2W	106.44401550 W
SFO2	125.7703443 MHz
====== GRADIENT CHANNEL ======	
GPNAM1	SINE.100
GPNAM2	SINE.100
GPNAM3	SINE.100
GPZ1	50.00 %
GPZ2	30.00 %
GPZ3	40.10 %
P16	1000.00 usec
NDO	2
TD	128
SFO1	125.7703 MHz
FIDRES	218.226349 Hz
SW	222.095 ppm
FnMODE	QF
SI	1024
SF	500.1300117 MHz
WDW	SINE
SSB	0
LB	0.00 Hz
GB	0
PC	1.40
SI	1024
MC2	QF
SF	125.7576222 MHz
WDW	SINE
SSB	0
LB	0.00 Hz
GB	0

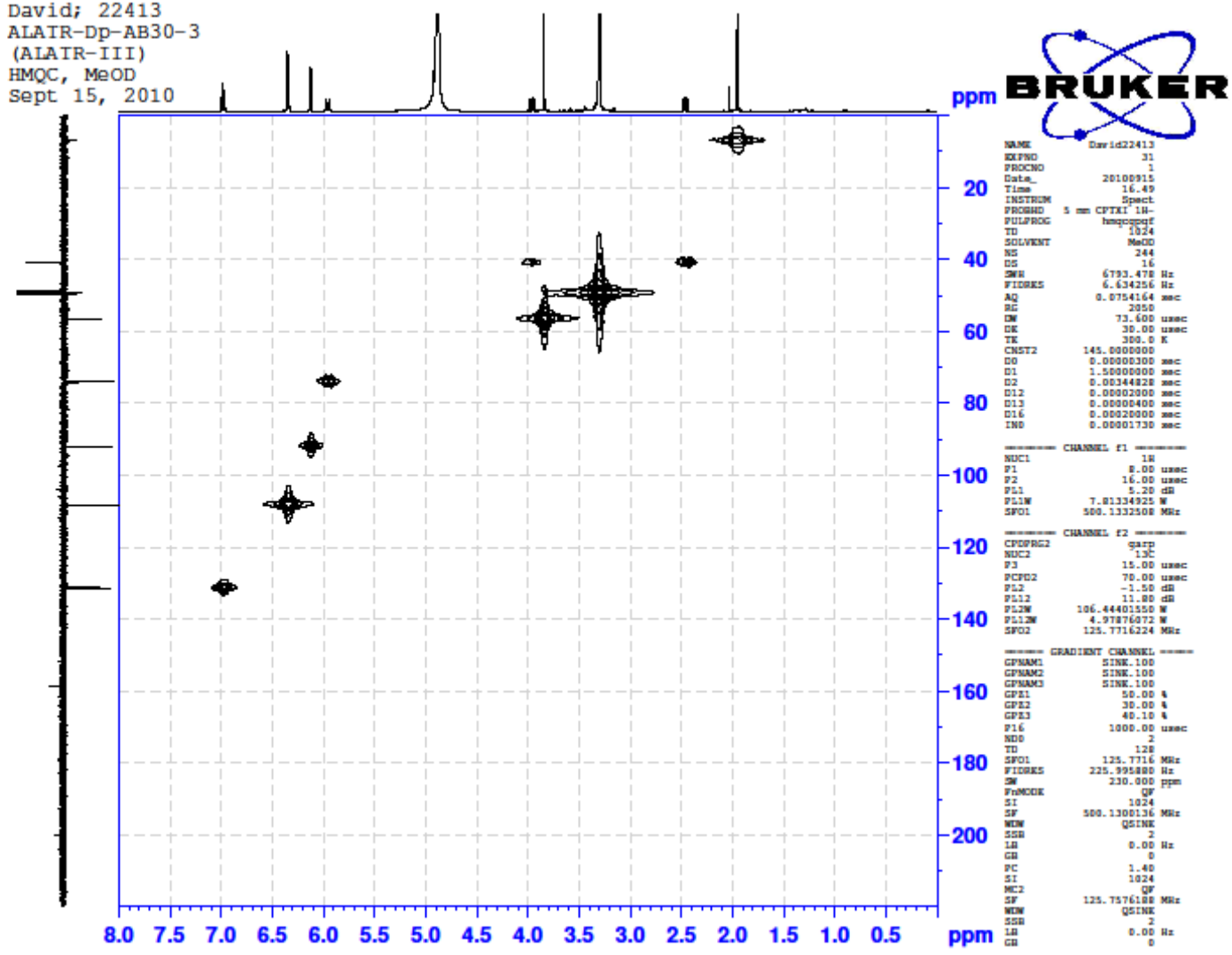

BRUKER

NAME	David22413	
EXPNO	31	
PROCNO	1	
Date_	20100915	
Time	16.49	
INSTRUM	Spect	
PROBHD	5 mm CPTXI 1H-	
PULPROG	hmqcgpqf	
TD	1024	
SOLVENT	MeOD	
NS	244	
DS	16	
SWH	6793.478	Hz
FIDRES	6.634256	Hz
AQ	0.0754164	sec
RG	2050	
DW	73.600	usec
DE	30.00	usec
TE	300.0	K
CNST2	145.0000000	
D0	0.00000300	sec
D1	1.50000000	sec
D2	0.00344828	sec
D12	0.00002000	sec
D13	0.00000400	sec
D16	0.00020000	sec
IN0	0.00001730	sec
====== CHANNEL f1 ======		
NUC1	1H	
P1	8.00	usec
P2	16.00	usec
PL1	5.20	dB
PL1W	7.81334925	W
SFO1	500.1332508	MHz
====== CHANNEL f2 ======		
CPDPRG2	garp	
NUC2	13C	
P3	15.00	usec
PCPD2	70.00	usec
PL2	-1.50	dB
PL12	11.80	dB
PL2W	106.44401550	W
PL12W	4.97876072	W
SFO2	125.7716224	MHz
====== GRADIENT CHANNEL ======		
GPNAM1	SINE.100	
GPNAM2	SINE.100	
GPNAM3	SINE.100	
GPZ1	50.00	%
GPZ2	30.00	%
GPZ3	40.10	%
P16	1000.00	usec
ND0	2	
TD	128	
SFO1	125.7716	MHz
FIDRES	225.995880	Hz
SW	230.000	ppm
FnMODE	QF	
SI	1024	
SF	500.1300136	MHz
WDW	QSINE	
SSB	2	
LB	0.00	Hz
GB	0	
PC	1.40	
SI	1024	
MC2	QF	
SF	125.7576188	MHz
WDW	QSINE	
SSB	2	
LB	0.00	Hz
GB	0	

APPENDDIX C

SUPPORTING INFORMATION FOR RNA-SEQ ANALYSIS

C.1. Tophat analysis parameters

min-anchor: 8
splice-mismatches: 0
min-report-intron: 50
max-report-intron: 500000
min-isoform-fraction: 0.15
max-multihits: 40
segment-length: 25
segment-mismatches: 2
min-closure-exon: 100
min-closure-intron: 50
max-closure-intron: 5000
min-coverage-intron: 50
max-coverage-intron: 20000
min-segment-intron: 50
max-segment-intron: 500000

Table C-1. Over-represented neighbour-based sets.

(3S,8S)-falcarindiol (1 μM)	(3R,8S)-falcarindiol (1 μM)	(3R,8S)-falcarindiol (10 μM)	(3R)-falcarinol (2 μM)	(R)-sulforphane (1 μM)	6-isovaleryl-umbelliferone (10 μM)	(Z)-ligustilide (10 μM)
HXK4	PO5F1	RS27	HXK4	SLMAP	MK01	SMCA4
GCKR	P4HA1	RS27A	SLBP	GSH0	ACTB	IKKA
PHAX	SMRC1	RPN1	GCKR	NR4A3	TBA1A	SMRC1
SLBP	KDM1A	RL40	PHAX	CSF1	1433G	PO5F1
SPN1	TIF1A	S61A2	GEMI2	GSHB	CTNB1	TF2L1
DDX20	MATR3	S61A1	SPN1	MALT1	2AAA	SMCA2
SMN	ARI3B	INS1	LMBL2		L1CAM	TF65
GEMI2	MTA1	SRPRB	DDX20		KS6A3	MATR3
GEMI5	CTBP2	SRPR	AAAS		1433E	KDM1A
AAAS	P66B	INS2	PCGF6		IKKA	MTA1
NUPL1	ZN513	SC11A	NUPL1		KAP3	MK01
NXF1	HELLS	IF1AX	SMN		KALRN	EPN1
RAE1L	JADE1	RS8	MGAP		SRC	TBCE
NUP93	MTA2	RL5	RAE1L		MYH11	D3YXI3
IF4E	XRCC5	RS15	KDM1A		AKT2	MED1
B2RQL0	SALL4	ERF1	NXF1		JIP1	CTBP2
Q6PFD9	CHD4	RS3	RING2		RALA	SMCA5
RBP2	A2A8L1	EF2	MAX		DYN1	DDB1
D3YXJ1	BRWD1	IF2P	MATR3		KPCG	PARP1
SMD3	NACC1	RL14	MTA1		NMDZ1	KIF5C
RSMB	ACINU	RL13A	NUP93		MYH9	ACL6A
NCBP1	ZBT43	RSSA	IF4E		Q4VA56	XRCC5
B1APM6	TRI33	D3YYM6	GEMI5		MYH10	SRC
MGN	DNLI3	RS11	ACL6A		MYO1B	TIF1A
CPSF1	ZIC2	RS19	XRCC5		CADH2	O35171
NFX1	HCFC1	D3YW44	B2RQL0		MYO5A	2AAA
D3Z4G3	RFX2	UBIM	Q6PFD9		KPCB	P4HA1
RNPS1	XRCC1	RL19	SMCA5		ARNT	ZFHX3

REFERENCES

Agurell, S., M. Halldin, J. E. Lindgren, A. Ohlsson, M. Widman, H. Gillespie and L. Hollister (1986). pharmacokinetics and metabolism of delta 1-tetrahydrocannabinol and other cannabinoids with emphasis on man. Pharmacological Reviews 38(1): 21-43.

Ahmad, R., D. Raina, C. Meyer, S. Kharbanda and D. Kufe (2006). Triterpenoid cddo-me blocks the Nf-Kb pathway by direct inhibition of Ikk-Beta on Cys-179. Journal of Biological Chemistry 281(47): 35764-35769.

Alam, J. and J. L. Cook (2007). How many transcription factors does it take to turn on the heme oxygenase-1 gene? American Journal of Respiratory Cell and Molecular Biology 36(2): 166-174.

Amit, I., M. Garber, N. Chevrier, A. P. Leite, Y. Donner, T. Eisenhaure, M. Guttman, J. K. Grenier, W. Li, O. Zuk, L. A. Schubert, B. Birditt, T. Shay, A. Goren, X. Zhang, Z. Smith, R. Deering, R. C. McDonald, M. Cabili, B. E. Bernstein, J. L. Rinn, A. Meissner, D. E. Root, N. Hacohen and A. Regev (2009). Unbiased Reconstruction of a Mammalian Transcriptional Network Mediating Pathogen Responses. Science 326(5950): 257-263.

Andreadi, C. K., L. M. Howells, P. A. Atherfold and M. M. Manson (2006). Involvement of Nrf2, p38, B-Raf, and nuclear factor-κB, but not phosphatidylinositol 3-kinase, in induction of hemeoxygenase-1 by dietary polyphenols. Molecular Pharmacology 69(3): 1033-1040.

Ansher, S. S., P. Dolan and E. Bueding (1986). Biochemical effects of dithiolthiones. Food Chemistry and Toxicology 24(5): 405-15.

Anwar-Mohamed, A. and A. O. S. El-Kadi (2009). Sulforaphane induces cyp1a1 mrna, protein, and catalytic activity levels via an ahr-dependent pathway in murine hepatoma hepa 1c1c7 and human hepg2 cells. Cancer Letters 275(1): 93-101.

Aoki, Y., H. Sato, N. Nishimura, S. Takahashi, K. Itoh and M. Yamamoto (2001). Accelerated DNA adduct formation in the lung of the nrf2 knockout mouse exposed to diesel exhaust. Toxicology and Applied Pharmacology 173(3): 154-160.

Apopa, P. L., Xiaoqing He and Q. Ma (2008). Phosphorylation of Nrf2 in the transcription activation domain by casein kinase 2 (CK2) is critical for the nuclear translocation and transcription activation function of Nrf2 in IMR-32 neuroblastoma cells. Journal of Biochemical and Molecular Toxicology 22(1): 63-76.

Appelt, G. D. (1985). Pharmacological aspects of selected herbs employed in Hispanic folk medicine in the San Luis Valley of Colorado, USA: I. *Ligusticum porteri* (osha) and *Matricaria chamomilla* (manzanilla). Journal of Ethnopharmacology 13(1): 51.

Appendino, G., F. Pollastro, L. Verotta, M. Ballero, A. Romano, P. Wyrembek, K. Szczuraszek, J. W. Mozrzymas and O. Taglialatela-Scafati (2009). Polyacetylenes from Sardinian *Oenanthe fistulosa*: a molecular clue to risus sardonicus. Journal of Natural Products.

Asher, G., P. Tsvetkov, C. Kahana and Y. Shaul (2005). A mechanism of ubiquitin-independent proteasomal degradation of the tumor suppressors p53 and p73. Genes & Development 19(3): 316-321.

auf dem Keller, U., M. Huber, T. A. Beyer, A. Kumin, C. Siemes, S. Braun, P. Bugnon, V. Mitropoulos, D. A. Johnson, J. A. Johnson, D. Hohl and S. Werner (2006). Nrf transcription factors in keratinocytes are essential for skin tumor prevention but not for wound healing. Molecular and Cellular Biology 26(10): 3773-3784.

Bacon, J. R., G. Williamson, R. C. Garner, G. Lappin, S. Langouet and Y. Bao (2003). Sulforaphane and quercetin modulate PhIP-DNA adduct formation in human HepG2 cells and hepatocytes. Carcinogenesis 24(12): 1903-1911.

Bae, S. H., S. H. Sung, E. J. Cho, S. K. Lee, H. E. Lee, H. A. Woo, D.-Y. Yu, I. S. Kil and S. G. Rhee (2011). Concerted action of sulfiredoxin and peroxiredoxin I protects against alcohol-induced oxidative injury in mouse liver. Hepatology 53(3): 945-953.

"BC Ministry of Environment: BC Species and Ecosystems Explorer." Retrieved January 12, 2010, from http://www.env.gov.bc.ca/atrisk/toolintro.html.
Beck, J. J. and S. C. Chou (2007). The structural diversity of phthalides from the Apiaceae. Journal of Natural Products 70(5): 891-900.
Beck, J. J. and F. R. Stermitz (1995). Addition of methyl thioglycolate and benzylamine to (Z)-ligustilide, a bioactive unsaturated lactone constituent of several herbal medicines. an improved synthesis of (Z)-ligustilide. Journal of Natural Products 58(7): 1047-1055.
Berger, S. L. (2007). The complex language of chromatin regulation during transcription. Nature 447(7143): 407-412.
Bertani, G. (1951). Studies on lysogenesis I.: the mode of phage liberation by lysogenic *Escherichia coli*. Journal of Bacteriology 62(3): 293-300.
Bhatt, L. R., M. S. Bae, B. M. Kim, G. S. Oh and K. Y. Chai (2009). A chalcone glycoside from the fruits of *Sorbus commixta* Hedl. Molecules 14(12): 5323-5327.
Bjelakovic, G., D. Nikolova, L. L. Gluud, R. G. Simonetti and C. Gluud (2007). Mortality in randomized trials of antioxidant supplements for primary and secondary prevention: systematic review and meta-analysis. Journal of the American Medical Association 297(8): 842-857.
Blanc, M. C., P. Bradesi and J. Casanova (2005). Enantiomeric differentiation of acyclic terpenes by 13 C NMR spectroscopy using a chiral lanthanide shift reagent. Magnetic Resonance in Chemistry 43(2): 176-179.
Bock, K. W., T. Eckle, M. Ouzzine and S. Fournel-Gigleux (2000). Coordinate induction by antioxidants of UDP-glucuronosyltransferase UGT1A6 and the apical conjugate export pump MRP2 (multidrug resistance protein 2) in Caco-2 cells. Biochemical Pharmacology 59(5): 467-70.
Bornheim, L. M., E. T. Everhart, J. Li and M. A. Correia (1993). Characterization of cannabidiol-mediated cytochrome P450 inactivation. Biochemical Pharmacology 45(6): 1323-1331.
Bornheim, L. M. and M. P. Grillo (1998). Characterization of cytochrome P450 3A inactivation by cannabidiol: possible involvement of cannabidiol-hydroxyquinone as a P450 inactivator. Chemical Research in Toxicology 11(10): 1209-1216.
Braida, D., S. Pegorini, M. V. Arcidiacono, G. G. Consalez, L. Croci and M. Sala (2003). Post-ischemic treatment with cannabidiol prevents electroencephalographic flattening, hyperlocomotion and neuronal injury in gerbils. Neuroscience letters 346(1-2): 61-64.
Buckley, B. J., S. Li and A. R. Whorton (2008). Keap1 modification and nuclear accumulation in response to S-nitrosocysteine. Free Radical Biology and Medicine 44(4): 692-698.
Bullard, J. H., E. Purdom, K. D. Hansen and S. Dudoit (2010). Evaluation of statistical methods for normalization and differential expression in mRNA-Seq experiments. BMC bioinformatics 11(1): 94.
Calabrese, E. J. (2008). Converging concepts: Adaptive response, preconditioning, and the Yerkes-Dodson Law are manifestations of hormesis. Ageing Research Reviews 7(1): 8-20.
Calabrese, E. J. (2008). Hormesis and medicine. British Journal of Clinical Pharmacology 66(5): 594.
Calabrese, E. J., K. A. Bachmann, A. J. Bailer, P. M. Bolger, J. Borak, L. Cai, N. Cedergreen, M. G. Cherian, C. C. Chiueh, T. W. Clarkson, R. R. Cook, D. M. Diamond, D. J. Doolittle, M. A. Dorato, S. O. Duke, L. Feinendegen, D. E. Gardner, R. W. Hart, K. L. Hastings, A. W. Hayes, G. R. Hoffmann, J. A. Ives, Z. Jaworowski, T. E. Johnson, W. B. Jonas, N. E. Kaminski, J. G. Keller, J. E. Klaunig, T. B. Knudsen, W. J. Kozumbo, T. Lettieri, S.-Z. Liu, A. Maisseu, K. I. Maynard, E. J. Masoro, R. O. McClellan, H. M. Mehendale, C. Mothersill, D. B. Newlin, H. N. Nigg, F. W. Oehme, R. F. Phalen, M. A. Philbert, S. I. S. Rattan, J. E. Riviere, J. Rodricks, R. M. Sapolsky, B. R. Scott, C. Seymour, D. A. Sinclair, J. Smith-Sonneborn, E. T. Snow, L. Spear, D. E. Stevenson, Y. Thomas, M. Tubiana, G. M. Williams and M. P. Mattson (2007). Biological stress response terminology: Integrating the concepts of adaptive response and preconditioning

stress within a hormetic dose-response framework. Toxicology and Applied Pharmacology 222(1): 122-128.
Calabrese, E. J. and L. A. Baldwin (2003). Chemotherapeutics and hormesis. CRC Critical Reviews in Toxicology 33(3-4): 305-353.
Calabrese, E. J. and L. A. Baldwin (2003). Hormesis: The dose-response revolution. Annual Review of Pharmacology and Toxicology 43(1): 175-197.
Cheng, Z., J. Moore and L. Yu (2006). High-Throughput Relative DPPH Radical Scavenging Capacity Assay. Journal of Agricultural and Food Chemistry 54(20): 7429-7436.
Cho, H. Y., S. P. Reddy, A. Debiase, M. Yamamoto and S. R. Kleeberger (2005). Gene expression profiling of NRF2-mediated protection against oxidative injury. Free Radical Biology and Medicine 38(3): 325-43.
Cho, H. Y., S. P. Reddy, M. Yamamoto and S. R. Kleeberger (2004). The transcription factor NRF2 protects against pulmonary fibrosis. FASEB J 18(11): 1258-60.
Choi, Y. H., A. Hazekamp, A. M. G. Peltenburg-Looman, M. Frédérich, C. Erkelens, A. W. M. Lefeber and R. Verpoorte (2004). NMR assignments of the major cannabinoids and cannabiflavonoids isolated from flowers of Cannabis sativa. Phytochemical Analysis 15(6): 345-354.
Ciaccio, P. J., A. K. Jaiswal and K. D. Tew (1994). Regulation of human dihydrodiol dehydrogenase by Michael acceptor xenobiotics. Journal of Biological Chemistry 269(22): 15558-62.
Clarke, J. D., A. Hsu, K. Riedl, D. Bella, S. J. Schwartz, J. F. Stevens and E. Ho (2011). Bioavailability and inter-conversion of sulforaphane and erucin in human subjects consuming broccoli sprouts or broccoli supplement in a cross-over study design. Pharmacological Research 64(5): 456-463.
Copple, I. M., C. E. Goldring, R. E. Jenkins, A. J. L. Chia, L. E. Randle, J. D. Hayes, N. R. Kitteringham and B. K. Park (2008). The hepatotoxic metabolite of acetaminophen directly activates the Keap1-Nrf2 cell defense system. Hepatology 48(4): 1292-1301.
Copple, I. M., A. Lister, A. D. Obeng, N. R. Kitteringham, R. E. Jenkins, R. Layfield, B. J. Foster, C. E. Goldring and B. K. Park (2010). Physical and functional interaction of sequestosome 1 with Keap1 regulates the Keap1-Nrf2 cell defense pathway. Journal of Biological Chemistry 285(22): 16782-16788.
Cui, F., L. Feng and J. Hu (2006). Factors affecting stability of *Z*-Ligustilide in the volatile oil of radix *Angelicae Sinensis* and *Ligusticum Chuanxiong* and its stability prediction. Drug Development and Industrial Pharmacy 32(6): 747 - 755.
Cullinan, S. B. and J. A. Diehl (2004). PERK-dependent activation of Nrf2 contributes to redox homeostasis and cell survival following endoplasmic reticulum stress. Journal of Biological Chemistry 279(19): 20108-20117.
Cullinan, S. B., J. D. Gordan, J. Jin, J. W. Harper and J. A. Diehl (2004). The Keap1-BTB protein is an adaptor that bridges Nrf2 to a Cul3-based E3 ligase: oxidative stress sensing by a Cul3-Keap1 ligase. Molecular and Cellular Biology 24(19): 8477-8486.
Cullinan, S. B., D. Zhang, M. Hannink, E. Arvisais, R. J. Kaufman and J. A. Diehl (2003). Nrf2 is a direct PERK substrate and effector of PERK-dependent cell survival. Molecular and Cellular Biology 23(20): 7198-7209.
Czepa, A. and T. Hofmann (2003). Structural and sensory characterization of compounds contributing to the bitter off-taste of carrots (*Daucus carota* L.) and carrot puree. Journal of Agricultural and Food Chemistry 51(13): 3865-3873.
Dannan, G. A., D. J. Porubek, S. D. Nelson, D. J. Waxman and F. P. Guengrich (1986). 17 beta-Estradiol 2-and 4-hydroxylation catalyzed by rat hepatic cytochrome P-450: roles of individual forms, inductive effects, developmental patterns, and alterations by gonadectomy and hormone replacement. Endocrinology 118(5): 1952-1960.

Dauchet, L., P. Amouyel, S. Hercberg and J. Dallongeville (2006). Fruit and vegetable consumption and risk of coronary heart disease: a meta-analysis of cohort studies. The Journal of Nutrition 136(10): 2588-2593.

De Long, M. J., H. J. Prochaska and P. Talalay (1986). Induction of NAD(P)H:quinone reductase in murine hepatoma cells by phenolic antioxidants, azo dyes, and other chemoprotectors: A model system for the study of anticarcinogens. Proceedings of the National Academy of Sciences of the United States of America 83(3): 787-791.

Denison, M. S. and S. R. Nagy (2003). Activation of the aryl hydrocarbon receptor by structurally diverse exogenous and endogenous chemicals. Annual Review of Pharmacology and Toxicology 43(1): 309-334.

Dieckhaus, C. M., C. L. Fernandez-Metzler, R. King, P. H. Krolikowski and T. A. Baillie (2005). Negative ion tandem mass spectrometry for the detection of glutathione conjugates. Chemical Research in Toxicology 18(4): 630-638.

Dietz, B. M., Y.-H. Kang, G. Liu, A. L. Eggler, P. Yao, L. R. Chadwick, G. F. Pauli, N. R. Farnsworth, A. D. Mesecar, R. B. van Breemen and J. L. Bolton (2005). Xanthohumol isolated from humulus lupulus inhibits menadione-induced DNA damage through induction of quinone reductase. Chemical Research in Toxicology 18(8): 1296-1305.

Dietz, B. M., D. Liu, G. K. Hagos, P. Yao, A. Schinkovitz, S. M. Pro, S. Deng, N. R. Farnsworth, G. F. Pauli and R. B. van Breemen (2008). *Angelica sinensis* and its alkylphthalides induce the detoxification enzyme NAD(P)H: quinone oxidoreductase 1 by alkylating Keap1. Chemical Research in Toxicology 21(10):1939-48.

Dinkova-Kostova, A. T., W. D. Holtzclaw, R. N. Cole, K. Itoh, N. Wakabayashi, Y. Katoh, M. Yamamoto and P. Talalay (2002). Direct evidence that sulfhydryl groups of Keap1 are the sensors regulating induction of phase 2 enzymes that protect against carcinogens and oxidants. Proceedings of the National Academy of Sciences of the United States of America 99(18): 11908-11913.

Dinkova-Kostova, A. T., W. D. Holtzclaw and N. Wakabayashi (2005). Keap1, the sensor for electrophiles and oxidants that regulates the phase 2 response, is a zinc metalloprotein. Biochemistry 44(18): 6889-6899.

Dinkova-Kostova, A. T., K. T. Liby, K. K. Stephenson, W. D. Holtzclaw, X. Gao, N. Suh, C. Williams, R. Risingsong, T. Honda, G. W. Gribble, M. B. Sporn and P. Talalay (2005). Extremely potent triterpenoid inducers of the phase 2 response: Correlations of protection against oxidant and inflammatory stress. Proceedings of the National Academy of Sciences of the United States of America 102(12): 4584-4589.

Dinkova-Kostova, A. T., M. A. Massiah, R. E. Bozak, R. J. Hicks and P. Talalay (2001). Potency of Michael reaction acceptors as inducers of enzymes that protect against carcinogenesis depends on their reactivity with sulfhydryl groups. Proceedings of the National Academy of Sciences of the United States of America 98(6): 3404-9.

Dinkova-Kostova, A. T. and P. Talalay (2008). Direct and indirect antioxidant properties of inducers of cytoprotective proteins. Molecular Nutrition & Food Research 52(S1): S128-S138.

Dinkova-Kostova, A. T. and P. Talalay (2010). NAD(P)H:quinone acceptor oxidoreductase 1 (NQO1), a multifunctional antioxidant enzyme and exceptionally versatile cytoprotector. Archives of Biochemistry and Biophysics 501(1): 116-123.

Eberle, D., B. Hegarty, P. Bossard, P. Ferre and F. Foufelle (2004). SREBP transcription factors: master regulators of lipid homeostasis. Biochimie 86(11): 839-848.

Eggler, A. L., G. Liu, J. M. Pezzuto, R. B. van Breemen and A. D. Mesecar (2005). Modifying specific cysteines of the electrophile-sensing human Keap1 protein is insufficient to disrupt binding to the Nrf2 domain Neh2. Proceedings of the National Academy of Sciences of the United States of America 102(29): 10070-10075.

Enomoto, A., K. Itoh, E. Nagayoshi, J. Haruta, T. Kimura, T. O'Connor, T. Harada and M. Yamamoto (2001). High Sensitivity of Nrf2 Knockout Mice to Acetaminophen Hepatotoxicity Associated with Decreased Expression of ARE-Regulated Drug Metabolizing Enzymes and Antioxidant Genes. Toxicological Sciences 59(1): 169-177.

Essaghir, A., F. Toffalini, L. Knoops, A. Kallin, J. van Helden and J.-B. Demoulin (2010). Transcription factor regulation can be accurately predicted from the presence of target gene signatures in microarray gene expression data. Nucleic Acids Research. 38: e120.

Fabricant, D. S. and N. R. Farnsworth (2001). The value of plants used in traditional medicine for drug discovery. Environmental Health Perspectives 109(Suppl 1): 69-75.

Fahey, J. W., A. T. Dinkova-Kostova, K. K. Stephenson and P. Talalay (2004). The "Prochaska" microtiter plate bioassay for inducers of NQO1. Methods in Enzymology 382: 243-58.

Fahey, J. W., Y. Zhang and P. Talalay (1997). Broccoli sprouts: an exceptionally rich source of inducers of enzymes that protect against chemical carcinogens. Proceedings of the National Academy of Sciences of the United States of America 94(19): 10367-72.

Favreau, L. V. and C. B. Pickett (1991). Transcriptional regulation of the rat NAD(P)H:quinone reductase gene. Identification of regulatory elements controlling basal level expression and inducible expression by planar aromatic compounds and phenolic antioxidants. Journal of Biological Chemistry 266(7): 4556-61.

Fontana, L., L. Partridge and V. D. Longo (2010). Extending healthy life span - from yeast to humans. Science 328(5976): 321-326.

Fujimoto, Y., M. Satoh, N. Takeuchi and M. Kirisawa (1991). Cytotoxic acetylenes from *Panax quinquefolium*. Chemical & Pharmaceutical Bulletin 39(2): 521-523.

Furger, A., J. M. O. S. Binnie, Alexandra, B. A. Lee and N. J. Proudfoot (2002). Promoter proximal splice sites enhance transcription. Genes & Development 16(21): 2792-2799.

Galloway, L. A. (1975). Systematics of the North American desert species of *Abronia* and *Tripterocalyx* (Nyctaginaceae). Brittonia 27(4): 328-347.

Gao, L., J. Wang, K. R. Sekhar, H. Yin, N. F. Yared, S. N. Schneider, S. Sasi, T. P. Dalton, M. E. Anderson, J. Y. Chan, J. D. Morrow and M. L. Freeman (2007). Novel n-3 fatty acid oxidation products activate Nrf2 by destabilizing the association between Keap1 and Cullin3. Journal of Biological Chemistry 282(4): 2529-2537.

Gao, X., L. Björk, V. Trajkovski and M. Uggla (2000). Evaluation of antioxidant activities of rosehip ethanol extracts in different test systems. Journal of the Science of Food and Agriculture 80(14): 2021-2027.

Gijbels, M. J. M., J. J. C. Scheffer and A. Baerheim Svendsen (1982). Phthalides in the essential oil from roots of *Levisticum officinale*. Planta Medica 44: 207-211.

Gong, P., D. Stewart, B. Hu, N. Li, J. Cook, A. Nel and J. Alam (2002). Activation of the mouse heme oxygenase-1 gene by 15-deoxy-Delta(12,14)-prostaglandin J(2) is mediated by the stress response elements and transcription factor Nrf2. Antioxidants and Redox Signalling 4(2): 249-57.

Goodacre, R., S. Vaidyanathan, W. B. Dunn, G. G. Harrigan and D. B. Kell (2004). Metabolomics by numbers: acquiring and understanding global metabolite data. Trends in Biotechnology 22(5): 245-252.

Goyak, K. M. O., M. C. Johnson, S. C. Strom and C. J. Omiecinski (2008). Expression profiling of interindividual variability following xenobiotic exposures in primary human hepatocyte cultures. Toxicology and Applied Pharmacology 231(2): 216-224.

Greenfield, N. J. (2007). Using circular dichroism spectra to estimate protein secondary structure. Nature Protocols 1(6): 2876-2890.

Grønbæk, M. (2004). Epidemiologic evidence for the cardioprotective effects associated with consumption of alcoholic beverages. Pathophysiology 10(2): 83-92.

Guarente, L. and F. Picard (2005). Calorie restriction–the SIR2 connection. Cell 120(4): 473-482.

Gundlach, H., Müller, M. J., Kutchan, T. M., and M. H. Zenk (1992). Jasmonic acid is a signal transducer in elicitor-induced plant cell cultures. Proceedings of the National Academy of Sciences of the United States of America 89 (6): 62389-62393.
Gunther, E. (1973). Ethnobotany of Western Washington: the knowledge and use of indigenous plants by Native Americans, Univ of Washington Pr.
Hampson, A., M. Grimaldi, M. Lolic, D. Wink, R. Rosenthal and J. Axelrod (2000). Neuroprotective antioxidants from marijuanaa. Annals of the New York Academy of Sciences 899(1): 274-282.
Hankinson, O. (1979). Single-step selection of clones of a mouse hepatoma line deficient in aryl hydrocarbon hydroxylase. Proceedings of the National Academy of Sciences of the United States of America 76(1): 373-376.
Hansen, L. and P. M. Boll (1986). Polyacetylenes in Araliaceae: Their chemistry, biosynthesis and biological significance. Phytochemistry 25(2): 285-293.
Haraldsdóttir, J., L. Jespersen, J. Hansen-Møller, S. L. Hansen, L. P. Christensen and K. Brandt (2002). Recent developments in bioavailability of falcarinol. DIAS Report Horticulture (Denmark).
Harborne, J. B. (1999). The comparative biochemistry of phytoalexin induction in plants. Biochemical Systematics and Ecology 27(4): 335-367.
Harikumar, K. B., A. B. Kunnumakkara, K. S. Ahn, P. Anand, S. Krishnan, S. Guha and B. B. Aggarwal (2009). Modification of the cysteine residues in IκBα kinase and NF-κB (p65) by xanthohumol leads to suppression of NF-κB-regulated gene products and potentiation of apoptosis in leukemia cells. Blood 113(9): 2003-2013.
Harris, T. K. and G. J. Turner (2002). Structural basis of perturbed pKa values of catalytic groups in enzyme active sites. IUBMB Life 53(2): 85-98.
Hayes, D. P. (2006). Nutritional hormesis. European Journal of Clinical Nutrition 61(2): 147-159.
He, F. J., C. A. Nowson, M. Lucas and G. A. MacGregor (2007). Increased consumption of fruit and vegetables is related to a reduced risk of coronary heart disease: meta-analysis of cohort studies. Journal of Human Hypertension 21(9): 717-728.
He, F. J., C. A. Nowson and G. A. MacGregor (2006). Fruit and vegetable consumption and stroke: meta-analysis of cohort studies. The Lancet 367(9507): 320-326.
Hedrick, U. P. (1972). Sturtevant's edible plants of the world, Dover Publications, New York.
Heiss, E., C. Herhaus, K. Klimo, H. Bartsch and C. Gerhauser (2001). Nuclear factor kappa B Is a molecular target for sulforaphane-mediated anti-inflammatory mechanisms. Journal of Biological Chemistry 276(34): 32008-32015.
Hertog, M. G. L., P. C. H. Hollman and M. B. Katan (1992). Content of potentially anti-carcinogenic flavonoids of 28 vegetables andnine fruits commonly consumed in The Netherlands. Food Chemistry 40: 2379-2383.
Hirakura, K., M. Morita, K. Nakajima, Y. Ikeya and H. Mitsuhashi (1991). Polyacetylenes from the roots of *Panax ginseng*. Phytochemistry 30(10): 3327-3333.
Hollman, P. C. H., J. M. P. van Trijp, M. N. C. P. Buysman, M. S. v.d. Gaag, M. J. B. Mengelers, J. H. M. de Vries and M. B. Katan (1997). Relative bioavailability of the antioxidant flavonoid quercetin from various foods in man. FEBS Letters 418(12): 152-156.
Holtzclaw, W. D., A. T. Dinkova-Kostova and P. Talalay (2004). Protection against electrophile and oxidative stress by induction of phase 2 genes: the quest for the elusive sensor that responds to inducers. Advances in Enzyme Regulation 44(1): 335-367.
Hong, F., M. L. Freeman and D. C. Liebler (2005). Identification of sensor cysteines in human Keap1 modified by the cancer chemopreventive agent sulforaphane. Chemical Research in Toxicology 18(12): 1917-1926.
Horton, J. D., N. A. Shah, J. A. Warrington, N. N. Anderson, S. W. Park, M. S. Brown and J. L. Goldstein (2003). Combined analysis of oligonucleotide microarray data from transgenic and knockout

mice identifies direct SREBP target genes. Proceedings of the National Academy of Sciences of the United States of America 100(21): 12027-12032.
Hoye, T. R., C. S. Jeffrey and F. Shao (2007). Mosher ester analysis for the determination of absolute configuration of stereogenic (chiral) carbinol carbons. Nature Protocols 2(10): 2451-2458.
Hu, R., C. Xu, G. Shen, M. R. Jain, T. O. Khor, A. Gopalkrishnan, W. Lin, B. Reddy, J. Y. Chan and A. N. Kong (2006). Gene expression profiles induced by cancer chemopreventive isothiocyanate sulforaphane in the liver of C57BL/6J mice and C57BL/6J/Nrf2 (-/-) mice. Cancer Letters 243(2): 170-92.
Hu, R., C. Xu, G. Shen, M. R. Jain, T. O. Khor, A. Gopalkrishnan, W. Lin, B. Reddy, J. Y. Chan and A. N. Kong (2006). Identification of Nrf2-regulated genes induced by chemopreventive isothiocyanate PEITC by oligonucleotide microarray. Life Sciences 79(20): 1944-55.
Huang, H. C., T. Nguyen and C. B. Pickett (2002). Phosphorylation of Nrf2 at Ser-40 by protein kinase C regulates antioxidant response element-mediated transcription. Journal of Biological Chemistry 277(45): 42769-42774.
Huang, W.-H., Q.-W. Zhang, C.-Z. Wang, C.-S. Yuan and S.-P. Li (2010). Isolation and identification of two new polyynes from a North American ethnic medicinal plant--*Oplopanax horridus* (Smith) Miq. Molecules 15(2): 1089-1096.
Ishii, Y., K. Itoh, Y. Morishima, T. Kimura, T. Kiwamoto, T. Iizuka, A. E. Hegab, T. Hosoya, A. Nomura, T. Sakamoto, M. Yamamoto and K. Sekizawa (2005). Transcription factor Nrf2 plays a pivotal role in protection against elastase-induced pulmonary inflammation and emphysema. Journal of Immunology 175(10): 6968-6975.
Itoh, K., T. Chiba, S. Takahashi, T. Ishii, K. Igarashi, Y. Katoh, T. Oyake, N. Hayashi, K. Satoh and I. Hatayama (1997). An Nrf2/Small Maf heterodimer mediates the induction of Phase II detoxifying enzyme genes through antioxidant response elements. Biochemical and Biophysical Research Communications 236(2): 313-322.
Itoh, K., M. Mochizuki, Y. Ishii, T. Ishii, T. Shibata, Y. Kawamoto, V. Kelly, K. Sekizawa, K. Uchida and M. Yamamoto (2004). Transcription factor Nrf2 regulates inflammation by mediating the effect of 15-deoxy-delta-12,14-prostaglandin J2. Molecular and Cellular Biology 24(1): 36-45.
Itoh, K., K. I. Tong and M. Yamamoto (2004). Molecular mechanism activating Nrf2–Keap1 pathway in regulation of adaptive response to electrophiles. Free Radical Biology and Medicine 36(10): 1208-1213.
Itoh, K., N. Wakabayashi, Y. Katoh, T. Ishii, K. Igarashi, J. D. Engel and M. Yamamoto (1999). Keap1 represses nuclear activation of antioxidant responsive elements by Nrf2 through binding to the amino-terminal Neh2 domain. Genes and Development 13(1): 76-86.
Iuvone, T., G. Esposito, R. Esposito, R. Santamaria, M. Di Rosa and A. A. Izzo (2004). Neuroprotective effect of cannabidiol, a non-psychoactive component from *Cannabis sativa*, on beta-amyloid-induced toxicity in PC12 cells. Journal of Neurochemistry 89(1): 134-141.
Jain, A. K., D. A. Bloom and A. K. Jaiswal (2005). Nuclear import and export signals in control of Nrf2. Journal of Biological Chemistry 280(32): 29158-68.
Jain, A. K., S. Mahajan and A. K. Jaiswal (2008). Phosphorylation and dephosphorylation of tyrosine 141 regulate stability and degradation of INrf2: A novel mechanism in Nrf2 activation. Journal of Biological Chemistry 283(25): 17712-17720.
Jeon, Y.-J., S.-K. Myung, E.-H. Lee, Y. Kim, Y. J. Chang, W. Ju, H.-J. Cho, H. G. Seo and B. Y. Huh (2011). Effects of beta-carotene supplements on cancer prevention: Meta-analysis of randomized controlled trials. Nutrition and Cancer 63(8): 1196-1207.
Jiang, T., Z. Huang, Y. Lin, Z. Zhang, D. Fang and D. D. Zhang (2010). The protective role of Nrf2 in streptozotocin-induced diabetic nephropathy. Diabetes 59(4): 850-860.
Johnson, B. M., J. L. Bolton and R. B. van Breemen (2001). Screening botanical extracts for quinoid metabolites. Chemical Research in Toxicology 14(11): 1546-51.

Johnson, D., L. Kershaw, A. MacKinnon and J. Pojar (1995). Plants of the Western boreal forest and aspen parkland. Canada, Lone Pine Publishing and the Canadian Forest Service.

Jowsey, I. R., Q. Jiang, K. Itoh, M. Yamamoto and J. D. Hayes (2003). Expression of the aflatoxin b1-8,9-epoxide-metabolizing murine glutathione *S*-transferase A3 subunit is regulated by the Nrf2 transcription factor through an antioxidant response element. Molecular Pharmacology 64(5): 1018-1028.

Kamburov, A., K. Pentchev, H. Galicka, C. Wierling, H. Lehrach and R. Herwig (2011). ConsensusPathDB: toward a more complete picture of cell biology. Nucleic Acids Research 39(suppl 1): D712-D717.

Kansanen, E., A. M. Kivelä and A.-L. Levonen (2009). Regulation of Nrf2-dependent gene expression by 15-deoxy-Δ12,14-prostaglandin J2. Free Radical Biology and Medicine 47(9): 1310-1317.

Kaspar, J. W. and A. K. Jaiswal (2010). An Autoregulatory Loop between Nrf2 and Cul3-Rbx1 Controls Their Cellular Abundance. Journal of Biological Chemistry 285(28): 21349-21358.

Katsuoka, F., H. Motohashi, J. D. Engel and M. Yamamoto (2005). Nrf2 transcriptionally activates the mafG gene through an antioxidant response element. Journal of Biological Chemistry 280(6): 4483-4490.

Kelly, V. P., E. M. Ellis, M. M. Manson, S. A. Chanas, G. J. Moffat, R. McLeod, D. J. Judah, G. E. Neal and J. D. Hayes (2000). Chemoprevention of aflatoxin B1 hepatocarcinogenesis by coumarin, a natural benzopyrone that is a potent inducer of aflatoxin B1-aldehyde reductase, the glutathione s-transferase A5 and P1 subunits, and NAD(P)H:quinone oxidoreductase in rat liver. Cancer Research 60(4): 957-969.

Kensler, T. W. and N. Wakabayashi (2010). Nrf2: friend or foe for chemoprevention? Carcinogenesis 31(1): 90-99.

Kim, E.-H. and Y.-J. Surh (2006). 15-Deoxy-Delta-12,14-prostaglandin J2 as a potential endogenous regulator of redox-sensitive transcription factors. Biochemical Pharmacology 72(11): 1516-1528.

Kim, J.-W., M.-H. Li, J.-H. Jang, H.-K. Na, N.-Y. Song, C. Lee, J. A. Johnson and Y.-J. Surh (2008). 15-Deoxy-Δ12,14-prostaglandin J2 rescues PC12 cells from H2O2-induced apoptosis through Nrf2-mediated upregulation of heme oxygenase-1: Potential roles of Akt and ERK1/2. Biochemical Pharmacology 76(11): 1577-1589.

Kim, Y. C., H. Masutani, Y. Yamaguchi, K. Itoh, M. Yamamoto and J. Yodoi (2001). Hemin-induced activation of the thioredoxin gene by Nrf2. A differential regulation of the antioxidant responsive element by a switch of its binding factors. Journal of Biological Chemistry 276(21): 18399-406.

Kimura, S., E. Warabi, T. Yanagawa, D. Ma, K. Itoh, Y. Ishii, Y. Kawachi and T. Ishii (2009). Essential role of Nrf2 in keratinocyte protection from UVA by quercetin. Biochemical and Biophysical Research Communications 387(1): 109-114.

Kobaisy, M., Z. Abramowski, L. Lermer, G. Saxena, R. E. W. Hancock, G. H. N. Towers, D. Doxsee and R. W. Stokes (1997). Antimycobacterial polyynes of Devil's Club (*Oplopanax horridus*), a North American native medicinal plant. Journal of Natural Products 60(11): 1210-1213.

Kobayashi, A., M.-I. Kang, H. Okawa, M. Ohtsuji, Y. Zenke, T. Chiba, K. Igarashi and M. Yamamoto (2004). Oxidative stress sensor Keap1 functions as an adaptor for Cul3-based E3 ligase to regulate proteasomal degradation of Nrf2. Molecular and Cellular Biology 24(16): 7130-7139.

Kobayashi, A., M.-I. Kang, Y. Watai, K. I. Tong, T. Shibata, K. Uchida and M. Yamamoto (2006). Oxidative and electrophilic stresses activate Nrf2 through inhibition of ubiquitination activity of Keap1. Molecular and Cellular Biology 26(1): 221-229.

Kobayashi, A., K. Tamagawa and K. Yamashita (1977). Synthesis of (±)-Dendrotrifidiol and its naturally occurring analogs. Agricultural and Biological Chemistry 41(4): 691-695.

Kobayashi, M., L. Li, N. Iwamoto, Y. Nakajima-Takagi, H. Kaneko, Y. Nakayama, M. Eguchi, Y. Wada, Y. Kumagai and M. Yamamoto (2009). the antioxidant defense system Keap1-Nrf2 comprises a

multiple sensing mechanism for responding to a wide range of chemical compounds. Molecular and Cellular Biology 29(2): 493-502.
Kobayashi, M. and M. Yamamoto (2006). Nrf2-Keap1 regulation of cellular defense mechanisms against electrophiles and reactive oxygen species. Advances in Enzyme Regulation 46: 113-40.
Kode, A., S. Rajendrasozhan, S. Caito, S.-R. Yang, I. L. Megson and I. Rahman (2008). Resveratrol induces glutathione synthesis by activation of Nrf2 and protects against cigarette smoke-mediated oxidative stress in human lung epithelial cells. American Journal of Physiology - Lung Cellular and Molecular Physiology 294(3): L478-488.
Kogan, N. M., R. Rabinowitz, P. Levi, D. Gibson, P. Sandor, M. Schlesinger and R. Mechoulam (2004). Synthesis and antitumor activity of quinonoid derivatives of cannabinoids. Journal of Medicinal Chemistry 47(15): 3800-3806.
Kraft, A. D., D. A. Johnson and J. A. Johnson (2004). Nuclear Factor E2-related factor 2-dependent antioxidant response element activation by tert-butylhydroquinone and sulforaphane occurring preferentially in astrocytes conditions neurons against oxidative insult. Journal of Neuroscience 24(5): 1101-1112.
Kuiper, G. G. J. M., J. G. Lemmen, B. Carlsson, J. C. Corton, S. H. Safe, P. T. van der Saag, B. van der Burg and J.-Ã. k. Gustafsson (1998). Interaction of estrogenic chemicals and phytoestrogens with estrogen receptor-alpha. Endocrinology 139(10): 4252-4263.
Kwak, M. K., N. Wakabayashi, K. Itoh, H. Motohashi, M. Yamamoto and T. W. Kensler (2003). Modulation of gene expression by cancer chemopreventive dithiolethiones through the Keap1-Nrf2 pathway. Identification of novel gene clusters for cell survival. Journal of Biological Chemistry 278(10): 8135-45.
Lai, E. C. (2002). Micro RNAs are complementary to 3'-UTR sequence motifs that mediate negative post-transcriptional regulation. Nature Genetics 30(4): 363-364.
Lami, N., S. Kadota and T. Kikuchi (1991). Constituents of the roots of *Boerhaavia diffusa* L. IV. Isolation and structure determination of boeravinones D, E, and F. Chemical & Pharmaceutical Bulletin 39(7): 1863-1865.
Langmead, B., C. Trapnell, M. Pop and S. L. Salzberg (2009). Ultrafast and memory-efficient alignment of short DNA sequences to the human genome. Genome Biology 10(3): R25.
Larsen, P. K., B. E. Nielsen and J. Lemmich (1970). Constituents of Umbelliferous Plants. Acta Chemica Scandinavica 24(3): 1113-1117.
Launer, A. E., D. D. Murphy, J. M. Hoekstra and H. R. Sparrow (1992). The endangered Myrtle's silverspot butterfly: present status and initial conservation planning. Journal of Research on the Lepidoptera 31(1-2): 132-146.
Lee-Hilz, Y. Y., A. M. Boerboom, A. H. Westphal, W. J. Berkel, J. M. Aarts and I. M. Rietjens (2006). Pro-oxidant activity of flavonoids induces EpRE-mediated gene expression. Chemical Research in Toxicology 19(11): 1499-505.
Lee, J.-M., M. J. Calkins, K. Chan, Y. W. Kan and J. A. Johnson (2003). Identification of the NF-E2-related factor-2-dependent genes conferring protection against oxidative stress in primary cortical astrocytes using oligonucleotide microarray analysis. Journal of Biological Chemistry 278(14): 12029-12038.
Lee, J.-M., J. M. Hanson, W. A. Chu and J. A. Johnson (2001). Phosphatidylinositol 3-kinase, not extracellular signal-regulated kinase, regulates activation of the antioxidant-responsive element in IMR-32 human neuroblastoma cells. Journal of Biological Chemistry 276(23): 20011-20016.
Lee, J.-M., A. Y. Shih, T. H. Murphy and J. A. Johnson (2003). NF-E2-related factor-2 mediates neuroprotection against mitochondrial complex I inhibitors and increased concentrations of intracellular calcium in primary cortical neurons. Journal of Biological Chemistry 278(39): 37948-37956.

Lee, L. S., K. K. Stephenson, J. W. Fahey, T. L. Parsons, P. S. Lietman, A. S. Andrade, X. Lei, H. Yun, G. H. Soon, P. Shen, S. Danishefsky and C. Flexner (2009). Induction of chemoprotective phase 2 enzymes by ginseng and its components. Planta Medica 75(10): 1129-1133.

Lee, O.-H., A. K. Jain, V. Papusha and A. K. Jaiswal (2007). An auto-regulatory loop between stress sensors INrf2 and Nrf2 controls their cellular abundance. Journal of Biological Chemistry 282(50): 36412-36420.

Lee, T. D., H. Yang, J. Whang and S. C. Lu (2005). Cloning and characterization of the human glutathione synthetase 5'-flanking region. Biochemical Journal 390(2): 521-528.

Leonti, M., L. Casu, S. Raduner, F. Cottiglia, C. Floris, K.-H. Altmann and J. Gertsch (2010). Falcarinol is a covalent cannabinoid CB1 receptor antagonist and induces pro-allergic effects in skin. Biochemical Pharmacology 79(12): 1815-1826.

Li, C. Y., X. Y. Liu, H. Bu, Z. Li, B. Li, M. M. Sun, Y. S. Guo, Y. L. Liu and Y. Zhang (2007). Prevention of glutamate excitotoxicity in motor neurons by 5,6-dihydrocyclopenta-1,2-dithiole-3-thione: implication to the development of neuroprotective drugs. Cellular and Molecular Life Sciences 64(14): 1861-1869.

Li, H. L. (1973). An archaeological and historical account of cannabis in China. Economic Botany 28(4): 437-448.

Li, J., T. Ichikawa, L. Villacorta, J. S. Janicki, G. L. Brower, M. Yamamoto and T. Cui (2009). Nrf2 protects against maladaptive cardiac responses to hemodynamic stress. Arteriosclerosis, Thrombosis, and Vascular Biology 29(11): 1843-1850.

Li, J., J.-M. Lee and J. A. Johnson (2002). Microarray analysis reveals an antioxidant responsive element-driven gene set involved in conferring protection from an oxidative stress-induced apoptosis in IMR-32 cells. Journal of Biological Chemistry 277(1): 388-394.

Li, J., T. D. Stein and J. A. Johnson (2004). Genetic dissection of systemic autoimmune disease in Nrf2-deficient mice. Physiological Genomics 18(3): 261-272.

Li, M., I. X. Wang, Y. Li, A. Bruzel, A. L. Richards, J. M. Toung and V. G. Cheung (2011). Widespread RNA and DNA sequence differences in the human transcriptome. Science 33(6038): 53-58.

Li, S. L., S. S. Chan, G. Lin, L. Ling, R. Yan, H. S. Chung and Y. K. Tam (2003). Simultaneous analysis of seventeen chemical ingredients of *Ligusticum chuanxiong* by on-line high performance liquid chromatography-diode array detector-mass spectrometry. Planta Medica 69(5): 445-51.

Lin, J., N. R. Cook, C. Albert, E. Zaharris, J. M. Gaziano, M. Van Denburgh, J. E. Buring and J. E. Manson (2009). Vitamins C and E and Beta carotene supplementation and cancer risk: A randomized controlled trial. Journal of the National Cancer Institute 101(1): 14-23.

Linares, E. and R. A. Bye (1987). A study of four medicinal plant complexes of Mexico and adjacent United States. Journal of Ethnopharmacology 19(2): 153-183.

Linnewiel, K., H. Ernst, C. Caris-Veyrat, A. Ben-Dor, A. Kampf, H. Salman, M. Danilenko, J. Levy and Y. Sharoni (2009). Structure activity relationship of carotenoid derivatives in activation of the electrophile/antioxidant response element transcription system. Free Radical Biology and Medicine 47(5): 659-667.

Liu, G.-H., J. Qu and X. Shen (2008). NF-κB/p65 antagonizes Nrf2-ARE pathway by depriving CBP from Nrf2 and facilitating recruitment of HDAC3 to MafK. Biochimica et Biophysica Acta (BBA) - Molecular Cell Research 1783(5): 713-727.

Liu, G., A. L. Eggler, B. M. Dietz, A. D. Mesecar, J. L. Bolton, J. M. Pezzuto and R. B. van Breemen (2005). Screening method for the discovery of potential cancer chemoprevention agents based on mass spectrometric detection of alkylated Keap1. Analytical Chemistry 77(19): 6407-6414.

Liu, H., A. T. Dinkova-Kostova and P. Talalay (2008). Coordinate regulation of enzyme markers for inflammation and for protection against oxidants and electrophiles. Proceedings of the National Academy of Sciences of the United States of America 105(41): 15926-15931.

Liu, M., D. N. Grigoryev, M. T. Crow, M. Haas, M. Yamamoto, S. P. Reddy and H. Rabb (2009). Transcription factor Nrf2 is protective during ischemic and nephrotoxic acute kidney injury in mice. Kidney International 76(3): 277-285.

Liu, X.-Y., C.-Y. Li, H. Bu, Z. Li, B. Li, M.-M. Sun, Y.-S. Guo, L. Zhang, W.-B. Ren, Z.-L. Fan, D.-X. Wu and S.-Y. Wu (2008). The neuroprotective potential of phase II enzyme inducer on motor neuron survival in traumatic spinal cord injury *in vitro*. Cellular and Molecular Neurobiology 28(5): 769-779.

Liu, X. M., K. J. Peyton, D. Ensenat, H. Wang, M. Hannink, J. Alam and W. Durante (2007). Nitric oxide stimulates heme oxygenase-1 gene transcription via the Nrf2/ARE complex to promote vascular smooth muscle cell survival. Cardiovascular Research 75(2): 381-389.

Lo, S.-C. and M. Hannink (2006). PGAM5, a Bcl-XL-interacting protein, is a novel substrate for the redox-regulated Keap1-dependent ubiquitin ligase complex. Journal of Biological Chemistry 281(49): 37893-37903.

Lu, W., G. Zheng, A. Aisa and J. Cai (1998). First total synthesis of optically active panaxydol, a potential antitumor agent isolated from *Panax ginseng*. Tetrahedron Letters 39(51): 9521-9522.

Lu, X., J. Zhang, H. Liang and Y. Zhao (2004). Chemical constituents of *Angelica sinensis*. Journal of Chinese Pharmaceutical Sciences 13(1): 1-3.

Lundholt, B. K., K. M. Scudder and L. Pagliaro (2003). A simple technique for reducing edge effect in cell-based assays. Journal of Biomolecular Screening 8(5): 566-570.

Luo, Y., A. L. Eggler, D. Liu, G. Liu, A. D. Mesecar and R. B. van Breemen (2007). Sites of alkylation of human Keap1 by natural chemoprevention agents. Journal of the American Society for Mass Spectrometry 18(12): 2226-2232.

Ma, Q., L. Battelli and A. F. Hubbs (2006). Multiorgan autoimmune inflammation, enhanced lymphoproliferation, and impaired homeostasis of reactive oxygen species in mice lacking the antioxidant-activated transcription factor Nrf2. American Journal of Pathology 168(6): 1960-1974.

Ma, W. G., M. Mizutani, K. E. Malterud, S. L. Lu, B. Ducrey and S. Tahara (1999). Saponins from the roots of Panax notoginseng. Phytochemistry 52(6): 1133-1139.

Malhotra, D., E. Portales-Casamar, A. Singh, S. Srivastava, D. Arenillas, C. Happel, C. Shyr, N. Wakabayashi, T. W. Kensler, W. W. Wasserman and S. Biswal (2010). Global mapping of binding sites for Nrf2 identifies novel targets in cell survival response through ChIP-Seq profiling and network analysis. Nucleic Acids Research 38(17):5718-34.

Malik, A. I. and K. B. Storey (2009). Activation of antioxidant defense during dehydration stress in the African clawed frog. Gene 442(1-2): 99-107.

Mattes, B. R., T. P. Clausen and P. B. Reichardt (1987). Volatile constituents of balsam poplar: The phenol glycoside connection. Phytochemistry 26(5): 1361-1366.

Mattson, M. P. (2008). Dietary factors, hormesis and health. Ageing Research Reviews 7(1): 43-48.

Mechoulam, R., Z. Ben-Zvi and Y. Gaoni (1968). Hashish-XIII: On the nature of the beam test. Tetrahedron 24(16): 5615-5624.

Mechoulam, R., M. Peters, E. Murillo-Rodriguez and L. O. Hanuš (2007). Cannabidiol – Recent advances. Chemistry & Biodiversity 4(8): 1678-1692.

Menon, V. P. and A. R. Sudheer (2007). Antioxidant and anti-inflammatory properties of curcumin. The Molecular Targets and Therapeutic Uses of Curcumin in Health and Disease: 105-125.

Miao, W., L. Hu, P. J. Scrivens and G. Batist (2005). Transcriptional regulation of NF-E2 p45-related factor (NRF2) expression by the aryl hydrocarbon receptor-xenobiotic response element signaling pathway: Direct cross-talk between phase i and ii drug-metabolizing enzymes. Journal of Biological Chemistry 280(21): 20340-20348.

Miranda, C. L., G. L. Aponso, J. F. Stevens, M. L. Deinzer and D. R. Buhler (2000). Prenylated chalcones and flavanones as inducers of quinone reductase in mouse Hepa 1c1c7 cells. Cancer Letters 149(1-2): 21-29.

Moerman, D. E. (1998). Native American Ethnobotany, Timber Pr (Portland).

Mortazavi, A., B. A. Williams, K. McCue, L. Schaeffer and B. Wold (2008). Mapping and quantifying mammalian transcriptomes by RNA-Seq. Nature Methods 5(7): 621-628.

Mulcahy, R. T. and J. J. Gipp (1995). Identification of a putative antioxidant response element in the 5'-flanking region of the human γ-glutamylcysteine synthetase heavy subunit gene. Biochemical and Biophysical Research Communications 209(1): 227.

Murphy, E. M., L. Nahar, M. Byres, M. Shoeb, M. Siakalima, M. Mukhlesur Rahman, A. I. Gray and S. D. Sarker (2004). Coumarins from the seeds of *Angelica sylvestris* (Apiaceae) and their distribution within the genus Angelica. Biochemical Systematics and Ecology 32(2): 203-207.

NatureServeExplorer. (2010). "Global Comprehensive Report." Retrieved Jan 9th, 2010, from http://www.natureserve.org/explorer/servlet/NatureServe?searchName=Oplopanax+horridus.

Nitz, S., M. H. Spraul and F. Drawert (1990). C17 Polyacetylenic alcohols as the major constituents in roots of *Petroselinum crispum* Mill. ssp. tuberosum. Journal of Agricultural and Food Chemistry 38(7): 1445-1447.

Noyan-Ashraf, M. H., L. Wu, R. Wang and B. H. Juurlink (2006). Dietary approaches to positively influence fetal determinants of adult health. FASEB Journal 20(2): 371-3.

Ogura, T., K. I. Tong, K. Mio, Y. Maruyama, H. Kurokawa, C. Sato and M. Yamamoto (2010). Keap1 is a forked-stem dimer structure with two large spheres enclosing the intervening, double glycine repeat, and C-terminal domains. Proceedings of the National Academy of Sciences of the United States of America 107(7): 2842-2847.

Ohnuma, T., T. Komatsu, S. Nakayama, T. Nishiyama, K. Ogura and A. Hiratsuka (2009). Induction of antioxidant and phase 2 drug-metabolizing enzymes by falcarindiol isolated from *Notopterygium incisum* extract, which activates the Nrf2/ARE pathway, leads to cytoprotection against oxidative and electrophilic stress. Archives of Biochemistry and Biophysics 488(1): 34-41.

Olsson, B., E. Bondesson, L. Borgstrom, S. Edsbaacker, S. Eirefelt, K. Ekelund, L. Gustavsson and T. Hegelund-Myrback (2011). Pulmonary Drug Metabolism, Clearance, and Absorption. Controlled Pulmonary Drug Delivery: 21-50.

Olsson, K. and R. Svensson (1996). The influence of polyacetylenes on the susceptibility of carrots to storage diseases. Journal of Phytopathology 144(9-10): 441-447.

Osei-Hyiaman, D., J. Liu, L. Zhou, G. Godlewski, J. Harvey-White, W. Jeong, S. BÃ¡tkai, G. Marsicano, B. Lutz and C. Buettner (2008). Hepatic CB1 receptor is required for development of diet-induced steatosis, dyslipidemia, and insulin and leptin resistance in mice. The Journal of Clinical Investigation 118(9): 3160.

Oshlack, A. and M. Wakefield (2009). Transcript length bias in RNA-seq data confounds systems biology. Biology Direct 4(1): 14.

Otieno, M. A., T. W. Kensler and K. Z. Guyton (2000). Chemoprotective 3H-1,2-dithiole-3-thione induces antioxidant genes in vivo. Free Radical Biology and Medicine 28(6): 944-52.

Ozgen, M., R. N. Reese, A. Z. Tulio, J. C. Scheerens and A. R. Miller (2006). Modified 2,2-azino-bis-3-ethylbenzothiazoline-6-sulfonic acid (ABTS) method to measure antioxidant capacity of selected small fruits and comparison to ferric reducing antioxidant power (FRAP) 2,2-diphenyl-1-picrylhydrazyl (DPPH) methods. Journal of Agricultural and Food Chemistry 54(4): 1151-1157.

Papajewski, S., J. H. Guse, I. Klaiber, G. Roos, R. Sussmuth, B. Vogler, C. U. Walter and W. Kraus (1998). Bioassay guided isolation of a new C18-polyacetylene, (+)-9(Z),17-octadecadiene-12,14-diyne-1,11,16-triol, from Cassonia barteri. Planta Medica 64(5): 479-81.

Park, H. J., Y. W. Lee, H. H. Park, Y. S. Lee, I. B. Kwon and J. H. Yu (1998). Induction of quinone reductase by a methanol extract of *Scutellaria baicalensis* and its flavonoids in murine Hepa 1c1c7 cells. European Journal of Cancer Prevention 7(6): 465.

Patil, N. S., K. S. Lole and D. N. Deobagkar (1996). Adaptive larval thermotolerance and induced cross-tolerance to propoxur insecticide in mosquitoes *Anopheles stephensi* and *Aedes aegypti*. Medical and Veterinary Entomology 10(3): 277-282.

Pearson, K. J., K. N. Lewis, N. L. Price, J. W. Chang, E. Perez, M. V. Cascajo, K. L. Tamashiro, S. Poosala, A. Csiszar, Z. Ungvari, T. W. Kensler, M. Yamamoto, J. M. Egan, D. L. Longo, D. K. Ingram, P. Navas and R. de Cabo (2008). Nrf2 mediates cancer protection but not prolongevity induced by caloric restriction. Proceedings of the National Academy of Sciences of the United States of America 105(7): 2325-2330.

Pergola, P. E., P. Raskin, R. D. Toto, C. J. Meyer, J. W. Huff, E. B. Grossman, M. Krauth, S. Ruiz, P. Audhya, H. Christ-Schmidt, J. Wittes and D. G. Warnock (2011). Bardoxolone methyl and kidney Function in CKD with type 2 diabetes. New England Journal of Medicine 365(4): 327-336.

Pertwee, R. G. (2008). The diverse CB1 and CB2 receptor pharmacology of three plant cannabinoids: Δ9-tetrahydrocannabinol, cannabidiol and Δ9-tetrahydrocannabivarin. British Journal of Pharmacology 153(2): 199-215.

Pietsch, E. C., J. Y. Chan, F. M. Torti and S. V. Torti (2003). Nrf2 mediates the induction of ferritin H in response to xenobiotics and cancer chemopreventive dithiolethiones. Journal of Biological Chemistry 278(4): 2361-9.

Pokharel, Y. R., E. H. Han, J. Y. Kim, S. J. Oh, S. K. Kim, E.-R. Woo, H. G. Jeong and K. W. Kang (2006). Potent protective effect of isoimperatorin against aflatoxin B1-inducible cytotoxicity in H4IIE cells: bifunctional effects on glutathione S-transferase and CYP1A. Carcinogenesis 27(12): 2483-2490.

Primiano, T., Y. Li, T. W. Kensler, M. A. Trush and T. R. Sutter (1998). Identification of dithiolethione-inducible gene-1 as a leukotriene B4 12-hydroxydehydrogenase: implications for chemoprevention. Carcinogenesis 19(6): 999-1005.

Prochaska, H. J. and A. B. Santamaria (1988). Direct measurement of NAD(P)H:quinone reductase from cells cultured in microtiter wells: a screening assay for anticarcinogenic enzyme inducers. Analytical Biochemistry 169(2): 328-36.

Pushan, W., G. Xuanliang, W. Yixiong, Y. Fukuyama, M. Iwao and M. Suguwara (1984). Phthalides from the rhizome of *Ligusticum wallichii*. Phytochemistry 23.

Radak, Z., H. Y. Chung, E. Koltai, A. W. Taylor and S. Goto (2008). Exercise, oxidative stress and hormesis. Ageing Research Reviews 7(1): 34-42.

Ratnayake, A. S. and T. Hemscheidt (2002). Olefin cross-metathesis as a tool in natural product degradation. The stereochemistry of (+)-falcarindiol. Organic Letters 4(26): 4667-9.

Reata Pharmaceuticals, I. (2012). Bardoxolone Methyl evaluation in patients with chronic kidney disease and type 2 diabetes (BEACON). ClinicalTrials.gov [Internet], Bethesda (MD). National Library of Medicine (US).

Reisman, S. A., R. L. Yeager, M. Yamamoto and C. D. Klaassen (2009). Increased Nrf2 activation in livers from Keap1-knockdown mice increases expression of cytoprotective genes that detoxify electrophiles more than those that detoxify reactive oxygen species. Toxicological Sciences 108(1): 35-47.

Ristow, M., K. Zarse, A. Oberbach, N. Klating, M. Birringer, M. Kiehntopf, M. Stumvoll, C. R. Kahn and M. Blaher (2009). Antioxidants prevent health-promoting effects of physical exercise in humans. Proceedings of the National Academy of Sciences of the United States of America.

Roberts, J., K. Bebenek and T. Kunkel (1988). The accuracy of reverse transcriptase from HIV-1. Science 242(4882): 1171-1173.

Rohman, M. and K. J. Harrison-Lavoie (2000). Separation of copurifying GroEL from glutathione-S-transferase fusion proteins. Protein Expression and Purification 20(1): 45-47.
Ross, D., J. K. Kepa, S. L. Winski, H. D. Beall, A. Anwar and D. Siegel (2000). NAD(P)H:quinone oxidoreductase 1 (NQO1): chemoprotection, bioactivation, gene regulation and genetic polymorphisms. Chemical and Biological Interactions 129(1-2): 77-97.
Rushmore, T. H. and C. B. Pickett (1990). Transcriptional regulation of the rat glutathione S-transferase Ya subunit gene. Characterization of a xenobiotic-responsive element controlling inducible expression by phenolic antioxidants. Journal of Biological Chemistry 265(24): 14648-53.
Sambrook, J., Fritsch, E.F., Maniatis, T. (1989). Molecular Cloning: A Laboratory Manual, Cold Spring Harbor Press (New York).
Sampath, H. and J. M. Ntambi (2004). Polyunsaturated fatty acid regulation of gene expression. Nutrition Reviews 62(9): 333-339.
Satoh, T., K. Kosaka, K. Itoh, A. Kobayashi, M. Yamamoto, Y. Shimojo, C. Kitajima, J. Cui, J. Kamins, S.-i. Okamoto, M. Izumi, T. Shirasawa and S. A. Lipton (2008). Carnosic acid, a catechol-type electrophilic compound, protects neurons both in vitro and in vivo through activation of the Keap1/Nrf2 pathway via S-alkylation of targeted cysteines on Keap1. Journal of Neurochemistry 104(4): 1116-1131.
Scapagnini, G., C. Colombrita, M. Amadio, V. D'Agata, E. Arcelli, M. Sapienza, A. Quattrone and V. Calabrese (2006). Curcumin activates defensive genes and protects neurons against oxidative stress. Antioxidants and Redox Signalling 8(3-4): 395-403.
Schaldach, C. M., J. Riby and L. F. Bjeldanes (1999). Lipoxin A4: A new class of ligand for the Ah receptor. Biochemistry 38(23): 7594-7600.
Schinkovitz, A., S. M. Pro, M. Main, S.-N. Chen, B. U. Jaki, D. C. Lankin and G. F. Pauli (2008). Dynamic nature of the ligustilide complex. Journal of Natural Products 71(9): 1604-1611.
Schmiech, L., C. Alayrac, B. Witulski and T. Hofmann (2009). Structure determination of bisacetylenic oxylipins in carrots (*Daucus carota* L.) and enantioselective synthesis of falcarindiol. Journal of Agricultural and Food Chemistry 57(22): 11030-11040.
See Waters, M., J. A. Cowen, J. C. McWilliams, P. E. Maligres and D. Askin (2000). Thiol addition to aryl propargyl alcohols under mild conditions: an accelerating neighboring group effect. Tetrahedron Letters 41(2): 141-144.
Sesso, H. D., J. E. Buring, W. G. Christen, T. Kurth, C. Belanger, J. MacFadyen, V. Bubes, J. E. Manson, R. J. Glynn and J. M. Gaziano (2008). Vitamins E and C in the Prevention of Cardiovascular Disease in Men. The Journal of the American Medical Association 300(18): 2123-2133.
Shan, Y., R. W. Lambrecht, S. E. Donohue and H. L. Bonkovsky (2006). Role of Bach1 and Nrf2 in up-regulation of the heme oxygenase-1 gene by cobalt protoporphyrin. FASEB Journal 20(14): 2651-2653.
Shen, G., C. Xu, R. Hu, M. R. Jain, A. Gopalkrishnan, S. Nair, M.-T. Huang, J. Y. Chan and A.-N. T. Kong (2006). Modulation of nuclear factor E2-related factor 2 mediated gene expression in mice liver and small intestine by cancer chemopreventive agent curcumin. Molecular Cancer Therapeutics 5(1): 39-51.
Shih, A. Y., P. Li and T. H. Murphy (2005). A small-molecule-inducible Nrf2-mediated antioxidant response provides effective prophylaxis against cerebral ischemia *in vivo*. Journal of Neuroscience 25(44): 10321-10335.
Shimada, T., C. L. Hayes, H. Yamazaki, S. Amin, S. S. Hecht, F. P. Guengerich and T. R. Sutter (1996). Activation of chemically diverse procarcinogens by human cytochrome P-450 1B1. Cancer Research 56(13): 2979-2984.
Siegel, D., D. L. Gustafson, D. L. Dehn, J. Y. Han, P. Boonchoong, L. J. Berliner and D. Ross (2004). NAD(P)H:quinone oxidoreductase 1: Role as a superoxide scavenger. Molecular Pharmacology 65(5): 1238-1247.

Smith, G. W. (1983). Arctic pharmacognosia II. Devil's club, *Oplopanax horridus.* Journal of Ethnopharmacology 7(3): 313.
Smith, P. K., R. I. Krohn, G. T. Hermanson and A. K. Mallia (1985). Measurement of protein using bicinchoninic acid. Analytical Biochemistry 150: 76–85.
Snyder, G. H., M. J. Cennerazzo, A. J. Karalis and D. Locey (1981). Electrostatic influence of local cysteine environments on disulfide exchange kinetics. Biochemistry 20(23): 6509-6519.
So, H. S., H. J. Kim, J. H. Lee, S. Y. Park, C. Park, Y. H. Kim, J. K. Kim, K. M. Lee, K. S. Kim and S. Y. Chung (2006). Flunarizine induces Nrf2-mediated transcriptional activation of heme oxygenase-1 in protection of auditory cells from cisplatin. Cell Death & Differentiation 13(10): 1763-1775.
Son, T., S. Camandola and M. Mattson (2008). Hormetic dietary phytochemicals. NeuroMolecular Medicine 10(4): 236-246.
Song, N.-Y., D.-H. Kim, E.-H. Kim, H.-K. Na and Y.-J. Surh (2009). 15-Deoxy-Δ12,14-prostaglandin J2 induces upregulation of multidrug resistance-associated protein 1 via Nrf2 Activation in Human Breast Cancer Cells. Annals of the New York Academy of Sciences 1171(1): 210-216.
Spencer, S. R., C. A. Wilczak and P. Talalay (1990). Induction of glutathione transferases and NAD(P)H:quinone reductase by fumaric acid derivatives in rodent cells and Tissues. Cancer Research 50(24): 7871-7875.
Spink, D. C., H. P. Eugster, D. W. Lincoln, J. D. Schuetz, E. G. Schuetz, J. A. Johnson, L. S. Kaminsky and J. F. Gierthy (1992). 17 beta-Estradiol hydroxylation catalyzed by human cytochrome P450 1A1: A comparison of the activities induced by 2, 3, 7, 8-tetrachlorodibenzo-*p*-dioxin in MCF-7 cells with those from heterologous expression of the cDNA. Archives of Biochemistry and Biophysics 293(2): 342-348.
Stevens, K. L. (1986). Allelopathic polyacetylenes from *Centaurea repens* (Russian knapweed). Journal of Chemical Ecology 12(6): 1205-1211.
Stewart, D., E. Killeen, R. Naquin, S. Alam and J. Alam (2003). Degradation of transcription factor Nrf2 via the ubiquitin-proteasome pathway and stabilization by cadmium. Journal of Biological Chemistry 278(4): 2396-2402.
Su, B. N., J. Q. Gu, Y. H. Kang, E. J. Park, J. M. Pezzuto and A. D. Kinghorn (2004). Induction of the phase II enzyme, quinone reductase, by withanolides and norwithanolides from solanaceous Species. Mini-Reviews in Organic Chemistry 1: 115.
Sun, Z., Z. Huang and D. D. Zhang (2009). Phosphorylation of Nrf2 at multiple sites by MAP kinases has a limited contribution in modulating the Nrf2-dependent antioxidant response. PLoS ONE 4(8): e6588.
Surh, Y. J. (2003). Cancer chemoprevention with dietary phytochemicals. Nature Reviews Cancer 3(10): 768-80.
Talalay, P., R. P. Batzinger, A. M. Benson, E. Bueding and Y. N. Cha (1978). Biochemical studies on the mechanisms by which dietary antioxidants suppress mutagenic activity. Advances in Enzyme Regulation 17: 23-36.
Tamehiro, N., Y. Shigemoto-Mogami, T. Kakeya, K.-i. Okuhira, K. Suzuki, R. Sato, T. Nagao and T. Nishimaki-Mogami (2007). Sterol regulatory element-binding protein-2- and liver X receptor-driven dual promoter regulation of hepatic ABC transporter A1 gene expression. Journal of Biological Chemistry 282(29): 21090-21099.
Tanaka, Y., L. M. Aleksunes, R. L. Yeager, M. A. Gyamfi, N. Esterly, G. L. Guo and C. D. Klaassen (2008). NF-E2-related factor 2 inhibits lipid accumulation and oxidative stress in mice fed a high-fat diet. Journal of Pharmacology and Experimental Therapeutics 325(2): 655-664.
Terada, A., Y. Tanoue and D. Kishimoto (1989). (-)-(9Z)-1, 9-Heptadecadiene-4, 6-diyn-3-ol as a principal component of the resinous sap of *Evodiopanax innovans nakai*, japanese name, takanotsume, and its role in an ancient golden varnish of japan. Bulletin of the Chemical Society of Japan 62(9): 2977-2980.

Terrell, B. and A. Fennell (2009). Osha (bear root) *Ligusticum porteri* JM Coult. & Rose var. *porteri*. Native Plants Journal 10(2): 110-118.
Thain, A., K. Gaston, O. Jenkins and A. R. Clarke (1996). A method for the separation of GST fusion proteins from co-purifying GroEL. Trends in Genetics 12(6): 209-210.
The Merck Index, t. e., Entry# 4369.
Thimmulappa, R. K., K. H. Mai, S. Srisuma, T. W. Kensler, M. Yamamoto and S. Biswal (2002). Identification of Nrf2-regulated genes induced by the chemopreventive agent sulforaphane by oligonucleotide microarray. Cancer Research 62(18): 5196-5203.
Tillett, S. S. (1967). The maritime species of *Abronia* (Nyctaginaceae). Brittonia 19(4): 299-327.
Tong, K. I., Y. Katoh, H. Kusunoki, K. Itoh, T. Tanaka and M. Yamamoto (2006). Keap1 recruits Neh2 through binding to ETGE and DLG motifs: Characterization of the two-site molecular recognition model. Molecular and Cellular Biology 26(8): 2887.
Tong, K. I., A. Kobayashi, F. Katsuoka and M. Yamamoto (2006). Two-site substrate recognition model for the Keap1-Nrf2 system: a hinge and latch mechanism. Biological Chemistry 387(10/11): 1311-1320.
Tong, K. I., B. Padmanabhan, A. Kobayashi, C. Shang, Y. Hirotsu, S. Yokoyama and M. Yamamoto (2007). Different electrostatic potentials define ETGE and DLG motifs as hinge and latch in oxidative stress response? Molecular and Cellular Biology 27(21): 7511-7521.
Trapnell, C., B. A. Williams, G. Pertea, A. Mortazavi, G. Kwan, M. J. van Baren, S. L. Salzberg, B. J. Wold and L. Pachter (2010). Transcript assembly and quantification by RNA-Seq reveals unannotated transcripts and isoform switching during cell differentiation. Nature Biotechology 28(5): 511-515.
Tung, Y. T., M. T. Chua, S. Y. Wang and S. T. Chang (2008). Anti-inflammation activities of essential oil and its constituents from indigenous cinnamon (*Cinnamomum osmophloeum*) twigs. Bioresource Technology 99(9): 3908-3913.
Uda, Y., K. R. Price, G. Williamson and M. J. C. Rhodes (1997). Induction of the anticarcinogenic marker enzyme, quinone reductase, in murine hepatoma cells in vitro by flavonoids. Cancer Letters 120(2): 213-216.
Ursini, F., M. Maiorino, P. Morazzoni, A. Roveri and G. Pifferi (1994). A novel antioxidant flavonoid (IdB 1031) affecting molecular mechanims of cellular activation. Free Radical Biology & Medicine 16(5): 547-553.
Vainio, H. and E. Weiderpass (2006). Fruit and vegetables in cancer prevention. Nutrition and Cancer 54(1): 111-142.
Valcic, S., A. Muders, N. E. Jacobsen, D. C. Liebler and B. N. Timmermann (1999). Antioxidant chemistry of green tea catechins. Identification of products of the reaction of epigallocatechin gallate with peroxyl radicals. Chemical Research in Toxicology 12(4): 382-386.
Vaquerizas, J. M., S. K. Kummerfeld, S. A. Teichmann and N. M. Luscombe (2009). A census of human transcription factors: function, expression and evolution. Nature Reviews Genetics 10(4): 252-263.
Velculescu, V. E., L. Zhang, B. Vogelstein and K. W. Kinzler (1995). Serial analysis of gene expression. Science 270(5235): 484-487.
Velichkova, M. and T. Hasson (2005). Keap1 regulates the oxidation-sensitive shuttling of Nrf2 into and out of the nucleus via a Crm1-dependent nuclear export mechanism. Molecular and Cellular Biology 25(11): 4501-4513.
Vollrath, V., A. M. Wielandt, M. Iruretagoyena and J. Chianale (2006). Role of Nrf2 in the regulation of the Mrp2 (ABCC2) gene. Biochemical Journal 395(Pt 3): 599.
Wakabayashi, N., K. Itoh, J. Wakabayashi, H. Motohashi, S. Noda, S. Takahashi, S. Imakado, T. Kotsuji, F. Otsuka, D. R. Roop, T. Harada, J. D. Engel and M. Yamamoto (2003). Keap1-null mutation leads to postnatal lethality due to constitutive Nrf2 activation. Nature Genetics 35(3): 238-245.

Wang, H. H., N. H. Afdhal and D. Q.-H. Wang (2006). Overexpression of estrogen receptor-alpha increases hepatic cholesterogenesis, leading to biliary hypersecretion in mice. Journal of Lipid Research 47(4): 778-786.
Wang, Z., M. Gerstein and M. Snyder (2009). RNA-Seq: a revolutionary tool for transcriptomics. Nature Reviews Genetics 10(1): 57-63.
WCMC (1994). Biodiversity Data Sourcebook, World Conservation Press.
WCRF-AICR (2007). Food, nutrition, physical activity, and the prevention of cancer: a global perspective, American Institute for Cancer Research (Washington).
WHO (2003). Diet, nutrition and the prevention of chronic diseases. Report of a Joint FAO/WHO expert Consultation. Geneva: World Health Organization WHO Technical Report, series 916.
Wiedman, S. J. and A. P. Appleby (1972). Plant growth stimulation by sublethal concentrations of herbicides. Weed Research 12(1): 65-74.
Williams, R. T. (1959). Detoxication mechanisms: the metabolism and detoxication of drugs, toxic substances, and other organic compounds, Wiley Blackwell (Hoboken).
Wink, M. (2010). Introduction: Biochemistry, Physiology and Ecological Functions of Secondary Metabolites. Annual Plant Reviews Volume 40: Biochemistry of Plant Secondary Metabolism, Wiley-Blackwell (Hoboken).
Wollenweber, E., S. Papendieck and G. Schilling (1993). A novel C-methyl isoflavone from *Abronia latifolia*. Natural Product Research 3(2): 119-122.
Wollenweber, E., R. d. Wehde, M. Darr, G. n. Lang and J. F. Stevens (2000). C-Methyl-flavonoids from the leaf waxes of some Myrtaceae. Phytochemistry 55(8): 965-970.
Wu, D., W. Li, P. Lok, F. Matsumura and C. F. Adam Vogel (2011). AhR deficiency impairs expression of LPS-induced inflammatory genes in mice. Biochemical and Biophysical Research Communications 410(2): 358-363.
Wu, K. C., J. Y. Cui and C. D. Klaassen (2011). Beneficial role of nrf2 in regulating NADPH generation and consumption. Toxicological Sciences 123(2): 590-600.
Wu, L., M. H. Noyan Ashraf, M. Facci, R. Wang, P. G. Paterson, A. Ferrie and B. H. Juurlink (2004). Dietary approach to attenuate oxidative stress, hypertension, and inflammation in the cardiovascular system. Proceedings of the National Academy of Sciences of the United States of America 101(18): 7094-9.
Yamamoto, T., T. Suzuki, A. Kobayashi, J. Wakabayashi, J. Maher, H. Motohashi and M. Yamamoto (2008). Physiological significance of reactive cysteine residues of keap1 in determining Nrf2 activity. Molecular and Cellular Biology 28(8): 2758-2770.
Yamaori, S., J. Ebisawa, Y. Okushima, I. Yamamoto and K. Watanabe (2011). Potent inhibition of human cytochrome P450 3A isoforms by cannabidiol: Role of phenolic hydroxyl groups in the resorcinol moiety. Life Sciences 88(15-16): 730-736.
Yan, R., N. L. Ko, S.-L. Li, Y. K. Tam and G. Lin (2008). Pharmacokinetics and metabolism of ligustilide, a major bioactive component in *Rhizoma chuanxiong*, in the rat. Drug Metabolism & Disposition 36(2): 400-408.
Yang, M., D. Seo, S. Choi, Y. Park and K. Lee (2008). Polyacetylenes from the roots of cultivated-wild ginseng and their cytotoxicity in vitro. Archives of Pharmacal Research 31(2): 154-159.
Yang, M. C., H. C. Kwon, Y.-J. Kim, K. R. Lee and H. O. Yang (2010). Oploxynes A and B, polyacetylenes from the stems of *Oplopanax elatus*. Journal of Natural Products 73(5): 801-805.
Yannai, S., A. J. Day, G. Williamson and M. J. Rhodes (1998). Characterization of flavonoids as monofunctional or bifunctional inducers of quinone reductase in murine hepatoma cell lines. Food Chemistry and Toxicology 36(8): 623-30.
Yates, M. S., Q. T. Tran, P. M. Dolan, W. O. Osburn, S. Shin, C. C. McCulloch, J. B. Silkworth, K. Taguchi, M. Yamamoto, C. R. Williams, K. T. Liby, M. B. Sporn, T. R. Sutter and T. W. Kensler (2009). Genetic versus chemoprotective activation of Nrf2 signaling: overlapping yet distinct

gene expression profiles between Keap1 knockout and triterpenoid-treated mice. Carcinogenesis 30(6): 1024-1031.

Yuan, J. H., Y. Q. Li and X. Y. Yang (2007). Inhibition of epigallocatechin gallate on orthotopic colon cancer by upregulating the Nrf2-UGT1A signal pathway in nude mice. Pharmacology 80(4): 269-278.

Zeng, L., H. Liao, Y. Liu, T.-S. Lee, M. Zhu, X. Wang, M. B. Stemerman, Y. Zhu and J. Y. J. Shyy (2004). Sterol-responsive element-binding protein (SREBP) 2 down-regulates ATP-binding cassette transporter A1 in vascular endothelial cells. Journal of Biological Chemistry 279(47): 48801-48807.

Zhang, D. D., S.-C. Lo, J. V. Cross, D. J. Templeton and M. Hannink (2004). Keap1 is a redox-regulated substrate adaptor protein for a Cul3-dependent ubiquitin ligase complex. Molecular and Cellular Biology 24(24): 10941-10953.

Zhang, Y.-K. J., R. L. Yeager, Y. Tanaka and C. D. Klaassen (2010). Enhanced expression of Nrf2 in mice attenuates the fatty liver produced by a methionine- and choline-deficient diet. Toxicology and Applied Pharmacology 245(3): 326-334.

Zhao, J., A. N. Moore, J. B. Redell and P. K. Dash (2007). Enhancing expression of Nrf2-driven genes protects the blood brain barrier after brain injury. Journal of Neuroscience 27(38): 10240-10248.

Zheng, G., W. Lu and J. Cai (1999). Stereoselective Total synthesis of (3R,8S)-falcarindiol, a common polyacetylenic compound from umbellifers. Journal of Natural Products 62(4): 626-628.

Zidorn, C., K. Johrer, M. Ganzera, B. Schubert, E. M. Sigmund, J. Mader, R. Greil, E. P. Ellmerer and H. Stuppner (2005). Polyacetylenes from the Apiaceae vegetables carrot, celery, fennel, parsley, and parsnip and their cytotoxic activities. Journal of Agricultural and Food Chemistry 53(7): 2518-2523.